



# Chemical analysis of resinous materials employed in artistic pre-hispanic Mexico : application to aztec and maya archaeological samples

Paola Lucero

► **To cite this version:**

Paola Lucero. Chemical analysis of resinous materials employed in artistic pre-hispanic Mexico : application to aztec and maya archaeological samples. Other. Université d'Avignon, 2012. English. <NNT : 2012AVIG0244>. <tel-00959989>

**HAL Id: tel-00959989**

**<https://tel.archives-ouvertes.fr/tel-00959989>**

Submitted on 17 Mar 2014

**HAL** is a multi-disciplinary open access archive for the deposit and dissemination of scientific research documents, whether they are published or not. The documents may come from teaching and research institutions in France or abroad, or from public or private research centers.

L'archive ouverte pluridisciplinaire **HAL**, est destinée au dépôt et à la diffusion de documents scientifiques de niveau recherche, publiés ou non, émanant des établissements d'enseignement et de recherche français ou étrangers, des laboratoires publics ou privés.



ACADEMIE D'AIX-MARSEILLE  
UNIVERSITE D'AVIGNON ET DES PAYS DE VAUCLUSE  
Ingénierie Appliquée à la Restauration  
des Patrimoines Naturel et Culturel  
UMR IMBE, CNRS 7263-IRD 237



## THÈSE

Présentée à l'Université d'Avignon et des Pays de Vaucluse  
Pour obtenir le diplôme de DOCTORAT

**SPÉCIALITÉ : Chimie**

**ANALYSE CHIMIQUE DES MATIÈRES RÉSINEUSES  
EMPLOYÉES DANS LE DOMAINE ARTISTIQUE PRÉ-  
HISPANIQUE AU MEXIQUE.  
APPLICATION AUX ÉCHANTILLONS ARCHÉOLOGIQUES  
AZTÈQUE ET MAYA.**

Présentée par

**Paola LUCERO**

En vue de l'obtention du grade de **Docteur en Sciences**  
Soutenue le 14 Septembre 2012

Directrice de Thèse : Cathy VIEILLES CAZES

Jury

REGERT Martine

Présidente du Jury

*Rapporteur, directrice de recherche CNRS, Université Nice Sophia Antipolis*

BUCIO-GALINDO Lauro

*Rapporteur, professeur à l'Université National Autonome du Mexique*

MATHE Carole

*Co-encadrant de thèse, maître de conférences à l'Université d'Avignon et des Pays de Vaucluse*

VIEILLES CAZES Catherine

*Directrice de thèse, professeur, HDR à l'Université d'Avignon et des Pays de Vaucluse*

*To my parents and siblings,  
to Val*

*Our Sun has hidden  
And has left us  
In complete darkness.  
We know that it will illuminate us again.  
But while it is in the underworld,  
We must get together.  
Hiding everything we love in our hearts.  
Our advanced study schools,  
Our houses of sing  
Our temples,  
Our ball fields will be destroyed  
We will abandon the streets,  
to lock ourselves in our homes.*

*Fathers and mothers,  
Do not forget to tell your children  
What life has been like  
Until today in Anahuac,  
Do not forget to tell your children  
That one day the Sun will shine again  
In Anahuac.*

**Last communicate of Aztec Emperor Cuauhtémoc to his people  
August 12<sup>th</sup> 1521**

*This thesis would not have been possible without the help and advice of many scientists, restorers, and archaeologist. It is my deep wish to thank all these people:*

*First of all, I wish to thank Prof. Dr. Cathy Vieillescazes for giving me the opportunity to work in her group on this exceptional research project. She supported me whenever necessary and made this thesis a great learning experience.*

*My most genuine gratitude is owed to Dr. Carole Mathe I thank her for her guidance. Her support and knowledge in conservation science was very valuable and helpful.*

*Many special thanks go to Prof Dr. Irma Belio and Prof Dr. Lauro Bucio. They contributed considerably to the success of this work with their brilliant ideas, on statistical and mathematical treatment of data. I thank them as well for their active collaboration in the collection of certified samples. I cordially thank them for his friendship and enthusiasm and unconditional support.*

*I am grateful to Dr. Rito Vega, without his precious knowledge in botanic, collection of certified samples would not have been possible.*

*I thank Dr. Leonardo López Luján director of the archaeological project of Templo Mayor, for granting us access to both the archaeological site and the archaeological samples, and for the confidence that he deposed on this scientific work and its results.*

*It was a great experience to talk with María Barajas and the members of the team of the Conservation Department of Templo Mayor Museum. I really appreciate the discussions with them, because they taught me what the problems in restoration are, and which improvements and knowledge would be helpful.*

*I also wish to thank Dr. Aurora Montúfar, who contributed to this research with samples from the paleo- botanical collection of the INAH.*

*I acknowledge National Mexican Council of Science and Technology (CONACYT) for the Ph D. scholarship that granted me.*

*I acknowledge the Academic body of biomaterials from the Autonomous University of Sinaloa., for their participation in the collection of certified resins.*

*I cordially thank the colleagues from the electronic microscope at the Physics Institute from the UNAM for their collaboration in the analysis of copal samples.*

*Most grateful I am to Niko for his support, patience and for following me in this project.*

*A very special thank goes to all my friends that always support me, I will always remember you.*

*Finally my love and gratitude goes to my family that helped me and guided me all along my studies.*

## Summary

Summary	I
List of Figures	V
List of Tables	X
Abbreviations	XIII
<b>PART A</b>	
<b>INTRODUCTION</b>	<b>1</b>
<b>CHAPTER I</b>	
<b>GENERAL PRESENTATION OF THE COPALS</b>	<b>4</b>
1.1 General presentation of Mexican copals	5
1.2 Botanical and geographical distribution	6
1.2.1 Botanical sources and collection	6
1.3 Historical Context	9
1.3.1 The Maya civilization	9
1.3.2 Chichén Itzá city	10
1.3.3 Importance of “Sacred Cenote” at Chichén Itzá and their offerings	11
1.4 The Aztec civilization	12
1.4.1 The foundation of Mexico-Tenochtitlán	13
1.4.2 The rise of Aztec empire	13
1.4.3 The importance of “Templo Mayor” site	13
1.4.4 The building stages in Templo Mayor construction	14
1.5 Uses and properties	15
1.5.1 Copal uses in ancient Mexico	15
1.5.2 Contemporary uses and applications of copal	17
1.6 Previous works on chemical composition of Mexican copals	18
1.7 Oleo-gum-resin: definitions	19
1.8 Gums	19
1.9 Gum composition of <i>Bursera simaruba</i>	19
1.10 Fats	20
1.11 Terpenic resins	20
1.12 Bio synthesis of terpenic precursors	20
1.13 The essential oils	21
1.13.1 Triterpens	23
1.13.2 The ursans	24
1.13.3 The oleanans	24
1.13.4 The lupans	25
1.13.5 Biological activity	26
<b>CHAPTER II</b>	
<b>PRESENTATION OF THE COPAL SAMPLES AND THE ANALYTICAL STRATEGY</b>	<b>28</b>
2.1 Extraction of copal	29

2.2 Resins from botanical certified origin	31
2.2.1 Botanical References	31
2.2.2 Choice of studied species	32
2.3 Archaeological samples from Templo Mayor site	33
2.3.1 Description of the offerings from Templo Mayor	34
2.3.2 Macroambiental conditions	38
2.3.3 Microambiental conditions	39
2.4 Description of archeological Aztec offerings	40
2.4.1 Offering 120	40
2.4.2 Offering 125	41
2.4.3 Offering 126	42
2.4.4 Offering 128	42
2.5 Archaeological sample from the “Sacred Cenote” of Chichén Itzá	42
2.5.1 Macroambiental conditions	43
2.5.2 The Chichén Itzá Cenote: microambiental conditions	45
2.5.3 Underwater Chichén Itzá cenote explorations	46
2.6 Commercial Samples	48
2.7 Presentation of the Analytical Strategy	51
2.8 Study by optical microscopy	53
2.9 Conclusion	56
<b>PART B Analytical Study of the resins and Discussion</b>	<b>57</b>
<b>CHAPTER III</b>	
<b>SPECTROSCOPIC TECHNIQUES: FTIR</b>	<b>57</b>
3.1 Mathematical Treatment of Experimental data: chemometric strategies	57
3.1.1 Principal Component Analysis	57
3.1.2 Linear discriminant analysis (LDA)	59
3.2 Chemotaxonomy. Correlation of resin composition and botanical origin	60
3.2.1 Terpenoids and chemotaxonomy	61
3.3 Study by Fourier-transformed infrared spectroscopy (FTIR)	62
3.3.1 FTIR spectra of terpene and terpene like molecules	62
3.4 Sampling Methods: transmission methods	64
3.5 Reflectance Methods	64
3.6 Results and discussion	65
3.7 PCA	67
3.8 Linear discriminant analysis	71
3.9 Application to a botanical origin certified sample	72
3.10 Application to two commercial samples of copal	73
3.11 Deconvolution of the bands in the region between 1200 and 1300 $\text{cm}^{-1}$ of the spectra. Application of the technique to two commercial resins	75
3.12 Application to archeological resins	78
3.13 Partial analysis of the surface of the samples	80
3.13.1 Comparison of partial analysis from commercial samples and a naturally aged sample of them.	81



3.13.2 Spectra variation between external and internal part of an archaeological sample TMT	84
3.14 Conclusions	86
<b>CHAPTER IV</b>	
<b>HIGH PERFORMANCE LIQUID CHROMATOGRAPHY -UV/VIS ANALYSIS</b>	<b>88</b>
4.1 High Performance Liquid Chromatography (HPLC)	89
4.2 Standard molecules	93
4.3 Quantification of triterpenoids: analytical calibration	93
4.4 Global analysis of certified resin samples	94
4.5 Comparison of global chromatograms from certified origin resins	96
4.6 Comparison of global chromatograms from commercial resins	102
4.7 Comparison of global chromatograms of archaeological resins	105
4.8 HPLC coupled to PCA analysis for botanical certified resins	108
4.9 Linear Discriminant Analysis	111
4.10 HPLC coupled to PCA analysis for archeological resins	112
4.11 Purification by Solid Phase Extraction (SPE)	115
4.12.1 General Methodology	115
4.13 Conclusion	117
<b>CHAPTER V</b>	
<b>GAS CHROMATOGRAPHY-MASS SPECTROMETRY</b>	<b>118</b>
5.1 Derivatization	120
5.2 The study of standard triterpenoic molecules	121
5.3 Results of the study on botanical certified samples	123
5.4 Comparison of global chromatograms from certified origin resins	124
5.5 Insight on triterpenic composition for samples of certificated origin	128
5.5.1 Comparison between <i>B. bipinnata</i> and <i>B. stenophylla</i> resins	128
5.5.2 <i>B. excelsa</i> triterpenic composition	129
5.5.3 <i>B. grandifolia</i> triterpenic composition	130
5.5.4 <i>B. laxiflora</i> triterpenic composition	131
5.5.5 <i>B. penicillata</i> triterpenic composition	132
5.5.6 <i>B. simaruba</i> triterpenic composition	133
5.5.7 <i>B. copallifera</i> triterpenic composition	134
5.6 Study of archeological samples	134
5.6.1 Molecular composition of archeological sample 26	135
5.6.2 Molecular composition of archeological sample 51	136
5.6.3 Molecular composition of archeological sample 52	137
5.6.4 Molecular composition of archeological sample 84	138
5.6.5 Molecular composition of archeological sample 173	139
5.6.7 Molecular composition of archeological sample TMT	139
5.6.8 Molecular composition of archeological sample 140	140
5.6.9 Molecular composition of archeological sample from Chichén Itzá	141

5.7 Study of commercial samples	143
5.7.1 Molecular composition of Sidral	143
5.7.2 Molecular composition of commercial sample SONB4	144
5.7.3 Comparison between molecular composition of ATZJ2 and SONB4	144
5.7.4 Molecular composition Oaxc2	145
5.7.5 Molecular composition IZUP1 and SONR1	146
5.8 Comparison of partial analysis from the surface and the inner part of the samples	150
5.8.1 Comparison between SONB4 and a sample naturally aged portion of it	151
5.8.2 Molecular variation between external and internal part of an archaeological sample TMT	150
5.9 Conclusions	152
<b>GENERAL CONCLUSION</b>	<b>154</b>
<b>PERSPECTIVES</b>	<b>159</b>
<b>MATERIALS AND METHODS</b>	<b>161</b>
<b>BIBLIOGRAPHY</b>	<b>167</b>
<b>ANNEXES</b>	<b>185</b>
<b>ANNEX 1</b>	<b>186</b>
<b>ANNEX 2</b>	<b>193</b>
<b>ANNEX 3</b>	<b>235</b>
<b>ANNEX 4</b>	<b>269</b>

## Liste of Figures

### PART A

#### Chapter I General Presentation of the Copals

<b>Fig 1</b>	Pages from the “De la Cruz-Badiano” codex	<b>5</b>
<b>Fig 2</b>	Botanical classification of resin producing trees	<b>7</b>
<b>Fig 3</b>	Phylogeny of Mexican <i>Bursera</i> based on ribosomal A.D.N.	<b>8</b>
<b>Fig 4</b>	Map of Mexico, with the number of <i>Bursera</i> species by region	<b>9</b>
<b>Fig 5</b>	Map with most important Mayan cities	<b>10</b>
<b>Fig 6</b>	Map of Chichén Itzá City	<b>11</b>
<b>Fig 7</b>	The seven stages of “Templo Mayor” a) Aveni, 1988 b) Picture from the National Museum of Anthropology and History, Mexico City	<b>14</b>
<b>Fig 8</b>	MVA pathway left (Eisenreich et al, 2004) and MEP pathway (Kashara et al, 2002) for terpenoids biosynthesis.	<b>16</b>
<b>Fig 9</b>	Structure of typical occurring monoterpenes (from I to XV) and sesquiterpenes (XVI to XXIV) in resins from Burseraceae family	<b>17</b>
<b>Fig 10</b>	Triterpenic skeleton of ursane type	<b>21</b>
<b>Fig 11</b>	Examples of skeletal types of triterpenes found in <i>Bursera</i> resins.	<b>22</b>
<b>Fig 12</b>	$\alpha$ -amyrin, $\alpha$ -amyrone and 3-epi- $\alpha$ -amyrin	<b>23</b>
<b>Fig 13</b>	$\beta$ -amyrin, $\beta$ -amyrone and 3-epi- $\beta$ -amyrin	<b>23</b>
<b>Fig 14</b>	Lupan compounds founded in commercial or archeological resins, described by several authors	<b>24</b>
<b>Fig 15</b>	Structure of lup-20 (29)- en 3 $\beta$ - 23-diol from <i>B. simaruba</i> resin	<b>24</b>
<b>Fig 16</b>	Primitive representation of Quetzalcoatl holding a copal bag on his hand	<b>25</b>
<b>Fig 17</b>	Archaeological Aztec pieces where copal is believed to be used as adhesive	<b>25</b>

#### Chapter II Presentation of the Analytical Strategy and the copal samples

<b>Fig 18</b>	A description of the general situation encountered when analyzing historical materials and, a general approach to their study.	<b>30</b>
<b>Fig 19</b>	Pictures of copals from different botanical origin, taken at our laboratory	<b>30</b>
<b>Fig 20</b>	From left to right: images of “piedra” copal in Cholula, White copal in Sonora, “lágrima” copal at Izúcar and “mirra” in Azcapotzalco markets.	<b>33</b>
<b>Fig 21</b>	Physical aspect of copals from certified botanical origin.	<b>35</b>
<b>Fig 22</b>	Picture of tree Aztec figurines made of copal, the first taken from Lehman, 1948 and the second and third from Naoli, 2004	<b>36</b>
<b>Fig 23</b>	Picture of the offering 120, level 3. (Alonso A. et al, 2008)	<b>37</b>
<b>Fig 24</b>	Offering “U” from Templo Mayor. It is notable the symmetrical disposition of the four copal balls in the corners and a ceremonial knife in the center (drawing from Carrisoza F. at Jimenez-Badillo, 2009)	<b>39</b>
<b>Fig 25</b>	Reconstruction of the sacred precinct of Tenochtitlán after Antonio Serrato Combé a) Templo Mayor b) Cuauhxiclco c) Tzompantli. d) Casa de las Águilas e) Area explored by the Archeological project of Templo Mayor	<b>40</b>
<b>Fig 26</b>	From left to right: Piedra del Sol (1790), Coyolxauhqui (1978) and	<b>44</b>

	Tlaltecuhlli (2006)	
<b>Fig 27</b>	Map of the cenotes at Yucatán peninsula (Pedroza, 2010)	<b>45</b>
<b>Fig 28</b>	The cenote of Chichén Itza	<b>47</b>
<b>Fig 29</b>	Archaeological objects recovered from the sacred cenote of Chichén Itzá:	<b>48</b>
<b>Fig 30</b>	Archaeological copal objects recovered from the sacred cenote of Chichén Itzá: a) animal shaped figurine, b) Tripod bowl with offering with jade beads c) Tripod bowl with offering d) copal ball with small balls of rubber, e) human face f) corn shaped copal (Catalog of Peabody museum)	<b>52</b>
<b>Fig 31</b>	Picture of non homogeneous archaeological samples referred A) sample 26 B) sample 173, C) sample TMT, D) sample 84 Homogeneous archeological sample M1	<b>54</b>
<b>Fig 32</b>	Fig 33 Homogeneous archeological samples A) 51, B) 52 C) M1	<b>55</b>
<b>Fig 33</b>	TMT sample A) from the surface and B) from the interior	<b>56</b>

## PART B Analytical Study of the resins and Discussion

### Chapter III Spectroscopic Techniques: FTIR

<b>Fig 34</b>	Principal components analysis (PCA) projects data along the directions where the data varies the most.	<b>58</b>
<b>Fig 35</b>	FTIR spectra of different species A) <i>B. bipinnata</i> , B) <i>B. excelsa</i> , C) <i>B. grandifolia</i>	<b>65</b>
<b>Fig 36</b>	FTIR spectra of different species A) <i>B. penicillata</i> , B) <i>B. simaruba</i> C) <i>B. stenophylla</i>	<b>66</b>
<b>Fig 37</b>	Band interpretation for the studied species : A) <i>B. bipinnata</i> , B) <i>B. excelsa</i> , C) <i>B. grandifolia</i> , D) <i>B. laxiflora</i> , E) <i>B. penicillata</i> , F) <i>B. stenophylla</i>	<b>68</b>
<b>Fig 38</b>	Distribution in the hyperspace of the first two components of the species according their botanical origin. Variables are shown with different symbols	<b>69</b>
<b>Fig 39</b>	Loading plot, variables with a high impact on first component are shown in orange, and variables with a high impact on second component are shown on black	<b>70</b>
<b>Fig 40</b>	Distribution in the hyperspace of the first two components of the species using 2 less band positions as variables (f and e)	<b>71</b>
<b>Fig 41</b>	PCA analysis for the samples of the six certified resins plus a sample of <i>B. copallifera</i>	<b>73</b>
<b>Fig 42</b>	PCA analysis for the samples of the six certified resins plus commercial sample MEXJ1	<b>74</b>
<b>Fig 43</b>	PCA analysis of the samples of the six certified resins plus commercial sample IZUM1	<b>74</b>
<b>Fig 44</b>	Deconvolution of bands between 1200 and 1300cm <sup>-1</sup> region. For a) <i>B. bipinnata</i> and b) <i>B. stenophylla</i>	<b>76</b>
<b>Fig 45</b>	IZUM1 deconvolution of 1300-1200 region: botanical origin <i>B. stenophylla</i> R <sup>2</sup> 99.17	<b>77</b>
<b>Fig 46</b>	MEXJ1 deconvolution of 1300-1200 region: botanical origin <i>B. bipinnata</i> R <sup>2</sup> 98.09	<b>77</b>

<b>Fig 47</b>	PCA with FTIR data from six species plus FTIR data from archeological samples: mathematical model was able to discriminate archeological samples, from different archeological sites.	<b>78</b>
<b>Fig 48</b>	Distribution in the hyperspace of archeological resins among fresh botanical origin certified resins. Aztec archeological samples are shown as follows	<b>80</b>
<b>Fig 49</b>	FTIR spectra of fresh and light aged sample of Huitzuco	<b>82</b>
<b>Fig 50</b>	FTIR spectra of fresh and light aged sample of SONB4	<b>82</b>
<b>Fig 51</b>	PCA analysis for the samples with FTIR data of six certified resins plus commercial sample HUITZUCO fresh and light aged	<b>83</b>
<b>Fig 52</b>	PCA analysis for the samples with FTIR data of six certified resins plus commercial sample SONB4 ● fresh, ● and light aged	<b>83</b>
<b>Fig 53</b>	FTIR spectra of inner part and surface of TMT	<b>84</b>
<b>Fig 54</b>	PCA analysis for the samples with FTIR data of six certified resins TMT sample from the ● inner part and ● the surface	<b>85</b>

#### Chapter IV High Performance Liquid Chromatography -UV/Vis Analysis

<b>Fig 55</b>	Schematic view of HPLC instrumentation and their components.	<b>90</b>
<b>Fig 56</b>	Chromatogram of <i>B. bipinnata</i> . triterpenic zone running from 24 to 35 min in retention time	<b>95</b>
<b>Fig 57</b>	Global chromatograms for certified origin samples by species	<b>97</b>
<b>Fig 58</b>	Comparison of <i>B. bipinnata</i> and <i>B. stenophylla</i> chromatograms	<b>98</b>
<b>Fig 59</b>	Chromatograms of samples type A and B of <i>B. stenophylla</i>	<b>99</b>
<b>Fig 60</b>	Molecular profile types A and B of <i>B. excelsa</i>	<b>100</b>
<b>Fig 61</b>	<i>B. simaruba</i> lot A with a richer polar fraction than lot B	<b>100</b>
<b>Fig 62</b>	The six different molecular profiles for <i>B. laxiflora</i>	<b>101</b>
<b>Fig 63</b>	Chromatograms of ATZB1, Huitzuco, IZUB2 and SONB3 that have the same molecular composition than <i>B. bipinnata</i> samples.	<b>102</b>
<b>Fig 64</b>	Chromatograms of commercial samples with a molecular profile close to <i>B. stenophylla</i> resin.	<b>103</b>
<b>Fig 65</b>	Chromatograms of some commercial samples from unknown botanical origin, presumably not within Burseraceae family.	<b>104</b>
<b>Fig 66</b>	Chromatograms of archeological sample with molecular profile A.	<b>105</b>
<b>Fig 67</b>	Chromatogram of archeological sample with triterpens and possible condensation products (A1-A4)	<b>106</b>
<b>Fig 68</b>	Chromatograms from archeological samples with B profile from Templo Mayor	<b>107</b>
<b>Fig 69</b>	Chromatogram of Chichén Itzá archeological sample	<b>108</b>
<b>Fig 70</b>	Distribution in the hyperspace of the first two components of PCA for 6 species according their botanical origin	<b>109</b>
<b>Fig 71</b>	Loading plot for PCA analysis using HPLC data	<b>110</b>
<b>Fig 72</b>	Distribution in the hyperspace of the first two components of PCA for 6 species according their botanical origin and Aztec samples and Maya sample	<b>113</b>
<b>Fig 73</b>	Distribution in the hyperspace of the first two components of PCA for 6	<b>114</b>

	species according their botanical origin plus archaeological sample and specific position of sample 84	
<b>Fig 74</b>	Chromatograms of A) washing product and B) elution product	<b>116</b>
<b>Chapter V Gas Chromatography-Mass Spectrometry</b>		
<b>Fig 75</b>	Schematic view of GC instrumentation and their components	<b>119</b>
<b>Fig 76</b>	Characteristic fragments from silylated compounds	<b>120</b>
<b>Fig 77</b>	Global gas chromatograms for resin samples of certified botanical origin and for A) <i>B. bipinnata</i> and B) <i>B. stenophylla</i> resins samples	<b>124</b>
<b>Fig 78</b>	Global gas chromatograms for resin samples of certified botanical origin and for A) <i>B. excelsa</i> and B) <i>B. laxiflora</i> resin samples	<b>125</b>
<b>Fig 79</b>	Global gas chromatograms for resin samples of certified botanical origin and for <i>B. penicillata</i> and <i>B. simaruba</i> resin sample	<b>126</b>
<b>Fig 80</b>	Global gas chromatograms for resin samples of certified botanical origin and for A) <i>B. grandifolia</i> and B) <i>B. copallifera</i> resin sample	<b>127</b>
<b>Fig 81</b>	GC chromatogram of <i>B. bipinnata</i> sample 11c1	<b>128</b>
<b>Fig 82</b>	Zoom into triterpenic zone of GC chromatogram of a sample of A) <i>B. bipinnata</i> and B) <i>B. stenophylla</i> resins	<b>129</b>
<b>Fig 83</b>	Zoom into triterpenic zone of GC chromatogram of a sample of a <i>B. excelsa</i> resin sample	<b>130</b>
<b>Fig 84</b>	Zoom into triterpenic zone of GC chromatogram of sample 34b1Q of a <i>B. grandifolia</i> resin sample	<b>131</b>
<b>Fig 85</b>	Zoom into triterpenic zone of GC chromatogram of sample 47a1Q of a <i>B. laxiflora</i> resin sample	<b>131</b>
<b>Fig 86</b>	Zoom into triterpenic zone of GC chromatogram of sample 47b1Q of a <i>B. laxiflora</i> resin sample	<b>132</b>
<b>Fig 87</b>	Zoom into first triterpenic zone of GC chromatogram of sample 63a4 of a <i>B. penicillata</i> resin sample	<b>132</b>
<b>Fig 88</b>	Zoom into second triterpenic zone of GC chromatogram of sample 63a4 of a <i>B. penicillata</i> resin sample	<b>133</b>
<b>Fig 89</b>	Zoom into triterpenic zone of GC chromatogram of sample 70a1Q of a <i>B. simaruba</i> resin sample	<b>133</b>
<b>Fig 90</b>	Zoom into triterpenic zone of GC chromatogram of the <i>B. copallifera</i> resin sample	<b>134</b>
<b>Fig 91</b>	Zoom into triterpenic zone of GC chromatogram of archaeological sample 26	<b>135</b>
<b>Fig 92</b>	A) Complete chromatogram and B) zoom into triterpenic zone of archeological sample 51	<b>136</b>
<b>Fig 93</b>	A) Complete chromatogram and B) zoom into triterpenic zone of archeological sample 52	<b>137</b>
<b>Fig 94</b>	A) Complete chromatogram and B) zoom into triterpenic zone of archeological sample 84	<b>138</b>
<b>Fig 95</b>	A) Complete chromatogram and B) zoom into triterpenic zone of archeological sample 173	<b>139</b>
<b>Fig 96</b>	A) Complete chromatogram and B) zoom into triterpenic zone of archeological sample TMT	<b>140</b>
<b>Fig 97</b>	A) Complete chromatogram and B) zoom into triterpenic zone of	<b>141</b>

	archeological sample M1	
<b>Fig 98</b>	A) Complete chromatogram and B) zoom into triterpenic zone of archeological sample Chichén Itzá	<b>142</b>
<b>Fig 99</b>	A) Complete chromatogram and B) zoom into triterpenic zone of commercial sample Sidral	<b>143</b>
<b>Fig 100</b>	Zoom into triterpenic zone of commercial sample SONB4	<b>144</b>
<b>Fig 101</b>	Global Chromatograms for SONB4 and ATZJ2	<b>145</b>
<b>Fig 102</b>	Global Chromatogram for Oaxc2	<b>145</b>
<b>Fig 103</b>	Zoom into triterpenic zones of the chromatograms for A) IZUP1 and B) SONR1	<b>146</b>
<b>Fig 104</b>	Global chromatograms for A) IZUP1 and B) SONR1	<b>147</b>
<b>Fig 105</b>	Global chromatograms for A) SONB4 resin and B) SONB4 aged resin	<b>148</b>
<b>Fig 106</b>	Zoom into triterpenic zones of SONB4 resin and SONB4 aged resin	<b>149</b>
<b>Fig 107</b>	Zoom into triterpenic zone of chromatograms of TMT resin in the inner part and from the surface	<b>151</b>
<b>Fig 108</b>	Mass fragmentation for the “N” compound, peak detected at 39.78 min in the resin TMT surface	<b>151</b>
<b>Annexes</b>		
<b>Fig 109</b>	Map of the GPS position of originating trees for certified resins	<b>189</b>
<b>Fig 110</b>	FTIR spectra of <i>B. bipinnata</i> samples	<b>172</b>
<b>Fig 111</b>	FTIR spectra of <i>B. excelsa</i> samples	<b>173</b>
<b>Fig 112</b>	FTIR spectra of <i>B. grandifolia</i> samples	<b>174</b>
<b>Fig 113</b>	FTIR spectra of <i>B. laxiflora</i> samples	<b>175</b>
<b>Fig 114</b>	FTIR spectra of <i>B. simaruba</i> samples	<b>176</b>
<b>Fig 115</b>	FTIR spectra of <i>B. stenophylla</i> samples	<b>177</b>
<b>Fig 116</b>	FTIR spectra of <i>B. penicillata</i> samples	<b>178</b>
<b>Fig 117</b>	PCA: First two components for certified resins plus commercial samples: ◀ATZM1, ◀CHOB1, ◀ATZB1, ◀IZUR1.	<b>213</b>
<b>Fig 118</b>	Chromatograms of commercial samples	<b>220</b>
<b>Fig 119</b>	Mass spectra of molecular markers for <i>B. bipinnata</i> and <i>B. stenophylla</i>	<b>279</b>
<b>Fig 120</b>	Mass spectra of molecular markers for <i>B. excelsa</i> and <i>B. laxiflora</i>	<b>280</b>
<b>Fig 121</b>	Mass spectra of molecular markers for <i>B. grandifolia</i> and <i>B. simaruba</i>	<b>284</b>
<b>Fig 122</b>	Mass spectra of molecular markers for <i>B. penicillata</i>	<b>291</b>
<b>Fig 123</b>	Mass spectra of molecular markers for <i>B. copallifera</i>	<b>294</b>

## Liste of Tables

### PART A

#### Chapter I General Presentation of the Copals

<b>Table 1</b>	Monosaccharide composition of <i>B. Simaruba</i> (Magaloni, 1996)	<b>19</b>
----------------	---	-----------

#### Chapter II Presentation of the Analytical Strategy and the copal samples

<b>Table 2</b>	Copals collected in 2004-2005	<b>34</b>
<b>Table 3</b>	Copals collected in 2008	<b>34</b>
<b>Table 4</b>	Copals collected in 2010	<b>49</b>
<b>Table 5</b>	Arqueological Aztec samples	<b>49</b>
<b>Table 6</b>	Archeological sample from Chichén Itzá	<b>50</b>

### PART B Analytical Study of the resins and Discussion

#### Chapter III Spectroscopic Techniques: FTIR

<b>Table 7</b>	Assignment for the most characteristic IR bands of some terpenoid compounds (Schulz and Baranska, 2007)	<b>62</b>
<b>Table 8</b>	Band positions taken into account as variables for the PCA matrix	<b>67</b>
<b>Table 9</b>	Results for LDA classification model: Fitting and validation matrix were identical. Rows represent the true class, and columns the assigned class. Wrong assignments are shown in red	<b>72</b>

#### Chapter IV High Performance Liquid Chromatography -UV/Vis Analysis

<b>Table 10</b>	Amount of resins used for the HPLC chromatographic study	<b>90</b>
<b>Table 11</b>	Gum and resin percentage in resin samples from studied species	<b>91</b>
<b>Table 12</b>	Unsoluble matter in apolar solvents in archeological samples.	<b>92</b>
<b>Table 13</b>	Arqueological Aztec samples	<b>93</b>
<b>Table 14</b>	Archeological sample from Chichén Itzá	<b>94</b>
<b>Table 15</b>	Unsoluble matter in apolar solvents in archeological samples	<b>95</b>
<b>Table 16</b>	Retention time of peak corresponding to non triterpenic compounds founded in each species (+ presence, -absence)	<b>96</b>
<b>Table 17</b>	Retention time of peaks corresponding to triterpenic compounds found in each species (+ presence, -absence)	<b>96</b>
<b>Table 18</b>	Fitting matrix of the LDA Rows represent the true class, and the columns the assigned class	<b>111</b>
<b>Table 19</b>	Validation matrix of LDA, Rows represent the true class and the columns the assigned class	<b>112</b>



## Chapter V Gas Chromatography-Mass Spectrometry

<b>Table 20</b>	TMS structure of the triterpenic standard molecules studied by GC-MS. O: Oleanane, U: Ursane, L: Lupane	<b>121</b>
<b>Table 21</b>	Time of retention of standard molecules under the designed GC-MS gradients	<b>122</b>
<b>Table 22</b>	Amount of resins used for the GC-MS study	<b>123</b>

## Conclusions and Perspectives

<b>Table 23</b>	Recapitulative of botanical origin for archaeological and commercial samples studied	<b>155</b>
-----------------	--	------------

## Materials and Methods

<b>Table 24</b>	HPLC Gradient 1, employed for the study of the terpenic compounds in fresh resins	<b>162</b>
<b>Table 25</b>	HPLC gradient 2 employed for the study of the terpenic compounds in archaeological resins	<b>162</b>
<b>Table 26</b>	Gradient 1, GC-MS temperature gradient for the global analysis of resins	<b>164</b>
<b>Table 27</b>	Gradient 2, optimal gradient for the analysis of triterpenoids GC-MS	<b>165</b>

## ANNEXES

<b>Table 28</b>	Table of certified copals <i>B. bipinnata</i> , <i>B. excelsa</i> and <i>B. grandifolia</i> , with GPS position of originating tree and date of collection	<b>186</b>
<b>Table 29</b>	Table of <i>B. laxiflora</i> y <i>B. penicillata</i> certified copals, with GPS position of originating tree and date of collection	<b>187</b>
<b>Table 30</b>	Table of <i>B. simaruba</i> , <i>B. stenophylla</i> certified copals, with GPS position of originating tree and date of collection	<b>188</b>
<b>Table 31</b>	Pictures of some commercial samples	<b>190</b>
<b>Table 32</b>	Selected pictures of optical microscopic study of certified origin samples from <i>B. bipinnata</i> species	<b>191</b>
<b>Table 33</b>	Selected pictures of optical microscopic study of certified origin samples from <i>B. bipinnata</i> species, and from archeological sample M1	<b>192</b>
<b>Table 34</b>	Selected pictures of electronic microscopic study of certified origin samples from <i>B. Bipinnata</i> species	<b>193</b>
<b>Table 35</b>	Selected pictures of electronic microscopic study of certified origin samples from <i>B. bipinnata</i> species	<b>194</b>
<b>Table 36</b>	Selected pictures of electronic microscopic study of certified origin samples from <i>B. bipinnata</i> species	<b>195</b>
<b>Table 37</b>	Picture of Sidral sample before and after light ageing	<b>196</b>
<b>Table 38</b>	Botanical differences between <i>B. bipinnata</i> and <i>B. stenophylla</i>	<b>197</b>
<b>Table 39</b>	FTIR bands of certified resins used in PCA	<b>206</b>
<b>Table 40</b>	FTIR bands of archaeological resins used in PCA	<b>207</b>
<b>Table 41</b>	LDA results of classification of FTIR data of certified resins	<b>208</b>
<b>Table 42</b>	FTIR data used on PCA on selected commercial sample	<b>208</b>

<b>Table 43</b>	HPLC data of peaks corresponding to non triterpenic compounds in botanical certified resins and archaeological resins used in PCA	<b>224</b>
<b>Table 44</b>	HPLC data of peaks corresponding to non triterpenic compounds in botanical certified resins and archaeological resins used in PCA	<b>225</b>
<b>Table 45</b>	HPLC data of peaks corresponding to non triterpenic compounds in botanical certified resins and archaeological resins used in PCA	<b>227</b>
<b>Table 46</b>	LDA results with HPLC data for certified samples: fitting and confusion matrix	<b>228</b>
<b>Table 47</b>	Concentration of standard molecules in botanically certified samples (mg/ ml)	<b>256</b>
<b>Table 48</b>	Concentration of standard molecules in archaeological samples (mg/ ml)	<b>256</b>
<b>Table 49</b>	Concentration of lupenone in <i>B. simaruba</i> samples (mg/ ml)	<b>256</b>
<b>Table 50</b>	Concentration of standard molecules in commercial samples (mg/ ml)	<b>257</b>
<b>Table 51</b>	Retention times of standard molecules under gradient 2 for the study of triterpenic compounds	<b>258</b>
<b>Table 52</b>	Retention times of standard molecules under gradient 1 for the study of archaeological samples	<b>259</b>
<b>Table 53</b>	Mass spectra and retention time for identified triterpenes in Mexican copal	<b>286</b>

## List of Abbreviations

<b>A.D.</b>	<i>Annus Domini</i> or current era
<b>B.C.</b>	Before Christ
<b>EI</b>	Electronic impact
<b>FTIR</b>	Fourier-transform infrared spectroscopy
<b>GC-MS</b>	Gas chromatography–mass spectrometry
<b>HPLC</b>	High-performance liquid chromatography
<b>ID</b>	Identification
<b>LDA</b>	Linear Discriminant Analysis
<b>MeOH</b>	Methanol
<b>MW</b>	molecular weight
<b>m/z</b>	mass-to-charge ratio
<b>N.B.</b>	<i>Nota bene</i>
<b>PCA</b>	Principal component analysis
<b>PDA</b>	Photodiode array detection
<b>RIC</b>	Reconstructed ion chromatogram
<b>TIC</b>	Total ion chromatogram
<b>tr</b>	Retention time
<b>UPLC-MS</b>	high-performance liquid chromatography –mass spectrometry
<b>UV</b>	ultraviolet (light)
<b>Vis</b>	visible (light)
<b>IPP</b>	isopentenyl diphosphate
<b>MVA</b>	mevalonate
<b>MEP</b>	methyl erythritol phosphate
<b>CYP1A</b>	cytochrome P1A
<b>CYP2A</b>	cytochrome P2A
<b>PD<sub>50</sub></b>	the dose or concentration that acts in 50% of population considered

# Part A

# Introduction

The research team “Engineering applied to restoration of natural and cultural patrimony” has two main research axes: the first one centered in the study of resins and the second one focused on the study of colorants.

During 2006 archaeological excavations at the Templo Mayor site, in Mexico City, a huge monolith representing Tlaltecutli, the Aztec Goddess of death and life, was uncovered by archeologists from Leonardo López Luján team. Further investigations of professionals conclude that this monolith was in fact part of the Cuauhxiccalco, a funerary monument where Aztecs emperors were cremated.

Following archaeological excavation at this site and its surroundings uncovered thirteen offerings until 2008. Offerings were extraordinary: they were conceived as scaled representations of Aztec universe, and counted from a few to several hundreds of objects.

Among the materials found in these offerings, the most abundant was copal. Copal is an organic material; nowadays the term is generic and refers to a number of resins present in Mexican and international markets. Along the years of work in this research, a number of voids in botanical classification of the producing trees of resin, and ambiguities in the designation of the resins themselves were remarked by our team.

The copal from the Aztec offerings presented different colors: going from light yellow, to black passing by orange and brown. The consistency of their surface was heterogeneous as well, it went from a solid compact state to a very fragile porous and some times cracked one.

At this stage of the archaeological and conservation research many questions arisen about these copals. Were all these copals sharing the same botanical origin? Or they were rather mixtures of resins with different origin? Given its different uses, was there a botanical origin preferred for a specific use? Was the state of preservation related to the botanical origin more than to the burial

conditions to what they were subjected to? What would be the conservation strategy that should be followed to preserve these materials? Could a correlation be made between the data obtained from the botanical origin to provisioning sources from the copal? Which analytical technique could be use in order to identify them? Should the study of these materials be based in samples taken from the inner part of the piece, rather from the outside? It was at this point that the present research was born.

For this study a first stage on documentary research was done, and Mexican copal was related to *Bursera* Genus. Burseraceae family is known around the world because their members produce exudates, depending on the species of the producing tree, the secreted resin could be oliban (encens), frankincense or Mexican copal.

An analytical strategy was developed then, in our laboratory and the first chemical analyses were conducted on commercial samples. FTIR spectra were collected and existing HPLC protocols were tested and consequently adapted for the analysis of these materials, the same happened to GC-MS protocols.

In the second stage resins from certified botanical origin were needed. To obtain them a collaboration with researchers from the National Autonomous University of Mexico and the Autonomous University of Sinaloa was established.

The focus of this research was fixed according to the multiple interests of all the partners, and common objectives were settled to:

- ✂ Establish the molecular profile of certified resins
- ✂ Identify into the composition of the resins as many triterpenic compounds as possible
- ✂ Compare the molecular composition of the botanically certified resins to that of archeological and commercial resins

- ⌘ Observe the behavior of these materials upon ageing, and asses if botanical origin of a sample can be found for aged materials, and finally
- ⌘ Establish a simple protocol that allows conservation professionals to find the botanical origin of both archeological and commercial resins.

# Chapter I

## General presentation of the copals



## Chapter I

### General presentation of the copals

#### 1.1 General presentation of Mexican copals

The modern word « copal » is derived from the Nahuatl word *copalli* which means resin. In other regions of Mexico nowadays exist other terms to name copal: it is known as *honté*, *hom* or *jom* in huastec, *pum* in totonac and *pom* or *cib* in maya (Garcia-Hernandez, 2000).

Nevertheless the term that was retained in XVI<sup>th</sup> century by the Spanish was “copal”, so they spread this term, in American and European markets, to refer to a large group of gums and resins (Case, 2002). In fact in our days there is great confusion, as this term covers a number of exudates that share certain hardness and have a relatively high melting point.

Natural resins have been employed since ancient times in varnishes, paints, as binders, in cosmetic preparations and, in ancient Mexican context as adhesives (Sahagún, 2006) for a wide variety of purposes going from feathered art-crafts to dental incrustations, passing by turquoise mosaics and, ritual knives.

Medicinal purposes have been documented in sources from sixteenth century as it is the “De la Cruz-Badiano” codex (figure 1) that records a series of traditional remedies for different illnesses (Fresquet, 1999), the “General history of the things from New Spain” from Bernardino de Sahagún and the “True history of the conquest of the New Spain” from Bernal Diaz del Castillo, that record as well traditional uses of copal among original cultures from Mexico.



Fig 1 Pages from the “De la Cruz-Badiano” codex

Fresh copal was used as well as a spiritual material (Viveros, 2007), commonly burnt as incense in Maya and Nahua societies, in prayer to ask for guidance and protection, it was believed to be - along with human blood - the preferred food for Gods.

This extensive use of the resin can be correlated to the relative easiness on their obtention and their wide availability. Resins are naturally exuded by certain kind of trees upon injury or insect attack. The practice of cuts on the tree bark produces a flow of resin that hardens with the air contact (Langenheim, 2003).

## **1.2 Botanical and geographical distribution**

### **1.2.1 Botanical sources**

The Burseraceae family includes over 20 genera and more than 600 species of trees and scrubs from tropical and subtropical regions from Asia, Africa and America. A characteristic of this family is to have resin products containing aromatic terpenes and essential oils. Often called the balsam or torchwood family, Burseraceae are widely distributed in tropical and subtropical regions worldwide and are divided into three subfamilies: Bursereae, Canarieae and Proteieae (Langenheim, 2003).

*Burseras* are related to the genus of frankincense (*Boswellia*) and myrrh (*Commiphora*) (figure 2). The genus *Bursera* comprises around 100 species in America that distribute between the Southwest of the United States and the North of Brasil, but reach their major diversity on the Pacific coast of Mexico (Rzedowski, 2004).

*Burseras* have been described as “typically low or medium size trees with colorful trunks in blue, green, yellow, red or purple” (Langenheim, 2003). The bark of some of them exfoliates in papery sheets. This genus is notable because its exudates are rich in terpenoids (Mooney and Emboden, 1968).

In Mexico, *Bursera* is one of the most important components of dry forest, in some parts of the Southern regions of Mexico the genre becomes dominant or co-dominant. In desert scrub and thorn scrub, they are also present and, occur in a lesser extent in lowland tropical rain forest and higher altitude woodland (Rzedowski, 2005).

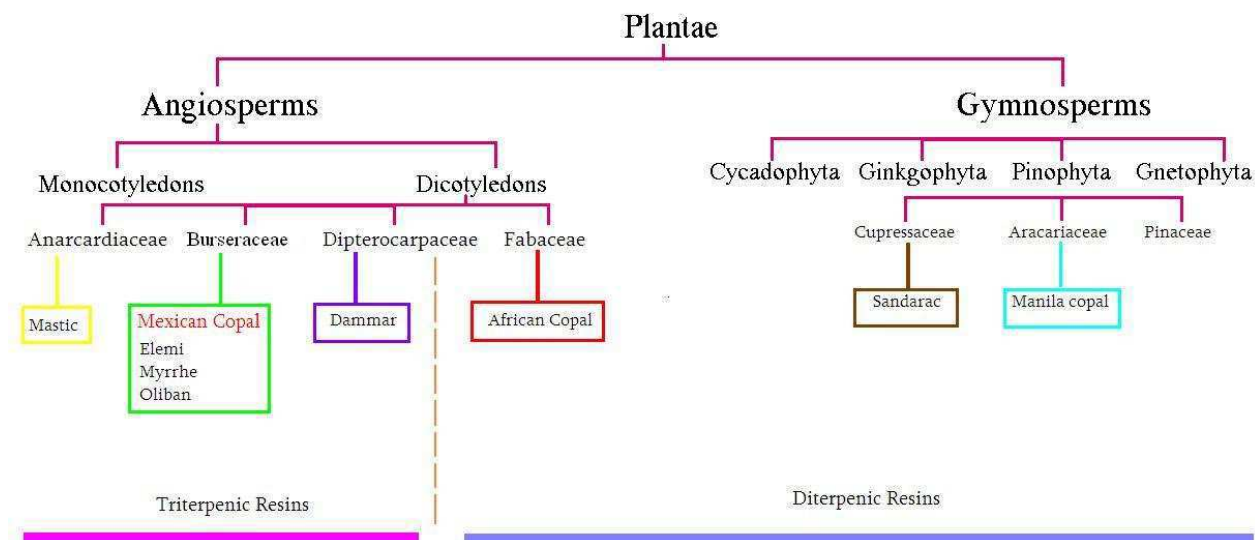


Fig 2 Botanical classification of resin producing trees (Langenheim, 2003)

Until now 82 species had been recenssed by botanists. Nevertheless, its classification remains problematic and its phylogenetic relationships are not well understood (Rzedowski, 1979). Molecular studies (Becerra and Venable, 1999) supported the view that *Bursera* is monophyletic and more closely related to *Commiphora* than *Boswellia*. The figure 3 shows a simplified version of the DNA classification of Mexican *Burseras* made by Becerra and Venable to show the two sections and the five groups in which they were divided.

Concerning distribution, the southern pacific regions of Mexico concentrate the highest richness in *Bursera* species. Guerrero registers 48 species while Michoacán and Oaxaca 37. Although it is evident that each species presents different affinities and ecological tolerances, most of Mexican varieties grow in the good drained soil of slopes and mountains, in heights going from the sea level to 1800 m, where a long dryness season of 5 to 8 months is present, with no frost (Gregorio-Martinez, 2005). In the pacific slopes of Mexico where the maximum degree of variability of this genus is present, the ecosystem is classified as tropical non-evergreen forest, with an annual average temperature of 20-29 °C and a precipitation of 600-1200 mm. This landscape is founded continuously from the south of Sonora and Chihuahua regions to Chiapas and Central America (Campos-Osorno, 2006).

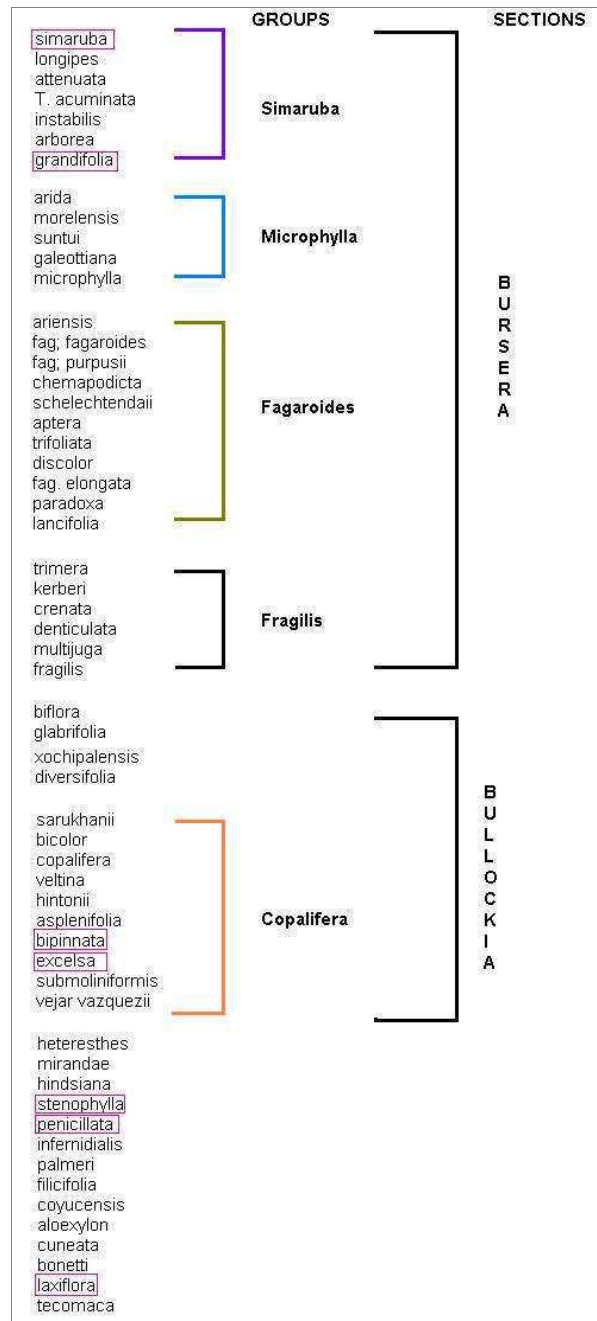


Fig 3 Phylogeny of Mexican *Bursera* based on ribosomal D.N.A. (Becerra and Venable, 1999)

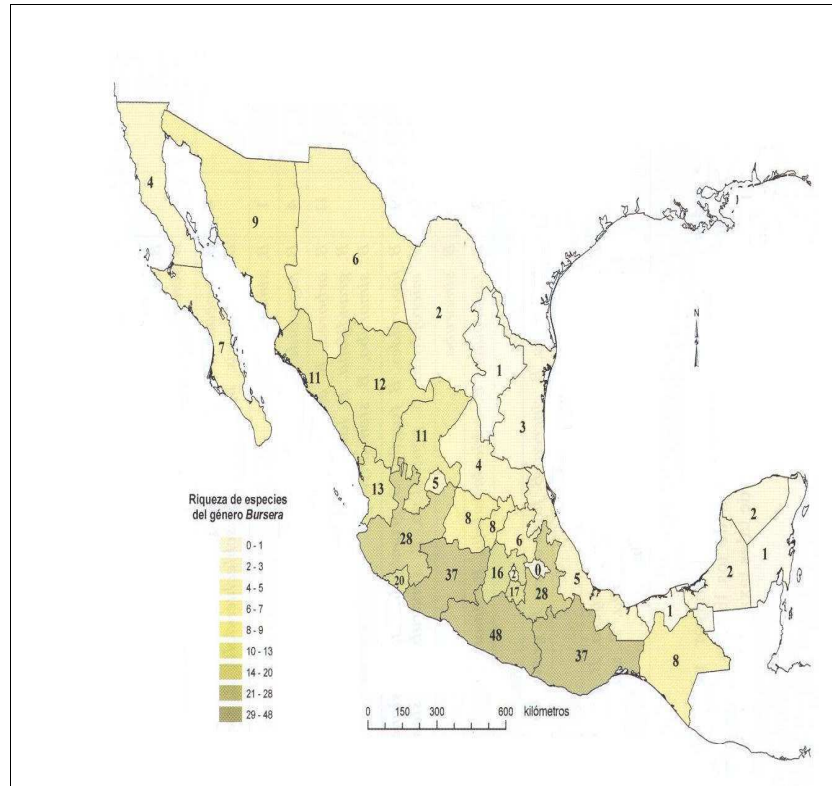


Fig 4 Map of Mexico, with the number of *Bursera* species by region (Rzedowski *et al*, 2005)

### 1.3 Historical context

#### 1.3.1 The Maya civilization

Yucatan peninsula climate is characterized by recurring hurricanes, savannas pound to flooding, a cave system that drain rainwater, a lack of surface groundwater, and a 6 to 7 months of dry season (Faust, 2001).

Maya culture is one of the most important and sophisticated ancient cultures, from the Mesoamerican cultural area of pre-Columbian time (Vandenabeele *et al*, 2005). The first settlements of Maya civilization date, from 3500 B.C., in the Yucatan peninsula and, continued until 200 A.D. in a phase known as the Preclassic period. Considering Yucatán environment, water provision was a major concern to the Maya and that is why during the Preclassic phase cities as Edzná and Tikal were constructed with extensive systems for collecting water, using reservoirs and underground tanks. While other cities as Ek Balám, Mayapán and Loltún constructed basins and ditching channels for the management of water (Andrews *et al*, 1960). In the next map (figure 5) the southern classical sites are showed and the northern post classical sites, including Chichén Itzá.



Fig 5 Map with most important Mayan cities (Gallareta, 2007)

### 1.3.2 Chichén Itzá city

Chichén Itzá extends near 15 km<sup>2</sup> and their constructions correspond to several styles related to the different stages of their evolution. The architectonic style that predominated in the first constructions was the Puuc, which is the style of southern and more ancient cities, like Uxmal and Sayil. Examples of this style in Chichén Itzá are the buildings of the Nuns, the Annex, the Church, the House of the Deer, the Akabdzib, among others.

Then the assimilation of the culture of other areas of Mesoamerica, especially of the Gulf and the Plateau, induced Chichén Itzá to develop a new style in decoration, planning and iconography. This style has been denominated Mayan-tolteca of Chichén Itzá. Examples of this style are constructions as the Castle, the Thousand Columns, the Game of Ball, the Tzomplantli and the Temple of the Soldiers. This city was an important center of the Mayan culture between the years 900 and 1200 A.D. The most formidable constructions are conserved date from this period (Cano, 2002).

But undoubtedly the most remarkable building of all the city is the Kukulcán pyramid (Mayan equivalent of Quetzalcóatl God), also known as “the Castle”. In this building twice a year: in the spring equinox and in autumn solstice a game of shades on the building simulates a serpent that descends until loosing itself in the Earth.

The Castle as other important pyramids in Mesoamerica (like the Templo Mayor) hides an older pyramid inside itself. In its interior there are a Chac Mool (God associated to the rain cult) and a throne of jaguar painted in red with incrustations of jade simulating their skin. This building has been interpreted like the material expression of a calendar. In fact if the number of steps of the four sides and those of the entrance of the temple are added, they sum 365, the same number than the days of the year.

### 1.3.3 Importance of “Sacred Cenote” at Chichén Itzá and their offerings

*Cenotes* are natural sinkholes in the limestone of rock that forms the geological base of the peninsula. Among Maya, *cenotes* were considered as sacred places, and offerings were common. Chichén Itzá is a Classic site, established on the Northern lowlands of Yucatán (figure 6), “In the border of the well of the Itzá” (Andrews, 1990), undoubtedly a reference to the sacrifice *cenote*. The city had a height towards years 600 and 900 B.C. soon to be lefted and to be refunded by the “itzáes” in 500 A.D. It was the Mayan priest Lakin Chan, known also as Itzamná that brought new blossoming to this large city. From that moment, their inhabitants named themselves chanes or itzáes.



Fig 6 Map of Chichén Itzá City (Cobos, 1997)

The Chichén Itzá complex counts with two cenotes: the “Xtoloc” in the west side, and the Sacred or Sacrificial on the east side.

Since the first explorations of Chichén Itzá, copal was recovered from sacred Cenote. It is no surprising as it was a worship place, where not only Chichén Itza inhabitants celebrated important ceremonies, but also a peregrination site where Mayas from distant places deposited offerings as well (Morley, 1972).

Between 1904 and 1911, Edward H. Thompson explored and, drained Sacred Cenote, finding over 100 gold objects, bones, ceramic vessels, shells, a scepter with anthropomorphic form, 250 objects of jade, pectorals, lances of flint, textiles of cotton, pumpkins but according to their notes “the most abundant material is some pom-incense pellets, often found into the bottom of blue painted vessels, where copal was “molded or poured before being deposited into the Cenote” (Coggings and Ladd, 1992).

Maya preparation of copal, was quite complex, the copal was worked until it became malleable, copal soot mixed with “Maya blue”, was applied to the surface of ceramic pieces. In other occasions, different tree exudates were applied to the surface of the object to offer, like *chicle* (from *Manilkara zapota*) or rubber (from *Castilla elastica*). The pattern of the copal varied with round, rolled pellets, bars in a conglomerate and cones.

In the archaeobotanical collection of the INAH (National Institute of Anthropology and History of Mexico) over 200 pieces of copal extracted from the Sacred Cenote of Chichén Itza are preserved. Among these pieces there is one ball molded with *ulli* (rubber) incrustations, another ball with corn grained applications on its surface, and a human face (Montufar, 2007).

#### **1.4 The Aztec civilization**

The Mexicas or Aztecs were an ethnic group with nahua filiation, that after a long peregrination founded México-Tenochtitlan, a city that between the XV<sup>th</sup> and XVI<sup>th</sup> centuries became the center of one of the biggest empires of all the times in Mesoamerica. Aztecs developed rich and complex religious, political, cosmologic, astronomic, philosophic and artistic traditions. In a good amount Aztecs were the heirs of the cultures of many other ancient Mesoamerican civilizations as the Olmecs, the Teotihuacans and the Toltecs.



### **1.4.1 The foundation of Mexico Tenochtitlán**

When Aztecs arrived to Mexico Valley the Tecpanecs from Azcapotzalco dominated the region, after a short period they established in Chapultepec where they were expelled. Then they settled in Tizapan a territory dominated by Culhuacan, they abandoned this settlement because of the hostile environment.

Finally they took the risk of resettle in a territory under the Tecpanecs control. A little island at Occident of Texcoco lake, in the year 1325 A.D. (year 2 Calli on Aztec calendar). This settlement implicated the subordination to Atzcapotzalco and the payment of tributes. This situation continued until the year 1428 A.D., when Aztec organized, along with Texcoco and Tlacolpan the “triple alliance”, which finally defeated Azcapotzalco.

### **1.4.2 The rise of Aztec empire**

The importance of this alliance relies on the fact that in barely 100 years, it conquered a big territory: from Atlantic to Pacific Oceans of current territory of Mexico. After a couple of years Aztecs took control over their allies, dominating them thus giving rise to the Aztec empire (Obregon-Rodriguez, 2001).

This empire, as many other empires in history, excerpted an effective political, economic and ideological control over the dominated territory, Aztecs got a big city, as capital of the empire: Mexico-Tenochtitlan, where the proclamations of imperial ideology where marked and reflected in the architecture of the buildings (Smith, 2001). At the heart of this imperial ideology we find the “Templo Mayor”.

### **1.4.3 The importance of “Templo Mayor” site**

The “Templo Mayor” was built at the geographical center of the city it was a precinct surrounded by a staggered platform, where the main buildings of the city where located. It was the tributary center of the empire. Merchandises from a vast territory either sold in markets, or paid as tribute (Carrasco, 1999) were put together in offerings and funerary deposits.

At this temple took place all ritual celebrations: from the regular ones, marked in pre Columbian calendar to the most extraordinary ones corresponding to the enthronization and funerary ceremonies for the emperor (Lopez-Luján, 2010). In each of these events offerings were buried (Matos-Moctezuma, 2011).

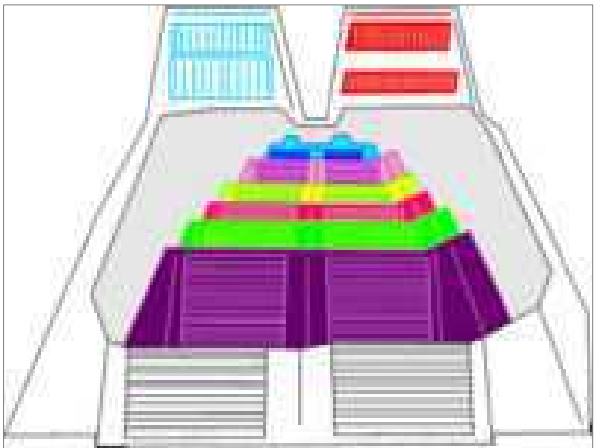
#### 1.4.4 The building stages in Templo Mayor construction

Although the position of Templo Mayor was known long time ago, it was believed to had been totally destroyed. Since at the moment of the defeat of the Aztecs, all the buildings of the city were destroyed and its materials employed in the construction of European style constructions. It was until 1978 that some excavations of the electricity company found the Coyolxhauqui (Moon Goddess) sculpture. This sculpture is important as documentary sources established its location at the foot of the stairs of Huitzilopoztli altar (Lopez Austin, 2001).

From this moment a program of excavation, conservation and preservation was designed (Renfrew, 1998). This archeological work, has shown that the construction of this ceremonial center was divided in 7 stages, corresponding more or less with each emperor reign, meaning that each ruler addressed a campaign of enlargement of the temple, that consisted in the construction of a superimposed pyramid onto the previous one, preserving the east-west orientation of the building (figure 7)

By the time the Spanish arrived to Tenochtitlan, Templo Mayor reached 60 m height (Matos-Moctezuma, 1987). It was a double Temple, the northern part was dedicated to Tlaloc (God of the rain), while the southern part was dedicated to Huitzilopochtli (God of War).

The Templo Mayor precinct measured 500 m on each side, having a total surface of 250 thousand square meters.



**Fig 7 The seven stages of “Templo Mayor” a) Aveni, 1988 b) Picture from the National Museum of Anthropology and History, Mexico City**

The first stage was probably made of wood, and to our days it is impossible to know if in the inside the remains of the pyramid there are still some remains of the first stage.

The second stage was constructed before 1428 A.D. and is visible now on, Mexico city downtown. There are some paintings preserved on the Tlaloc adulatory as well as a Chac-Mool. In the last staircase just before a sacrificial stone there is a glyph that identifies this stage with a date that in our calendar would correspond to 1390 A.D. This is the earliest fully exposed structure, so its orientation, dimensions and structural characteristics have been measured and described (Aveni, 1988).

The third stage dates from 1431 A.D. (year 4 cane in pre Columbian calendar) that corresponds to Itzcoatl reign. From this period only some stairs and part of the paved are preserved.

The fourth stage present two constructive periods: the first one (dating from around 1454 A.D.) corresponds to Moctezuma I government. From this period, were recovered a good number of ornamental elements such as braziers dedicated to the regent gods of the temple, and the Coyolxauqui sculpture.

The second constructive period corresponds maybe to the Axayacatl reign, where a platform ornamented with undulating serpents, was added to the front of the pyramid.

From the fifth constructive stage, remain few elements: a stuccoed platform and, part of the ceremonial floor dated from 1470 A.D.

From the sixth stage survived a fragment of the main facade with a wall that shows as ornamentation a sculpture of the head of three serpents. This stage dates from 1500 A.D.

Finally from the seventh 7 stage, which is dated between 1500 and 1521 A.D., remain the floor and the stairs that gave access to the Templo Mayor.

After and during the Spanish conquest of Mexico, all the buildings of the city were partially or totally destroyed, their remains as it was said before, were used as quarry for the edification of European buildings, and their foundations some times were re-used for these new constructions.

## **1.5 Uses and properties**

### **1.5.1 Copal uses in ancient Mexico**

As it has been said before on section 1.1 of this work, the first Spanish in American continent retained the term mexican term “copal” as well as the term “*incienso de indias*” (incense from

India) to refer to the natural resins, produced by New World trees, that were burnt in religious ceremonies, probably because of the parallel use in Europe of *Boswellia* resins.

Mesoamerican cultures considered copal as a protector. It was called “iztacteteo” or “White gods”; this material was believed to have magic and religious powers. After the Spanish chronicles from Bernal Díaz del Castillo, Bernardino Sahagún and Diego Landa, ancient Mexicans use copal quite often, at least twice a day, one in the morning and one in the afternoon. It was used as an offering to the gods, to “clean” the holy places, during funerals, in offerings to ask for rains, etc. There was no important ceremony that took place without it. The representation of copal can often be found in codex where priest are offering it to the gods, or are keeping it in a special bag (figure 8).

In addition copal was used as a binder mixed with pigments, for the decoration of murals. In goldsmith, copal was used as the wax is used in our days, in the “lost wax” technique. It was part of the formulations that were used as adhesives for masks, small rocks, and even in dentistry (figure 9) where it was used in dental incrustations in teeth cavities and for dental restorations as well (Bucio *et al* 2006).



**Fig 8. Primitive representation of Quetzalcoatl holding a copal bag on his hand**

According to Orta Amaro, 2007, there are evidences that Mesoamerican cultures, from X<sup>th</sup> to VI<sup>th</sup> centuries A.D. used both copal and calcium phosphate-based cement to fix precious stones to perform dental incrustations, some reports in the literature indicate that pyrite, hematite, jadeite and turquoise were typically used for this purpose. The technique probably consisted in creating a cavity on the tooth surface (of frontal teeth) by means of a drill like tool and perhaps also using

powdered quartz with water as an abrasive. The stone was then fixed to obtain the incrustation in the dental tissue (Orta Amaro, 2007).



Scale 1 cm picture: 2cm

1 cm picture: 10cm

1 cm picture: 1cm

1 cm picture: 12cm

**Fig 9 Archaeological Aztec pieces where copal is believed to be used as adhesive**

About rituals in pre-Columbian time the priest Sahagún wrote “women used [copal] as make up, on their faces and as corporal paint for their foot”. They painted themselves with red, yellow and dark preparations that were obtained mixing the resin with colorants; these mixtures were sometimes heated to obtain different gradation in colors (Anaya, 1998).

In traditional medicine copal has been reported to be used in catapasm, for the treatment of skin infections (Campos-Osorno, 2006).

Miguel Venegas, a jesuit misioner, from XVIII<sup>th</sup> century, wrote in his book “Natural and civil history of California” that in San Bernabé bay, California, “the abundance of copal and incense trees allows to use their resin mixed with grease for waterproofing wooden ships, instead of pitch” (Venegas, 1757).

In the other hand, the gum produced by *B. simaruba* has been established to enter in the composition of the mural paintings binders from the Maya site of Bonampak (Magaloni, 1996).

### **1.5.2 Contemporary uses and applications of copal**

Currently, the ancient curative and adivinatory ritual uses of copal are maintained in some Mexican villages (Viveros, 2007). Copal can be easily found in several seasonal and permanent markets that will be furthered described in the second part of this chapter.

In traditional contemporary markets, copal is sold and recommended in infusion, as a cure for bronchitis. As a catapasm, it is used to relief rheumatic pain. For the treatment of skin infections

and ulcers, traditional medicine recommends to heat copal until melting and to apply it, directly into the skin (Caralampio, 2000).

A few years ago, before the industrialization, along with *Manilkara zapota* resin, copal was used as chewing gum, that prevented cavities, and other dental affections, due to its chemical composition.

In the first days of November the “day of the dead” is still celebrated everywhere through the center and southern regions of actual Mexican territory. These celebrations include the elaboration of altars for the dead ancestors, that always include copal. In a notable synthesis, where Christian and Native American rites are mixed (Purata, 2008).

In the industry it is known to be part of the formulation of paintings, adhesives, artificial fireworks, soap, inks, varnishes and cosmetics creams (Montufar, 2007).

The essential oils are used widely like additives in food, fragrances, aromatherapy and traditional and alternative medicine. Synthetic and natural terpenoids have expanded the variety of used aromas.

In the patrimony field a binder made on copal has been used by outstanding painters such as Gerardo Murillo (1875-1964), Diego Rivera (1886-1957), and David Alfaro Siqueiros (1896-1974). Rivera specifically used this type of resin in the mural «La creación». In this case he used a mixture of Mexican copal, elemi resin and wax (López, 2002).

## **1.6 Previous works on chemical composition of Mexican copals**

To our knowledge, there are few scientific studies that deal with chemical composition of Mexican “copal”. It is worthy to mention here, the works from De la Cruz-Cañizares in 2005 and Hernandez-Vazquez in 2010, which analyzed commercial samples of resin from Mexico. As well as the work of Stacey and Cartwright 2006, who performed studies in objects from the British Museum collection and the study of a mosaic disc from Magar and Menar in 1995.

Nevertheless, up to now none of these studies had studied resins from certified botanic origin. The importance of the present work relies on the fact that our team, in collaboration with specialists in botanic from the Autonomous University of Sinaloa as well as the National University of Mexico, collected in situ the resins from certified botanical trees.

The important disadvantage of using commercial samples is that in many cases, as our colleague Irma Belio referred (personal communication) “the artisans collect resins, using the same

recipient for two or more trees”. It is also noteworthy to say that in some regions, like in the Mexican community of Teotlalco in Puebla up to six species of *Bursera* (*B. bipinnata*, *B. jorullensis*, *B. odorata*, *B. copallifera*, *B. bicolor*, *B. glabrifolia*) can coexist (Garcia-Hernandez, 2000).

### 1.7 Oleo-gum-resin: definitions

Tree exudates are chemically complex mixtures of fluid terpenoids, with a variable ratio of volatile and non volatile components depending on their botanical origin. Triterpenoids are the primary constituents of resins in Burseraceae that produce a balsamic type terpenoid resin, while diterpenoids are the primary components in non volatile fraction from Conifers and most Angiosperms. Finally the gum fraction is composed by polysaccharides.

### 1.8 Gums

Chemically gums are formed by complex chains of hydrophilic polysaccharides (complex sugars) derived from simple sugars such as galactose, arabinose, rhamnose. In 1993 Whistler described in detail, the complex structure of gum exudates (Langenheim, 2003). The Burseraceae family also yields several resins, which may contain gum in some extent (De la Cruz-Cañizares, 2005).

### 1.9 Gum composition of *Bursera simaruba*

Among the gums produced by Mexican *Bursera* species, only the gum of *B. simaruba* has been studied (Magaloni, 1996). Using an hydrolysis treatment before a GC-MS analysis, she found its monosaccharide composition (Table 1).

	Peak relative intensity
Arabinose	38
Ramnose	4
Galactose	100
Glucose	3

Table 1 Monosaccharide composition of *B. Simaruba* (Magaloni, 1996)

### 1.10 Fats

Fats are chemically constituted by fatty acids. In the synthesis of fatty acids from carbohydrates, that is followed by the enzymatic combination of the carbohydrates with glycerol some esters may be formed. Plant fats differ from oils in having more or less solid fatty acid constituents, at normal temperature. Fatty acids occur in some Conifer resins (Langenheim, 2005). A study conducted by Van Gemert and Armitage in 2007 identified by means of GC-MS the next fatty acids in commercial copals: capric, decanoic, palmitic, tetradecanoic, caproic, propanoic and nonanoic acids. Nevertheless because of the uncertainty on botanical origin it is not possible to know if these acids were present originally in the resin or are due to pollution of the samples.

### 1.11 Terpenic resins

Resins are chemically constituted by terpens. They are a diverse family of compounds present in all living organism but they attain their greatest structural and functional diversity in plants, (Langenheim, 2003) particularly Conifers, and *Buseraceae*. The name terpen is derived from the word turpentin (turpentine spirit). When the terpens are chemically modified by oxidation, the resulting compounds are referred generally as “terpenoids”, some authors use invariably both terms.

This family includes the monoterpenes, sesquiterpenes, diterpenes, steroids, carotenes, polyprenoids such as ubiquinone side chain, and the polymer rubber. Although, their variability they are all synthesized by two pathways that will be further discussed.

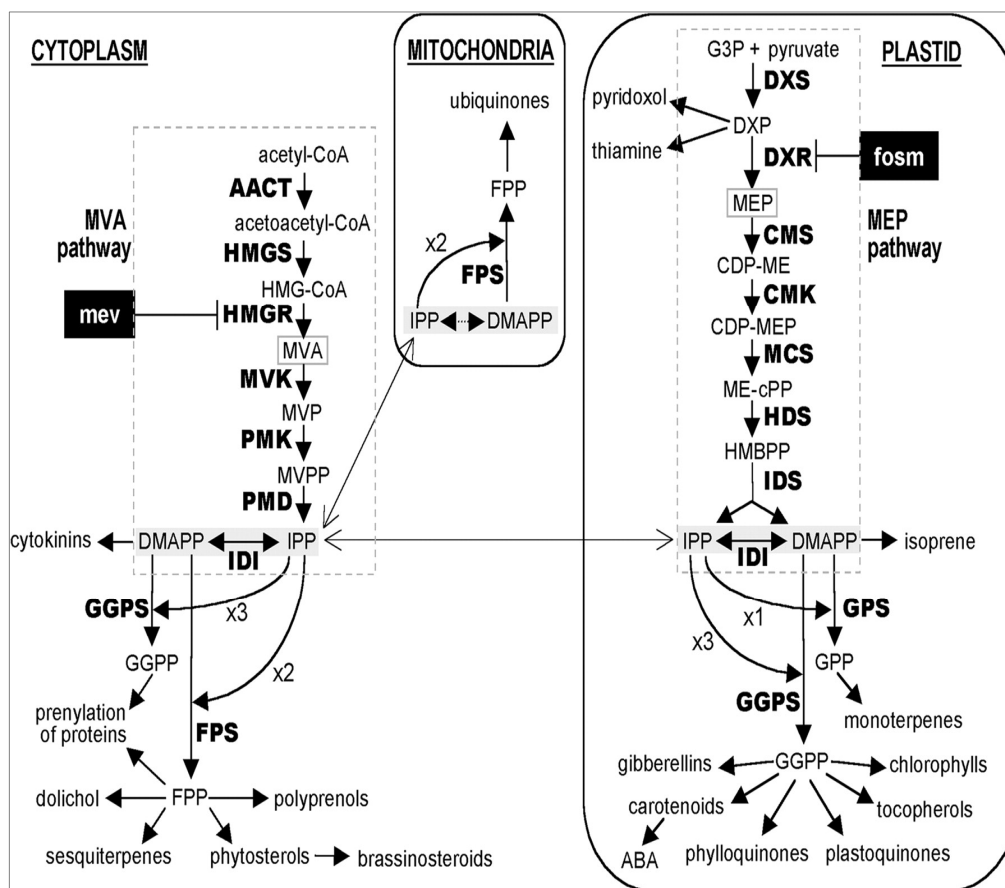
### 1.12 Bio synthesis of terpenic precursors

The basic biological isoprenoid unit is isopentenyl diphosphate (IPP). For many years it was assumed that the early stages of the terpenoid biosynthetic pathway were the same for all types of terpenoids. This is now known to be untrue. In plants, IPP can be synthesized in either the cytosol or in the stroma of plastids, using different precursors at each site. The cytosolic pathway utilizes acetate and is named the mevalonate (MVA) pathway after the important intermediate, mevalonic acid. This is the only pathway that operates for terpenoid biosynthesis in fungi and animals.

The plastidic pathway in the green parts of plants and in algae uses glyceraldehyde 3-phosphate and pyruvate, and again the pathway is named for an important intermediate, methyl erythritol phosphate (MEP) (Kashara *et al*, 2002). A synthetic overview of the two pathways is shown on



figure 10, for a detailed account on MVA pathway refer to Eisenreich *et al*, 2001 and on MEP to Kashara *et al*, 2002

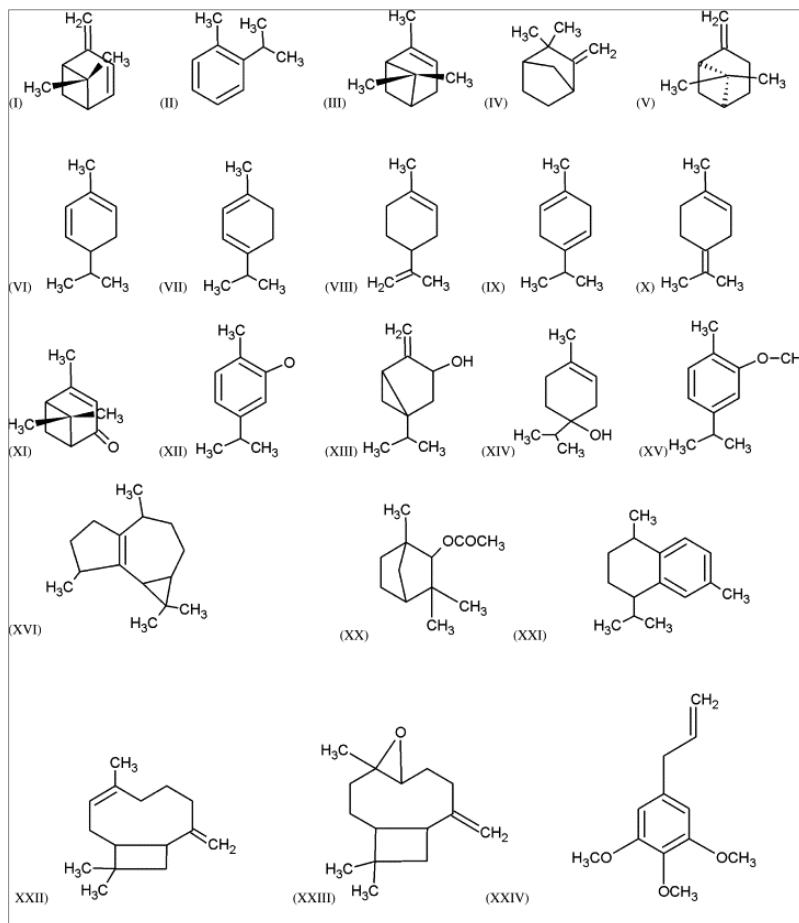


**Fig 10** MVA pathway left (Eisenreich *et al*, 2004) and MEP pathway (Kashara *et al*, 2002) for terpenoids biosynthesis.

### 1.13 The essential oils

Some components of resins are referred as “essential oils” (Mills and White, 1977). In the case of Burseraceae resins, these oils are chemically mainly mono and sesquiterpens. The concentration of monoterpens in natural fresh resins always dominates over that of sesquiterpens and triterpenes. Monoterpens and sesquiterpens play a major defense role against insects and pathogens (Langenheim, 2003).

The structure of the mono and sesquiterpens found by De la Cruz Cañizares, from commercial samples of Mexican copal are shown on figure 11. Similar studies with commercial copal samples lead to equivalent results (Van Gemert, 2007).



**Fig 11** Structure of typical occurring monoterpens (from I to XV) and sesquiterpens (XVI to XXIV) in resins from Burseraceae family.

**I** verbene, **II** *o*-cimene, **III**  $\alpha$ -pinene, **IV** camphene, **V**  $\beta$ -pinene, **VI**  $\alpha$ -phellandrene, **VII**  $\alpha$ -terpinene, **VIII** limonene, **IX**  $\gamma$ -terpinene, **X**  $\alpha$ -terpinolene, **XI** verbenone, **XII** carvacrol, **XIII** sabinol, **XIV** 4-terpineol, **XV** carvacrol methyl ether, **XVI** isoldene, **XX** fenchyl acetate, **XXI** *cis*-calamenene, **XXII** *trans*-caryophyllene, **XXIII** caryophyllene oxide, **XVIV** elemicin: a compound appearing in the monoterpenoid and sesquiterpenoid intervals (De la Cruz Canizares, 2005).

In the other hand the study conducted by Van Gemert in 2007 found the next mono and sesquiterpenoids: cadinene,  $\gamma$  muurolene,  $\gamma$  mururolol, spathulenol,  $\alpha$ -cubebene,  $\alpha$ -caracolene and

ledol. As well as the macroditerpenoids: verticiol and thunbengene. Again caution is need when interpreting this results because of the uncertainty on the origin of this samples.

### 1.13.1 Triterpenes

Concerning the “heavy” fraction of *Burserseraceae* resins, triterpenes with tetra or pentacyclic skeletons characterize them (figure 12).

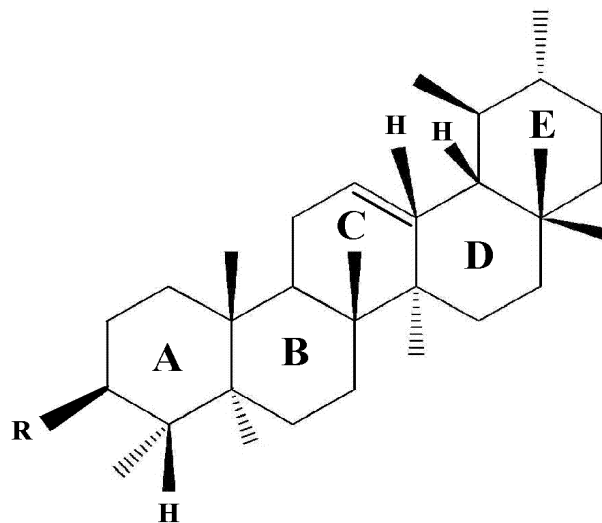


Fig 12 Triterpenic skeleton of ursane type

Resins from tropical *Bursera* family have been reported to contain resins constituted by lupane, ursane and oleanane like compounds (Khalid, 1985) (figure 13).

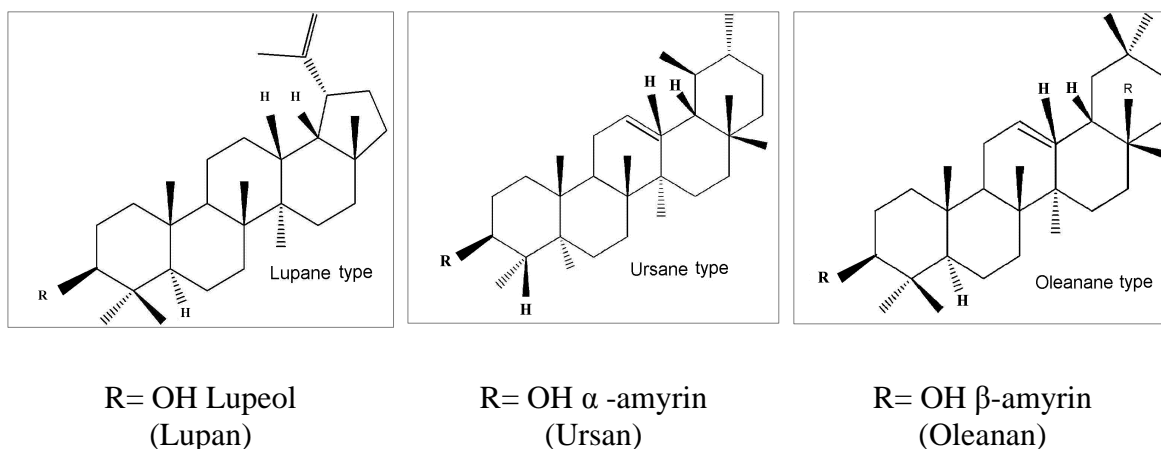


Fig 13 Examples of skeletal types of triterpenes found in *Bursera* resin

### 1.13.2 The ursans

Ursan family has a triterpenic pentacyclic skeleton. All the rings count six carbons. In resins from Mexican trees ursan compounds have been identified (figure 14).

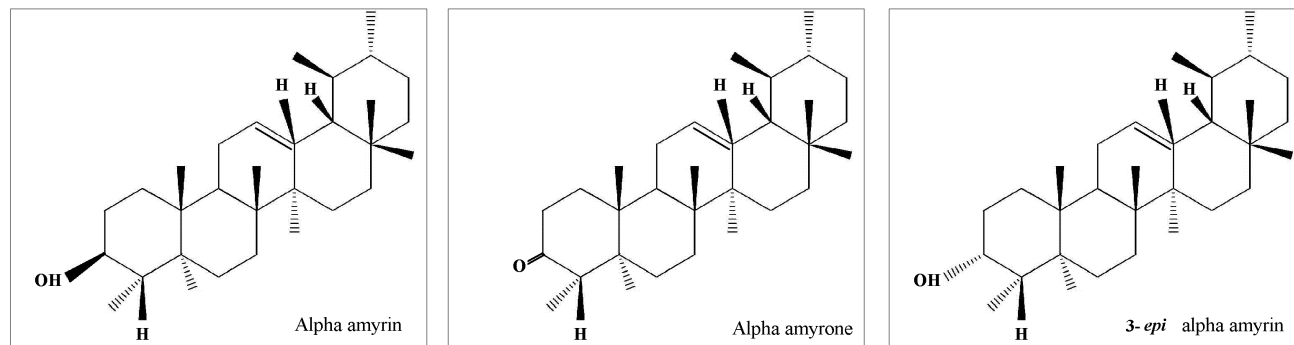


Fig 14  $\alpha$ -amyirin,  $\alpha$ -amyrone and 3-*epi*- $\alpha$ -amyirin

### 1.13.3 The oleanans

Oleanan family differs from ursan family by its methylated 29 position in the ring E. Three molecules of this family have been described as entering in the composition of Mexican copal (figure 15).

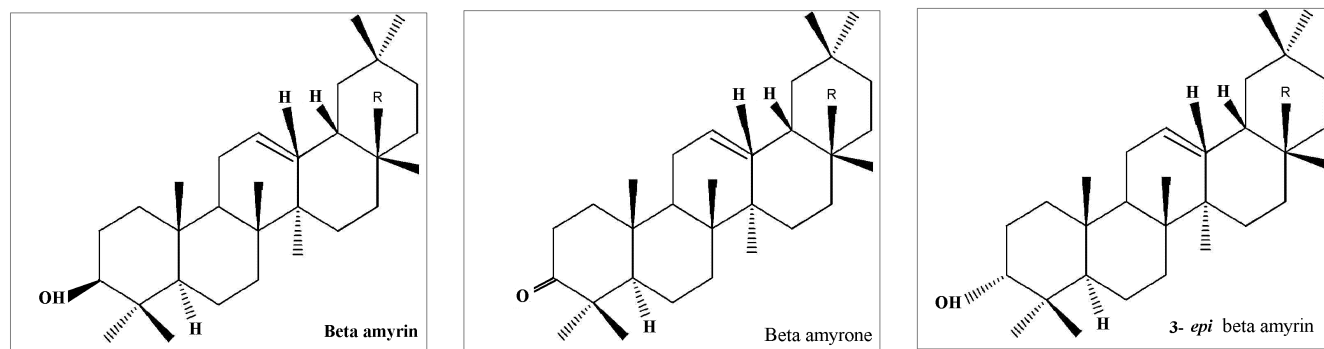


Fig 15  $\beta$ -amyirin,  $\beta$ -amyrone and 3-*epi*- $\beta$ -amyirin

Although  $\alpha$ - and  $\beta$ -amyirins occur in other plants, they are only known to be components of Burseraceae resins including elemi, myrrh and olibanum (Langenheim, 2003) and copal (De la Cruz-Cañizares, 2005)

### 1.13.4 The lupans

Lupans have a triterpenic skeleton, in with a five ringed cycle E. Various authors had described the presence of three lupan type triterpenoids either in commercial (Hernandez, 2010; De la Cruz-Cañizares, 2005) or archeological mexican resins (Stacey, 2006). Their structures are shown below, figure 16.

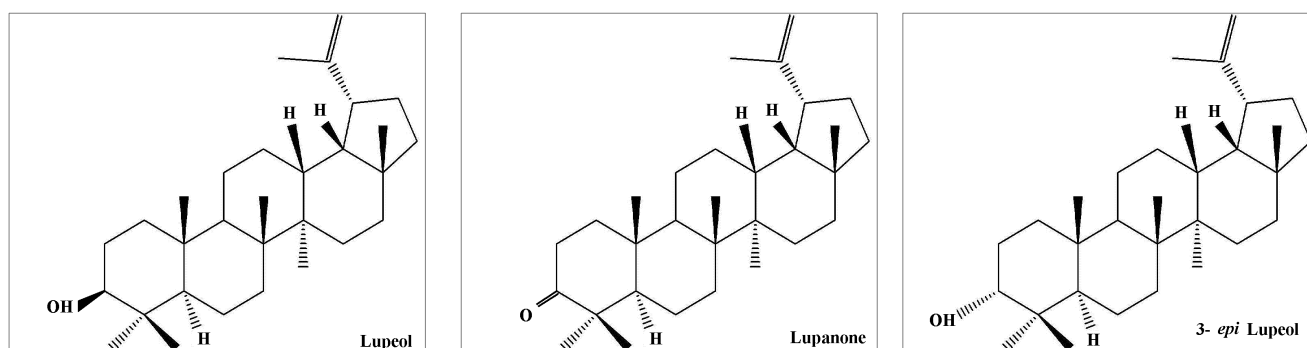


Fig 16 Lupan compounds founded in commercial or archeological resins, described by several authors

In the other hand, Peraza-Sanchez described four lupans from the resin of *B. simaruba* collected in the region of Yucatan (figure17).

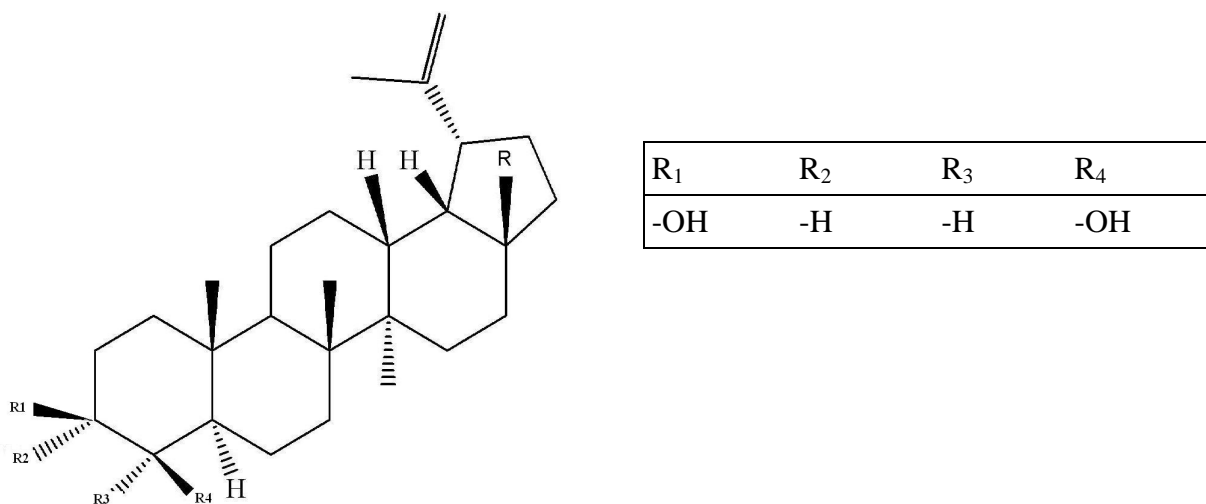


Fig 17 Structure of lup-20(29)-en-3β-23-diol from *B. simaruba* resin ( Peraza Sanchez, 1995)

### 1.13.5 Biological activity

Pentacyclic triterpenes are ubiquitously distributed throughout the plant kingdom, and copal is one of its sources. They exist in a free form as aglycones or in combined forms, and have long been known to have a number of biological effects (Ikeda, 2008). The compounds:  $\alpha$ -amyrin,  $\beta$ -amyrin and lupeol, found in copal resins, have many bio-active properties.

Lupeol, a phytosterol and triterpene, is widely found in edible fruits, and vegetables. Extensive research over the last three decades suggest that lupeol has potential as an anti-inflammatory, anti-microbial, anti-protozoal, antiproliferative, anti-invasive, anti-angiogenic and cholesterol lowering agent (Rahman *et al*, 2011). Other properties of lupeol include a positive effect over conditions such as arthritis, diabetes, cardiovascular ailments, renal disorder, hepatic toxicity, microbial infections and cancer (Al-Rehaily *et al*, 2001; Fernández *et al*, 2003; Rahman *et al*, 2011). The available literature suggests that lupeol is a non-toxic agent and does not cause any systemic toxicity in animals at doses ranging from 30 to 2000 mg/kg (Al-Rehaily *et al*, 2001; Rahman, *et al*, 2011; Dzubak *et al*, 2006).

Ursolic and oleanolic acids have been investigated for their hepatoprotective effects. The mechanism of effect is complex. It includes suppression of enzymes that play a role in liver damage such as cytochrome P450, cytochrome b5, CYP1A and CYP2A, and an increase in antioxidant substances such as glutathione, metalothionein, zinc, glutathione-S-transferase and glucuronosyltransferase, with simultaneous protective effects on liver mitochondria.

Concerning anticancerous effects the first study, centered on oleanolic acid, was published by Hunan as early as 1995 when Pesha *et al* reported cytotoxicity of betulin acid onto human melanoma cell lines. To our days the spectrum of cytotoxicity has enlarged to large lung cell cancer, epidermic carcinoma, melanoma and small cell lung cancer (Dzubak *et al*, 2006). Its efficiency against cell line proliferation has been probed (Jing, 1999; Wang, 2006).

Betulinic acid has inhibitory action against HIV replication in H9 lymphocytes with an  $EC_{50}$  = 1.4  $\mu$ M and a therapeutic index (TI) = 9.3 (Yu, 2007). Synthetic derivatives of these molecules are under study for the treatment of these diseases.

These compounds had the advantage of being lipophilic, which allows them to cross the blood-brain barrier. In the ursolic family, ursolic acid for instance has the potential of an antiproliferative agent, because of its inhibitory activity against DNA polymerases  $\alpha$  and  $\beta$ . It also has radioprotective effects in hematopoietic tissue (Dzubak, 2006).

Concerning the oleanane families and their derivatives, it is widely accepted that boswellic acid have an effective anti inflammatory and ant arthritic effects, that have been profited in Indian Ayurvedic medicine.

On the other hand,  $\alpha$ - and  $\beta$ -amyrin acetates, ursolic and 23-hydroxyursolic acids have analgesic properties ( $PD_{50} = 18.6\text{--}50 \text{ mg kg}^{-1}$ ), which are comparable and in one case, even outclass the activity of acetylsalicylic acid (Dzubak, 2006).

All the chemical, botanical, taxonomical, physical data that had been described until now in this work, were studied and used as a departure point for the collection of the samples, that will be present in the next chapter and that constitute the core of our research.

# Chapter II

## Presentation of the copal samples and the analytical strategy



## Chapter II

### Presentation of the copal samples and the analytical strategy

#### 2.1 Extraction of copal

Studying the process of collection of copal in Mexico, implicates the study of a millenary technique (Cruz-León, 2006). The survival of this practice is related with cultural motivations, as copal is intimately linked with ritual pre-Columbian practices that did not disappear upon the contact with European culture.

To this respect one can cite the Mendoza codex also known as “*Matrícula de tributos*”. This document was elaborated immediately after Spanish conquest, and details the Aztec empire’s administration, with the name of the over 30 provinces under Aztec domination and the taxes that should be paid. It contains information about the type of product, the amount and the frequency of tribute merchandise. Concerning copal this codex mentions “400 small baskets of white copal and 8000 small balls of refined copal” to be paid annually.

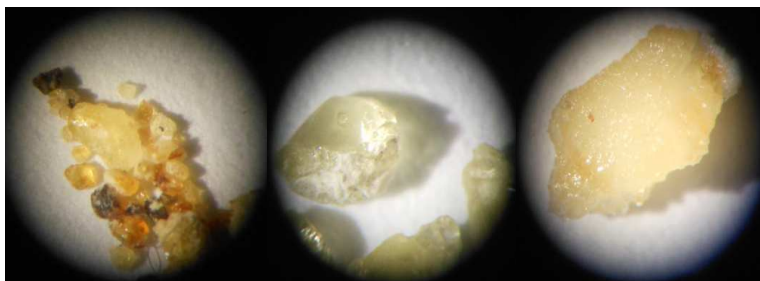
The actors of the collection of copal are known as “copaleros”, in our days there are few people dedicated to this activity. They work in the collection of copal in the season comprised between July and September from each year.

The knowledge on the techniques of extraction of copal, on the conservation of the trees and the selection of them constitute a heritage from a generation to another. Usually the “copalero” is assisted by a son or a grandchild from young age.

A study performed in the region of Morelos (Cruz-León, 2006) showed that each “copalero” may collect resin from up to 200 hundred trees in each season. During collection, the journey last eleven or twelve hours.

For the extraction of copal, some cuts are practiced perpendicularly to the tree trunk, in the phloem. Then the resin is collected in leaves of maguey (*Agave angustifolia*). The size of maguey leaves goes from 35 to 45 cm long and 3 to 8 cm width. This size is related to the bars of copal that can be bought at commercial markets.

In American context, «copals» are collected from *Bursera* or *Protium* species from the Burseraceae family (Becerra and Venable, 1995). The quality and color of the copal depends on the tree species from which is extracted (figure 18), when collected it is a translucent liquid that shortly after turns into yellow, white or amber solid (García-Hernández, 2000).



Scale                    1mm :80x                    3mm: 80x                    5mm: 80x

**Fig 18 Pictures of commercial copals with different colors from unknown botanical origin, taken at our laboratory**

The technique of harvesting copal also has an impact into the final commercial product. While white copal is the main product, exuded directly from the incisions practiced in the bark of the tree, “copal piedra” is the result of a defense reaction against the attack of an insect: *Chyptodes dejeani* (Montufar, 2007).

The “lágrima copal” (copal in tears) is the product remaining in the recipient of collection and the incision at the bark of the tree (Cruz-Leon, 2006).

The section of the bark that was cut upon the extraction of the resin and, that is fully impregnated with it, is also collected in Mexico. In the traditional markets it is sell as “Mirra” which has no relation to the actual myrrh (as it has been said previously on this work, it is produced by another tree species corresponding to *Commiphora myrrha*). In figure 19 are presented some pictures of the different kinds of copal, found in traditional markets from Mexico.



Scale 1 cm picture: 2cm    1cm picture: 15cm                    1cm picture: 20 cm                    1cm picture: 1cm

**Fig 19 Images from left to right: white copal, “piedra” copal at Cholula market, yellow “lágrima” copal at Izúcar market, and “mirra” at Azcapotzalco market.**

## 2.2 Resins from botanical certified origin

### 2.2.1 Botanical References

For our research we included 8 species, among the 80 different *Bursera* trees in Mexico. Here we present the botanical references for each species:

***B. bipinnata*** (DC.) Engl. (*B. elemifera* (Royle) Bail, *B. gracilis* Engl.). Description in Rzedowski and Calderón de Rzedowski (1996b); Rzedowski *et al.* (2004); all with illustrations. Engler (1931) also proposed and illustration.

***B. copallifera*** (DC.) Bullock. (*B. jorullensis* H.B.K., *B. palmeri* var. *glabrescens* S. Wats.) Description in Toledo Manzur (1982), Guizar-Nolazco and Sanchez-Velez (1991); the last work has illustrations as well.

***B. excelsa*** (H.B.K.) Engl. (*B. sphaerocarpa* Sprague & Riley). Plant description in Toledo Manzur (1982) and in Pennington and Sarukhan (1998); illustration in the last work and in McVaugh y Rzedowski (1965).

***B. grandifolia*** (Schltdl.) Engl. (*Elaphrium occidentale* Rose). Description in Toledo Manzur (1982), in Guizar-Nolazco and Sanchez-Velez (1991) and in Johnson (1992); the last two works also has illustrations.

***B. laxiflora*** S. Wats (*B. concinna* Sandw.) description in Johnson (1992).

***B. penicillata*** (DC.) Engl. (*B. inopinata* Bullock). Description in Bullock (1937, under the name of *B. inopinata*) and in Rzedowski and Guevara Fefer (1992). Illustration in McVaugh and Rzedowski (1965).

***B. simaruba*** (L.) Sarg. (*B. gummifera* L.) Description in Toledo Manzur (1982), Rzedowski and Guevara-Fefer (1992), Rzedowski and Calderón de Rzedowski (1996b) and Rzedowski *et al.* (2004); illustration on the last work.

***B. stenophylla*** Sprague & Riley. Description in Riley (1923) and Johnson (1992); the last work includes illustrations.

For the collection of the certified origin samples this research counted with the invaluable collaboration of experts in botanic (Dr. Rito Vega) and in biomaterials (Dr. Irma Belio) from the Autonomous University of Sinaloa (UAS), as well as with the cooperation of the academic body of Biomaterials from the UAS (UAS CA-208).

The collection proceeded from summer to fall, as in these times of the year trees have both leaves and fruits, which are necessary for botanical identification. After practicing a small cut into barks tree, resin was collected in glass tubes.

The criteria for the discrimination of the tree species was based on the bibliographical works mentioned at the beginning of the present section. A research work containing detailed information on this subject and a in-depth approximation to botanical aspects is under preparation of Dr. Rito Vega. As an example reference leaves showing the differences between leaves of *B. bipinnata* and *B. stenophylla* can be consulted in annex 1, table 37.

### 2.2.2 Choice of the studied species

Regarding the inclusion of each species in the study, our choice was oriented by several factors that will be discussed below.

We include *B. bipinnata* as its pollen has been founded by paleobotanist, in archaeological context in the site of Templo Mayor (Montufar, 2007). *B. bipinnata* is a species with a wide geographical presence and sometimes it produces hybrids with other members of the *Bullockia* section. As the botanical distinction between *B. stenophylla* and *B. bipinnata* is unclear, we decided to include this second specie as well (Rzedowski, 2005).

As it has been said on section 5.1.1 of chapter 1, Bonampak murals from the Maya Culture had been studied and researchers conclude that the gum of *B. simaruba* might have been used as agglutinant (Magaloni, 1996). So we include this specie to contribute to the knowledge of the chemical composition of this oleo-gum-resin.

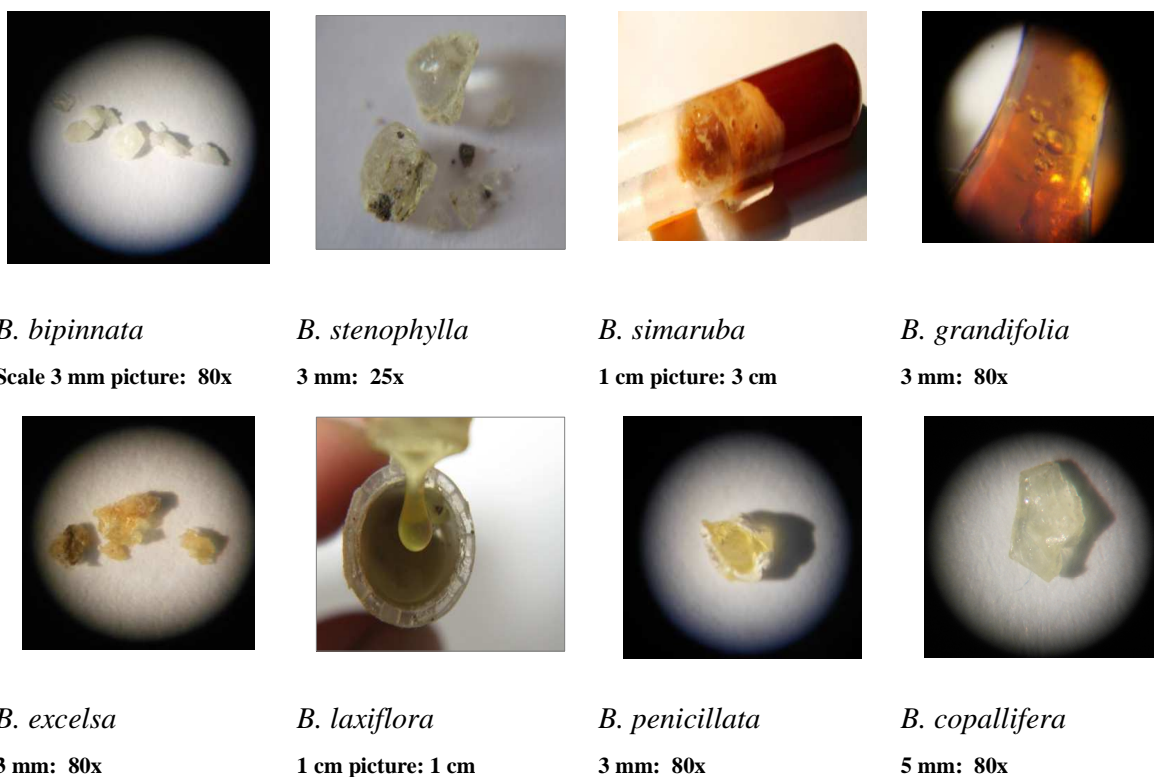
As *B. grandifolia* is a well defined *Bursera* tree and it is related to *B. simaruba*, we included it in the study to compare its chemical composition to the first one.

It is important to note that the genus *Bursera* has been divided into two subgenera or sections: *Bullockia* and *Bursera* (McVaugh and Rzedowski, 1965; Rzedowski, 1968; Becerra, 1997). *B. simaruba* and *B. grandifolia* belong to the section *Bursera* (subgenus *Bursera*), while the rest of the studied species belong to the section *Bullockia* (Rzedowski, 2005). See figure 3 chapter 1 of this work.

Colloquially *B. simaruba*, *B. grandifolia* and the other species from the subgenus *Bursera* are known as “cuajjotes” a *Nahuatl* word which means leprous tree and that refers to a botanic characteristic of this subgenus, as tree bark exfoliates (Becerra and Venable, 1999).

To have an idea on the variability of the chemical composition of *Bursera* resins from Mexico, other three species were chosen: *B. excelsa*, *B. laxiflora* and *B. penicillata* wich are not related to the other 4 species. Only one sample of resin from *B. copallifera* was collected, this sample was studied by all the analytical techniques described in the strategy for this

research and was included as external reference when statistical analysis tools were applied. In figure 20 we present a photo of a sample of resin from each of the studied species.



**Fig 20 Physical aspect of copals from certified botanical origin.**


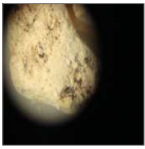
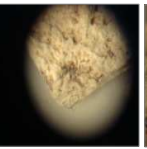


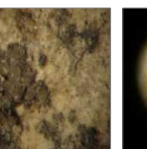
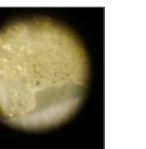
For orientation along this work, we included in annex 1 (tables 27, 28 and 29) data of certified resins concerning: the tree species, its GPS localization with a map and the date of collection.

For selected cases of commercial resins, pictures were also included.

### 2.3 Archaeological samples from Templo Mayor Site

In table five we present information corresponding to each studied archaeological sample from this site. It concerns the number of artifact from which sample was taken as well as the number of offering where artifact came from.

The nature of the samples was variable: sample 84 was taken from the adhesive material found in the base of a ceremonial knife, sample M1 was part of the molding material of a Aztec god figurine, sample 26 was part of a conglomerate of bars, probably offered liquid and contained in maguey leaves. The other samples come from amorphous artifacts.

ID	26	51	52	84	173	TMT	M1
Artifact number	A133	A 252	A260	A957	Unknown	Unknown	A5
Nature of the material	Spiritual offering, probably deposited in liquid state, preserved as part of a conglomerate	Amorphous material	Amorphous material	Adhesive from the base of a pectoral-ceremonial knife	Amorphous material	Amorphous material	Molding material from an Aztec figurine
Weight of sample (g)	0.25	0.04	0.02	0.39	0.32	1.5	2.3
Number of Offering	128	126	126	125	120	Unknown, Paleo botanical Collection of the INAH	140
Picture							
Scale	5 mm: 800x	5 mm: 80x	5mm: 80x	5mm: 25x	5mm: 25x	5mm: 25x	3 mm: 80x

**Table 2** Archaeological Aztec samples

**N.B.** The number appearing as ID for each archaeological sample, on table 2, will be retained all along the present work to refer and differentiate each Aztec resin sample.

In further sections of this chapter the offerings, the physical location and the physico-chemical conditions that surrounded these samples for over 500 years are described. After excavation the conservation treatments that they were subjected to, are described here as well. This information was taken from activities report of conservation and restoration of the collection of archaeological materials, 7<sup>th</sup> season (Alonso A. *et al*, 2008).

### 2.3.1 Description of the offerings from Templo Mayor

The offerings deposited in the Templo Mayor of Tenochtitlan are constituted by sets of objects carefully ordered. Some of them were placed in stone boxes underneath the buildings, whereas others were buried directly in the constructive filling material between constructive

stages of Templo Mayor (cf figure 7). Among the elements founded there are: sculptures representing deities (like the ones presented on figure 21), devices with symbolic connotations such as rings, scepters, pectoral, masks, lappets, flutes, whistles, drums, instruments of sacrifice, a wooden mask, etc. and flora and fauna elements.



Height: 35cm

Aproximative height: 35cm

**Fig 21** Picture of tree Aztec figurines made of copal, the first taken from Lehman, 1948 and the second and third from Lona-Naoli, 2004

The garments found in the offerings may be identified to the Aztec priesthood. Some offerings include vestiges of flora and animals. Between the identified fauna there are crocodiles, jaguars, pumas, lynxes, serpents, as well as a great diversity of birds, fish, shells and marine snails (Lopez-Lujan, 2009) and a wolf in the case of offering 120. A picture of one of the levels of these offerings is presented on figure 22.



Fig 22 Picture of an Aztec offering 120. (Alonso A. *et al*, 2008)

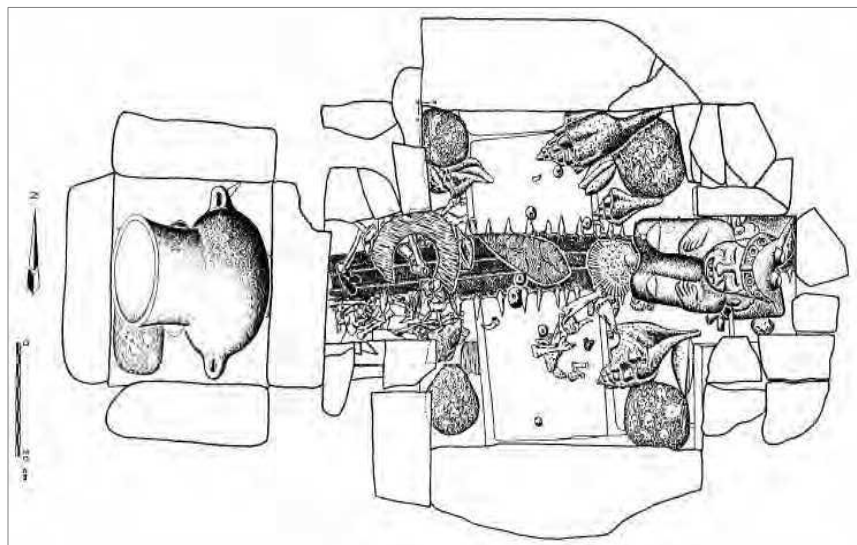
The variety and abundance of objects may be explained by the importance of the non verbal communication among the Aztecs: olfaction and vision, played a key role in their rituals of communication with the Gods, for instance only Tezcatlipoca could smell the scent of the flowers in an offering (Hayden, 1980).

Therefore these characteristics of the offerings opened a new line of investigation around Mexica's Cosmovision. One of most interesting, approaches lies in the relation between objects distribution and the meaning of the offerings. (Jimenez-Badillo, 2009). Previous investigations (López Lujan, 1993 and 1997; Lopez Austin, 2004; Contel 2008; Jimenez-Badillo, 2009) concluded that Mexica priest, that were in charge of the composition and deposition of the offerings, used a very sophisticated symbolic code to communicate with Mexica gods.

This code determined not only the location of each element of the offering, but also the categories of objects that had to be combined in order to express a specific concept. For instance, in some deposits, the image of the God of the fire was located next to other objects symbolically related to the “hot” portion of cosmos. At the same time, these sets were in symmetrical opposition to objects with “cold” connotation, the former ones related to God of rain and the fertility. An obvious interpretation of this code is that it expresses the concept of



balance arisen from the “complementary opposition” of cosmic energies, a ruling idea of the pre-Columbian religion. (Jimenez-Badillo, 2009).



**Fig 23 Offering “U” from Templo Mayor. It is notable the symmetrical disposition of the four copal balls in the corners and a ceremonial knife in the center (drawing from Carrisoza F. at Jimenez-Badillo, 2009)**

Another appelland and recurring arrangement of several offerings is the positioning of an object in the center and four more in the corners. This seems to be a reference to the geometric model of the Mexica universe, whose scheme included the center of the world and the four cardinal directions. (Jimenez-Badillo, 2009) A clear example of both schemes is founded in offering U (figure 23). These cosmic symbols turn the offering into an authentic scaled image of the Universe, where the lower levels represent the different infra world spheres and the higher ones the celestial spheres (Lopez-Lujan, 2009). Consequently, when approaching the study of these offerings it is precise to consider in one side the type and variety of objects that contain, and on the other side their distribution in the space.

Considering the artifacts in the offerings, physical and chemical factors play a key role into degradation processes: the compression of the materials owed to gravity, the erosion generated by the contact with abrasive particles, the fluctuations in water level (as the site is placed on a water source) that inundated the offerings and its partial evaporation, the pH of this water and the action of biological agents, the temperature and the concentration of oxygen, had a major impact into the differences that arise in the preservation state of archaeological objects from buried deposits.

The archeology in Mexico City faces the same challenges than in Rome, Jerusalem or Istanbul: it is constrained to the circumstance that ancient and highly valuable remains of a sophisticated civilization lie under the ground of a modern city (Lopez-Lujan, 2010).

The particularity of Mexico remains in the fact that, at this particular moment of the history, is the most populated city in the world and at the same time, it hoards the richest set of historical monuments of American continent (Lopez-Lujan, 2010).

### 2.3.2 Macroambiental conditions

Mexico City is located at a height of 2240 meters above sea level; the weather is temperate with two seasons along the year: a dry one and a rainy one, the last one, going from May to October. The difference of humidity between the two seasons is of about 40%.

Along Mexico runs the volcanic transversal axe thus, Mexico City is a telluric zone. Earthquakes related to volcanic activity are common, and may produce harm onto buried elements as in urban pipelines of the network of distribution and water collection.

Templo Mayor is placed, on a desiccated lacustrine soil, where the freatic nap is located close to the soil surface.

The ground is composed of clay and lime that interact with water, allowing the mobility of materials and a differential compactation (Alonso *et al*, 2008). This type of soil is permeable and allows the dragging of salts, pollution and clay onto the interior of offerings.

Concerning the buildings surrounding the site they have considerably different foundation systems: some colonial buildings were erected on the remains of Aztec buildings, while some others were constructed with Spanish technology. All the enumerated factors contribute to the sinking and/ or inclination of some areas.

As the site is located within an urban emplacement it is subjected to the presence of air pollution, and in some cases acid rain. Global warming had impacted the site as well, as ground temperature has certainly been increasing through the last years.

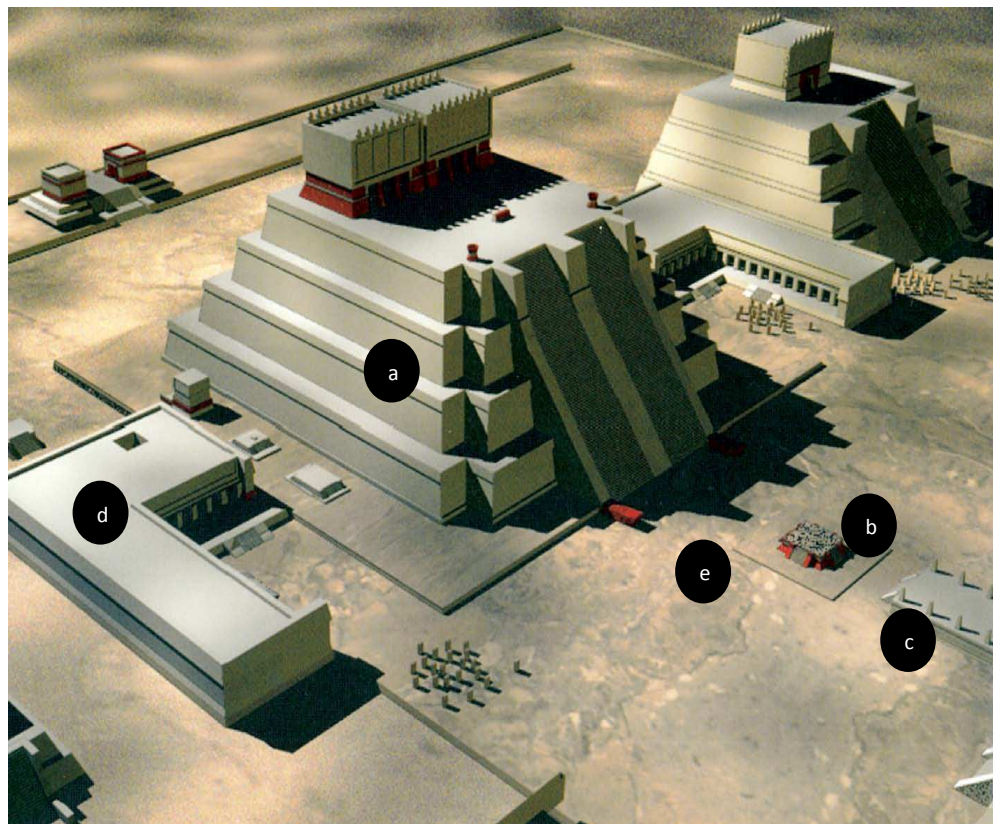
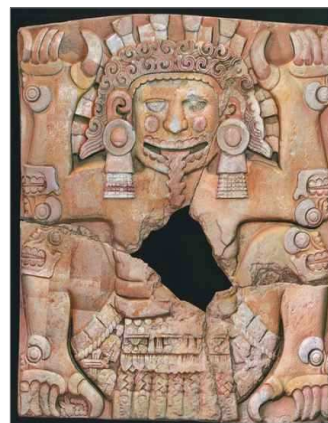


Fig 24 Reconstruction of the sacred precinct of Tenochtitlán after Antonio Serrato Combé. a) Templo Mayor, b) Cuauhxicalli, c) Tzompantli, d) House of the Eagle Warriors order, e) Area explored by the Archaeological project of Templo Mayor.

### 2.3.3 Microambiental conditions of Templo Mayor offerings

Offerings 120, 125, 126, 128 and 140 were excavated in what was once a colonial building known as “Casa de las Ajaracas” or in the esplanade just before this building. The principal stairs of the sixth constructive stage of the Templo Mayor were constructed in the physical space of this lot, as well as the esplanade in front of the temple, and the vestiges of what is supposed to be the Cuauhxicalli: the temple where Aztec emperors were cremated (figure 24).

These offerings are associated to the Tlaltecuhтли monolith, a superb piece of lapidary Aztec art, of 3.57 for 4 m long andesite, carved in relief. It was partially stuccoed, painted in red, ochre white, black and blue (figure 25).

**Diameter: 3.58m****Size: 3.26m x 3.08m****Size: 4m x 3.57m****Fig 25 From left to right: Piedra del Sol (1790), Coyolxauhqui (1978) and Tlaltecuhтли (2006)**

Generally speaking objects from the mentioned offerings that are manufactured in copal present heterogeneous states of preservation. A tendency towards a yellow coloration is verified with ageing. More than the half of the unburied copal is fragmented, its exterior is dusty and the surface presents layer or flake separation.

## **2.4 Description of archaeological Aztec offerings**

### **2.4.1 Offering 120**

It was excavated from June 2007 to November 2008.

It corresponds to the VI<sup>th</sup> constructive stage of Templo Mayor (built between the years 1486-1502 A.D.). The offering was placed inside a wrought stone box, the walls were constructed with flat smoothed blocks of andesite and a seal of the same material. When it was excavated the archaeological objects that constituted it, had a high content of water but it was not flooded. Nevertheless during some months during the excavation the offering was flooded due to broken pipelines of the public service of water. The nature of water was potable but also from sewage. Its pH was 7.82.

The presence of sewage water had a high impact onto copals within the offering: their surface was blackened.

Among the materials founded into the offering are: bars of copal with fibers of maguey onto their surface, maguey thorns rests of basketworks and hard fibers, objects of different materials like shell, bone, alloys of copper, flint, obsidian stone and green marble.

Comparatively speaking to the general state of preservation of the objects in this offering, it is inferior to the one of the objects of offerings 125 and 126.

The copal from the offering 120, was stick to maguey bars, are light yellow and brown colored, owing to the presence of organic material that polluted the context.

### **Conservation and Restoration Treatments**

The copal from this offering was cleaned, dry under controlled conditions, consolidated, when it was possible fragmentized pieces were joint, and then it were fumigated, finally they were conditioned for its storing.

#### **2.4.2 Offering 125**

It was excavated from April 2008.

The offering was found in a tunnel constructed with polished tezontle walls, sealed under two other offerings, between different seals of stone and stucco. From the entrance of the tunnel to the offering there are 2 m and a half. This situation created a good preservation environment with stable conditions of temperature, light, oxygen and elevated ambience moisture of around 92%, which allowed the conservation of a lot of organic materials such as wooden objects, seeds, animal hair and bones, basketworks, maguey thorns, copal and “guajes” (which are the dried fruits of *Lagenaria siceraria*, and were used as liquid containers by prehispanic cultures).

Among the remarkable inorganic materials from this offering are the turquoise tesels associated to the ornament of a pedernal knife and golden bells and ornaments from the wardrobe of the representations of Gods.

The objects were covering by sedimentary clay, and decomposed organic material.

During excavations some potable water infiltrations that affected the offering were registered, causing its flooding. This water had high content of chlorine and zinc, therefore water content was drained from the offering.

### **Conservation and Restoration Treatments**

The copal from this offering was cleaned with soft brush and water to wash out the sedimentary layer that covered it.

### 2.4.3 Offering 126

It was excavated from May 2008.

It was founded in a 2 m long and 1.1 m width box, constituted by four walls and a cover, from flat smoothed plaques of andesite. The interior walls were made of stone covered with clay and lime.

As the offering 125 and 120 it was flooded and the pH of the water was between 6.8 and 7. A particularity that is worth to mention, is that water presented an oily phase that may be owed to the dissolution of the essential oils from the copal bars; copal was very abundant in this offering, along with marine and botanical remains.

Objects were covered with a thin layer of sedimentary clay of 3 to 4 mm thickness.

This offering was colonized by black and white millipedes and fungi so it was subjected to a biocide treatment.

#### Conservation and restoration treatments

The copal from this offering followed a very similar process than the one from offering 120: it was cleaned, dry under controlled conditions, consolidated; when it was possible, fragmented pieces were joint, fumigated and finally conditioned for its storing.

### 2.4.4 Offering 128

This offering was found to the east and under the level of offering 125. The offerings are comprised into the constructive filling between two stages of the temple. It was located 12 m under the ground level. It was flooded, as the filling material is made of clay and lime and the water nap is located close to the surface. In this case the weight of the superior layers had produced harm owing to compaction.

Owing to its deep localization fluctuations of temperature and humidity were minimal, and concentration of oxygen was also limited.

### 2.5 Archaeological sample from the “Sacred Cenote” of Chichén Itzá

The first professional archaeological research project organized by the National Institute of Anthropology and History (INAH) in Chichén Itzá took place between 1960 and 1961 under the

direction of Roman Piña Chán. On this occasion, use was made of propelled-air equipment with a suction hose, but researcher soon change the technique for diving as the propelled air equipment was inadequate for the extraction of fragile items.

The sample of copal that was analyzed in this work (*cf* table 6) is likely to be recovered by this archaeological project. It was part of the paleobotanical collection of the INAH, where it has been stored for around 45 years, under museum conditions. It is constituted of a series of yellow fragments in tear shape and size, mixed with sable from the bottom of the cenote.

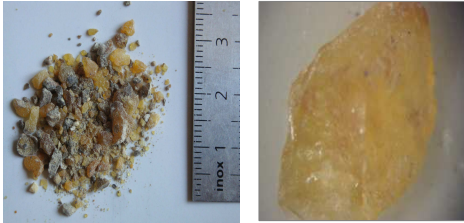
ID	Photos	Total weight of the sample (g)	Provenance, additional information
Chichén Itzá		23.47	<p>Paleo botanical Collection of the INAH</p> <p>Sample with small fragments of resin mixed to sable from the <i>cenote</i></p>
	<p>Fragment of 0.3cm x 0.15cm</p>		

Table 3 Archaeological sample from Chichén Itzá

### 2.5.1 The Chichén Itzá Cenote: macroambiental conditions

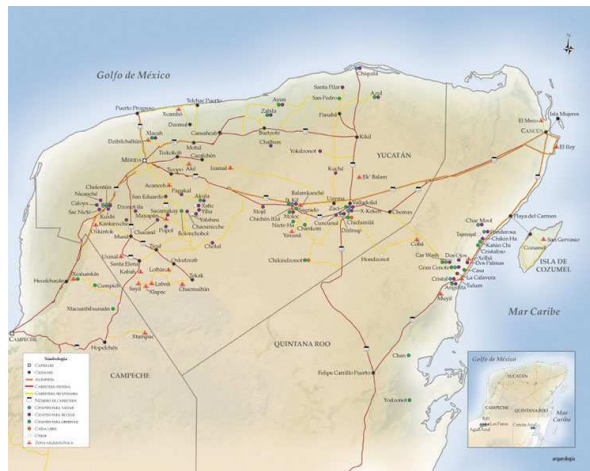
Yucatán peninsula is geologically speaking a flat calcareous platform without folding. The karstic constitution of Yucatán is mainly composed on calcium carbonate ( $\text{CaCO}_3$ ) limestone rock (Martos-López, 2007), with an average elevation of 20 m over the sea level, and tropical weather: intense pluvial precipitations, high temperature and dense vegetation are characteristics of this zone (Pedroza, 2010).

Its current morphology is the result of a series of geological and geomorphical events: karstic rock is highly permeable, allowing therefore the infiltration of meteoric water. This water cumulates in the underground, floating over a mass of marine water. The process of filtration together with changes in temperature the collapse, construction and dissolution of carbonates, contributed to form the biggest system of submerged caverns of the world, shelters, dolines, rivers and “cenotes”, (Beddows, 2007) *cf* figure 26.

The word “cenote” is a regional, mayan term derived from the word *ts'ono'ot* or *d'zonot* that means fresh water lake or cavern with deposited water (Rojas-Sandoval, 2007). In fact this term

defines any underground space with water, regardless its dimensions or characteristics (Martos-López, 2007).

It is important to note that the only source of fresh water in the whole peninsula is that of “cenotes”, the “Hondo” river being the only source of superficial water in the entire peninsula of Yucatán. Not all the cenotes in Yucatán present archaeological remains on its depth. Which demonstrates that among ancient Mayas two types of cenotes existed: for water supply and for ritual use.



**Fig 26 Map of the cenotes at Yucatán peninsula (Pedroza, 2010)**

For the Maya people, caverns and water bodies were the symbolic entrance to infra world and cenotes were the home of the *Chaacs* Gods of the rain. Therefore these sites were object of veneration (Martos-López, 2007). They were also considered as well as places of born and dead (Rojas-Sandoval, 2007). Soon after their arrival Cenotes caught the attention of the Spanish, who, amazed at their singularity, devoted space to describing them in their chronicles and accounts.

Cenotes can be classified according to their geological, hydrological, biological and chemical characteristics, so that we speak of ‘young’ or ‘lotic’ cenotes, and ‘old’ or ‘lentic’ cenotes. The first ones communicate freely with the aquifer through the galleries of the cavern, so that the water flow is horizontal and the water is present for only a very short time. Consequently, there is little organic matter as sediment and or in suspension.

In the lentic ones, the cenotes experience a blockage caused by the collapse of walls over centuries, and by natural sedimentation processes. These factors restrict exchanges with underground waters and makes refilling much slower. In this case there is sedimentation and



dissolution of particles of organic matter and detritus, which has a direct impact on the water's biological, physical and chemical processes.

While water clarity is a feature of young cenotes, the water in old cenotes tends to be turbid because of the presence of suspended particles. In fact, the production of organic matter in a cenote depends on the degree of opening or exposure of the aquifer to the outside and on the incidence of light. Such characteristics must of course be taken into account in underwater exploration work.

### 2.5.2 Microambiental conditions

One of the more appealing and outstanding features in Chichén Itzá is the Sacred Cenote or Cenote Chenkú (Cobos, 2007). It is located at the end of *Sacbé I* (avenue 1), 300 m to the north of the pyramid known as the Castle. It is a circular cenote of 60 m diameter and the maximal depth of its water is 13.5 m, *cf* figure 27. The distance from the ground surface to its water is 22 m depth, its walls are vertical and it belongs to the older or “lentic” type.



60 m diameter cenote

Fig 27 The cenote of Chichén Itza (Gallareta, 2007)

Chichén Itzá Sacred cenote being a closed system, has no water streams, therefore an accumulation of organic and particled material is observed (Beddows, 2007). The amount of organic material deposited onto this cenote depends directly onto its diameter.

Owing to this organic material accumulation, there is low penetration of UV-Visible light, exposition to direct sun light takes place only at noon each day (Rojas-Sandoval, 2007).

The amount of oxygen solved in the water and the pH decreases with the depth of the water of the cenote (Beddows, 2007). These factors along with the turbidity of its water, its low, and its fine sediments allow an extraordinary preservation of archaeological evidence.

There are two periods of height of the Sacred cenote as a worship place in the Classic (800-1100 A.D.) and the Postclassic (1100-1550 A.D.).

During the Classic Chichén Itzá dominated a great portion of the north of the Yucatán peninsula. The source of its power was the long distance commerce of different merchandises.

It is important to note that among all the cenotes in Yucatán, Sacred cenote is extraordinary because there is no other cenote, with such a variety and number of archaeological objects and offerings. Among the materials recover from its bottom can be found gold, jade, copper, textiles and of course copal (Rojas-Sandoval, 2007).

The origin of these objects can be related to the current territories of Guatemala, Costa Rica, Panamá, the south-east of the United States, and of course the Yucatan peninsula.

### **2.5.3 Underwater Chichén Itzá cenote explorations**

Along the XIX<sup>th</sup> century many explorers and adventurers with no actual formation to the archaeology were attracted to the cenote. This attraction was due in good part to the XVI<sup>th</sup> century chronicle “Relation of the things of Yucatán” from Diego the Landa.

In 1882, the eccentric French explorer Désiré Charnay tried to dredge the cenote with a Toselli sounder. However, the irregular bed of the well, the presence of stones, trunks and roots prevented the explorer from extracting anything, so he gave up (Martos-López, 2007).

In 1894, E. Thompson the first consul of the United States in Yucatan bought the Hacienda of Chichén Itzá. This hacienda included the remains of the ancient city and the cenote. From this year and up to 1907 the cenote was systematically dredged.

Between 1909 and 1911, Thompson changed its dredging technique for a diving one. In all the recover more than 30 000 objects (figure 28) among them where: ceramic vessels, carved jade beads with inscriptions, obsidian and quartz, figurines, shells, gold plated copper cups, gold bells, discs and pendants and human bones. Many of these vessels were filled with copal (figure 28i and 28j), and there were found also figurines moulded in copal, shaped as faces, corn, etc (figure 28h and 28k to m), (Cobos, 2007).

The bells along with wooden lances with flint ends, witness of a first identifiable phase of offerings associated with a warrior cult.



Fig 28 Archaeological objects recovered from the sacred cenote of Chichén Itzá:

a) golden bell, b) copper ring, c) ceramic vessel, d) gold monk pendant e) fragment of jadeite sculpture f) gold helmet, g) jade carved with glyphs animal shaped figurine, h) animal shaped figure, i) tripod bowl with offering with jade beads j) tripod bowl with offering k) copal ball with small balls of rubber, l) human face m) corn shaped copal (Catalog of Peabody museum, for scales consult catalog online).

## 2.6 Commercial samples

The interest of studying commercial copals is that these materials are traditionally used by artist in paintings but also for restorers, solved with ethanol as adhesive (personal communication from Maria Barajas). Among the painters that included copal in their paintings are Diego Rivera and Murillo (De la Cruz Cañízares, 2005).

Traditional markets in Mexico can be classified in two categories: the seasonal ones, that are associated with religious festivities and, that are settled in a location only for few days and the permanent markets like the Sinaloa and Azcapotzalco markets in Mexico City or the Tepoztlán market in Morelos.

“Copaleros” usually sell their products in seasonal markets were merchants from permanent markets buy copal for the year.

For this study commercial copal was collected by the author of this work, from seasonal markets in different locations like: Izúcar de Matamoros and Cholula in Puebla, Huitzucó in Guerrero and, from Azcapotzalco and Sonora permanent markets in Mexico City.

Dr. Lauro Bucio, and Dra Irma Belio also collected copal from Oaxaca, Colima and Estado de México.

In this way the geographical zone of collection of commercial copals cover a good part of the geographical zone that was once Aztec territory (figure 29).



**Fig 29** Map of Mexico. Orange zones represent the regions from wich commercial samples were collected and studied, green region plus orange region correspond to geographical extention of Aztec empire.

It is important to note that in traditional markets, resins from other botanical origin than *Bursera* may be found: for instance “zumaque” (*Rhus sp.*) and “estoraque” (*Liquidambar styraciflua*), a black copal looking resin (*Myroxylon balsamum*) among others (Montúfar, 2007). Their differentiation only by organoleptic analysis (physical characteristics) being impossible (Régert, 2008). The physical characteristics of the samples are present on tables: 4, 5 and 6. Samples were collected on glass tubes after a small incision had been made in the tree.

Reference	Description	Color, physical state	Geographical origin, year of collection
OaxC1	Copal “lágrima”	Opaque, yellow , solid	Oaxaca, Sep. 2005
OaxC2	Black copal	Black-redish, solid	Oaxaca, Sep. 2005
OaxC3	Yellow copal	Brown, sand looking powder, solid	Oaxaca, Sep. 2005
L1	White copal	Transparent, light yellow,solid	Colima, unknown
L2	White copal	Opaque light yellow powder, solid	Colima, unknown
M6	White copal	Transparent light yellow powder, solid	Texcoco
M6Q	White copal	Light yellow, solid	Texcoco

**Table 4 Copals collected in 2004-2005**

Reference	Description	Color, physical state	Geographical origin, year of collection
ATZB1	White copal	Light yellow resin, totally opaque, dusty in the surface	Unknown, 2008
ATZM1	Wooden fragments impregnated with resin	Resin: withish, opaque, solid.	Unknown, 2008
CHOB1	White copal	Light yellow opaque powder.	Puebla, 2008
CHOB2	White copal	White opaque resin solid	Puebla, 2008
CHOB3	White copal	Yellow opaque resin, solid.	Puebla, 2008
CHOB4	White copal	Light yellow resin with translucent and opaque localized zones	Puebla, 2008
CHOM1	Wooden fragments impregnated with resin	Resin: withish, opaque, solid.	Puebla, 2008
CHOR1	Red Copal	Brownish translucent resin with red	Puebla, 2008

		dots of solid material.	
Sidral	White copal	The most translucent fragment, solid.	Jolalpan, Puebla, 2008
Huitzucó	White copal	Half opaque, half translucent white fragments, solid.	Huitzucó, Guerrero, 2008
Inciense	Copal "lagrima"	Tears of yellow, opaque and translucent fragments, solid.	Unknown, 2008
IZUB2	White copal	Whitish opaque fragments, solid	Oaxaca, 2008
IZUM1	Wooden fragments impregnated with resin	Resin: white, opaque, solid.	Oaxaca, 2008
IZUP1	Copal "piedra"	Translucent, bright yellow, solid	Oaxaca, 2008
IZUR1	Red copal	Conglomerates of dusty surface with reddish-brown	Oaxaca, 2008
SONB1	White copal	White, translucent, solid.	Unknown, 2008
SONB2	White copal	Light yellow, translucent, solid.	Unknown, 2008
SONB3	White copal	White, translucent, solid.	Unknown, 2008
SONR1	Red copal	Brown, translucent, solid.	Unknown, 2008

Table 5 Copals collected in 2008

Reference	Description	Colour, physical state	Geographical origin, year of collection
ATZB2	White copal	Light yellow, solid, soft odour	Unknown, 2010
ATZJ2	Copal "lagrima"	Colour varies from light opaque yellow to orange, fragments solid	Unknown, 2010
SONR2	Red copal	Brownish resin conglomerated into big fragments of around 200g, dusty surface	Unknown, 2010
SONB4	White copal	White translucent resin, shiny surface. In barrels of 15 cm, quite sticky, solid.	Unknown, 2010
MEXB1	White copal	Bright yellow resin, shiny, shaped into bars of 20cm long for 8cm width.	Unknown, 2010
MEXJ1	Yellow copal	Tears in different colours ranging from translucent yellow to brown passing by orange and bright yellow.	Unknown, 2010
MEZM1	Wooden fragments impregnated with resin	Hard, bright yellow resin	Unknown, 2010

Table 6 Copals collected in 2010

## 2.7 Presentation of the analytical strategy

Based on the principle that the knowledge of the art and archaeological objects should be based on the examination of the artwork itself (Domenech-Carbó, 2008) an analytical strategy was created. This approach was necessary, in this case as the knowledge of the manufacturing of aircrafts in Ancient Mexico is quite ambiguous and most of the time is fragmentary and scarce, due to the lack of documentary sources.

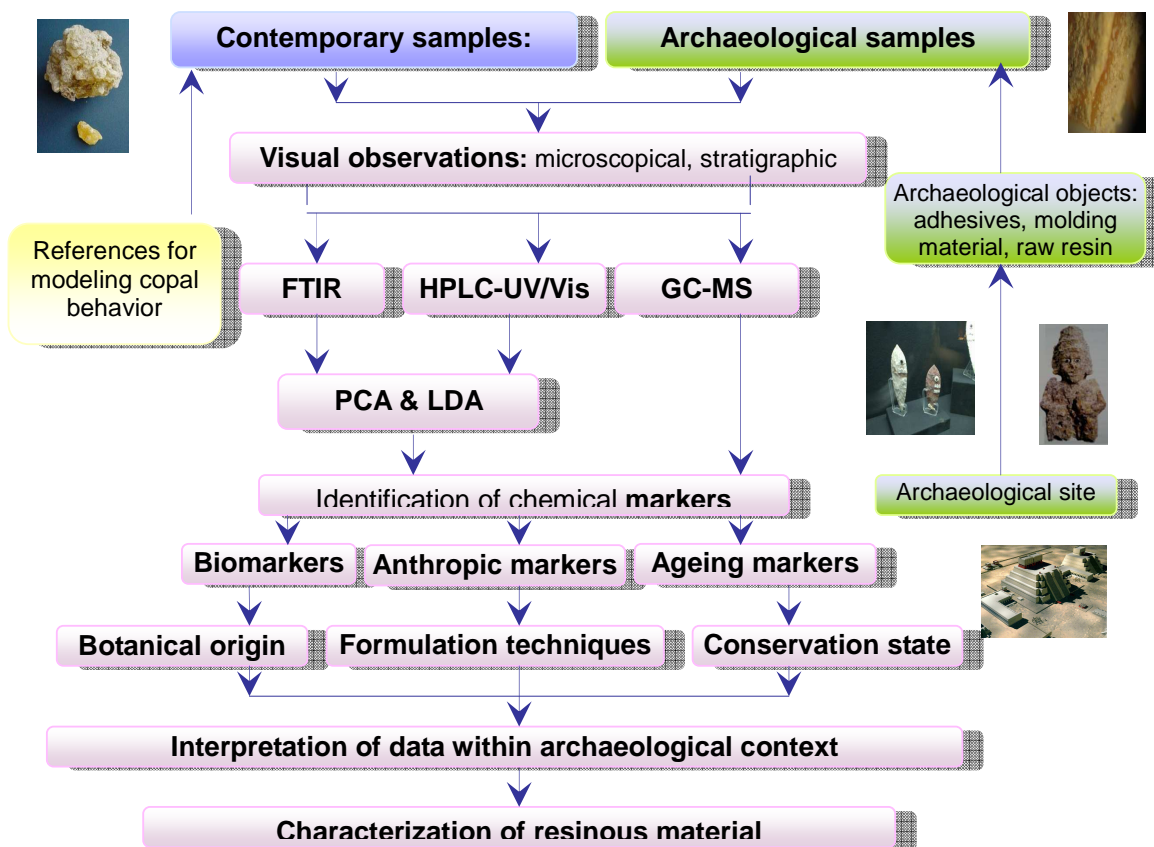
Even more studying the chemical composition of organic biomaterials associated to archaeological artifacts can give an important contribution to archaeological, conservation and ethnographic studies. Additionally the molecular analysis of the residues of these copal materials can answer questions relating to their botanical origin, their collection and preparation procedures, and their geographical origin. Chemical diagnosis helps to establish the extent and nature of degradation of the materials, important factors in conservation and restoration.

As it has been said in section 5 of chapter 1, the study of natural products– as resins - may be difficult owing to the complexity of these materials. The stability of an organic compound depends on its chemical structure, which determines the alteration mechanisms observed in organic materials. In consequence no general analytical technique exists to identify these substances and their degradation products, because they contain the same common elements (Colombini, 2000).

Nevertheless analyses on archaeological samples are difficult given the restrictions imposed on the number and size of the samples. Therefore the creation of an analytical strategy was necessary. A schematic view of the situation is presented on figure 30.

In this strategy certified origin samples and commercial samples were considered as reference materials to study the behavior of ancient copal.

A series of test was performed in a parallel way in both historical and fresh resins: the first step of the series was to perform a detailed visual examination, in both macro and microscopically levels.



**Fig 30** A description of the general situation encountered when analyzing historical materials and, a general approach to their study.

As archaeological samples exhibit a heterogeneous nature a stratigraphical analysis was performed. This analysis made evident an accelerated deterioration process on the surface of some archaeological samples.

The second step of this strategy consisted in a FTIR analysis of all samples. Spectral fingerprints for each botanical origin in certified samples were established.

The third stage in the strategy consisted in the HPLC/UV-Vis analysis of the samples, molecular differences in composition of resins from certified origin were remarked.

In order to achieve a better interpretation of both FTIR and HPLC-UV-Vis data two statistical methods were applied: PCA (Principal Component Analysis) and LDA (Linear Discriminant Analysis). The first one is a descriptive mathematical method which can help to recognize patterns, it produces a graphical where data is positioned according to their description. LDA is a classification method that uses linear combinations to minimize intra-species variations at the same time that it maximizes interspecies variations.



Statistical results have the advantage of being more easily interpretable by non chemist professionals, like conservators and archaeologist. Statistical results also allowed to compare the performance of the classification correlated to the analytic technique used (FTIR and HPLC). Results can be consulted in Chapter III and IV of this work.

The next step in the analysis consisted in the GC-MS analysis focused on the triterpenic fraction of the resins. This highly sensitive technique allowed identifying molecular markers for each studied resin species, at the same time that it opened new perspectives in the understanding of aging phenomena.

The last step of the strategy consisted in the consideration of all results to characterize effectively the origin of archaeological samples, as well as the changes experiences by copal under natural and accelerated ageing.

This strategy is based in the interpretation of analytical results based on artistic, archaeological, iconographic and iconological considerations following the model proposed by Tchaplá, 1999.

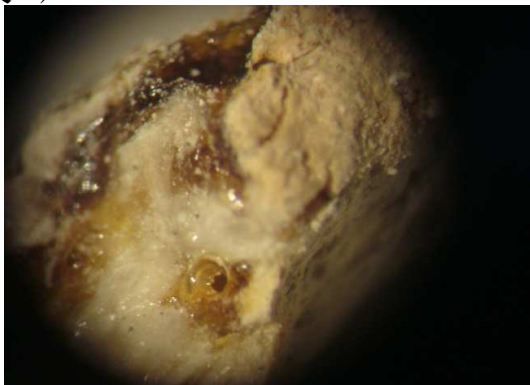
## **2.8 Study by optical microscopy**

In order to obtain the maximum information from one sample, a systematic preliminary analysis by optical microscopy on cross sections was performed. For some selected samples a study by electronic microscopy was performed, their nature is quite heterogeneous, some selected pictures of these results are shown on annex 1 (table 31 to 35) of this work.

Concerning archaeological samples, a first approach by optical microscopy allowed us to establish the heterogeneous nature of some of them (figure 31).

The microscopic examination of these samples revealed the presence of multilayer in archaeological samples, a difference in density between the outside of the samples (subject to a more intense ageing) and the inside was noticed: the inner part of the samples therefore showed to be much less deteriorated. Variations of color towards yellowing and/or blackening, lost of transparency and greater porosity, were also noticed on the surface.

A)



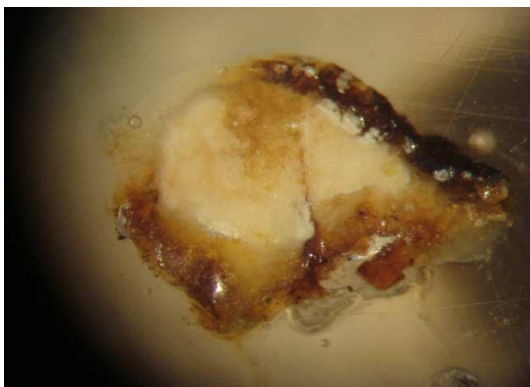
Size: 5mm  
80x

B)



Size: 5mm  
80x

C)



Size: 4 mm x 2 mm  
80x

D)



Size: 5 mm x 2mm  
80x

**Fig 31** Picture of non homogeneous archaeological samples referred A) sample 26, B) sample 173, C) sample TMT, D) sample 84

In sample no 26, two phases were observed: a white opaque one and a darker, amber coloured bright one.

Some other samples like M1 and 51, 52 were quite homogeneous, with no amber phase but instead some black dots on a whitish matter (figure 32).

Also remarkable is the closeness of aspect of samples 51 and 52. This fact can be explained considering that both samples come from the same archaeological offering, and therefore they were subjected to the same ageing conditions.

A)



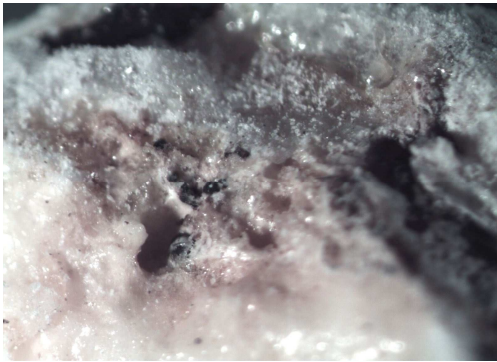
Size: 3mm x 2mm  
80x

B)



Size: 3mm x 2mm  
80x

C)



Global size 2 cm  
80x

**Fig 32 Homogeneous archaeological samples A) 51, B) 52, with inclusion of hair C) M1**

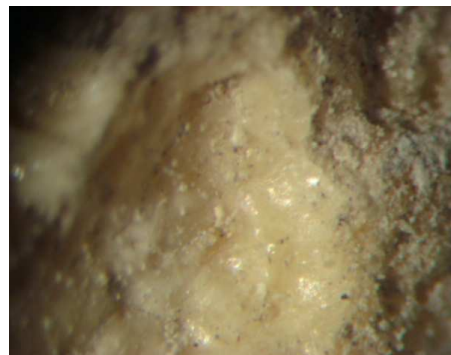
Sample TMT exhibit a very deteriorated and blackened surface, while the interior of the sample was white and brilliant as it was the surface of fresh resins (figure 33).

A)



Size: 3mm x 2mm  
80x

B)



Same sample, zoom  
120 x

**Fig 33 TMT sample A) from the surface and B) from the interior**

In consequence, partial analysis -by FTIR and GC/MS- of the different phases were performed when possible. Then the result was compared to that of global analysis, to assess degradation products, and the quality of the information obtained from deteriorated surfaces.

## 2.9 Conclusion

Even if the contribution of optical microscopy is modest to the results of this research, its utility is undeniable. It allowed us to distinguish a difference between the state of conservation of the surface of archaeological samples and its inner part.

In aged samples important physical changes could be observed. In fact along ageing resins oxidize by a mechanism of radical formation in a chain of events that begins with the attack of oxygen to double bonds, present in triterpenoids (Dietemann, 2003). These phenomena may lead to the formation of new insaturations that may act as chromophores, which yellow or darken resins appearance (De la Rié, 1988). At the same time these insaturations due to oxidation, enhanced resin sensibility to radiation and humidity, contributing to cracking and oat formation that were observed at the surface of some samples, all these phenomena were observed in archaeological resins, to different extents.

Degradation state of resins is connected to both original composition of the material and to ageing conditions, as ageing seems to be more intense in the surface of the resin a partial study of these more deteriorated parts will be performed, as part of this study.

# Part B

## Analytical Study of the resins and Discussion

### Chapter III

#### Spectroscopic Technique: FTIR Analyses

## Chapter III

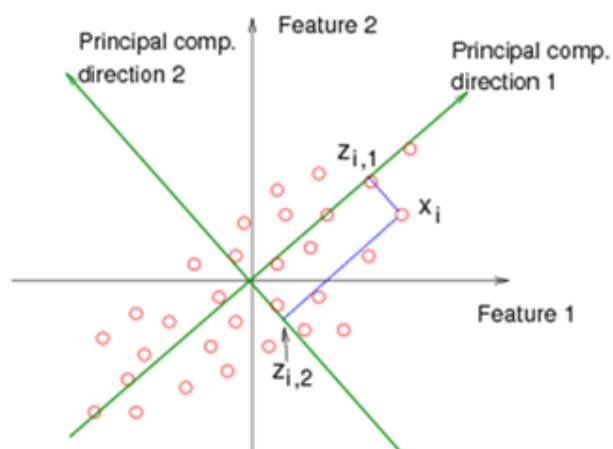
### FTIR Analysis

#### 3.1 Mathematical treatment of experimental data: chemometric strategies

##### 3.1.1 Principal Component Analysis (PCA)

A number of papers have identified natural materials by means of chemometric approaches (Tapp, 2003; Rezzi, 2005; Armanino, 2008; Casale, 2010a, Casale 2010b). In the artistic field, the most common is PCA (Principal Component Analysis), which has been applied to the discrimination of proteinaceous media (Andreotti, 2006; Colombini, 1999; Gautier, 2007; Bonaduce, 2006), seccative oils (Andreotti, 2006; Colombini 1999) polysaccharides (Colombini, 2002) and resins (Vieillescazes, 1995).

Up to now, characterisation of natural resins has been based on the use of specific markers, which can vary depending on materials ageing (Mills and White, 1977 and 1987) being this a disadvantage in case of degradation of molecules. As it has been said composition of plant resins is quite complex and is not entirely known yet for the majority of plant species (Colombini, 2000).



**Fig 34** Principal components analysis (PCA) projects data along the directions where the data varies the most (Terradez, 2000)

The objective of this technique is to capture the intrinsic variability in the data at the same time that reduces the dimensionality of a data set, either to ease interpretation or as a way to avoid over fitting and to prepare for subsequent analysis (Terradez, 2000).

Principal components are linear combinations of the original variables with the first principal component having the largest variance, the second having the second largest variance and so on (Cosio, 2007).

The aim of principal components analysis is to explain the maximum amount of variance with the fewest number of principal components (the smallest lost of information). It allows to consider the preferred directions of the data and to ignore those variables that do not have a big influence in the separation of the groups (Barreto, 2008). When data is projected in two dimensions (or three), is possible to distinguish visually the different classes that could appear, grouped in the projection. The different classes will be formed by those observations that display a uniform behaviour to each other and different from other existing groups (García, 2002).

PCA can be used to reduce the number of variables when there are too many predictors relative to the number of observations.

PCA is one of the most used classification techniques: and to sum up is a probabilistic parametric classification technique that maximizes the variance between categories and minimizes the variance within categories, by means of a data projection from a high dimensional space (Ferré, 1995).

### 3.1.2 Linear discriminant analysis (LDA)

LDA is a powerful chemometric tool that allows finding a predictive classification model, meaning that allows the construction of model able to foretell the property of a sample to a category previously defined, or to investigate how variables contribute to the separation in categories. This means that it allows studying the degree in which different populations, established *a priori*, differ from each other. It deals with two kinds of problems: descriptive discrimination, in which it describes if two or more populations are different from each other; and classification in strict sense, where given two or more populations and an object that belongs to some of them, it finds out to which of them it corresponds. The discriminating analysis requires to obtain combinations linear (or nonlinear) of independent variables that

will discriminate between defined groups *a priori*, so that the errors of the bad classification must be minimum (Barreto, 2009).

The LDA model is constructed from a set of samples of well-known category, denominated training data set, and then a regression equation is used as discriminating function (Casale, 2010 a).

Once the model is obtained, this one is used for the prediction of the category of property of the samples of unknown category. LDA can be linear or quadratic. The linear one assumes that all the groups have the same covariance matrix, while quadratic ones do not make this assumption.

In this research a level-one-out procedure was used. This means that each sample is removed once from the data set. The classification model is rebuilt and the removed sample is classified in this new model. All the samples of the data set are sequentially removed and reclassified. Finally a percentage of the correct classification is calculated (Lachlan, 1992). The quality of the LDA classification model was considered on the basis of the validation results.

The statistic analysis (PCA and LDA) in this work was performed using Minitab 16 (Minitab Inc. PA, California).

### **3.2 Chemotaxonomy. Correlation of resin composition and botanical origin**

Botanical systematic or plant taxonomy is the science of delimiting, describing or naming of, any group of plants considered to represent a distinct unit (Hegnauer, 1985). In many instances phylogeny of taxa is reconstructed with the aid of character comparison of living plants. The task of taxonomists is rendered very difficult, however, by relatively rapid divergences of characters and taxa in the course of adaptive radiation and, by several types of convergence known to occur during taxon evolution. Inevitably all existing systems of classification are imperfect in part. In such cases chemical characters may be very helpful.

In its broadest sense, chemotaxonomy is the use of chemical diversity as a taxonomic tool (Frisvad, 2008).

Plants are stunning chemical factories and, chemotaxonomy provide some broad assessments regarding the distribution of various structural classes of secondary metabolites such as alkaloids, quassinoids, flavonoids and triterpenes (Cordell, 2011). These compounds may



vary in their distribution within the plant. The amount and composition of classes of compounds such as alkaloids, flavonoids, essential oils and, many others are governed by the age of the plant or its parts, by the plant's locality (a geographical component) and its habitat (an ecological component). A solid knowledge of chemical variation is essential. Geographical and ecological variation has two main aspects. It may be the result of the plasticity of individual genotypes (modifications), or of a genetic heterogeneity of plant taxa. Genetical variation in local populations is called *genetical polymorphism*. Polymorphism is one of the starting points of differentiation: individual variants (inclusive of chemical ones) are able to become new races by migration and selection. Species which comprise several races or subspecies (units with their own combination of characters and area and/or habitats) are called polytypic (Hegnauer, 1985).

The composition of plant resin is quite complex and, not entirely known yet for the majority of plant species, it may also depend on climate and on the characteristics of soil (Colombini, 2000).

### 3.2.1 Terpenoids and chemotaxonomy

Secondary metabolites are chemical compounds produced by a limited number of species in a genus, order or even a phylum. Usually they occur in low concentrations and are not essential to plant cell survival. It is assumed that their function or importance is mainly related to ecological aspects, as they are often used as a defense against predators, parasites and diseases, for interspecies competition and, to facilitate the reproductive processes (Shulz and Baranska, 2007).

Terpens represent a large group of plant substance that occur in flowers, stems, leaves, roots and resins. It has been found that considerable variability in terpenoid composition is under genetic control and therefore terpenoids can be often acts as biochemical markers for chemotaxonomic classification (Shulz and Baranska, 2007).

Therefore some of the main components of the oleoresin (mono-, sequi- and triterpenes) have been used when studying other species as chemotaxonomic indicators and biochemical markers for instance of provenance of *Pinus* (Arrabal, 2005), *Boswellia sp* (Mathe, 2003) and dammar from Dipterocarpaceae (Burger, 2008).

### 3.3 Study by Fourier-transformed infrared spectroscopy (FTIR)

In the context of cultural heritage, the use of non destructive diagnostic techniques such as infrared spectroscopy (FTIR) had been used since 1954. This tool is highly valuable, in fact is one of the most widely used techniques in this field (Van Keulen, 2009), because of its ability for providing structural information of both organic and inorganic materials.

The scope of classical IR spectroscopic analysis was extended by the incorporation on IR Fourier transform spectroscopy owing to its superiority in terms of signal-to-noise ratio and resolution, while only a extremely amount of sample is needed to perform the analysis (Doménech, 2008). Infrared spectroscopy is based upon the study of the absorption of a sample of electromagnetic radiation with a wavelength between 10 000 and 10  $\text{cm}^{-1}$ . This range is divided itself into near infrared (from 10 000 to 4 000  $\text{cm}^{-1}$ ), medium infrared (from 4 000 to 400  $\text{cm}^{-1}$ ) and far infrared (under 400  $\text{cm}^{-1}$ ) (Rouessac, 1998).

The richest part of the spectra and the most accessible from the experimental point of view is that of medium infrared. In this region, absorption under 800  $\text{cm}^{-1}$  corresponds to a molecular fingerprint and, those over this wavelength are characteristic from the chemical functions present in the sample, which allow its analytical and structural analysis. In some cases the observation between the reference value and the experimental data allows to establish the surrounding environment of a given function in a molecule. For instance electronic delocalization and formation of hydrogen bonds shift down the absorption value (Bellamy, 1954).

#### 3.3.1 FTIR spectra of terpen and terpen like molecules

When dealing with natural resins, and being these ones constituted by many different compounds, it is impossible to perform a work structural identification by means of this technique (Hovanessian, 2005).

Nevertheless according to a previous study (Shulz and Barnska, 2007), it was possible to assign some band features to specific compounds (table 7).

Terpenes	Compounds	ATR-IR ( $\text{cm}^{-1}$ )	Assignment	Occurrence (example)
Acyclic monoterpenes	Myrcene	1637	$\nu(\text{C}=\text{C})$	Pepper ( <i>Piper nigrum</i> L.) (fruit)
		1595		
		989	$\omega(\text{CH}_2)$	

Terpenes	Compounds	ATR-IR (cm <sup>-1</sup> )	Assignment	Occurrence (example)	
	Citronellal	890	$\omega(\text{C-H})$	Eucalyptus ( <i>Eucalyptus citriodora</i> Hook) (leaf)	
		1725	$\nu(\text{C=O})$		
		1116			
	Citronellol	1058	$\delta(\text{C-C-OH})$	Eucalyptus ( <i>E. citriodora</i> Hook) (leaf)	
		1377			
	Geranyl acetate	1738	$\nu(\text{C=O})$	Eucalyptus ( <i>Eucalyptus macarthurii</i> , D. & M.) (leaf)	
		1365	$\delta_{\text{sym}}(\text{CH}_3(\text{C=O}))$		
		1227	$\nu_{\text{as}}(\text{C-O-C})$		
		1021	$\nu_{\text{s}}(\text{C-O-C})$		
	Monocyclic monoterpenes	<i>p</i> -Cymene			Thyme ( <i>Thymus vulgaris</i> L.) (leaf)
			1515		
			813	$\omega(\text{C-H})$	
Limonene		1644	$\nu(\text{ethylene C=C})$	Grapefruit <i>Citrus x paradise</i> MacF.) (fruit)	
		886	$\omega(\text{C-H})$		
Terpinen-4-ol		1050	$\delta(\text{C-C-OH})$	Marjoram ( <i>Origanum majorana</i> L.) (leaf)	
		924	$\omega(\text{CH}_2)$		
		887	$\omega(\text{C-H})$		
$\alpha$ -Terpinene		823	$\omega(\text{C-H})$	Marjoram ( <i>O. majorana</i> L.) (leaf)	
$\gamma$ -Terpinene		947	$\omega(\text{CH}_2)$	Marjoram ( <i>O. majorana</i> L.) (leaf)	
		781	$\omega(\text{C-H})$		
Bicyclic monoterpenes		1,8-Cineol	1374	$\delta_{\text{sym}}(\text{CH}_3(\text{CO}))$	Eucalyptus ( <i>Eucalyptus polybractea</i> RT Baker) (leaf)
	1214		$\nu_{\text{as}}(\text{C-O-C})$		
	1079		$\nu_{\text{s}}(\text{C-O-C})$		
	984		$\omega(\text{CH}_2)$		
	843		$\omega(\text{C-H})$		
	$\alpha$ -Pinene	1658	$\nu(\text{C=C})$	Pine tree ( <i>Pinus</i> sp.) (leaf)	
		886	$\omega(\text{CH}_2)$		
		787	$\omega(\text{C-H})$		
	$\beta$ -Pinene	1640	$\nu(\text{C=C})$	Pine tree ( <i>Pinus</i> sp.) (leaf)	
		873	$\omega(\text{CH}_2)$		
	Sabinene	1653	$\nu(\text{C=C})$	Pepper ( <i>P. nigrum</i> L.) (fruit)	
		861	$\omega(\text{CH}_2)$		
	Sesquiterpenes	$\alpha$ -Bisabolol	1437	$\delta(\text{CH}_2)$	Chamomile <i>Matricaria recutita</i> L.

Terpenes	Compounds	ATR-IR (cm <sup>-1</sup> )	Assignment	Occurrence (example)
		1375	$\delta_{\text{sym}}(\text{CH}_3)$	(flower)
		828	$\omega(\text{CH}_2)$	
		780	$\omega(\text{C-H})$	
	$\beta$ -Caryophyllene	1635	$\nu(\text{C=C})$	Pepper ( <i>P. nigrum</i> L.) (fruit)
		1447	$\delta(\text{CH}_2)$	
		1369	$\delta_{\text{sym}}(\text{CH}_3)$	
		887		
		877		

**Table 7 Assignment for the most characteristic IR bands of some terpenoid compounds (Schulz and Baranska, 2007)**

### 3.4 Sampling Methods: transmission methods

Transmission spectroscopy is the oldest and most straightforward IR method. The method is based upon the absorption of IR radiation at specific wavelengths as it passes through a sample. It is possible to analyze samples in liquid, solid, or gaseous form using this approach. There are three general methods for examining solid samples in transmission IR spectroscopy: alkali halide disks, mulls, and films.

### 3.5 Reflectance Methods

Reflectance techniques may be used for samples that are difficult to analyze by the conventional transmittance methods. Attenuated total reflectance spectroscopy (ATR) utilizes the phenomenon of total internal reflection. A beam of radiation entering a crystal will undergo total internal reflection when the angle of incidence at the interface between the sample and crystal is greater than the critical angle. The critical angle is a function of the refractive indexes of the two surfaces. The beam penetrates a fraction of a wavelength beyond the reflecting surface and when a material that selectively absorbs radiation is in close contact with the reflecting surface, the beam loses energy at the wavelength where the material absorbs. The resultant attenuated radiation is measured and plotted as a function of wavelength by the spectrometer and gives rise to the absorption spectral characteristics of the sample.

The crystals used in ATR cells are made from materials that have low solubility in water and are of a very high refractive index. Such materials include zinc selenide (ZnSe), germanium (Ge), and thallium / iodide (TII).

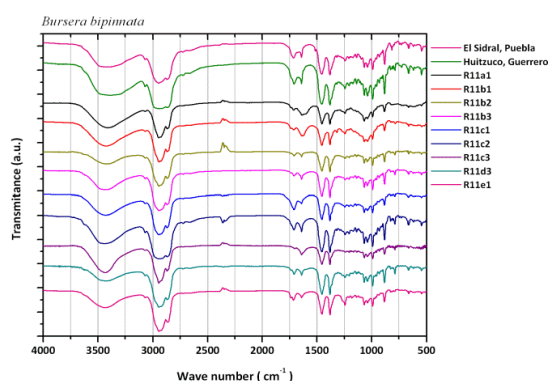
Different designs of ATR cells allow both liquid and solid samples to be examined.

Owing to the solid nature of the samples of resins, and the equipment present in the laboratory, this research work was performed in transmission mode (*cf* Materials and Methods section).

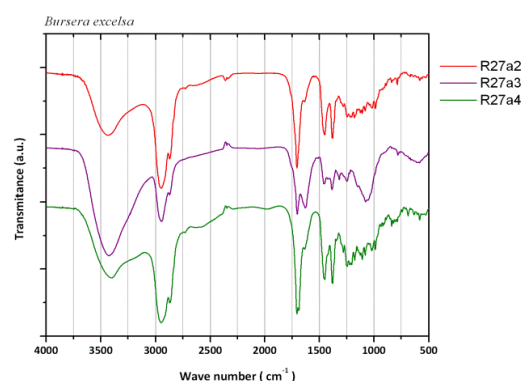
### 3.6 Results and discussion

After the collection of FTIR spectra of certified botanical resins, some spectral band positions were chosen owing to its contribution to differentiate spectra from different species (figures 35 and 36).

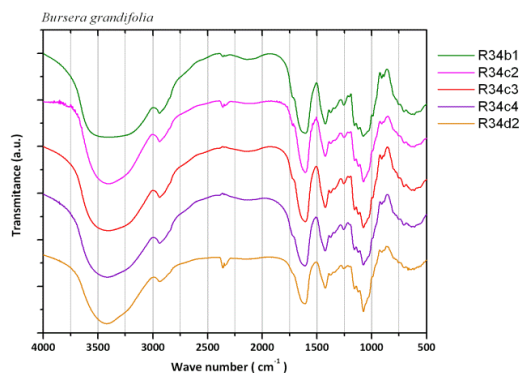
⌘ A)



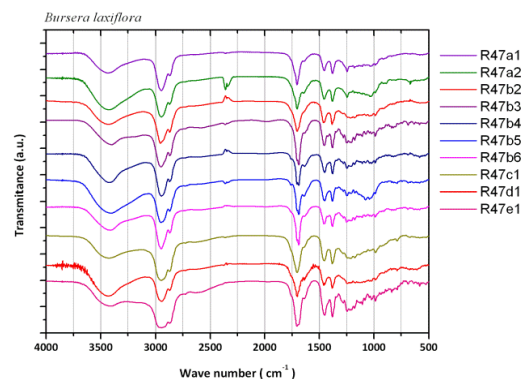
⌘ B)



⌘ C)



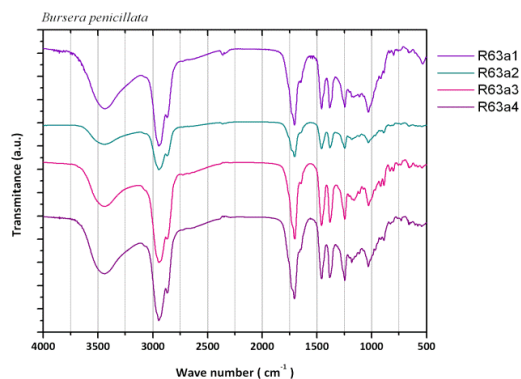
⌘ D)



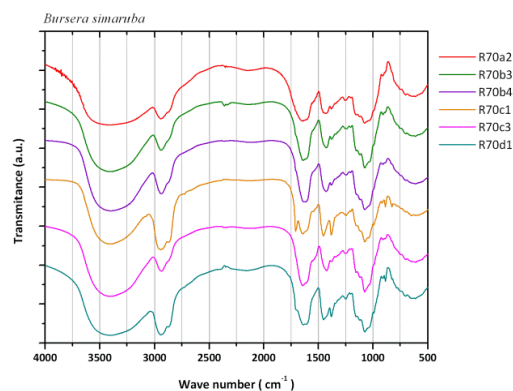
**Fig 35 FTIR spectra of different species A) *B. bipinnata*, B) *B. excelsa*, C) *B. grandifolia*, D) *B. laxiflora*. (Intra species variation in spectra can be remarked).**

A full page view of each of a comparative of the spectra for each studied species can be seen on annex 2 (Figures 110-116) of this work.

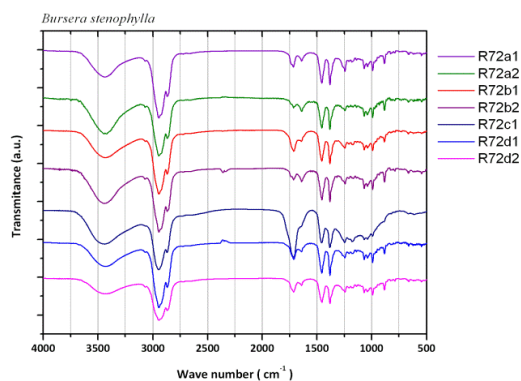
A)



B)



C)



**Fig 36** FTIR spectra of different species A) *B. penicillata*, B) *B. simaruba* C) *B. stenophylla* (Intra species variation in spectra can be remarked).

This data was then used into chemometric analysis. Sample distribution patterns were investigated with principal component analysis (PCA). Score graphics using the first two components, revealed a sample agglomeration with good differentiation in 5 out of the 6 species. This method was validated by LDA with a 95,2 % of positive recognition. The aim was to establish a spectral databank in order to identify the botanical provenance of fresh resins.

### 3.7 PCA

A data matrix with 42 rows (certified origin samples of resin) and 11 columns (variables) was built (*cf* annex 2, table 38). When it was possible, the assignment of the band to functional groups was made (table 9, figure 37). The variables were the band positions of FTIR spectra, in transmittance mode. Initially the matrix was analyzed by means of principal component analysis (PCA) in order to display the structure of the multivariate data, covariance matrix was used.

The following table gives the band color code of the figure 37:

	<b>Band position <math>\text{cm}^{-1}</math></b>	<b>Color</b>	<b>Interpretation</b>
<b>a</b>	3425	purple	Tension $\nu$ O-H broad band
<b>b</b>	2945	green	Tension $\nu$ C-H from alkans $\text{CH}_3$ and alkenes $\text{CH}_2$
<b>c</b>	1710-1720	light blue	Stretching $\nu$ C=O from carboxylic acid
<b>d</b>	1638	pink	Tension $\nu$ C=C
<b>e</b>	1454	green	Symmetric deformation $\delta$ $\text{CH}_2$
<b>f</b>	1380	green	Deformation of deflection $\delta$ $\text{CH}_3$
<b>g</b>	1242	blue	Tension $\nu$ C-O-C
<b>h</b>	1037	purple	Tension $\nu$ C-O symmetrical from alcohol
<b>i</b>	883	non colored	Intramolecular vibrations
<b>j</b>	687	light yellow	Intramolecular vibrations
<b>k</b>	584	non colored	Intramolecular vibrations

**Table 8** Band positions taken into account as variables for the PCA matrix.

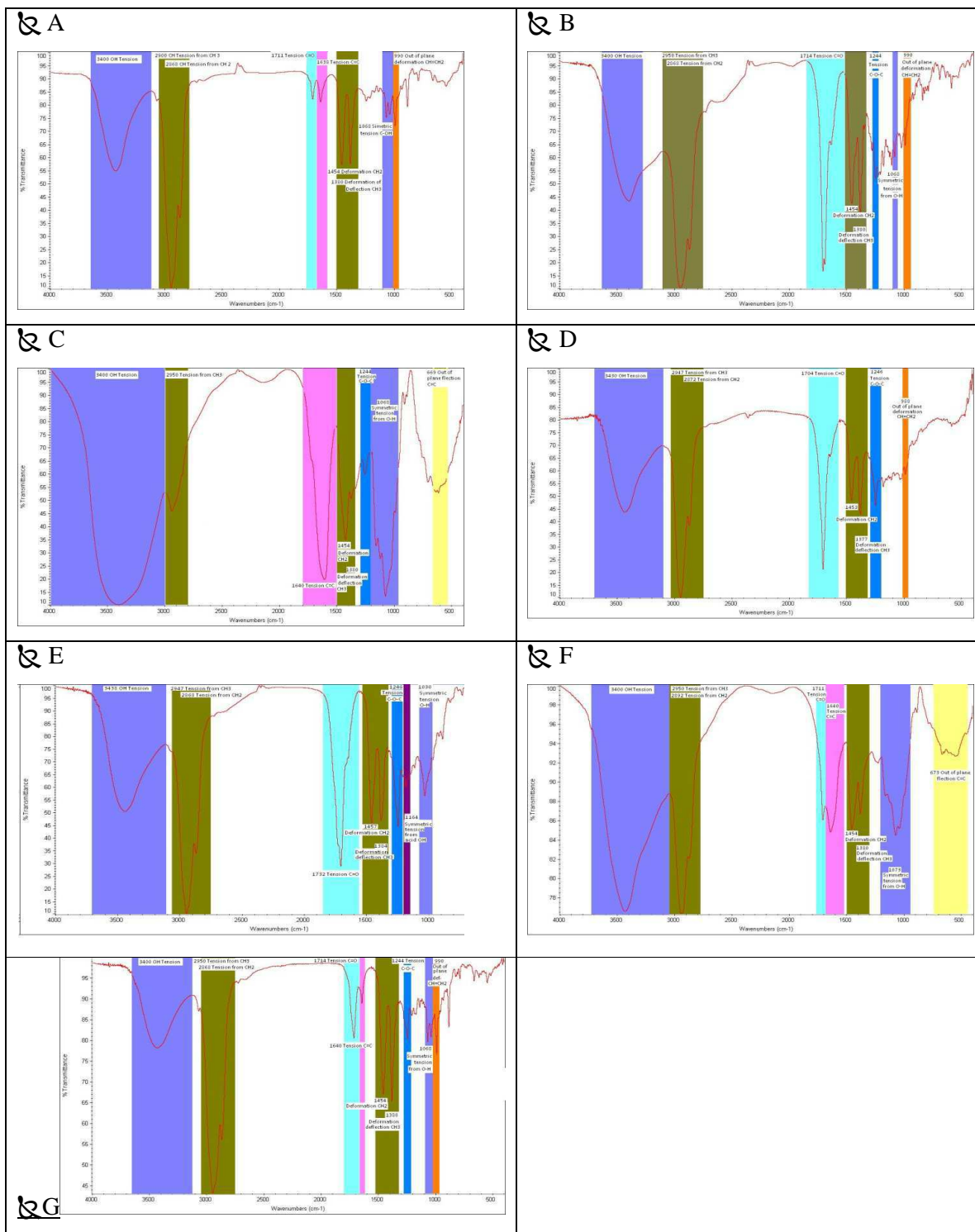
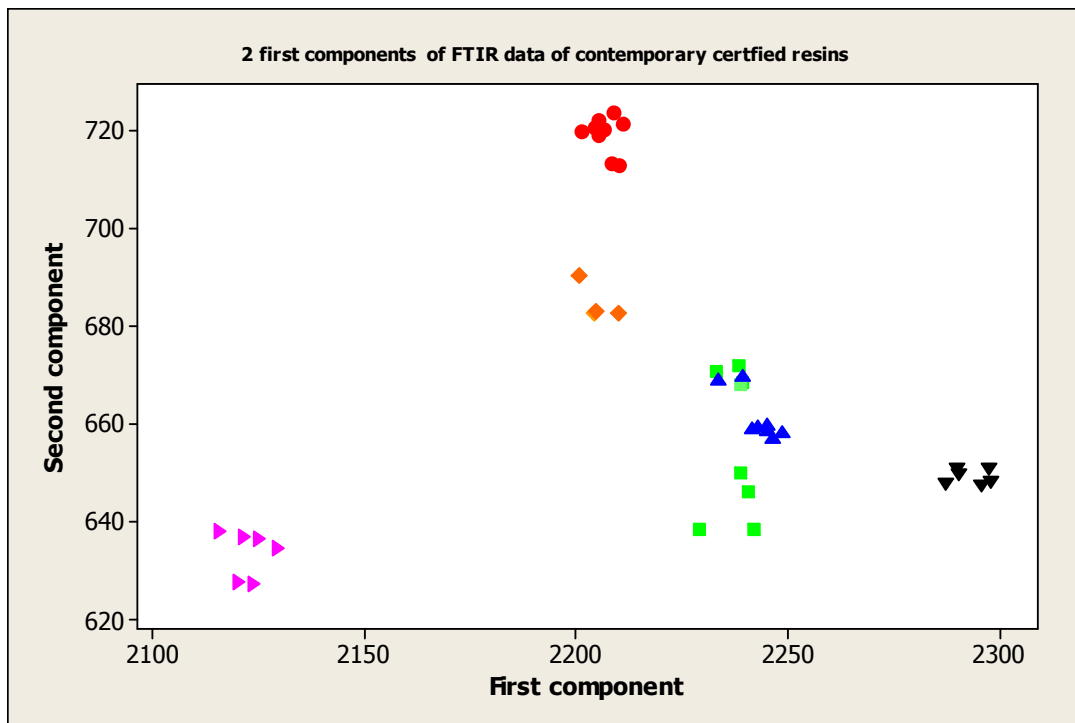


Fig 37 Band interpretation for the studied species : A) *B. bipinnata*, B) *B. excelsa*, C) *B. grandifolia*, D) *B. laxiflora*, E) *B. penicillata*, F) *B. stenophylla*



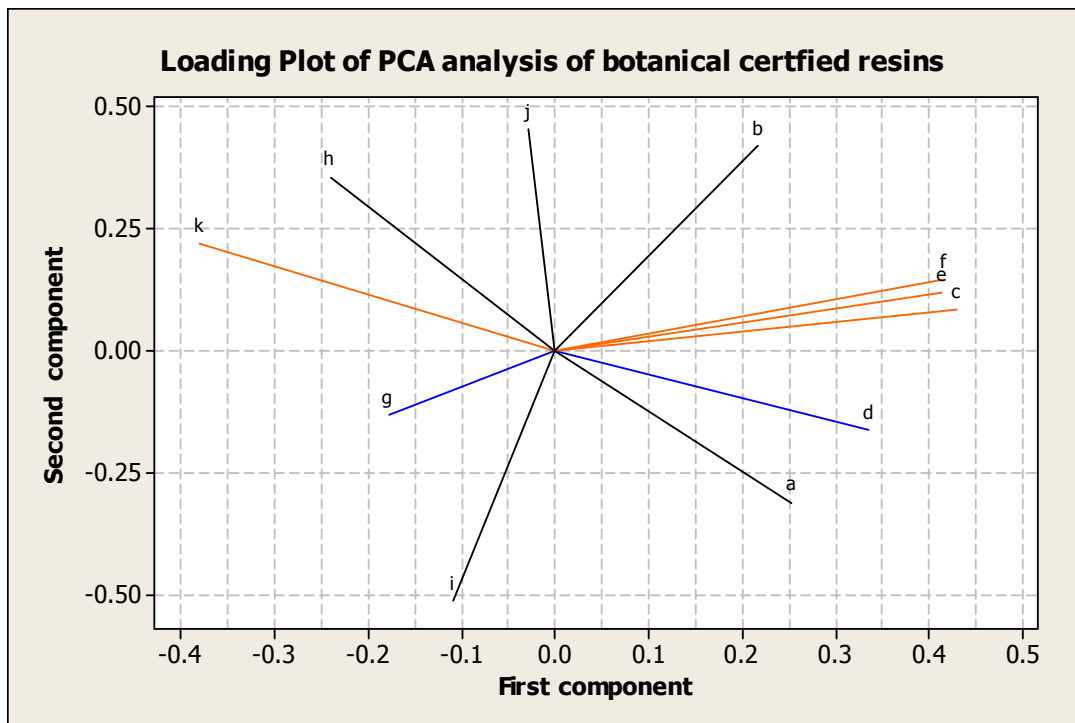
Afterwards according to the result of the projection of the 2 first components in a graphic (figure 38) five well defined groups were obtained.



**Fig 38** Distribution in the hyperspace of the first two components of the resins certified origin. Legend different species are shown as follows: ● *B. laxiflora*, ◆ *B. excelsa*, ■ *B. stenophylla*, ▲ *B. bipinnata*, ► *B. grandifloia*, ▼ *B. penicillata*.

The first principal and the second principal components were enough to display the data structure, since they explained 79% of the total variance. Examining the score plot in the area defined by the first two principal components, a separation of the samples into five groups was found according to the different botanical species, except for *B. stenophylla* that overlapped the zone comprised by *B. bipinnata*. It is important to note that their distribution into the hyperspace is not the same: while *B. bipinnata* forms a single compact group, *B. Stenophylla* forms 2 groups one compact and the other overlapping the *B. Bipinnata* region. These data are consistent with botanical findings, as it has been said on section two of chapter two, there are uncertainties that persist into the taxonomical classification of these two species: some authors consider *B. stenophylla* as a variation of *B. bipinnata*.

Since samples were well described in the score plot, the loading plot (figure 39) was analyzed in order to show which variables influenced the group separation.

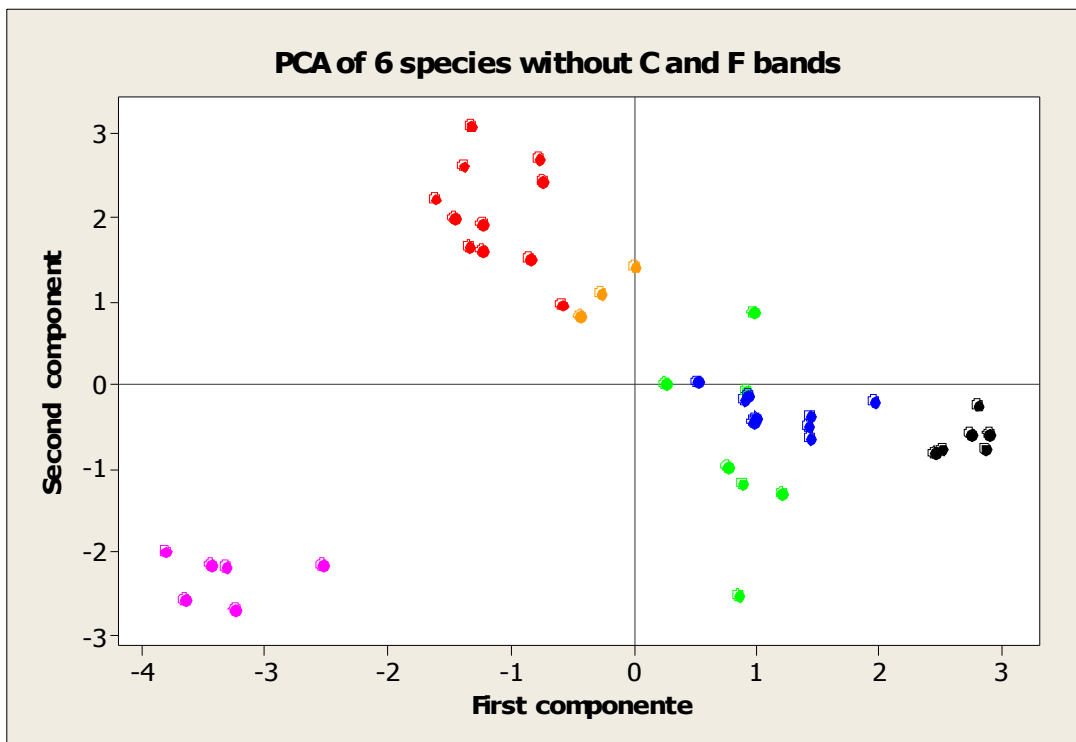


**Fig 39 Loading plot, variables with a high impact on first component are shown in orange, and variables with a high impact on second component are shown on black.**

As can be seen in the loading plot of the first two principal components, the bands f, e, c and b corresponding to deformation of  $\text{CH}_3$ ;  $\text{CH}_2$ ; tension of  $\text{C}=\text{O}$  and tension of alkanes  $\text{CH}_3$  respectively characterized the first principal component.

Nevertheless f, e and c were placed close in the graph, meaning that these variables have almost the same information, therefore f and e columns could be removed from the data matrix without a big decrease of discrimination capability.

The result of doing so is shown on figure 40, where a greater dispersion of the data can be appreciated, although classes can still be recognized.



**Fig 40** Distribution in the hyperspace of the resins samples from botanical certified origin, using the first two components with two less variables in the matrix (band positions f and e). Legend different species are shown as follows: ● *B. laxiflora*, ◆ *B. excelsa*, ■ *B. stenophylla*, ▲ *B. bipinnata*, ► *B. grandifloia*, ▼ *B. penicillata*.

Bands b, j, k and h (tension C-O from alcohol), were relevant on the second component. They were displayed in different regions of the loading plot meaning that the all of them were relevant for the classification model. Most of all, b band appeared more informative, since it showed high values on both components.

Band g (C-O-C tension) was the variable that was placed closest to the center of the plot, therefore its impact on groups separation, is minimal in compared to the other bands in the model.

### 3.8 Linear discriminant analysis

Since the data structure analysis gave a good sample characterization, a classification model was built. LDA analysis was applied in order to find a predictive classification model, able to separate the 6 botanical species.

Put into Group	<i>B. bipinnata</i>	<i>B. excelsa</i>	<i>B. grandifolia</i>	<i>B. laxiflora</i>	<i>B. penicillata</i>	<i>B. stenophylla</i>
<i>B. bipinnata</i>	6	0	0	0	0	0
<i>B. excelsa</i>	0	4	0	0	0	0
<i>B. grandifolia</i>	0	0	6	0	0	0
<i>B. laxiflora</i>	0	0	0	10	0	0
<i>B. penicillata</i>	0	0	0	0	6	0
<i>B. stenophylla</i>	2	0	0	0	0	8
Total N	8	4	6	10	6	8
N correct	6	4	6	10	6	8
Proportion	0.75	1	1	1	1	1

**N = 42      N Correct = 40      Correct Proportion = 0.952**

**Table 9 Results for LDA classification model: Fitting and validation matrix were identical. Rows represent the true class, and columns the assigned class. Wrong assignments are shown in red.**

As can be seen in the confusion matrix (table 9), LDA applied to the complete data set gave a recognition percentage of 95.2%, while only two resin samples were not correctly classified in the validation procedure. Complete statistical results can be consulted in annex 2.

### 3.9 Application to a botanical origin certified sample.

As there are over 80 species that produce resin in Mexico, we decided to perform a test with a resin with botanical certified origin, different from the six species that were included in the original FTIR study. After collection of the infrared spectra of a sample of *B. copallifera* species, PCA was performed. Results are shown on figure 41 and as it can be seen on the graph, the model assigns, as expected, the new sample in a different region which would correspond to a new category.

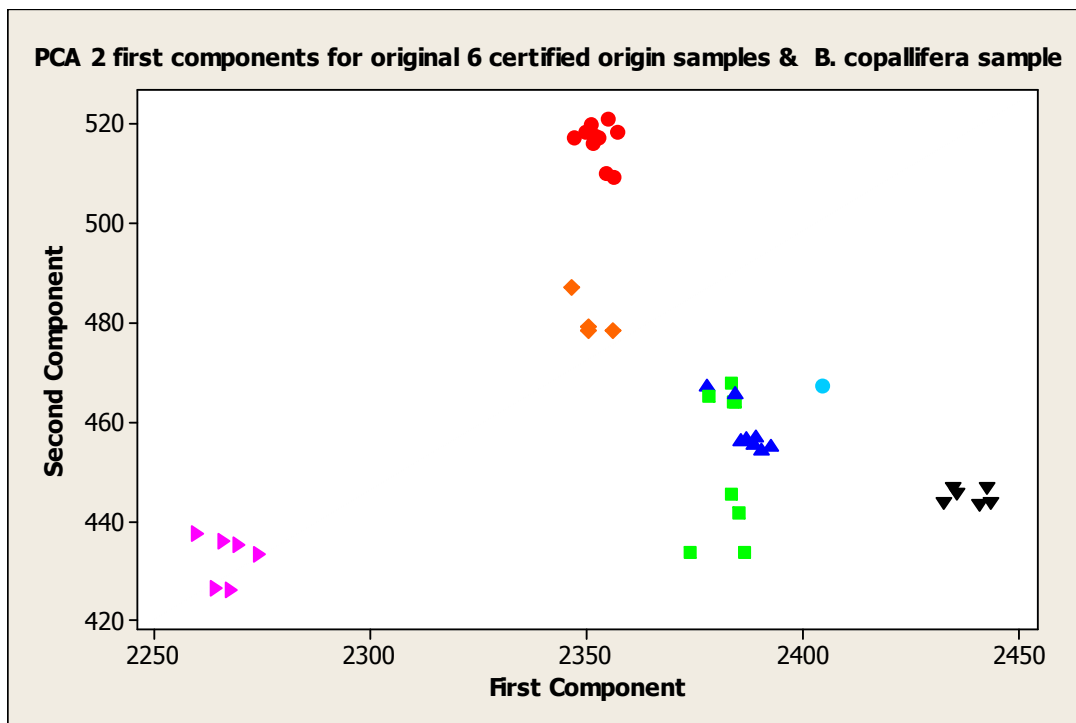


Fig 41 Distribution in the hyperspace of the resins samples from botanical certified origin, using the first two components, plus a certified sample from *B. copallifera*. Legend different species are shown as follows: ● *B. laxiflora*, ◆ *B. excelsa*, ■ *B. stenophylla*, ▲ *B. bipinnata*, ► *B. grandiflora*, ▼ *B. penicillata*.

### 3.10 Application to two commercial samples of copal.

The next step into the test of our model was to analyze a commercial sample as it can be seen on figure 42 for MEXJ1 and graph 43 for IZUM1, when PCA analysis was performed with FTIR data from these samples, both were placed into the hyperspace corresponding to both *B. bipinnata* and *B. stenophylla* species.

It is important to remember that MEXJ1 is a sample of yellow resin bought in a market from Mexico City, while IZUM1 is a sample of wood impregnated with a translucent resin that was bought at a seasonal market at Izúcar de Matamoros. Both cities are apart 200 km, confirming that even on fresh resins assignment of a botanical origin based in physical parameters is not possible.

Given the obtained results, a deconvolution of the area of FTIR spectra between 1200 and 1300  $\text{cm}^{-1}$  was performed.

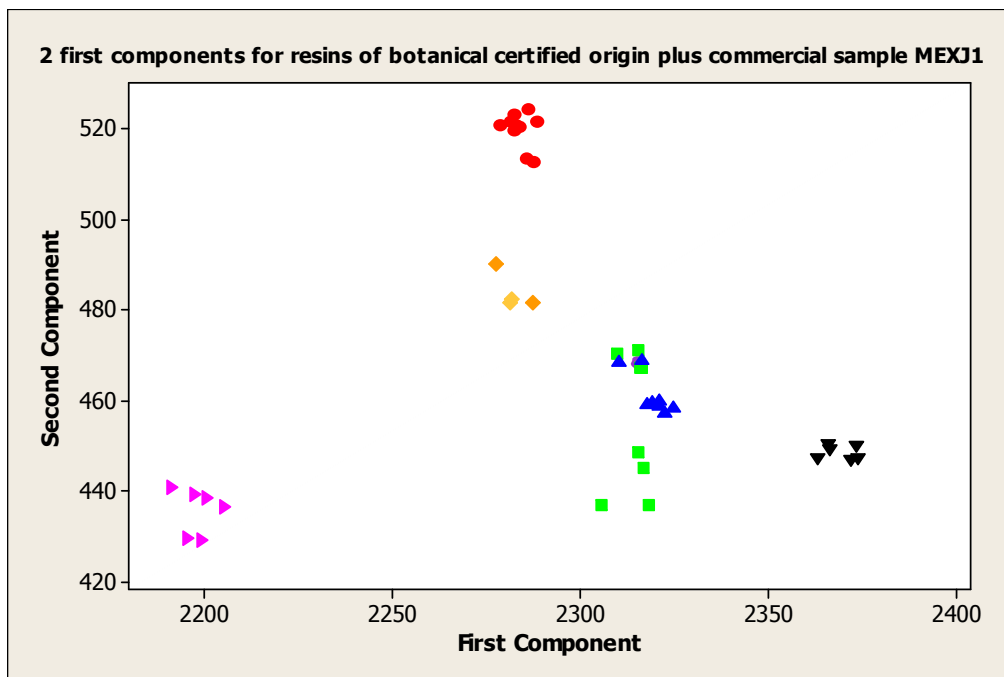


Fig 42 Distribution in the hyperspace of the resins samples from botanical certified origin, using the first two components plus commercial sample • MEXJ1. Legend different species are shown as follows: • *B. laxiflora*, ◆ *B. excelsa*, ■ *B. stenophylla*, ▲ *B. bipinnata*, ► *B. grandifloia*, ▼ *B. penicillata*.

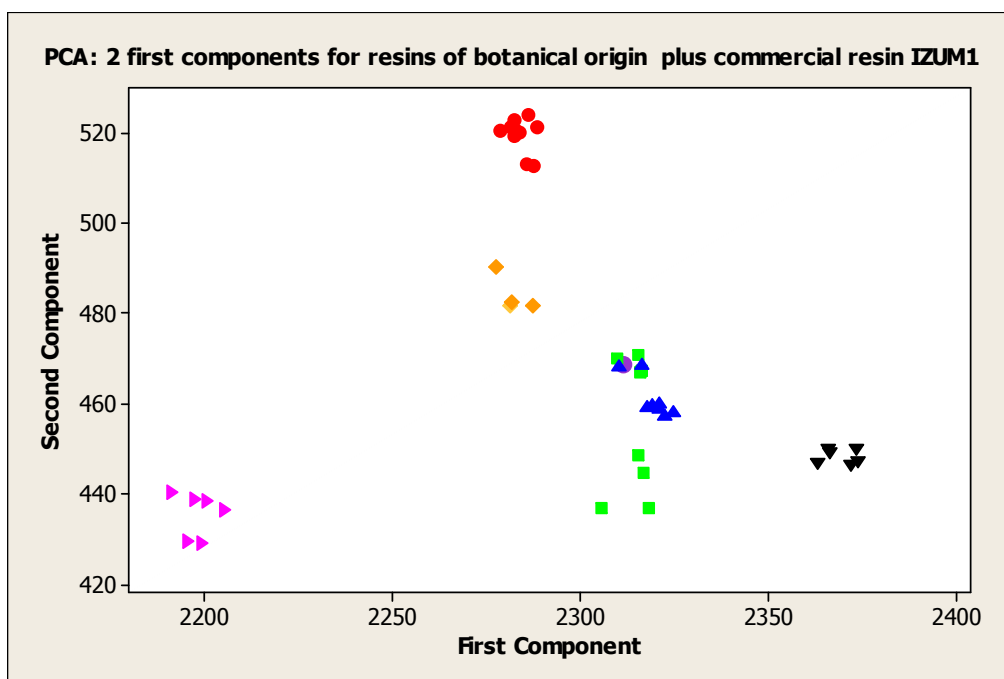


Fig 43 Distribution in the hyperspace of the resins samples from botanical certified origin, using the first two components plus commercial resin • IZUM1. Legend different species are shown as follows: • *B. laxiflora*, ◆ *B. excelsa*, ■ *B. stenophylla*, ▲ *B. bipinnata*, ► *B. grandifloia*, ▼ *B. penicillata*.

### 3.11 Deconvolution of the bands in the region between 1200 and 1300 $\text{cm}^{-1}$ of the spectra. Application of the technique to two commercial resins

One of the inconvenient that may arise when working with spectra of complex mixtures is the overlapping of the bands that different wavelengths, this phenomena is caused by the absorption of the radiation, at close frequencies, by different molecular bonds (of the radiated molecules) that vibrate to those same frequencies, or the same type of bonds placed in different environments within a same molecule. This phenomenon causes an increase of the amplitude of the signal in the spectra of the bond producing massive bands.

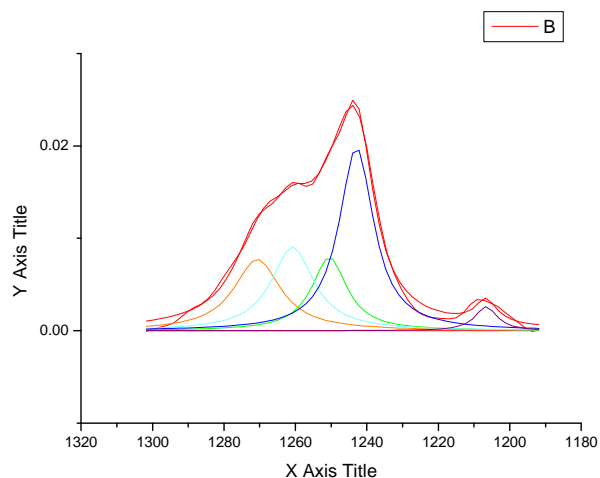
In the next stage of the research, we propose the decomposition of the massive signal from FTIR comprised between 1200 and 1300  $\text{cm}^{-1}$ , to differentiate two close botanical species. This region was chosen because there were found more differences between *B. bipinnata* and *B. stenophylla* species.

As can be seen on figure 44, as a result of the differences in chemical composition of resins, differences in the number of signals arisen in some regions of the FTIR spectra can be appreciated. This feature allows the differentiation between botanical origins of fresh samples.

A) *B. bipinnata*

$R^2$  0.99428

5 bands at : 1206.6, 1242.9, 1250.5, 1260.8, 1270.7



```
Data: A72A1_B
Model: Lorentz

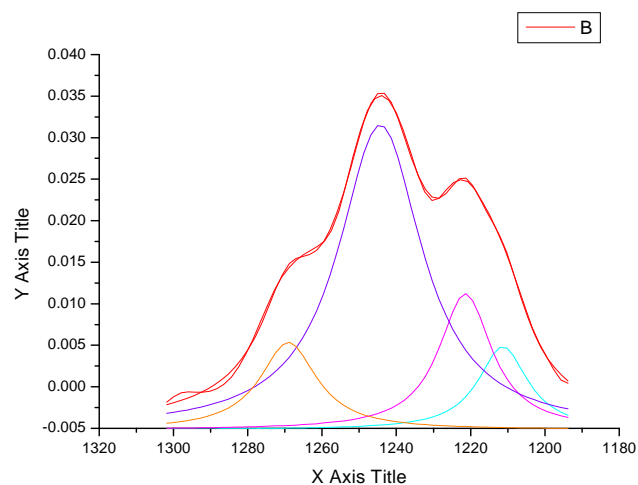
Chi² = 4.213E-7
R² = 0.99428

y0 0 ±0
xc1 1270.70959 ±1.90559
w1 15.92102 ±3.42698
A1 0.19315 ±0.12644
xc2 1250.51474 ±1.28473
w2 11.91148 ±3.86639
A2 0.14849 ±0.20933
xc3 1260.79631 ±1.23029
w3 14.43326 ±9.14298
A3 0.20544 ±0.23967
xc4 1242.93273 ±0.58563
w4 11.7045 ±1.12227
A4 0.36562 ±0.10309
xc5 1206.64098 ±0.75395
w5 7.43576 ±2.24147
A5 0.0304 ±0.00668
```

B) *B. stenophylla*

$R^2$  0.99888

4 bands at: 1211.3, 1221.4, 1244.3, 1269.1



```
Data: R11D1CORR_B
Model: Lorentz

Chi² = 1.8888E-7
R² = 0.99888

y0 -0.00517 ±0.00024
xc1 1211.30589 ±0.85139
w1 16.21574 ±1.83919
A1 0.25461 ±0.07447
xc2 1221.4362 ±0.5772
w2 17.30905 ±1.97577
A2 0.44573 ±0.09777
xc3 1244.33831 ±0.15209
w3 27.37031 ±0.80145
A3 1.57924 ±0.06077
xc4 1269.05838 ±0.29242
w4 18.53873 ±1.24322
A4 0.30693 ±0.02785
```

Fig 44 Deconvolution of bands between 1200 and 1300  $\text{cm}^{-1}$  region. For A) *B. bipinnata* and B) *B. stenophylla*.



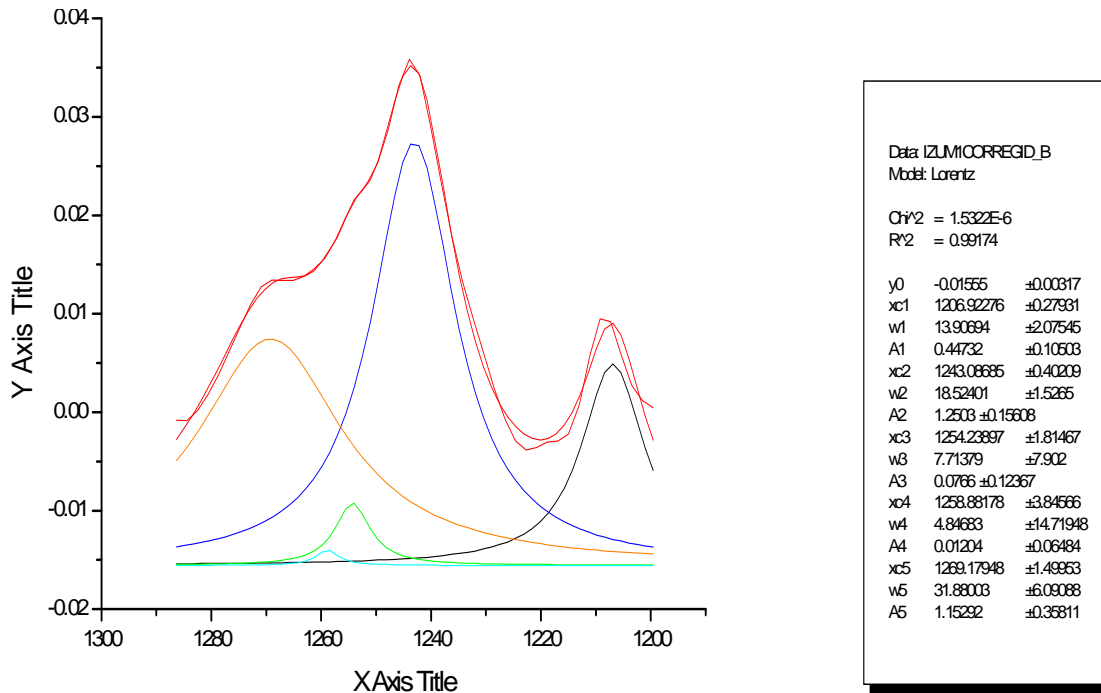


Fig 45 IZUM1 deconvolution of 1300-1200 region: botanical origin *B. stenophylla*  $R^2$  99.17 %

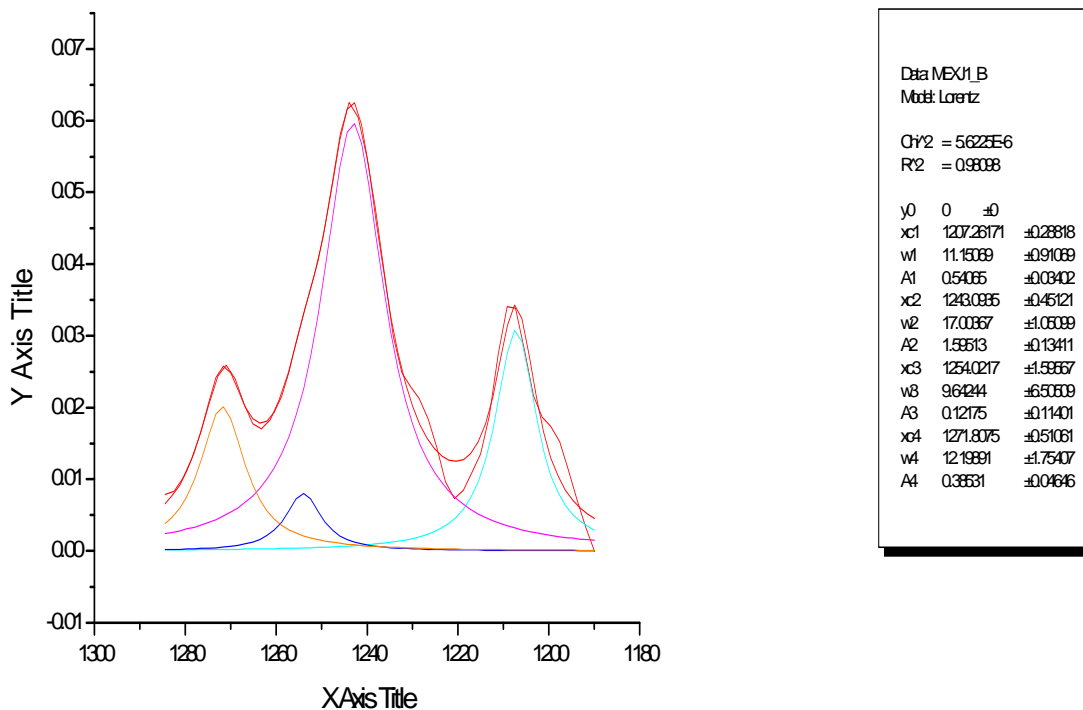
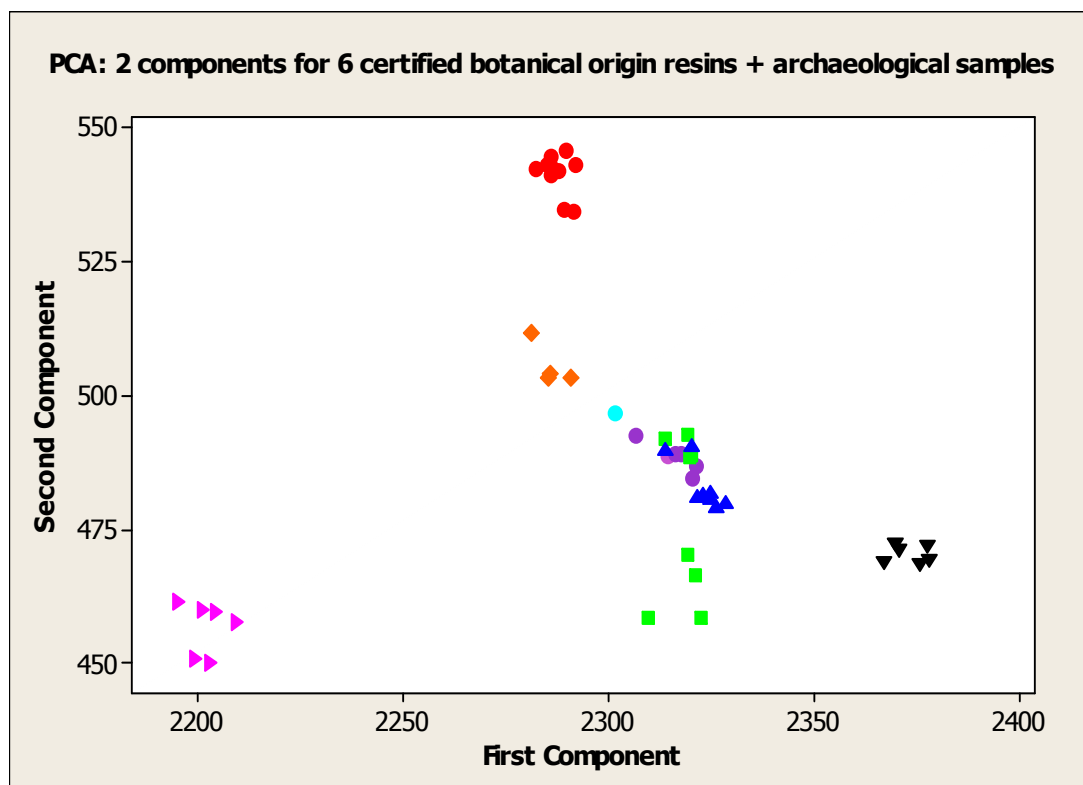


Fig 46 MEXJ1 deconvolution of 1300-1200 region: botanical origin *B. bipinnata*  $R^2$  98.09 %

When the procedure was applied to commercial resins, MEXJ1 and MEZM1, different botanical origins were attributed to each resin, based upon the number of signals in the mentioned region (figures 45 and 46):  $R^2$  was 99.17% for IZUM1 and  $R^2$  for MEXJ1 was 98.09 %

### 3.12 Application to archaeological resins

Archaeological samples were included into the analysis, and the graphic for the two first components was made. Here we present it in figure 47. From this graph it is important to note that archaeological sample from Chichén Itzá is located in a very distant region than the rest of the samples. Therefore, and considering firstly our previous study with *B. copallifera*, secondly the distance between both archaeological sites and oral tradition, different botanical origin can be assumed for this sample.



**Fig 47** Distribution in the hyperspace of the resins samples from botanical certified origin, using the first two components plus FTIR data from archaeological samples: mathematical model was able to discriminate archaeological samples, from different archaeological sites. ● Sample from Chichén Itzá, ● Samples from Templo Mayor. Legend different species are shown as follows: ● *B. laxiflora*, ◆ *B. excelsa*, ■ *B. stenophylla*, ▲ *B. bipinnata*, ► *B. grandifloia*, ▼ *B. penicillata*.

Regarding archaeological samples from Templo Mayor, except from 173 (see yellow dot on figure 48), all of them were graphed in the region of the hyperspace corresponding to *B. bipinnata* and *B. stenophylla* origins.

Considering that sample 173 was part of offering 120 (see 2.4.1 of chapter 2, page 40) and that the general state of preservation of objects in this offering was inferior to that of objects from offerings 125 and 126, one can attribute the location out of the area comprised between *B. bipinnata* and *B. stenophylla* species to degradation process. To have a better understanding of this phenomena complementary separative techniques were applied, the results can be consulted on chapter four and five of this work.

Regarding ageing the sample that under microscopic observation seemed to be less deteriorated was sample 51, from offering 126 as its surface was not yellowed, has not great porosity and only exhibits some black dots on its surface. Position of sample 51 in the hyperspace was located between *B. bipinnata* group and mixed *B. bipinnata* and *B. stenophylla* groups; together with all the other Aztec archaeological samples.

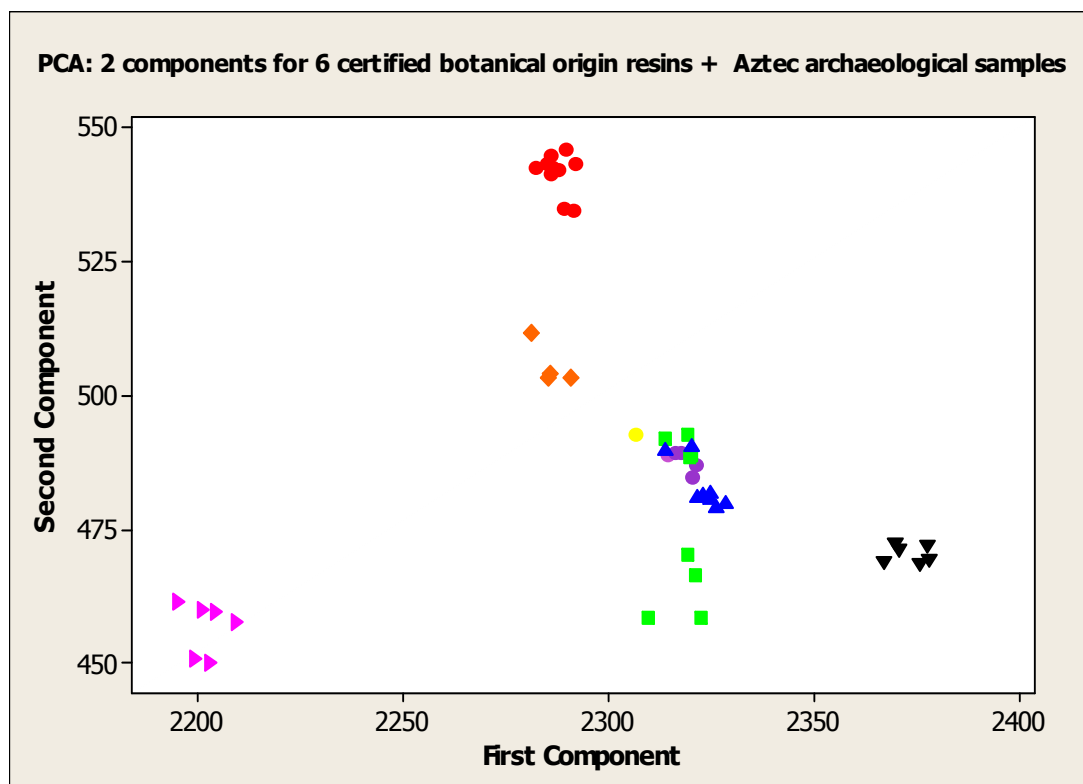


Fig 48 Distribution in the hyperspace of the resins samples from botanical certified origin, using the first two components plus Aztec archaeological samples. Legend different species are shown as follows: ● *B. laxiflora*, ◆ *B. excelsa*, ■ *B. stenophylla*, ▲ *B. bipinnata*, ► *B. grandiflora*, ▼ *B. penicillata*, ● 173, ● 26, 51, 52, 84, TMT, M1.

Therefore, taking into consideration that production of secondary metabolites and, specifically triterpenes from resins, are strictly gene regulated, molecular composition can be used as indicator for the producing tree species. Given the genetic distance of the repertoire species of *Bursera* known at this day is highly possible that the botanical origin of archaeological Aztec samples is comprised between *B. stenophylla* and *B. bipinnata* species. To probe this conclusion, additional studies using chromatographic techniques were performed (refer to chapters four and five of this work).

### 3.13 Partial analysis of the surface of the samples

Considering that the surface of the copal is the part that is more exposed to degradation factors, but also the more accessible when sampling patrimony objects, a study of the variations of FTIR spectra of this kind of materials was performed.

Previous studies (De la Cruz-Cañizares, 2005) had shown that Mexican copal contain many of the typical functional groups that promote auto-oxidation reactions, such as carbonyl groups,

carbon-carbon double bonds and tertiary carbon atoms. These reactions lead to degradation that manifests as yellowing and cracking (De la Rié, 1988).

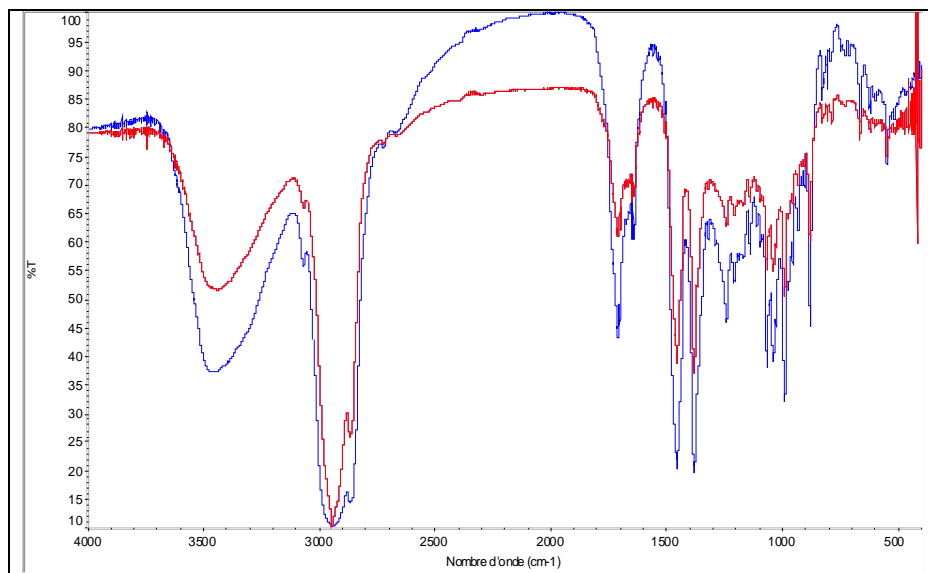
Light basically increases the initiation of the radical chain reactions, and oxidation proceeds mainly by light independent pathways (Dietemann, 2003). Nevertheless some differences have been remarked regarding the composition of resins under and without light exposition by other authors (Van der Doelen, 1988; Dietemann, 2003).

For this reason the most degraded surface found among the archaeological resins that we disposed (TMT), and two commercial samples (Huitzucó and SONB4) aged under natural light, were studied.

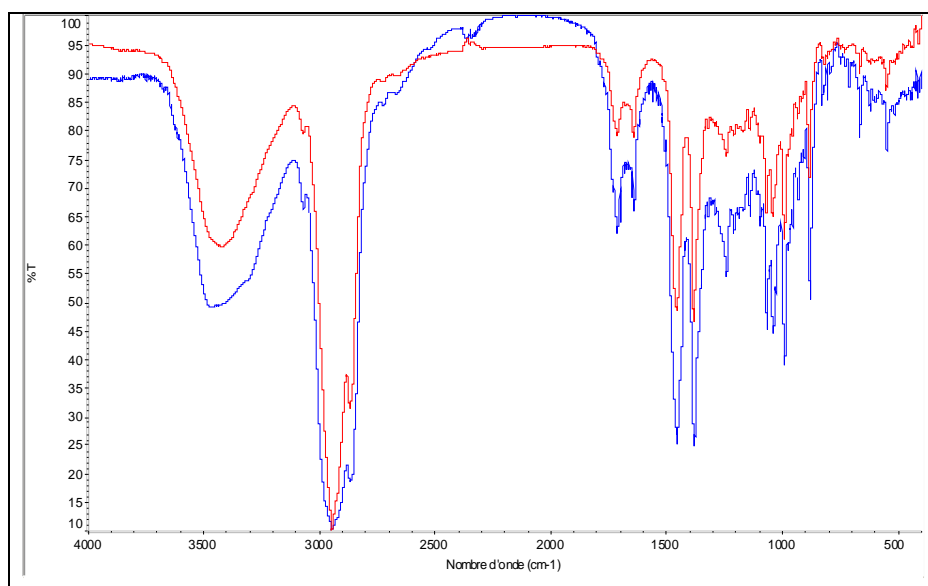
### **3.13.1 Comparison of partial analysis from commercial samples and a naturally aged sample of them**

Aging of a sample of Huitzucó and a sample of SONB4 were conducted as follows: a mass of 30 g of each commercial copal was exposed to natural light behind a window facing south, during two months and a half (September-December), in Avignon, France. The material subjected to FTIR analysis was taken from the surface of the sample in a deep not exceeding 3 mm, as UV does not penetrate to deeper layers.

A comparative of the FTIR spectra of fresh and aged samples is shown on figures 49 and 50. As expected considering the changes occurring when ageing, the spectra of both intentionally aged samples developed much increased absorption in areas correlated to hydroxy groups ( $3450\text{cm}^{-1}$ ), carboxylic acid groups ( $3200\text{-}2500\text{cm}^{-1}$ ) and carbonyl groups ( $1700\text{cm}^{-1}$ ) absorption .



**Fig 49** Comparative of FTIR spectra of — fresh and — light aged sample of Huitzuco (commercial sample).



**Fig 50** Comparative of FTIR spectra of — fresh and — light aged sample of SONB4 (commercial sample).

Together with the broadening of the bands a shifting in transmittance is observed, in order to assess the impact of this shifting of bands when using a FTIR-PCA model for the prediction of the botanical origin of a sample, tests were performed using both data from fresh and aged samples. The results can be seen in figures 50 and 51.

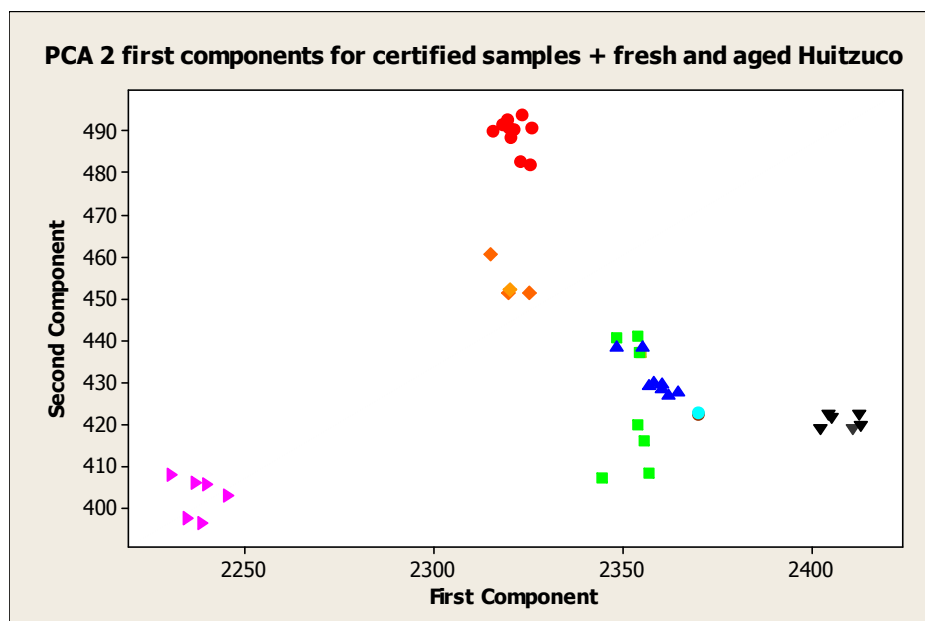


Fig 51 Distribution in the hyperspace of the resins samples from botanical certified origin, using the first two components plus samples of HUITZUCO fresh and aged. Legend different species are shown as follows: ● *B. laxiflora*, ◆ *B. excelsa*, ■ *B. stenophylla*, ▲ *B. bipinnata*, ► *B. grandiflora*, ▼ *B. penicillata*, ● fresh Huitzucó sample ● aged Huitzucó sample.

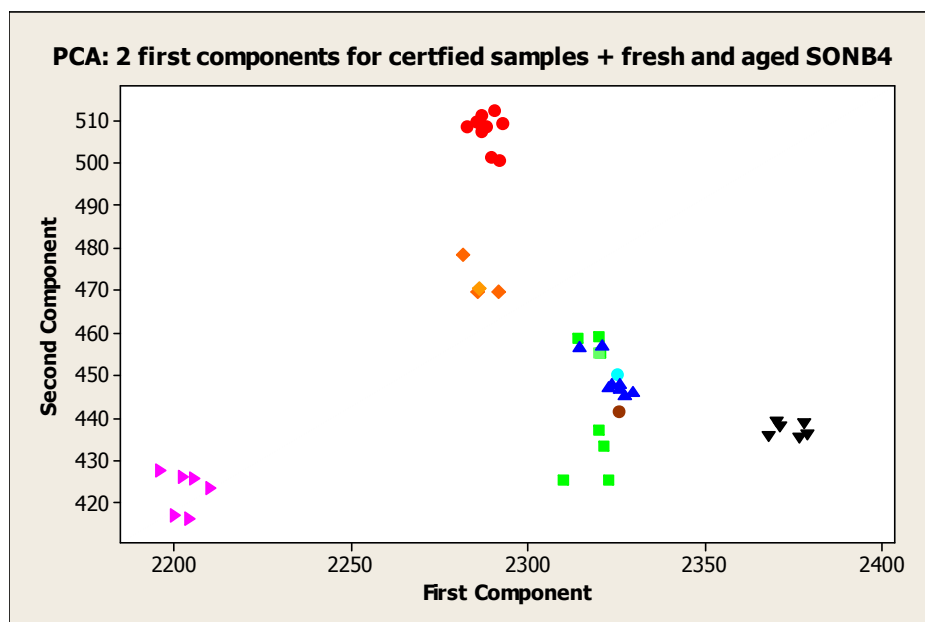


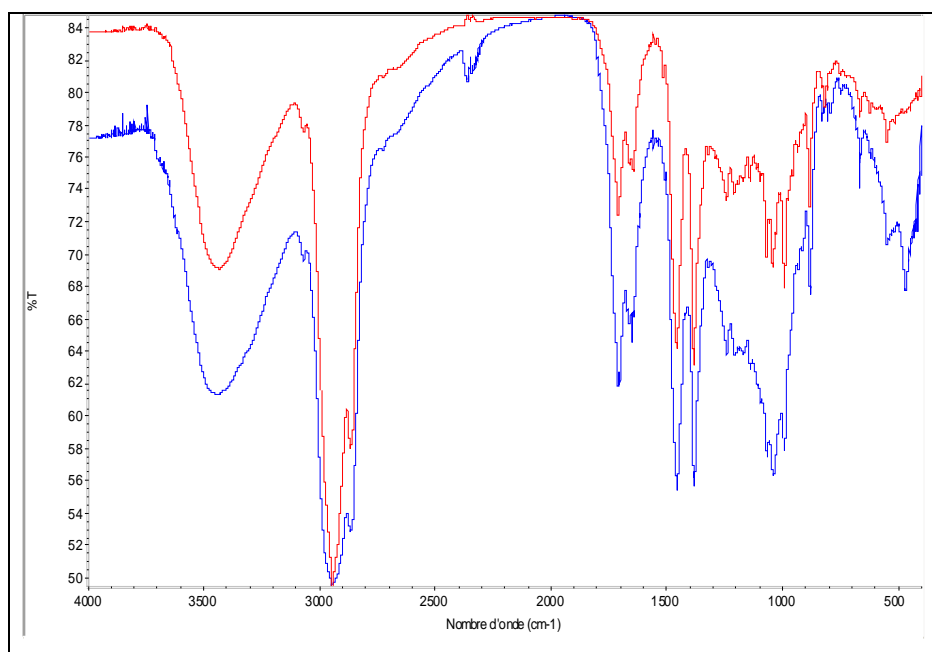
Fig 52 Distribution in the hyperspace of the resins samples from botanical certified origin, using the first two components plus samples of HUITZUCO fresh and aged SONB4. Legend different species are shown as follows: ● *B. laxiflora*, ◆ *B. excelsa*, ■ *B. stenophylla*, ▲ *B. bipinnata*, ► *B. grandiflora*, ▼ *B. penicillata*, ● fresh SONB4 sample ● aged SONB4 sample.

When PCA analysis was performed an almost imperceptible differences in the position of the sample Huitzuco were observed, and a slight more perceptible difference was observed in the SONB4 case.

For samples both fresh and aged the botanical origin remained between the *B. bipinnata* and *B. stenophylla* regions.

### 3.13.2 Spectra variation between external and internal part of an archaeological sample TMT

An equivalent study to that one performed on light aged samples was conducted on an archaeological sample. Samples from the outer (more degraded) and the inner part of the fragment were collected. Separated spectra from these samples were collected and are shown on figure 53. Again a broadening in the bands of hydroxy groups ( $3450\text{cm}^{-1}$ ), carboxylic acid groups ( $3200\text{-}2500\text{cm}^{-1}$ ) and carbonyl groups ( $1700\text{cm}^{-1}$ ) can be appreciated in the spectra of the surface sample, changes in spectra certainly seem to be more dramatic, which is natural considering the age of the sample (around 500 years).



**Fig 53** Comparative of FTIR spectra of the — inner part of TMT and — the more degraded surface of TMT

When PCA analysis was performed the location of the dot representing the inner part of the sample, it allowed us to establish *B. bipinnata* as the most probable origin for this sample, as it



falls right into the region corresponding to this species. In order to better appreciate this result some *B. bipinnata* triangles corresponding to *B. bipinnata* certified samples are not displayed as solid figures in figure 54.

Concerning the sample taken from the surface of the sample, it falls into the zone comprised between *B. bipinnata* and *B. stenophylla* species, and therefore from the data obtained from the surface the correlation to one of these two botanical origins can still be made. This results certified that ageing had an impact in spectra nevertheless even in the cases of very degraded archaeological samples, spectra still retain a good amount of information and can be useful when samples of the inner part of a piece are unavailable or when chromatographic methods can not be used.

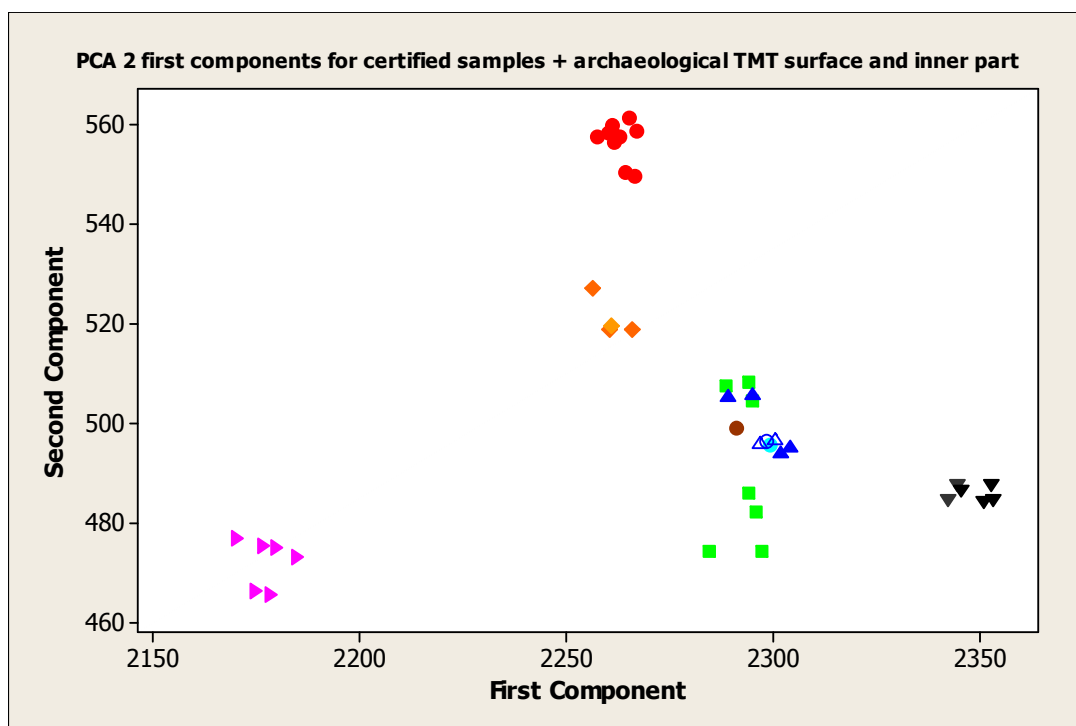


Fig 54 Distribution in the hyperspace of the resins samples from botanical certified origin, using the first two components plus TMT samples from its inner part and its surface. Legend different species are shown as follows: ● *B. laxiflora*, ◆ *B. excelsa*, ■ *B. stenophylla*, ▲ *B. bipinnata*, ► *B. grandiflora*, ▼ *B. penicillata* ● TMT sample from the inner part, ◆ TMT sample from the surface.

### 3.14 Conclusions

Usually the sensitivity of vibrational methods is considered lower in comparison to other analytical techniques but in some cases, also components occurring in low concentration can be successfully analyzed. In this chapter we prove that global molecular profiling with FTIR can be successfully applied in combination to powerful chemometrics tools like PCA and LDA to validate and analyze complex data from spectra, to be used into the classification of resinous material from unknown origin.

The homogeneity of modern resins of certified origin made their analysis easier, and permitted to establish a spectral bank of data for these species.

The genetic closeness of *B. stenophylla* and *B. bipinnata*, was confirmed indirectly by the closeness of their resin composition.

In this chapter the deconvolution of the bands of the region between 1200 and 1300  $\text{cm}^{-1}$  was performed onto fresh resins spectra, for the discrimination of samples from *B. stenophylla* and *B. bipinnata*. This method proved to be of great assistance when it comes to the classification of resins from close botanical origin.

It is important to note that conditions under which a sample aged significantly contribute to its chemical composition and consequently to its characteristic spectrum. This phenomenon was confirmed at different stages of this research, firstly when FTIR-PCA model was applied to the classification of archaeological resins as some of them fall in slightly different regions and secondly when partial analysis of the surface of aged resins was conducted, when partial spectra of fresh and more deteriorated resins were compared.

Auto-oxidation, condensation phenomena and degradation of triterpenoids can be cited among the processes that occur along time (Dietemann 2003). Along ageing, hardness and consistency of a resin change, due to the evaporation of the volatile fraction (Peris, 2008).

From these considerations caution should be kept when applying a discrimination model based on FTIR data of fresh resins into archaeological samples, but still reliable information can be obtained from this method. Additional information coming from archaeological reports may contribute with invaluable information about these materials.

To sum up this method seems to be a fast tool that can help to reduce possible botanical origins when great diversity of botanical sources is found.

As it has been stated before considering their strong gene regulation on the secondary metabolites as triterpenes, and considering genetic distances among the 80 species of *Bursera* threes, the archaeological Aztec resins may have their origin between *B. bipinnata* and

*B.stenophylla*. This turns FTIR spectroscopy in an invaluable tool for the conservator professionals implicated in archaeological works.

Assessing of the botanical origin of resins used in restoration of archaeological objects or even paintings is a must.

As stated by Dietemann in his work from 2003, “With increasing compositional complexity the reactivity of the reference substances increases, thus even greater reactivity is then expected in natural resins.” Therefore mixture of resins from different botanical origins may modify the original materials of a patrimony object and even worst it can result in accelerated degradation of them. In the authentication field, this method can be also used, as it has discriminated botanical origin for archaeological samples from different archaeological sites.

# Chapter IV

## Chromatographic techniques

### HPLC UV/Vis

## Chapter IV

### High Performance Liquid Chromatography -UV/Vis Analysis

Chromatographic techniques have been applied in several laboratories specialized in artworks. This came as consequence of their ability of separating organic compounds, from complex mixtures (Domenech, 2009). Chromatography comprises a group of methods for the separating molecular mixtures that depend on the differential affinities of the solutes between two immiscible phases.

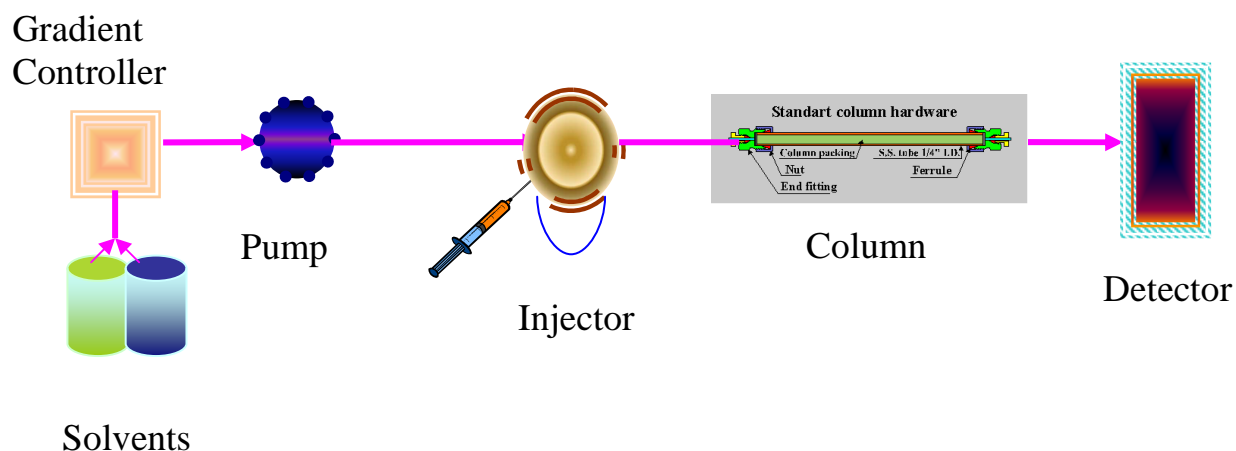
In the last years, high performance liquid chromatography (HPLC), and gas chromatography (GC) coupled to a mass detector (MS), have progressively replaced other less sophisticated techniques such as paper chromatography or thin layer chromatography because they can reach a higher discrimination of the type of the materials present in artistic objects. These techniques can also provide a more complete description of the alteration products present in the sample. In this aspect their superiority compared to spectroscopic techniques is undeniable (Doménech, 2009).

Their major drawbacks are that they are that depending on the type of detection they may be destructive, and cannot document the organization of heterogeneous samples (Daher, 2010). They also implicate pretreatments, like purification, extraction and derivatization that may be time consuming and modify original composition.

#### 4.1 High Performance Liquid Chromatography (HPLC)

HPLC is a form of liquid chromatography used to separate compounds that are dissolved in solution. Separation is based on the partition coefficient of a given analyte. Partition refers to the relative solubility of the analyte between two liquid phases: a mobile one and a static one. There are two operation modes: Normal phase with polar stationary phase and non-polar solvent and reverse phase with a non-polar stationary phase and a polar solvent.

A classical HPLC device is constituted by a gradient controller, a pump, an injector, a column and a detector. A schematic view of their arrangement is presented on figure 55.



**Fig 55 Schematic view of HPLC instrumentation and their components**

For this research we have chosen to study both the totality of the resins for its convenience for molecular profiling when applying the statistical methods of PCA and LDA, and the triterpenic fraction because of the resistance of these compounds to degradation, and its possible utility as molecular markers.

The first difficulty for the study of resins by HPLC arisen, when studying samples from certified botanical origin, because of the need of different amounts of sample depending on their terpenoid content of the studied species: from 2 mg up to 30 mg, refer to table 10.

Type of sample	Mass of sample used for HPLC analysis
<i>B. bipinnata</i>	3 mg
<i>B. stenophylla</i>	3 mg
<i>B. excelsa</i>	6 mg
<i>B. laxiflora</i>	6 mg
<i>B. penicillata</i>	3 mg
<i>B. simaruba</i>	30 mg
Commercial resins	From 2 mg up to 30 mg
Archeological resins	2 mg

**Table 10 Amount of resins used for the HPLC chromatographic study**

In this study the amount of resin needed for the analysis was directly correlated to the amount of gum present in the sample: at higher amount of gum, less terpenoids and more needed sample for the analysis. This study was performed by solving a known amount of rough resin in diethyl ether. After sonication and centrifugation, the residue left in the bottom of the solution was dried and weight. The percentage of gum was calculated from this data.

Finally, water was added to ensure the polarity of the residue. This data is consistent with, FTIR spectra. As presented in chapter 3, the samples from these species (*B. simaruba* and *B. grandifolia*) afforded a broaden band in  $3430\text{ cm}^{-1}$ .

Table 11 resumes the percentage of gum (non soluble material in apolar solvents) found in each studied species.

	% Gum	% Resin
<i>B. bipinnata</i>	0	100
<i>B. excelsa</i>	0.5	99.5
<i>B. simaruba</i>	25	75
<i>B. penicillata</i>	0	100
<i>B. stenophylla</i>	0	100
<i>B. laxiflora</i>	8	92
<i>B. grandifolia</i>	75	25

**Table 11 Gum and resin percentage in resin samples from certified species**

Generally speaking gum ratio is correlated to the producing species but this fact it cannot constitute a reliable factor for botanical identification, as gums are water soluble, widely distributed, and easy degradable materials. The big proportion of gum in *B. grandifolia* exudates prevented its study by HPLC, in fact some attempts were done but we concluded that for this kind of study, a much larger quantity than the actual amount of sample from what we dispose would be needed.

We performed the same type of analysis into archeological samples, solving a known amount of resin in ether; the ratios on non soluble matter founded are here reported (table 12). Nevertheless further test showed that this material was also insoluble in polar solvents.

	% Non soluble matter	% Resin
<b>TMT</b>	0.20	99.80
<b>Chicén Itzá</b>	4.38	95.62
<b>173</b>	1.73	98.23
<b>84</b>	2.68	97.32
<b>52</b>	0.16	99.84
<b>51</b>	0	100
<b>26</b>	5.72	94.28

**Table 12 Insoluble matter in apolar solvents in archeological samples**

Therefore we believe that the percentage of insoluble matter could be constituted in a good amount by particular matter, possibly from mineral origin as. Owing to its low quantity it was not possible to determinate the nature of this material by this or any other analytical technique in our hands FTIR, and FTIR- ATR included.

To sum up, the ratio of gum present in archeological samples is almost zero, this fact can be correlated either to the botanical origin of the sample or to the fact that these samples were exposed during a long time to high moisture and even under-water conditions.

The second difficulty of analyzing these materials by HPLC relies in the nature of the resins themselves, which are chemically very complex: Witte *et al.* described the analysis of terpenoids like problematic and indicates that their complete chromatographic separation is almost impossible, even by using sufficiently long chromatographic colons, some of these compounds may not be totally resolved (Witte, 1986). Indeed, *Bursera* resins consist of compounds with very similar structure, and some of them may present identical times of retention. This complexity increases further with degradation process. The identification of composed on the basis of their time of retention or their order of elution is consequently not always reliable (Burger, 2003).

For the HPLC study, both standards and global resins were solved on methanol, the designed protocol can be consulted in the materials and methods section of this work.



## 4.2 Standard molecules

Liquid chromatography was applied to the study of six standard molecules (table 13), at 210 nm, which is the general wavelength number for the study of resins.

The availability of triterpenic standards, and other materials often found in artworks like extended the application of chromatography to their identification, and the present research take advantage of this fact. In contrast the difficulty of obtaining standards of the oxidised alteration product formed during ageing from terpenoid compounds makes difficult the application of this technique to the identification of ancient materials. Therefore a GC-MS study was performed afterwards on resin samples to obtain a better characterization of concerned materials.

N°	Molecule	Retention time (min)
1	3- <i>epi</i> -lupeol	26.5
2	lupeol	27.6
3	3- <i>epi</i> - $\beta$ -amyrin	28.2
4	lupenone	28.7
5	3- <i>epi</i> - $\alpha$ -amyrin	29.4
6	$\beta$ -amyrin	29.9
7	$\alpha$ -amyrin	31.3
8	$\beta$ -amyrone	31.4
9	$\alpha$ -amyrone	32.2

**Table 13 Time of retention of standard molecules under the designed HPLC gradient**

Molecules  $\alpha$ - amyrin,  $\beta$ -amyrin, lupeol, and lupenone were purchased from Extrasynthèse (Genay, France),  $\alpha$ - amyrone and  $\beta$ -amyrone were purchased from BCP instruments (Irigny, France). 3-*epi*-lupeol, 3-*epi*- $\alpha$ -amyrin, 3-*epi*- $\beta$ -amyrin were isolated by our team from commercial samples.

## 4.3 Quantification of triterpenoids: analytical calibration

Standard solutions containing the above triterpenic compounds, at different concentrations were prepared and then injected by triplicate into the HPLC system. The outflow from the column was monitored by a diode array detector, operating at 210 nm.

Then the concentration of each of these molecules was calculated in each sample by introducing the peak-area into the equation of the curve.

<b>Triterpenic standard</b>	<b>Linearity range (<math>\mu\text{g/mL}</math>)</b>	<b>Calibration equation</b>	<b>LOD (<math>\mu\text{g/mL}</math>)</b>	<b>LOQ (<math>\mu\text{g/mL}</math>)</b>	<b>Correlation coefficient (<math>R^2</math>)</b>
$\alpha$ -amyrin	2.75-0200	$Y = 24499375.88 * X - 100187.19$	<b>3.52</b>	<b>11.7</b>	0.9993
$\alpha$ -amyrone	0.6041-290	$Y = 11485526.05 * X + 25383.31$	<b>2.5</b>	<b>10.6</b>	0.9995
$\beta$ -amyrin	2.2-100	$Y = 116395 * X - 37759.24$	<b>3.7</b>	<b>12.5</b>	0.9992
$\beta$ -amyrone	2.1-100	$Y = 8693057.33 * X + 31615.5$	<b>2.97</b>	<b>9.9</b>	0.9989
lupeol	0.5-100	$Y = 8862571 * X + 40562.44$	<b>2.07</b>	<b>6.9</b>	0.9996
lupenone	0.6-100	$Y = 11235316.61 * X + 26491.86$	<b>6.25</b>	<b>20.8</b>	0.9995

**Table 14 Statistical data from calibration. Chromatographic conditions: detection at 210 nm for standard compounds**

The linear calibration ranges, regression equations and, detection limits of these standard compounds were calculated. The results are listed in table 14. The linearity was tested in a variable concentration range according each molecule; their correlation coefficients are from 0.9989 to 0.9996. The limit of detection (LOD  $S/N = 3/1$ ) and the limit of quantification (LOQ  $S/N = 10/1$ ) were respectively lower than 3.7  $\mu\text{g/mL}$  and 20  $\mu\text{g/mL}$ .

Peaks were identified by co-injection with standard molecules, then corresponding area was taken into calibration equation and concentration of the concerned molecule was calculated. The results of these calculations are presented in annex 3 (tables 45-48).

#### **4.4 Global analysis of certified resin samples**

Chromatograms in liquid phase allowed a very clear interspecies distinction.

It is noteworthy to say that two regions of peaks can be distinguished on each chromatogram: the first one going from 0 to 24 minutes and the second running from 24 to 35 minutes.

The first zone corresponds with components from lower molecular weight and highest polarity (compounds with a molecular mass that corresponds to mono and sesquiterpens in UPLC-MS).

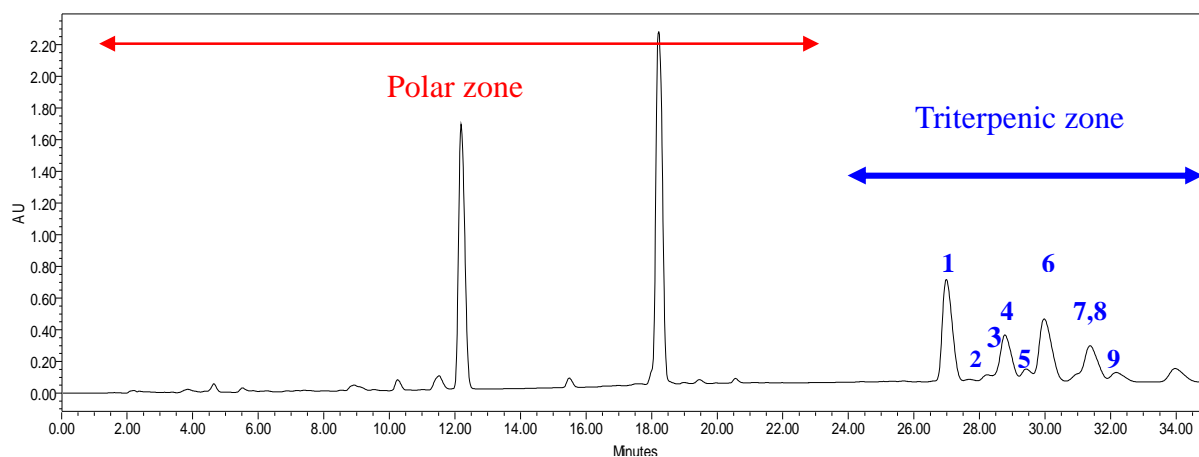
The second group of peaks in the chromatogram corresponds to molecules of higher molecular weight and lower polarity; these molecules were identified by co-injection with standard molecules as triterpenes.

In one hand, the composition of the more polar fraction is very different in both quantitative and qualitative terms for both species.

In the other hand a very homogeneous composition of the triterpenic fraction in qualitative terms was found for all resins (botanically certified, archeological and commercial samples) nevertheless the relative amount of each compound, for each species is quite particular.

These facts allowed us to model a molecular fingerprint by means of PCA this subject will be further discussed in this chapter.

In figure 56 we present a chromatogram of *B. bipinnata* where the two above mentioned areas of peaks are distinguished: in red the polar one, and in blue the triterpenic one. All triterpenes, identified in this research were assigned a number, according to their elution order. Number assignment will be kept all along this chapter for the identification of these molecules in other chromatograms.



**Fig 56** Chromatogram of *B. bipinnata* (sample 11d2), triterpenic zone running from 24 to 35 min in retention time

Number	Compound
1	3- <i>epi</i> -lupeol
2	lupeol
3	3- <i>epi</i> - $\beta$ amyryl
4	lupenone
5	3- <i>epi</i> - $\alpha$ amyryl
6	$\beta$ -amyryl
7/8	$\alpha$ -amyryl/ $\beta$ -amyryl
9	$\alpha$ -amyryl

**Table 15** Number assignment for identified triterpenoid compounds

#### 4.5 Comparison of global chromatograms from certified origin resins

As it was said before, differences can be remarked concerning the global molecular composition of each species. In one hand table 16 resume the presence and absence compounds of lower molecular weight and more polarity (from the red zone), in the other hand table 17 resumes the presence and absence of triterpenoids (blue zone) in each species of resins.

Concerning the second part of the chromatograms it is worthy to say that other triterpenic compounds were present in each sample, nevertheless it is at this point that UV/Vis reach is limits concerning differentiation of molecules with close structure, and therefore a more sensitive method as GC-MS was used for the detection and identification of these molecules, for an account into this matter refer to the GC-MS chapter of this work.

ID of the peak	A4	A3	A2	A1	B1	B2	B3	B4	B5	B6	B7	B8
Ret. time (min)	8.9	10	11.4	12	16	16.5	17	18	19.4	20	20.6	24
<i>B. bipinnata</i>	-	+	+	+	-	-	-	+	+	-	+	-
<i>B. excelsa</i>	-	+	-	+	+	-	-	-	+	+	-	+
<i>B. laxiflora</i>	+	+	+	+	+	+	-	-	-	-	-	+
<i>B. laxiflora</i>	-	-	+	+	+	+	-	-	-	-	-	+
<i>B. penicillata</i>	-	-	-	+	+	-	+	+	+	-	-	-
<i>B. simaruba</i>	-	+	+	+	-	-	-	-	-	+	-	-
<i>B. stenophylla</i>	+	+	+	+	-	-	-	+	-	-	-	-

Table 16 Retention time of peak corresponding to non triterpenic compounds founded in each species (+ presence, -absence)

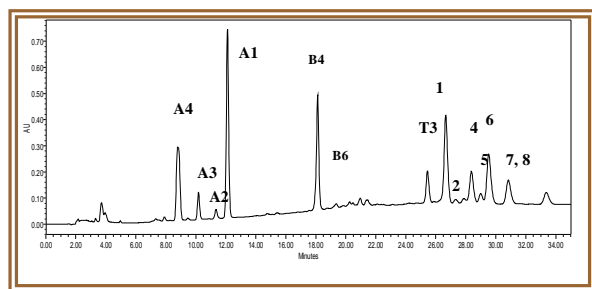
ID of the peak	3- <i>epi</i> -		3- <i>epi</i> - $\beta$		3- <i>epi</i> - $\alpha$	$\beta$ -	$\alpha$ -amyrin/		T4	
	T3	lupeol	lupeol	amyrin	lupenone	amyrin	amyrin	$\beta$ -amyrone		$\alpha$ -amyrone
Ret. time (min)	25.5	26.5	27.6	28.2	28.7	29.4	29.9	31.3	32.1	33.5
<i>B. bipinnata</i>	-	+	+	+	+	+	+	+	+	-
<i>B. excelsa</i>	+	+	+	-	+	-	+	-	-	-
<i>B. laxiflora</i>	-	+	+	+	+	-	+	+	+	-
<i>B. laxiflora</i>	-	+	+	-	+	-	+	+	+	-
<i>B. penicillata</i>	-	+	+	+	+	+	+	+	+	-
<i>B. simaruba</i>	-	+	+	+	+	+	+	+	+	-
<i>B. stenophylla</i>	+	+	+	+	+	+	+	+	+	+

Table 17 Retention time of peaks corresponding to triterpenic compounds found in each species (+ presence, -absence)

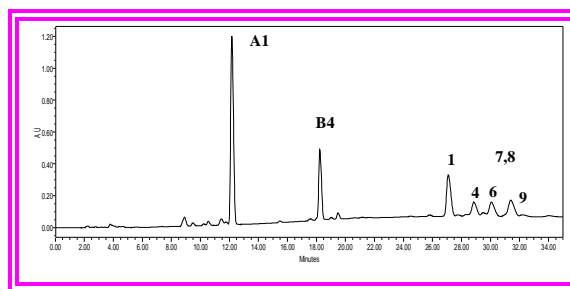
Regarding the first part of the chromatogram we chose a notation for compounds beginning either with letters A or B.

Compounds with an “A” notation are widely distributed in the 6 species, most of the time A1 is a major peak in their chromatograms. While “B” compounds are specific for each species, meaning that their presence and quantity varies a lot among species.

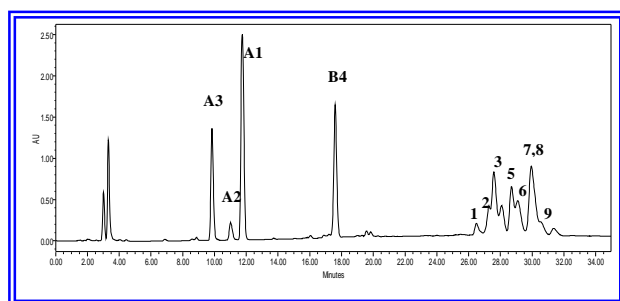
*B. stenophylla*



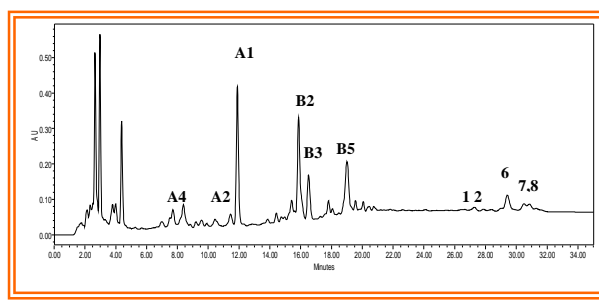
*B. bipinnata*



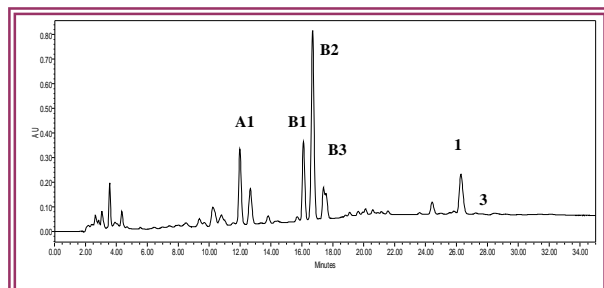
*B. simaruba*



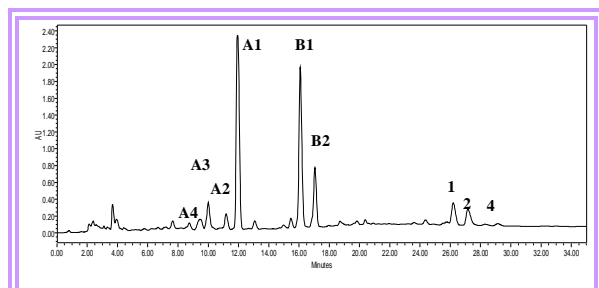
*B. penicillata*



*B. laxiflora*



*B. excelsa*

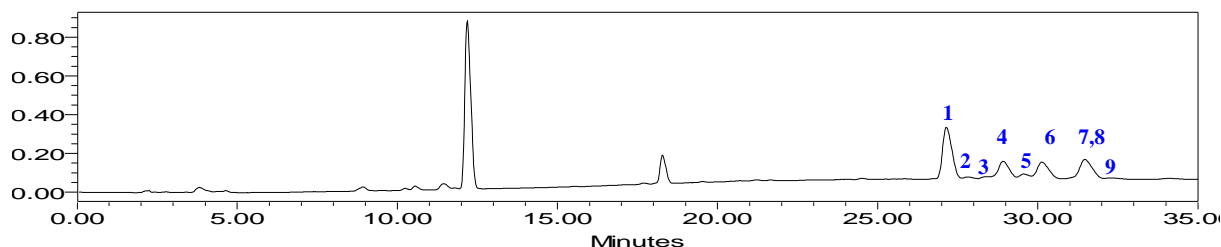


**Fig 57 Chromatograms for certified resins.** Identification of triterpenic compounds is as follows: 1) 3-*epi*-lupeol, 2) lupeol, 3) 3-*epi*- $\beta$ -amyrin, 4) lupenone, 5) 3-*epi*- $\alpha$  amyirin, 6)  $\beta$ -amyirin, 7/8  $\alpha$ -amyirin/  $\beta$ -amyirone, 9)  $\alpha$ -amyirone

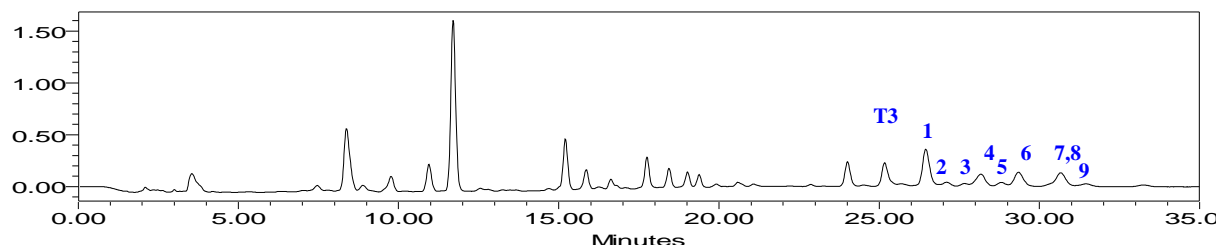
Figure 57 presents the chromatogram for each species and an account on the detection of the major peaks for both polar and triterpenic molecules.

When looking to these chromatograms, we conclude that the closest triterpenic molecular composition in qualitative terms is found between *B. bipinnata* and *B. stenophylla*. A difference between *B. bipinnata* and *B. stenophylla*, is the absence of the compound **T3** at 25.4 min in *B. bipinnata* (cf figure 58). Concerning the polar zone *B. stenophylla* seems to be richer qualitatively speaking, as at least 4 major peaks can be distinguished in this species. For *B. bipinnata* only two major peaks can be seen, in the polar zone.

*B. bipinnata*, sample 11b2 sample

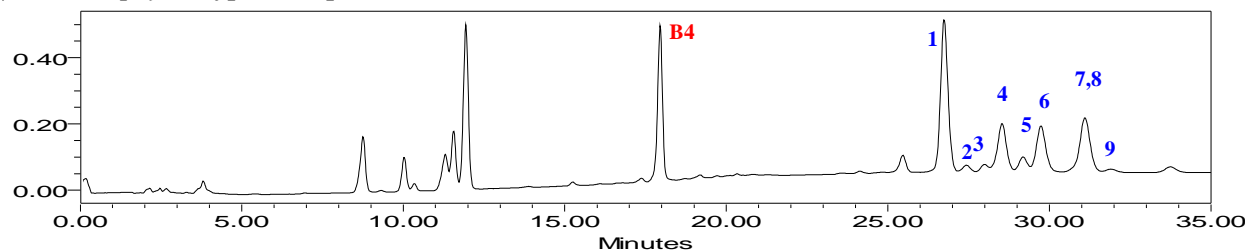
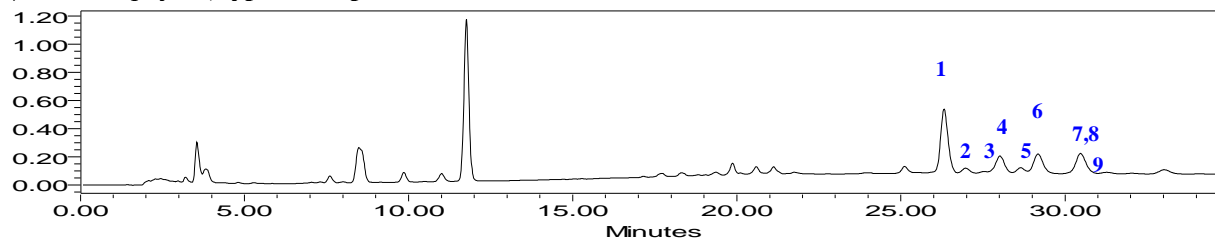


*B. stenophylla*, sample 72c2 sample



**Fig 58 Comparison of *B. bipinnata* and *B. stenophylla* chromatograms.** Identification of triterpenic compounds is as follows: 1) 3-*epi*-lupeol, 2) lupeol, 3) 3-*epi*- $\beta$ -amyrin, 4) lupenone, 5) 3-*epi*- $\alpha$  amyrin, 6)  $\beta$ -amyrin, 7/8  $\alpha$ -amyrin/  $\beta$ -amyrone, 9)  $\alpha$ -amyrone

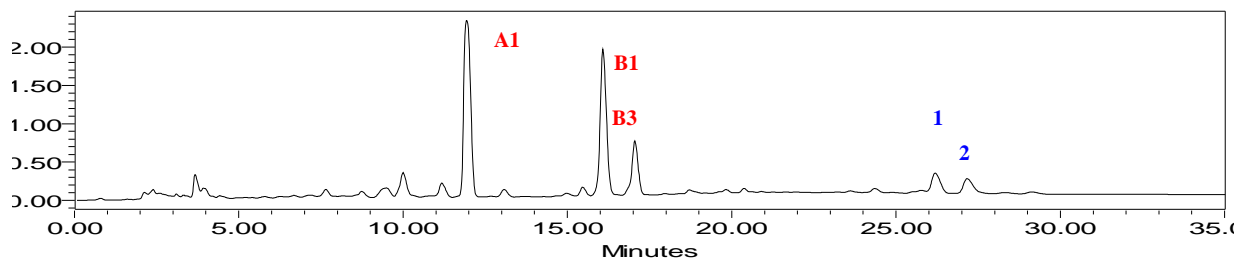
It is important to note that for *B. stenophylla* two lots can be distinguished: one with the presence of B4 and another one without it. Here in figure 59 we present a chromatogram of each type of *B. stenophylla* resin.

*B. stenophylla*, type 1 sample 72 a2*B. stenophylla*, type 2 sample 72d2

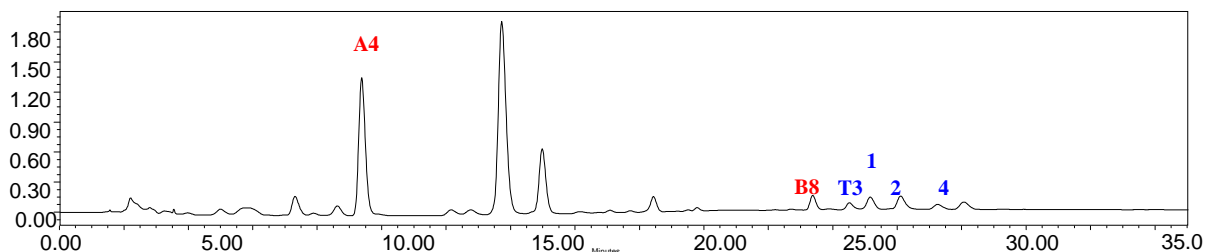
**Fig 59 Chromatograms of samples type A and B of *B. stenophylla*.** Identification of triterpenic compounds is as follows: 1) 3-*epi*-lupeol, 2) lupeol, 3) 3-*epi*- $\beta$ -amyrin, 4) lupenone, 5) 3-*epi*- $\alpha$  amyrin, 6)  $\beta$ -amyrin, 7/8  $\alpha$ -amyrin/  $\beta$ -amyrone, 9)  $\alpha$ -amyrone

Concerning *B. excelsa* two lots can be distinguished as well, based in the molecular composition of both more polar and triterpenic fractions, these differences can be appreciated on figure 60.

Although three major peaks can be distinguished in the polar zone, based upon their retention times, different identifications can be attributed to each one. Concerning the triterpenic fraction, type 1 seems to have a wider variety of different molecules than type 2.

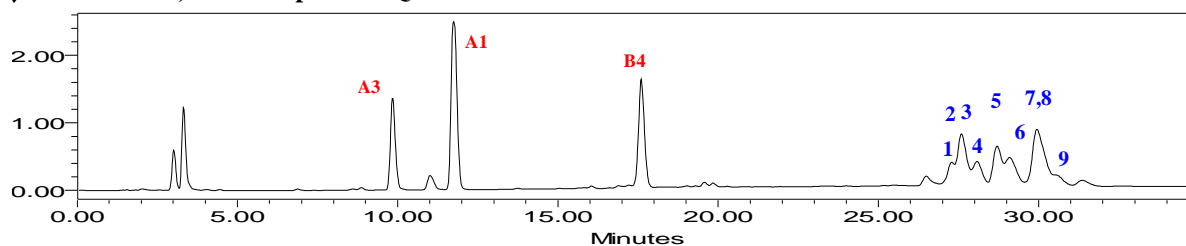
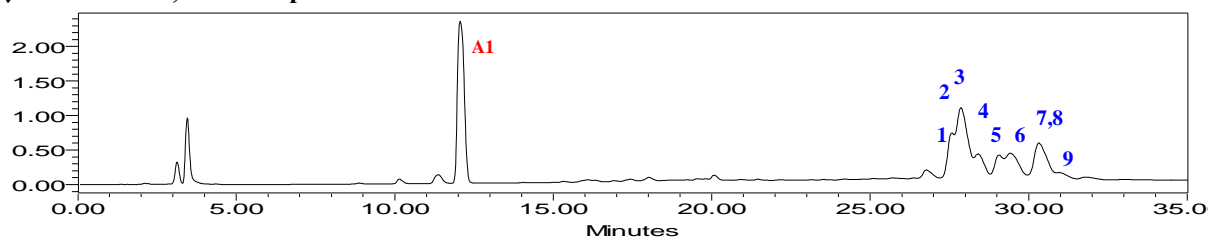
*B. excelsa*, type 1 sample 27a2

Identification of triterpenic compounds is as follows: 1) 3-*epi*-lupeol, 2) lupeol.

*B. excelsa*, type 2 sample 27a4

**Fig 60** Molecular profile types 1 and 2 of *B. excelsa*. Identification of triterpenic compounds is as follows: 1) 3-*epi*-lupeol, 2) lupeol, 4) lupenone.

Similarly in the case of *B. simaruba*: two molecular profiles based upon the composition of the resin can be described: a first one which contains three major peaks in the more polar zone (A3, A4 and B4) of the chromatogram, while the second one has a single major peak (A1) in the same chromatographic region (figure 61). Concerning the triterpenic fraction of the resin, both profiles have an identical composition.

*B. simaruba*, lot 1 sample 70a1Q*B. simaruba*, lot 2 sample 70d2

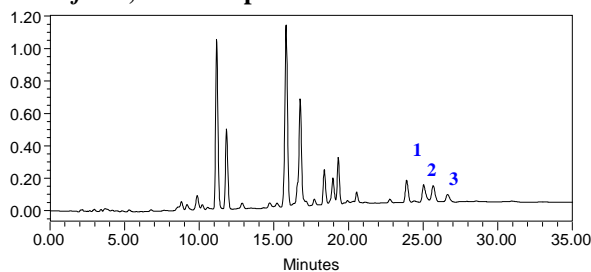
**Fig 61** *B. simaruba* lot 1 with a richer polar fraction than lot 2. Identification of triterpenic compounds is as follows: 1) 3-*epi*-lupeol, 2) lupeol, 3) 3-*epi*- $\beta$ -amyrin, 4) lupenone, 5) 3-*epi*- $\alpha$  amyirin, 6)  $\beta$ -amyrin, 7/8  $\alpha$ -amyrin/  $\beta$ -amyrone, 9)  $\alpha$ -amyrone

In contrast to the already mentioned species *B. penicillata* shows a very homogeneous composition which has already reflected in figure 57 of this work.

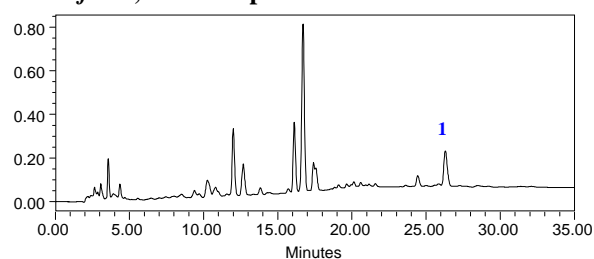


Finally the species that exhibits the greater diversity in molecular composition is *B. laxiflora*, within this species six groups could be distinguished and two of these groups (lots 1 and 2) counted more than five individuals (*cf* figure 62).

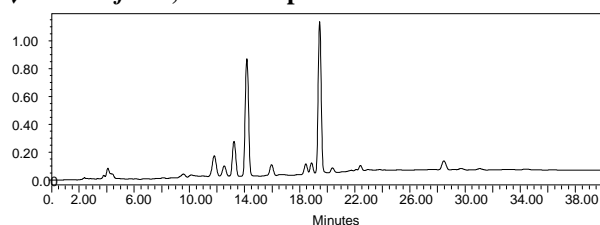
*B. laxiflora*, lot 1 sample 47a1



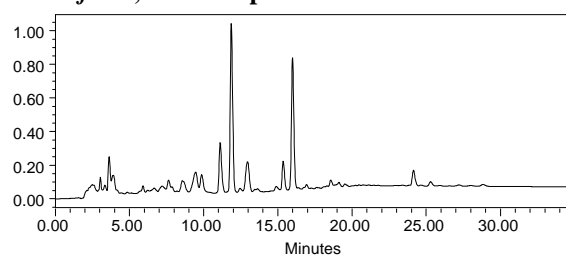
*B. laxiflora*, lot 2 sample 47b2



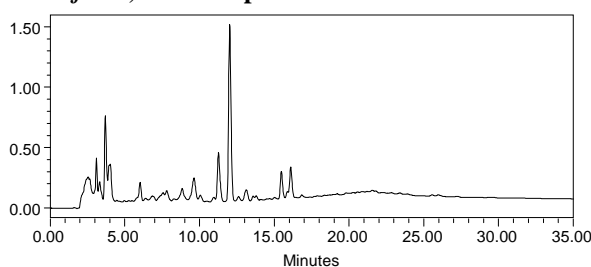
*B. laxiflora*, lot 3 sample 47e1 \*



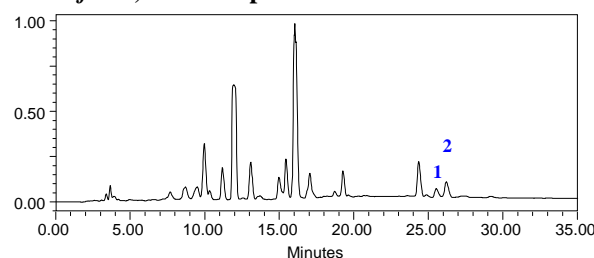
*B. laxiflora*, lot 4 sample 47d1



*B. laxiflora*, lot 5 sample 47c1



*B. laxiflora*, lot 6 sample 47f1



**Fig 62** The six different molecular profiles for *B. laxiflora*

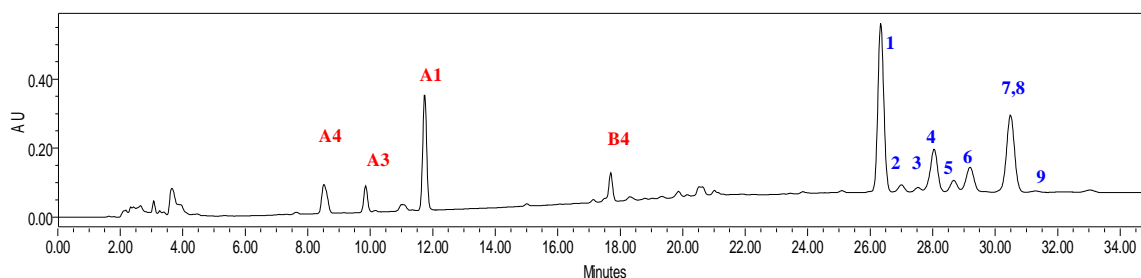
\* Due to a change in the instrumentation mode of injection (from a manual to an automatic injector) times of retention were enlarged, therefore to analyze this sample an enlarged protocol described in the Materials and methods section was used. The gradient remains the same, but 5 extra minutes were added to the running time.

#### 4.6 Comparison of global chromatograms from commercial resins

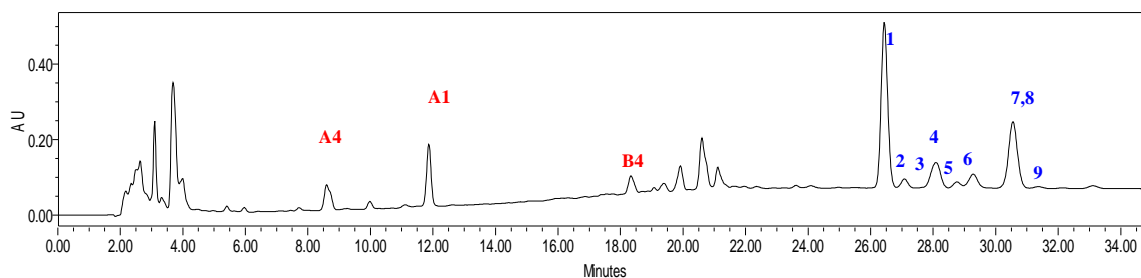
Concerning commercial copals with a whitish to yellow aspect two species were certainly differentiated by HPLC : *B. bipinnata* and *B. steophylla*. An important remark to these results is that no correlation can be established between botanical origin and physical aspect (color) of a resin, confirming data from the literature (Régert, 2008)

From this point of view, commercial samples ATZB1 and Huitzuco are likely to be *B bipinnata* resins, as the molecular composition determined by HPLC-UV/Vis means, seems to be the same. Here in figure 63, we present some chromatograms of these samples.

##### ATZB1



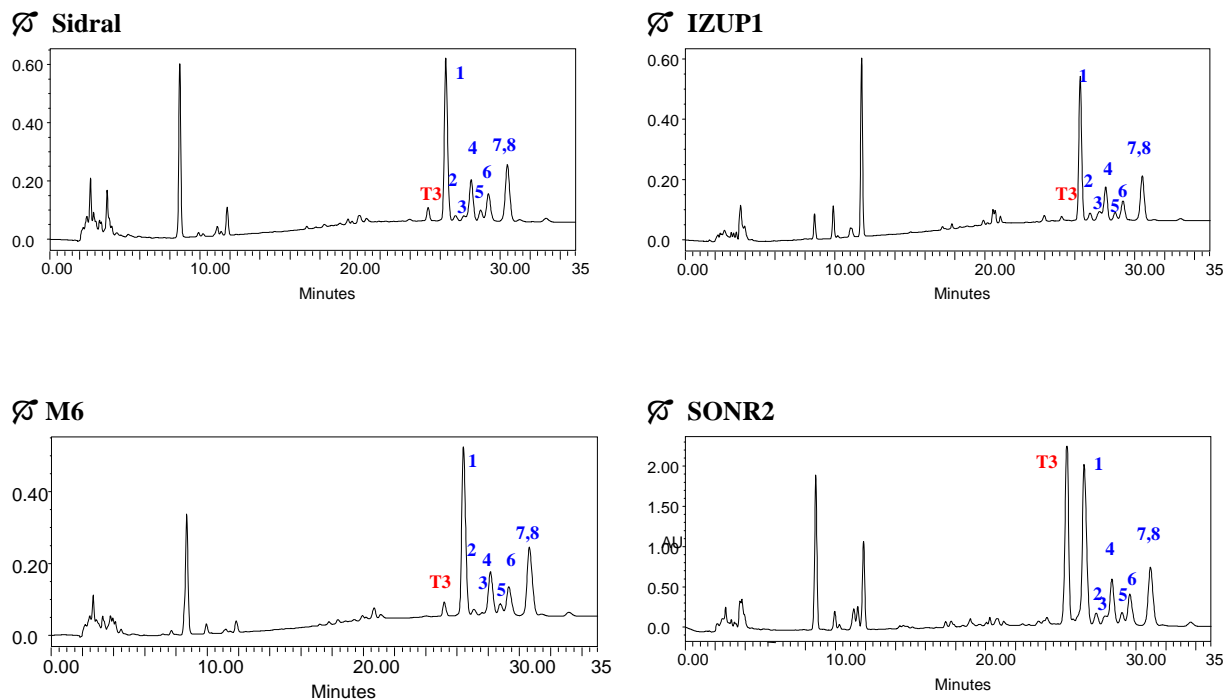
##### Huitzuco



**Fig 63 Chromatograms of ATZB1 and Huitzuco commercial samples that have the same molecular composition than *B. bipinnata* samples.** . Identification of triterpenic compounds is as follows: 1) 3-*epi*-lupeol, 2) lupeol, 3) 3-*epi*- $\beta$ -amyrin, 4) lupenone, 5) 3-*epi*- $\alpha$  amyrin, 6)  $\beta$  -amyrin, 7/8  $\alpha$ -amyrin/  $\beta$  -amyrone, 9)  $\alpha$ -amyrone

In the other hand based upon the great variation observed among the molecular profile of the studied certified resins, it is highly possible that commercial resins CHOB1, CHOB3, CHOM1,

Sidral, IZUM1, IZUP1, M6, M6Q, and red copal SONR2, are from *B. stenophylla* origin. (cf figure 64). As they present a molecular profile similar to that of this species.



**Fig 64 Chromatograms of commercial samples with a molecular profile close to *B. stenophylla* resin.**

Identification of triterpenic compounds is as follows: 1) 3-*epi*-lupeol, 2) lupeol, 3) 3-*epi*- $\beta$ -amyrin, 4) lupenone, 5) 3-*epi*- $\alpha$  amyrin, 6)  $\beta$ -amyrin, 7/8  $\alpha$ -amyrin/  $\beta$ -amyrone, 9)  $\alpha$ -amyrone

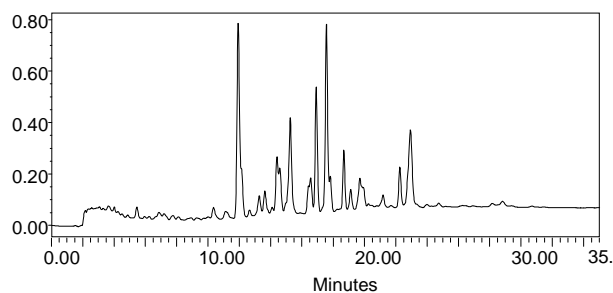
Many commercial samples, afforded chromatograms with too few or no triterpenes at all (figure 65), The physical aspect of this copals was white in the case of: MEXM1, ATZB2, Colima L2, OAXC1, OAXC2 and OAXC3, yellow for Incienso ATZJ2, and red for IZUR1. This information is a sign of a very different botanical origin, for these resins.

In many cases, most of their molecular compounds are located in the intermediate part of the chromatogram. Further studies need to be done upon these resins in order to find their botanical origin, again a more sensitive technique as GC-MS

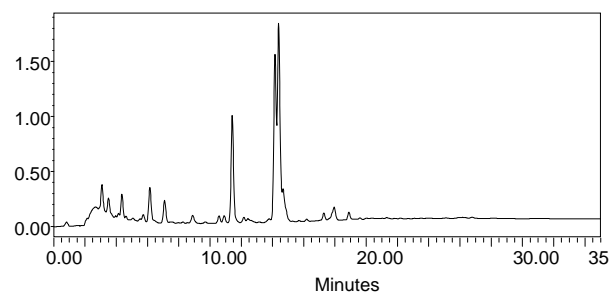
Some of these resins were bought within the same geographical location and nevertheless have a very different botanical origin. This has an impact towards the utilisation of commercial resins into restoration works: all commercial resins should be tested in order to ensure that its

composition is as close to original material as possible, to avoid possible interactions, and accelerated degradation from a more complex mixture of compounds (Dietemann, 2003).

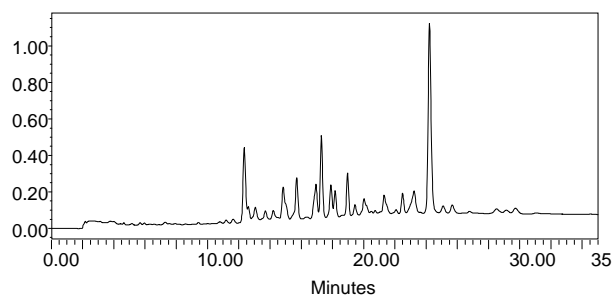
☞ ATZJ2



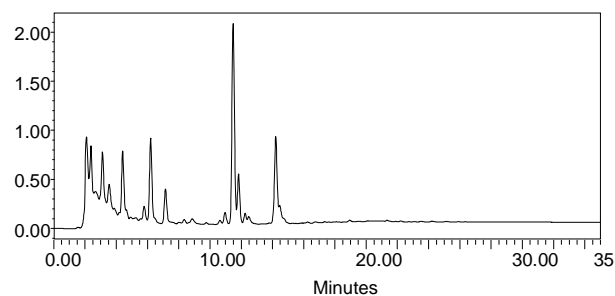
☞ Colima L2



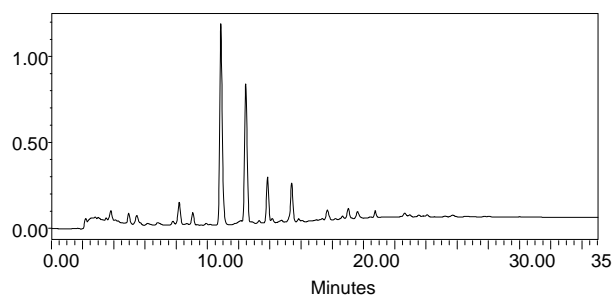
☞ OAXC1



☞ OAXC3



☞ OAXC2



**Fig 65** Chromatograms of some commercial samples from unknown botanical origin, presumably not within *Bursera* species

#### 4.7 Comparison of global chromatograms of archaeological resins

The purpose of the study of the archeological resin samples was to offer a methodology that can corroborate some assumptions about the use of copal in pre-Columbian times as adhesive, and molding material.

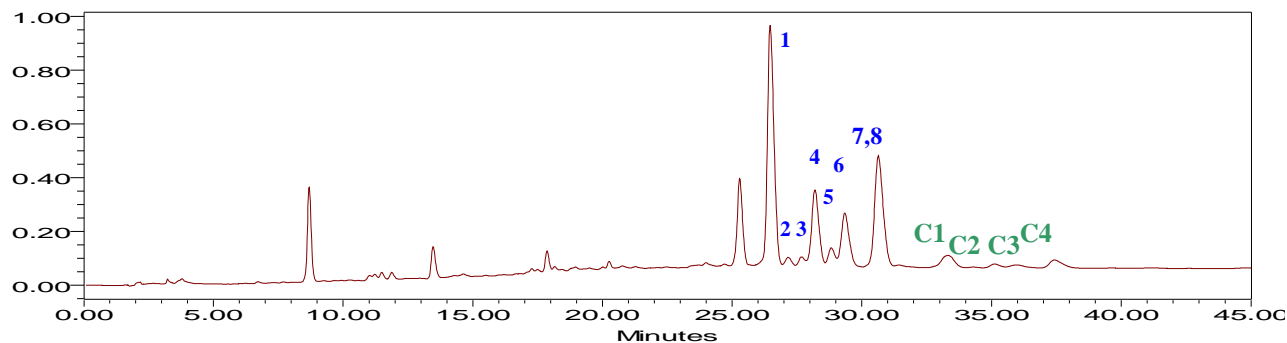
Despite the age of archeological samples, and their preservation under different conditions of relative humidity, pH, and temperature, their molecular composition retained most of the triterpenic fraction compounds except for 3-*epi*- $\beta$  amyrin and T3.

Considering the chromatogram profiles of Aztec materials coming from Templo Mayor, and those from botanical certified samples, HPLC results may suggest as botanical origin for these samples either *B. bipinnata* or *B. stenophylla*. In order to corroborate these results PCA was coupled to HPLC data, GC-MS was applied as well, and results of this analysis will be presented below and in chapter V.

The main molecular difference between these two species is compound T3, unfortunately it tends to disappear from aged resins.

In the molecular level, the study of archeological resins by this technique allowed us to detect molecules that were not present in fresh samples, the peaks corresponding to these molecules can be appreciated from minutes 32.5 to 36, in figure 66. Here we present the chromatogram of sample 173, the triterpenes present in fresh samples are marked in black, while C1 to C4 in green, represent the molecules either from higher molecular weight or higher polarity than molecules present in fresh samples. An adapted protocol for the study of these samples can be found in the materials and methods section of this work.

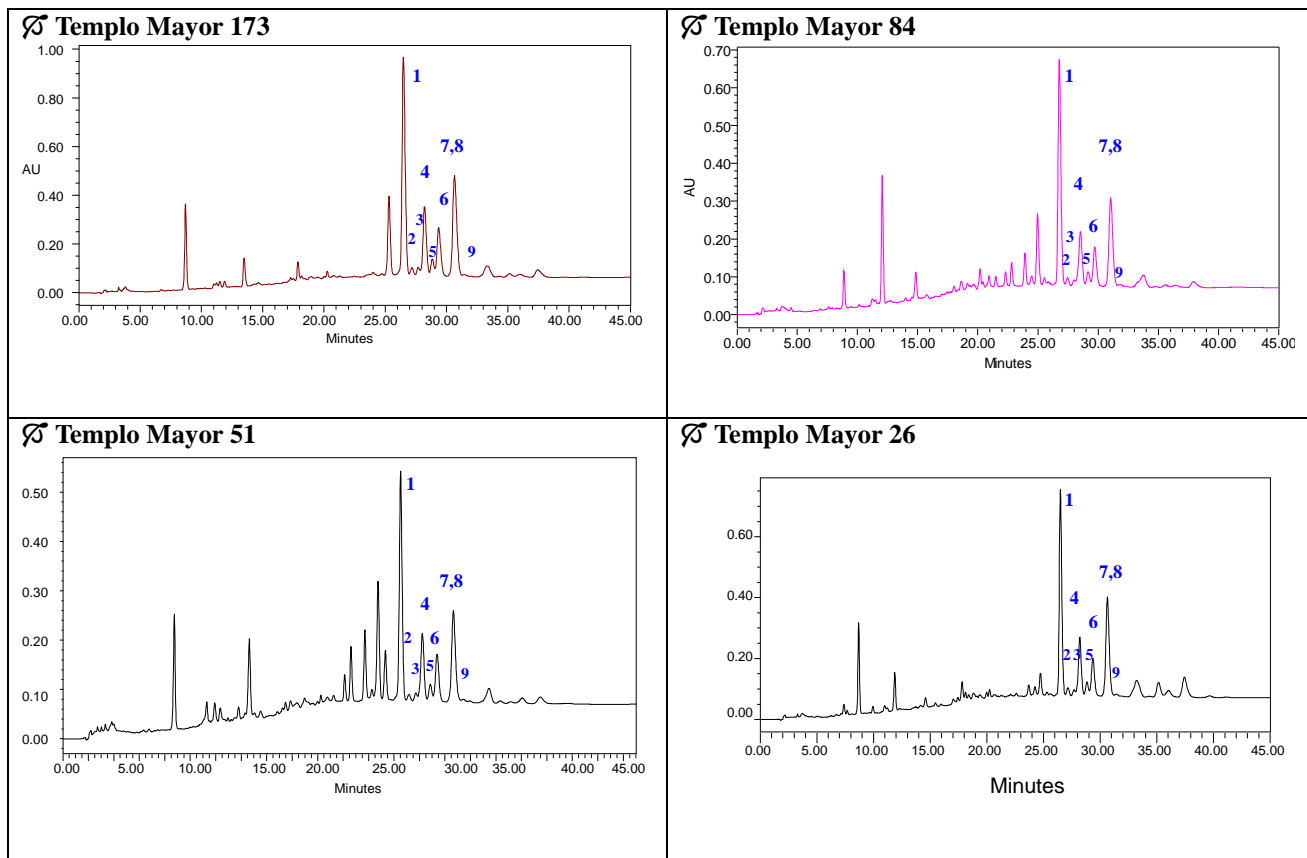
We defined this profile for archeological samples as **profile A**.



**Fig 66 Chromatogram of archeological sample with triterpenes and ageing related products (C1-C4).**

Identification of triterpenic compounds is as follows: 1) 3-*epi*-lupeol, 2) lupeol, 3) 3-*epi*- $\beta$ -amyrin, 4) lupenone, 5) 3-*epi*- $\alpha$  amyrin, 6)  $\beta$ -amyrin, 7/8  $\alpha$ -amyrin/  $\beta$ -amyrone.

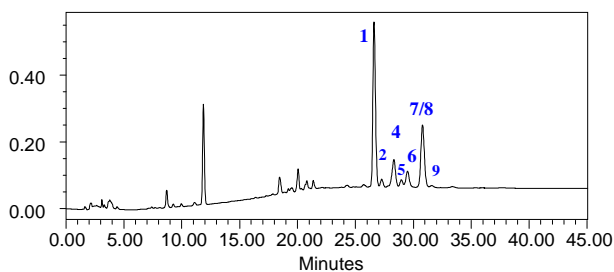
In figure 67 we present the whole chromatograms of archaeological samples with molecular profile “A” which are: 26, 51, 84 and 173.



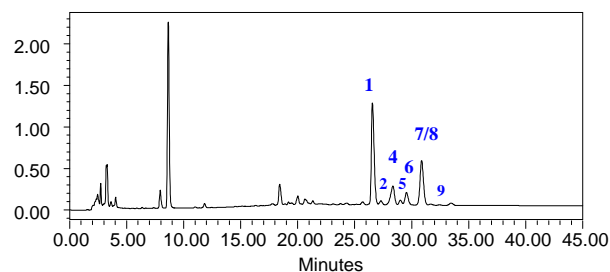
**Fig 67** Chromatograms of archeological sample with molecular profile A. Identification of triterpenic compounds is as follows: 1) 3-*epi*-lupeol, 2) lupeol, 3) 3-*epi*- $\beta$ -amyrin, 4) lupenone, 5) 3-*epi*- $\alpha$  amyirin, 6)  $\beta$ -amyrin, 7/8  $\alpha$ -amyrin/  $\beta$ -amyrone, 9)  $\alpha$ -amyrone

It is important to note that these molecules are not always present in archeological materials; they are absent in TMT and 52 (figure 68) these profile was defined as profile “B”.

## ☞ Templo Mayor 52



## ☞ Templo Mayor TMT



**Fig 68 Chromatograms from archeological samples with B profile from Templo Mayor.** Identification of triterpenic compounds is as follows: 1) 3-*epi*-lupeol, 2) lupeol, 3) 3-*epi*- $\beta$ -amyrin, 4) lupenone, 5) 3-*epi*- $\alpha$  amyryn, 6)  $\beta$ -amyryn, 7/8  $\alpha$ -amyryn/  $\beta$ -amyryone, 9)  $\alpha$ -amyryone

From these results as well as from the solubility test we conclude that no other organic material enters in a great proportion in the composition of these samples. Concerning inorganic materials a small amount of a particle matter maybe insoluble in both polar and apolar solvents was found as it was said on section 4.1 of this chapter.

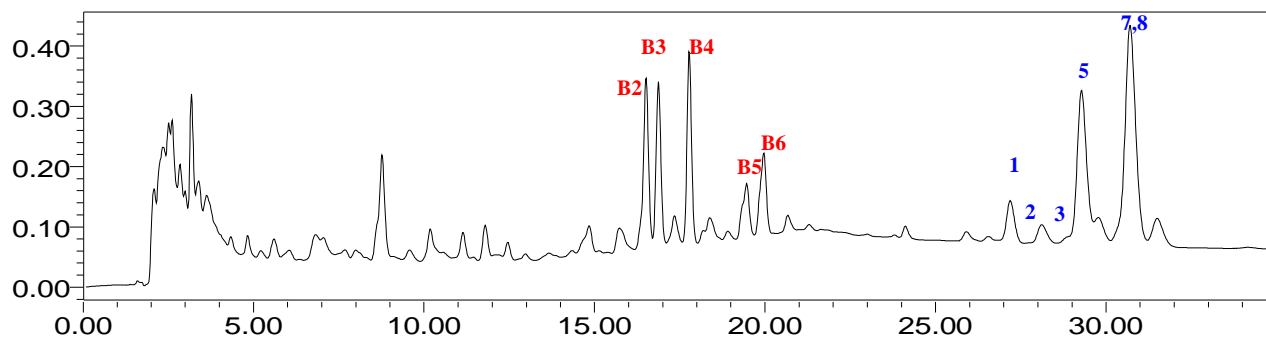
The results of this experiments yield important information for archeologist that were previously unavailable. Firstly this work confirms that a botanical origin of copal among the great variety of over 80 possible species was preferred by the Aztec priest. This origin is the same either for molded figurines, offerings to the Gods or used as adhesives for ceremonial knives.

In our days botanical distinction between *B. stenophylla* and *B. bipinnata* is unclear only with very sophisticated techniques slight differences in molecular compositions of their resins can be detected.

Concerning the botanical origin of Maya sample from Chichén Itzá (figure 69) we can hypothesize a very different botanical origin from the samples coming from Templo Mayor. Firstly the qualitative content of its triterpenic fraction is quite different quantitatively from the resins that we studied before, even more the peak area for the  $\alpha$  amyryn/  $\beta$  amyryone mixture is the major peak in the triterpenes zone, while in the rest of the archaeological samples, it was the 3-*epi*-lupeol peak which has the greatest area.

Its triterpen composition may correspond to a *Burseraceae* genus origin, but we can definitively discard a *B. simaruba* origin, that was related to Bonampak murals in Yucatán region (Magaloni,

1996). Certainly more studies should be performed on resins produced of endemic trees of the Yucatan peninsula, in order to identify the botanical origin of this sample.



**Fig 69 Chromatogram of Chichén Itzá archeological sample.** Identification of triterpenic compounds is as follows: 1) 3-*epi*-lupeol, 2) lupeol, 3) 3-*epi*- $\beta$ -amyrin, 4) lupenone, 5) 3-*epi*- $\alpha$  amyrin, 6)  $\beta$ -amyrin, 7/8  $\alpha$ -amyrin/  $\beta$ -amyrone, 9)  $\alpha$ -amyrone

#### 4.8 HPLC coupled to PCA analysis for botanical certified resins

As seen on the previous sections natural terpenoid resins have been identified by HPLC, coupled with PDA detectors in certified, commercial and archeological resins of *Bursera*. In order to compare the performance of FTIR and HPLC discrimination power, PCA was applied to HPLC data.

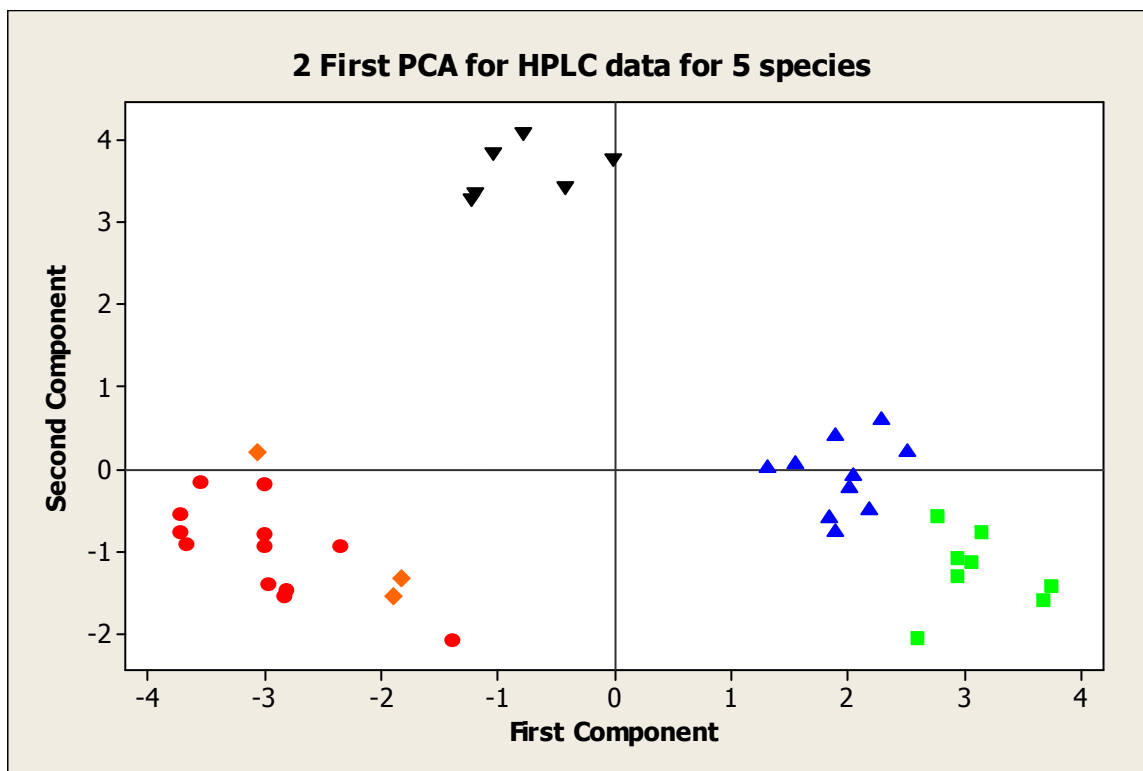
For this part of the study, both volatile (table 16) and triterpenic (table 17) compounds were selected in chromatograms, according to their retention times, peak areas were used in an indirect way: considering that the analysis was performed on different amounts of crude resin (and therefore different concentrations) according to the species of resin, the percentage of relative area was chosen for PCA analysis, to build the discrimination model.

*B. simaruba* was excluded from PCA analysis because lupeol and *epi*- $\beta$ -amyrin were never resolved into different peaks, the same happened to 3-*epi*  $\alpha$ -amyrin and  $\beta$ -amyrin in this species.

A data matrix with 40 rows (resin of certified origin samples) and 22 columns (variables, in this case relative area of the peaks in the chromatogram) was built (annex 3, tables 41, 42 and 43).

In figure 70 the structure of the data, using the first two principal components, is displayed.





**Fig 70** Distribution in the hyperspace of the resins samples from botanical certified origin, using the first two components, with HPLC data. Species are shown as follows: ● *B. laxiflora*, ◆ *B. excelsa*, ■ *B. stenophylla*, ▲ *B. bipinnata*, ▼ *B. penicillata*

In this case the first two principal components were enough to display the data structure, and they explained 46.5% of the total variance. Examining the score plot in the area defined by the first two principal components, good discrimination results were achieved, even more *B. bipinnata* and *B. stenophylla* were correctly discriminated also *B. penicillata* is well separated from the other species. Concerning *B. excelsa* and *B. laxiflora* they were grouped into the same area of hyperspace. Both species have a lower content of triterpenes compared to the other studied species, and this factor leads to a loss of sensibility in their discrimination using PCA with HPLC data.

When analyzing loading plot (figure 71) the molecules that exhibit the highest influence onto first component (in green) in the positive side are triterpenes: lupenone, 3-*epi*- $\alpha$ -amyrin,

lupenone,  $\alpha$ -amyrin/  $\beta$ -amyrone. In negative side with the highest impact B8 and B1 from the more polar fraction have the highest discrimination power.

As can be seen in the loading plot B2, B5, A3 and and A4, all volatile compounds show to have the higher impact on second component together with 3-*epi*-lupeol of the triterpenic fraction.

Generally speaking all triterpenes play a major role into discrimination except for lupeol which seems to have little impact on both components, together with A1.

On the second component B3 and B5 have the higher impact in discrimination, they both seem to content the same information so for further analysis B5 may be taken out of the analysis as it exhibits a slightly lower impact on both components. Along with B3 and B5,  $\alpha$ -amyrone was found to have a high impact on second component. On the negative part of the second component A3, A4 and 3-*epi*-lupeol display the higher discrimination power.

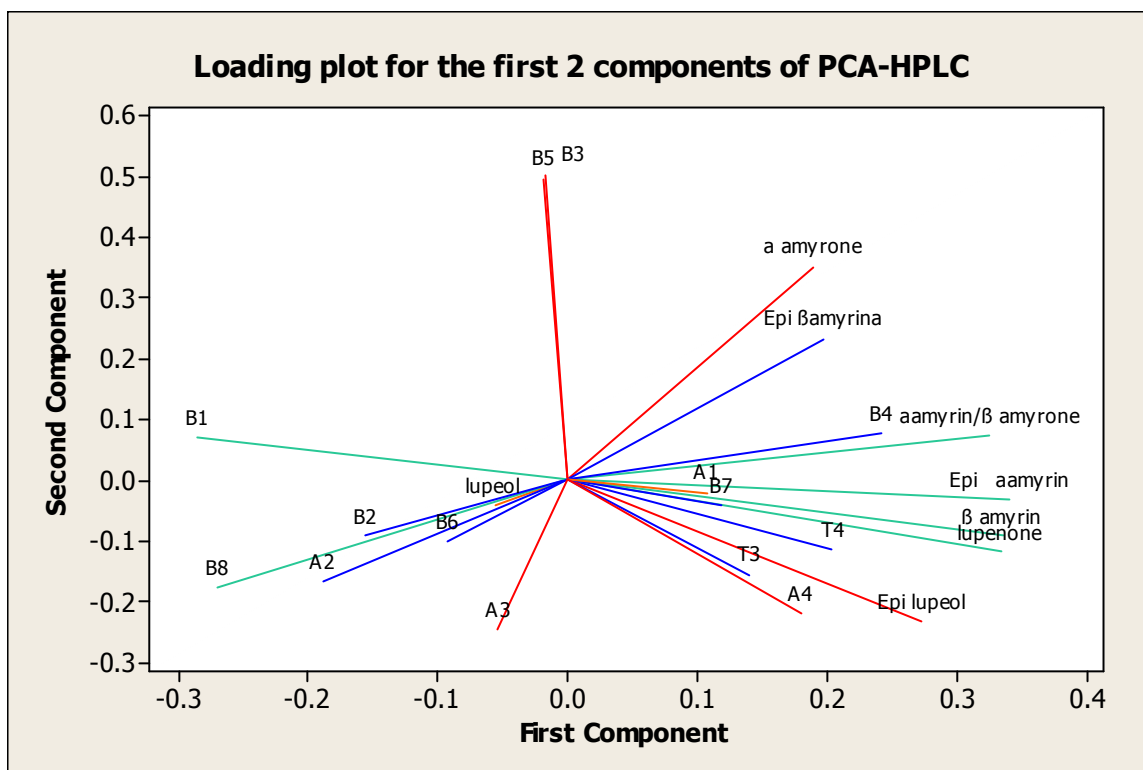


Fig 71 Loading plot for PCA analysis using HPLC data for botanical certified resins

#### 4.9 Linear Discriminant Analysis

As previously with FTIR data, a classification model was built. LDA analysis was applied in order to find a predictive classification model, able to separate the 5 botanical species. Results for fitting are shown on table 18 and for validation matrix on table 19.

Put into group	<i>B. bipinnata</i>	<i>B. excelsa</i>	<i>B. laxiflora</i>	<i>B. penicillata</i>	<i>B. stenophylla</i>
<i>B. bipinnata</i>	10	0	0	0	0
<i>B. excelsa</i>	0	4	0	0	0
<i>B. laxiflora</i>	0	0	12	0	0
<i>B. penicillata</i>	0	0	0	6	0
<i>B. stenophylla</i>	0	0	0	0	8
<b>Total N</b>	10	4	12	6	8
<b>N correct</b>	10	4	12	6	8
<b>Proportion</b>	1	1	1	1	1

**N = 40    N Correct = 40    Proportion Correct = 1.000**

**Table 18 Fitting matrix of the LDA Rows represent the true class, and the columns the assigned class**

As can be seen on fitting matrix this model seems to be more robust than the one constructed with FTIR data, affording a 100% of correct recognition. Complete statistical results can be consulted in annex 3.

The confusion matrix (table 19) afforded a global recognition percentage of 95.0% while only one sample of *B. excelsa* and one from *B. stenophylla* samples were incorrectly classified in the validation procedure.

Put into group	<i>B. bipinnata</i>	<i>B. excelsa</i>	<i>B. laxiflora</i>	<i>B. penicillata</i>	<i>B. stenophylla</i>
<i>B. bipinnata</i>	10	0	0	0	<b>1</b>
<i>B. excelsa</i>	0	3	0	0	0
<i>B. laxiflora</i>	0	<b>1</b>	12	0	0
<i>B. penicillata</i>	0	0	0	6	0
<i>B. stenophylla</i>	0	0	0	0	7
Total N	10	4	12	6	8
N correct	10	3	12	6	7
Proportion	1	0.75	1	1	0.875

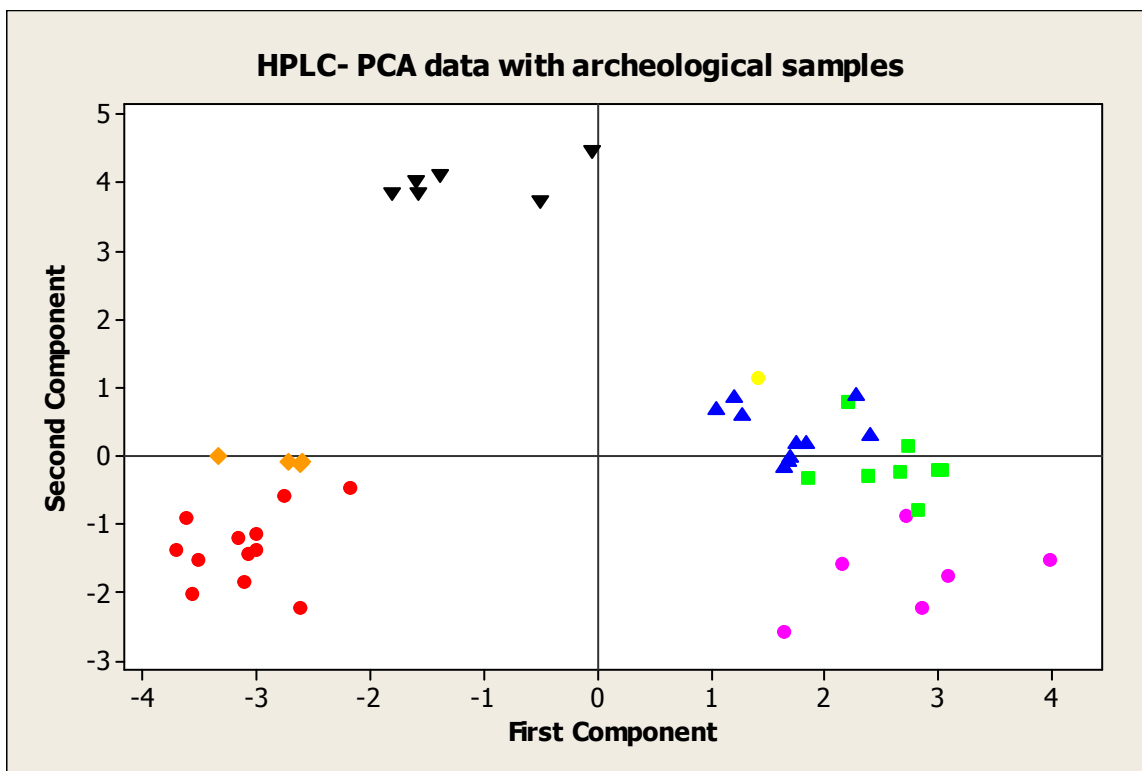
**N = 40    N Correct = 38    Correct Proportion = 0.950**

**Table 19** Confusion matrix of LDA, rows represent the true class, and the columns the assigned class. Wrong assignments are shown in red.

This affords as a consequence that when dealing with classification from a sample of *B. stenophylla* their probability to be correctly classified by this model is 87.5 %, on the other side *B. bipinnata* was always correctly classified. When looking at the graphic 69 a greatest dispersion of the *B. stenophylla* data in the hyperspace can be noticed, this fact may be correlated to a greater possibility of misclassification.

#### **4.10                    HPLC coupled to PCA analysis for archeological resins**

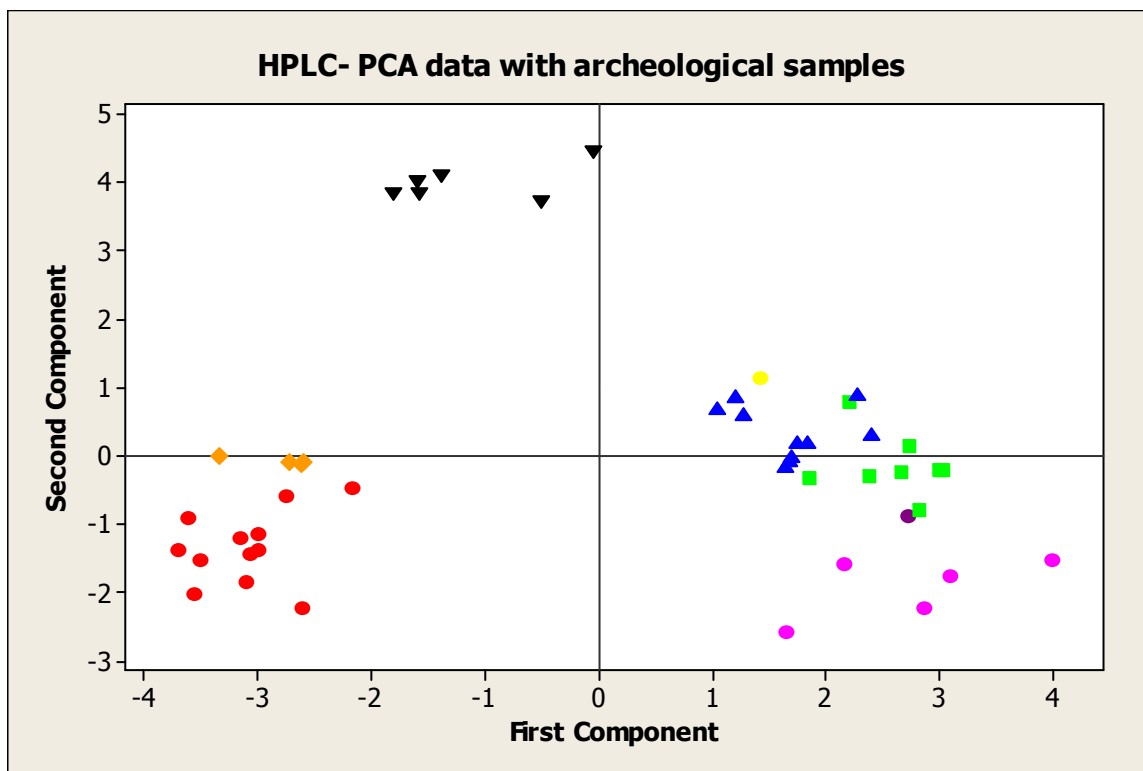
When HPLC data for archaeological samples was introduced into the model, a good discrimination was achieved between the archaeological sample from Chichén Itzá and the archaeological samples from Templo Mayor, this comes as a logical consequence of their great molecular difference, corroborated by HPLC chromatograms (figure 72).



**Fig 72** Distribution in the hyperspace of the resins samples from botanical certified origin, using the first two components, with HPLC data. Species are shown as: ● *B. laxiflora*, ◆ *B. excelsa*, ■ *B. stenophylla*, ▲ *B. bipinnata*, ▼ *B. penicillata*. Archeological samples are shown as: ● Samples from Templo Mayor, ● Sample from Chicén Itzá

Finally concerning botanical origin determination we hypothesized that the most probable origin for the 84 sample from Templo Mayor is likely to be *B. stenophylla*, as its position in the PCA graphic is close to the region of the hyperspace, where this species is distributed (figure 73).

Concerning the other samples of Templo Mayor it was not possible, to assess with certainty their botanical origin, given the botanical closeness of the species, and the many molecular changes that take place during ageing processes, giving place to the disappearance of some compounds sometimes (A2, A3, B8, *epi*- $\beta$ -amyrin,  $\alpha$ -amyrone,  $\beta$ -amyrone) or always (B1, B2, B3, B5) and the apparition of others (C1 to C4).



**Fig 73** Distribution in the hyperspace of the resins samples from botanical certified origin, using the first two components, with HPLC data. Species are shown as: ● *B. laxiflora*, ◆ *B. excelsa*, ■ *B. stenophylla*, ▲ *B. bipinnata*, ▼ *B. penicillata*. Archeological samples are shown as: ● Sample from Chicén Itzá, ● Samples 84 from Templo Mayor, ● The rest of the samples from Templo Mayor

In order to achieve a better botanical discrimination in aged samples further studies need to be conducted into degradation processes, comprising an identification of both volatile molecules and molecules arisen in aged samples by means of R.M.N.

In a second step the establishment of correlations between products of degradation and stages of ageing could be established. This type of work was beyond the scope of the present work, because of time constraints.

## 4.11 Purification by Solid Phase Extraction (SPE)

Sample preparation is necessary when molecules that interfere with the determination of the analyte are present within a matrix. To eliminate those interferences a number of techniques may be applied, namely: filtration, liquid-liquid and solid-solid extraction, etc.

In the last years solid-solid extraction has evolved a lot, not only allowing the purification but also the concentration of the target(s) molecule(s) within a sample.

### 4.11.1 General Methodology

For SPE cartridges, columns and plaques filled up with adsorbents are used. In the present work a reverse phase Chromabond C-18ec phase was chosen. Adsorbent was chosen considering its good affinity to triterpen molecules and its low affinity to other compounds. The volume of the cartouche was defined by the volume of the sample and the quantity of analyte present in the rough resin. In the present case for the analysis of commercial resins a 6 mL cartridges was selected, while a 1 mL was chosen for archaeological samples.

Generally speaking every SPE protocol has at least 4 steps:

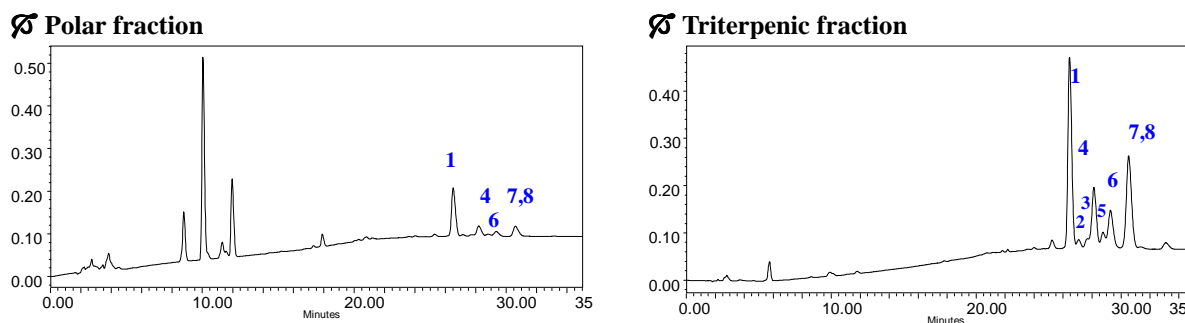
- 1) Conditioning. This stage allows the elimination of pollutants from the adsorbent at the same time that allows its activation. For this stage 6 mL of methanol were used. It is important to not let run the column dry.
- 2) Deposit of the sample. This step consists in the deposit of the sample onto adsorbent surface. To ensure better purification efficiency the velocity of filtration should be controlled. Experimental data show that for cartridges with 1 mL volume an adsorbent granulometry of 50 $\mu$ m a optimal time of deposit is 0.7 to 1 mL/ minute, for 6ml volume cartridges of 5 -6 mL are recommended.
- 3) Washing of the adsorbent. It is at this stage that the impurities without any affinity with the adsorbent will be eliminated from the solid phase. For this purpose a solvent or a mixture of solvents with good affinity for impurities and poor affinity to the analyte, should be used.

- 4) Elution. At this stage a solvent with the maximum affinity to the analyte must be used, to recover it. Its volume must be low as it will provide a higher pre-concentration. An adsorbent with lower particle diameter will afford lower elution volumes.

The “lit volume” is the amount of solvent used for conditioning, rinsing and elution and is about two to three times the volume of adsorbent

In the present work for the study of commercial samples the column was conditioned prior to use by drawing 2 times 3 mL of methanol followed by the same volume of distilled water. The prepared sample (2 mg/mL) was loaded onto and drawn through the column. The column was then washed with 3 mL of a mixture methanol-water (5:95, v/v). The cover of the manifold was then removed and the cover was wiped with a tissue, to remove drops of washing solution. Triterpenoids were then eluted from the column with 2 x 2 mL of methanol. The eluate collected was then analysed by means of HPLC.

The result of applying this technique are shown on figure 74 as it can be see on these chromatograms SPE show that it effectively separated the compounds corresponding to A) polar compounds and B) apolar compounds .



**Fig 74 Chromatograms of A) the washing product and B) the elution product.** Identification of triterpenic compounds is as follows: 1) 3-*epi*-lupeol, 2) lupeol, 3) 3-*epi*- $\beta$ -amyrin, 4) lupenone, 5) 3-*epi*- $\alpha$  amyirin, 6)  $\beta$ -amyirin, 7/8  $\alpha$ -amyirin/  $\beta$ -amyrone, 9)  $\alpha$ -amyrone

The extraction method described here for the qualitative analysis of triterpenoids in the matrix of a natural resin proved to be useful in terms of simplicity and general applicability. It should prove to be valuable in further studies in natural resins from Mexican *Bursera* origin and generally speaking with a triterpenic composition.



## 4.12 Conclusion

The usefulness of this technique is undeniable concerning molecular profiling, for differentiation between resins with different botanical origin. HPLC data coupled to PCA was able to discriminate botanical origin of fresh resins from very close species as *B. bipinnata* and *B. stenophylla*, which were hard to differentiate with FTIR-PCA.

The performance of the mathematical model constructed with HPLC data in PCA and validated by LDA exhibit a high performance with a 100% recognition in the fitting matrix and a 95% of positive recognition in the cross validation matrix.

The study of chromatograms from commercial resins show as well very interesting results: from these samples, two were identified as *B. bipinnata* resins, 9 as *B. stenophylla* resins, nine afforded chromatograms with too few or no triterpenes at all.

From the *B. bipinnata* both of them were white, concerning the *B. stenophylla* resins, one was white, one was red and one was a “myrrhe”.

From the 9 resins from unknown origin 2 were yellow, one was red and the rest were white. Confirming that no correlation can be established between the physical aspect and presentation of resins and their botanical origin.

Concerning ageing, liquid chromatography allow us to confirm that *Bursera* resins seem to undergo significant changes along time: from one side the evaporation of the volatile fraction and in the other one the oxidation and maybe the polymerization of the triterpenic fraction. These modifications can be assessed only partially by means of HPLC-UV/Vis, as it was show in the chromatograms from archaeological samples and therefore a deepened study should comprise the isolation of compounds C1 to C4 and its formal study by R.M.N.

Interestingly these changes nevertheless are not always present in archaeological resins, and therefore an insight into the mechanism of their formation and maybe a correlation between ageing conditions and their presence should be done.

Finally only few chemical species seem to be stable during natural aging: A4 of the non triterpenic fraction at retention time of nine min and all the triterpenic molecules except from 3-*epi*- $\alpha$ -amyrin, which nevertheless exhibited a tendency towards a changing on its proportions.

# Chapter V

## Chromatographic techniques GC-MS

## Chapter V

### Gas Chromatography-Mass Spectrometry

Gas Chromatography (GC) is a technique described, for the first time, by Martin and James in 1952. It is based upon the partition of the analytes between two phases: an inert, not very viscous, highly pure carrier gas as mobile phase and a liquid or solid stationary phase (Bartle, 2002). The use of this technique alone is limited when facing complex mixtures of compounds (Domenech-Carbó, 2008). This drawback can be resolved by coupling this technique to gas chromatography (GC-MS).

In a Mass Spectrometer (MS), the identification of an analyte is achieved by the ionization of a molecule, its fragmentation into smaller ions and their separation on the basis of the mass/charge ratio by an analyzer. This may be a quadrupole, an ion trap or a magnetic sector. In the present work an ion trap was used. This technique yields information about the molecular mass of a compound, its global formula and from the fragmentation pattern, about its molecular structure. When analyzing complex mixtures it is possible to draw qualitative and quantitative information (Colombini, 2006). Mass spectrometry is therefore a powerful tool for analysis involved in the identification of organic materials from artworks, as it has the potential to resolve molecular structures.

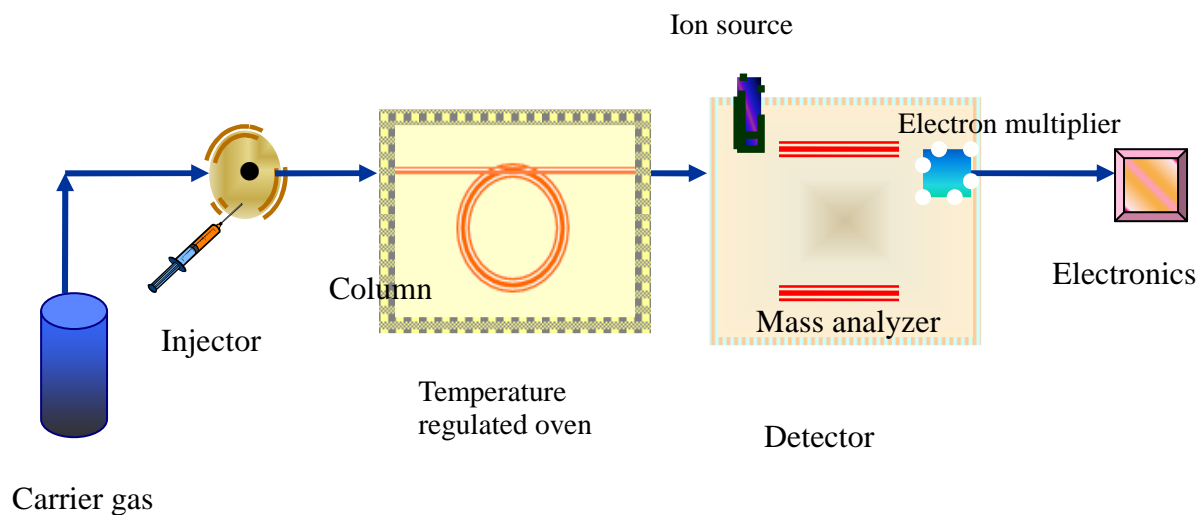


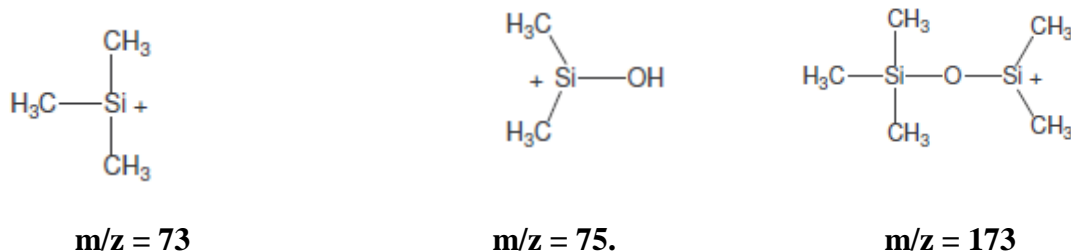
Fig 75 Schematic view of GC instrumentation and their components

Typical equipment for modern GC-MS consists of a cylinder containing the carrier gas -Helium, in this work-, an injector, a capillary column inside a temperature regulated oven, an interface (by which most of the carrier gas is depleted), a mass detector and the electronics (figure 75). More detailed information about the technique and its theory can be found elsewhere (Hubschmann, 2008).

## 5.1 Derivatization

It is a preliminary chemical treatment which main goals are to make compounds more volatile or less polar and consequently suitable for GC analysis, to lessen absorption phenomena into column due to functions alcohol and acid type, to stabilize thermally substances analyzed and to contribute to a better separation of compounds from similar structure (Hovanessian, 2005). The used of derivatization process is reported in the materials and methods section of this work. Trimethylsilylation of carboxylic and hydroxyl groups was achieved by a method previously described by Mathe *et al.* in 2004. Using silylation reagents like hexamethyldisilazane (HMDS) and chlorotrimethylsilane (TMSCl) presents the advantage of derivatizing in a single and fast step both carboxylic and hydroxyl groups. This enabled a more complete characterization of the composition of resins.

Indeed, the presence of trimethylsilylated (TMS) compounds induced the formation of characteristics ions. For molecules containing a hydroxyl group, it is important to note the existence of fragments  $m/z = 73$  and  $m/z = 75$  (Fig 76).



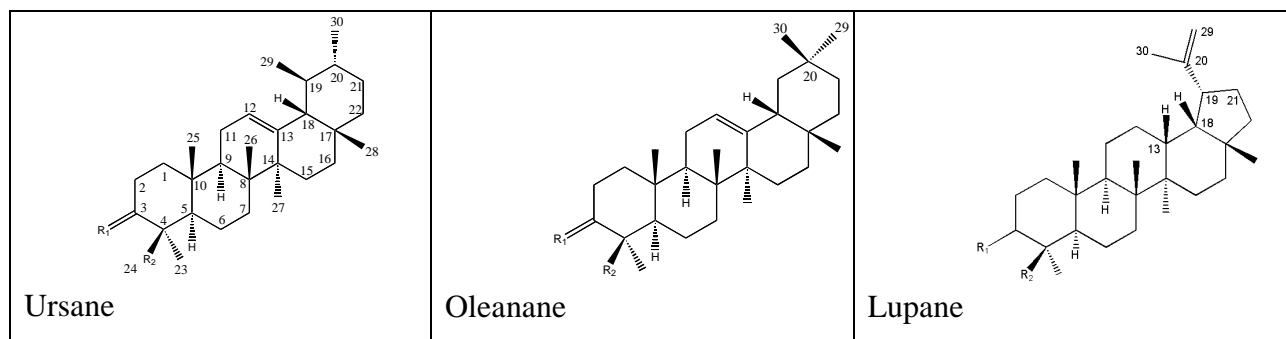
**Fig 76 Characteristic fragments from silylated compounds**

If the molecule counts on its structure more than one hydroxyl group either from an alcohol or a carboxylic acid functions, the presence of an ion  $m/z = 147$  resulting from the addition of the two previous fragments is observed.

In the present research, this technique was firstly used for the analysis of freshly collected resins from 6 species. Then triterpenoid composition was compared to that of selected commercial and of archaeological samples.

## 5.2 The study of standard triterpenoid molecules

As in the HPLC study of this work the same 9 standard molecules were studied; they presented ursane, oleanane and lupane skeletons and their TMS structure is presented on table 20.



Triterpenes		Structure type	R <sub>1</sub>
Common name	Systematic name		
$\alpha$ -amyrin, $\beta$ -OTMS ether	3 $\beta$ -hydroxy-urs-12-en-3-ol, $\beta$ -OTMS ether	U	$\alpha$ -H, $\beta$ -OH
3- <i>epi</i> - $\alpha$ -amyrin, $\alpha$ -OTMS ether	3 $\alpha$ -hydroxy-urs-12-en-3-ol, $\alpha$ -OTMS ether	U	$\alpha$ -OH, $\beta$ -H
$\beta$ -amyrenone	olean-12-en-3-one	O	O
$\beta$ -amyrin, $\beta$ -OTMS ether	3 $\beta$ -hydroxy-olean-12-en-3-ol, $\beta$ -OTMS ether	O	$\alpha$ -H, $\beta$ -OH
3- <i>epi</i> - $\beta$ -amyrin, $\alpha$ -OTMS ether	3 $\alpha$ -hydroxy-olean-12-en-3-ol, $\alpha$ -OTMS ether	O	OH, $\beta$ -H
lupeol, $\beta$ -OTMS ether	3 $\beta$ -lup-20(29)-en-3-ol, $\beta$ -OTMS ether	L	$\alpha$ -H, $\beta$ -OH
3- <i>epi</i> -lupeol, $\alpha$ -OTMS ether	3 $\alpha$ -lup-20(29)-en-3-ol, $\alpha$ -OTMS ether	L	$\alpha$ -OH, $\beta$ -H

**Table 20** TMS structure of the triterpenic standard molecules studied by GC-MS. O: Oleanane, U: Ursane, L: Lupane

Two gradients of temperature were used for the study of molecular composition of copals, one for the study of global resins and one for the study of triterpenoids. In table 21 are reported the retentions times under both gradients (protocols are described in the materials and methods

section). Each compound was attributed a roman number. This notation is used along the present chapter, in the chromatograms, to identify these molecules.

N°	Molecules	Global study	Triterpenoid study
		(Protocol 1)	(Protocol 2)
		Retention Time (min)	Retention Time (min)
<b>I</b>	3- <i>epi</i> - $\beta$ -amyrin $\alpha$ -OTMS	40.6	32.5
<b>II</b>	3- <i>epi</i> - $\alpha$ -amyrin $\alpha$ -OTMS	41.1	33.0
<b>III</b>	3- <i>epi</i> -lupeol $\alpha$ -OTMS	41.2	33.2
<b>IV</b>	$\beta$ -amyrone	42.6	34.8
<b>V</b>	$\beta$ -amyrin $\beta$ -OTMS	42.9	35.2
<b>VI</b>	$\alpha$ -amyrone	43.4	35.8
<b>VII</b>	$\alpha$ -amyrin $\beta$ -OTMS	43.5	36.2
<b>VIII</b>	lupenone	43.7	36.7
<b>IX</b>	Lupeol $\beta$ -OTMS	43.9	37.8

**Table 21** Time of retention of standard molecules under the designed GC-MS gradients

The obtained mass spectra of standard compounds were stored for the construction of a bank of mass spectra adapted to the study of triterpenes. Later, the comparison between the mass spectra of the chromatographic peaks obtained when analyzing commercial, archaeological and botanically certified samples, allowed the identification of the compounds present in each sample.

According to earlier studies of our research team (Mathe, 2004), the retention time of the compounds was influenced by the number and the type of functional groups present, and generally increased with increasing molecular weight. Concerning the chemical skeleton in the retention mechanism, lupane standards are retained longer than their ursane isomers and even longer than oleanane ones. In the other hand the absolute configuration of C-3 has a great influence into retention times:  $\beta$ -configuration gave a longer retention time than  $\alpha$ -configuration. This fact allows to differentiate  $\beta$ -amyrin (**V**),  $\alpha$ -amyrin (**VII**) and lupeol (**IX**), from their respective 3-*epimer* (**I**, **II** and **III**) in the chromatogram. Under the chromatographic conditions

described in the materials and methods section, compounds of a same family are always eluted according to the following order: 3- $\alpha$ -alcohol, 3-ketone and 3- $\beta$ -alcohol. A depth comment on fragmentation patterns of triterpenes can be found in Mathe, 2004.

### 5.3 Results of the study on botanical certified samples

The main objective of this type of work was to establish a molecular profile, to distinguish chemically resins from different botanical origin, and to identify as many compounds as possible into their chromatograms.

As in the HPLC study, for the study of certified samples, different amounts of sample depending on the studied species were needed (as much as possible the amount of sample was tried to be kept at 2 mg). The amount used for each different botanical origin of the resins is given in table 22.

Studied species	Mass of sample used for GC-MS analysis
<i>B. bipinnata</i>	2 mg
<i>B. stenophylla</i>	2 mg
<i>B. excelsa</i>	3-5 mg
<i>B. laxiflora</i>	From 2 mg up to 20mg
<i>B. penicillata</i>	2 mg
<i>B. grandifolia</i>	60 mg
<i>B. simaruba</i>	70 mg
Commercial resin	From 2 mg up to 30 mg
Archaeological resins	2 mg

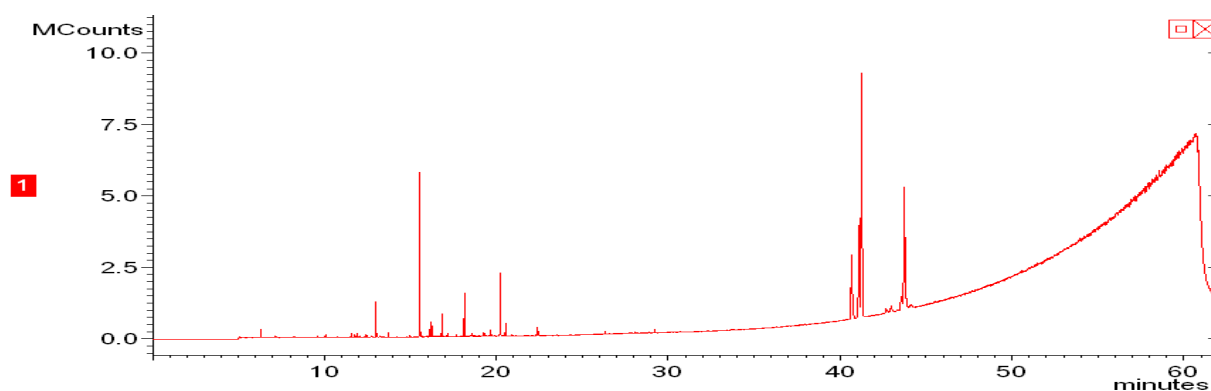
**Table 22** Amount of resins used for the GC-MS study

#### 5.4 Comparison of global chromatograms from certified botanical origin resins

As Fig 73 shows, gas chromatograms allow a clear distinction between resins. When analyzing chromatograms obtained using protocol 1, sesqui- and monoterpenes were located between minutes 11 and 38.5 of the chromatogram while triterpenes can be identified from 39 min.

Some general observations about composition of resins will be addressed in this section, but the main analysis of the triterpenic fraction will be done in the next section of this chapter, using protocol 2 chromatograms. It is worthy to comment some correlations and differences between HPLC and GC chromatograms, as a striking difference can be remarked between GC chromatograms and HPLC ones.

##### *B. bipinnata*



##### *B. stenophylla*

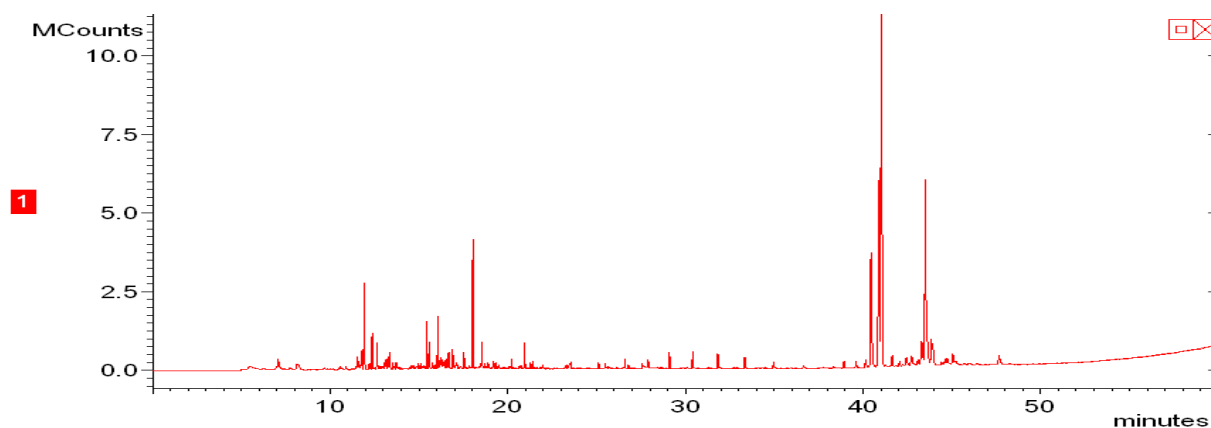


Fig 77 Global gas chromatograms for resin samples of certified botanical origin and *B. bipinnata* and *B. stenophylla* resin samples

While *B. bipinnata* and *B. stenophylla* exhibited a richer triterpenic fraction than the other resins, when analyzed by HPLC, GC shows that in fact their triterpenic fraction can be judged as

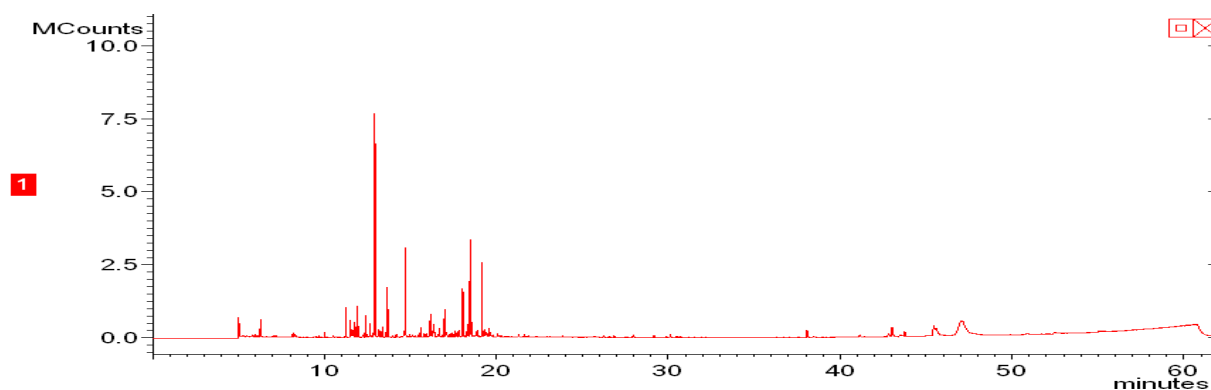


intermediate (figure 77) considering the number of different molecules in their chromatograms. Somewhere between *B. excelsa* that is rather poor in triterpenes and *B. penicillata* that is really rich on them.

Although our study was not focused on the characterization of the compounds on the volatile fraction of these resins, some observations can be made.

Concerning the volatile fraction, *B. bipinnata* and *B. stenophylla* volatile fraction differ in composition from what we can see chromatograms. In *B. bipinnata*, caryophyllene,  $\alpha$ -pinene and a sesquiterpenoid related to limonene were identified. The complete characterization of the volatile fraction is impossible as the derivatization protocol followed may volatilize most of these compounds.

### ♂ *B. excelsa*



### ♂ *B. laxiflora*

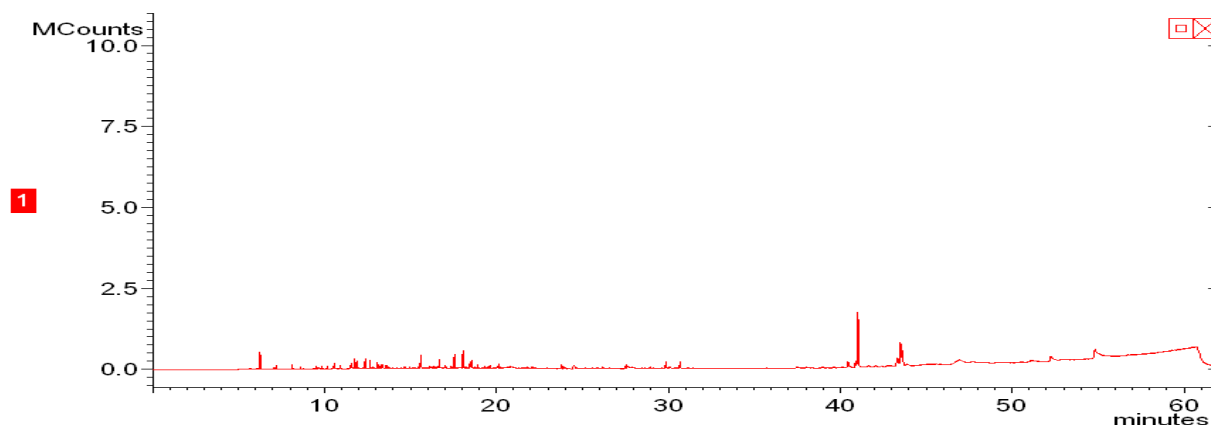


Fig 78 Global gas chromatograms for resin samples of certified botanical origin and for *B. excelsa* and *B. laxiflora* resin samples

*B. excelsa* contrary to other species as *B. penicillata* and *B. simaruba*, does not exhibit any further richness on its terpenoid tenure. The same can be said regarding *B. laxiflora* triterpenoid

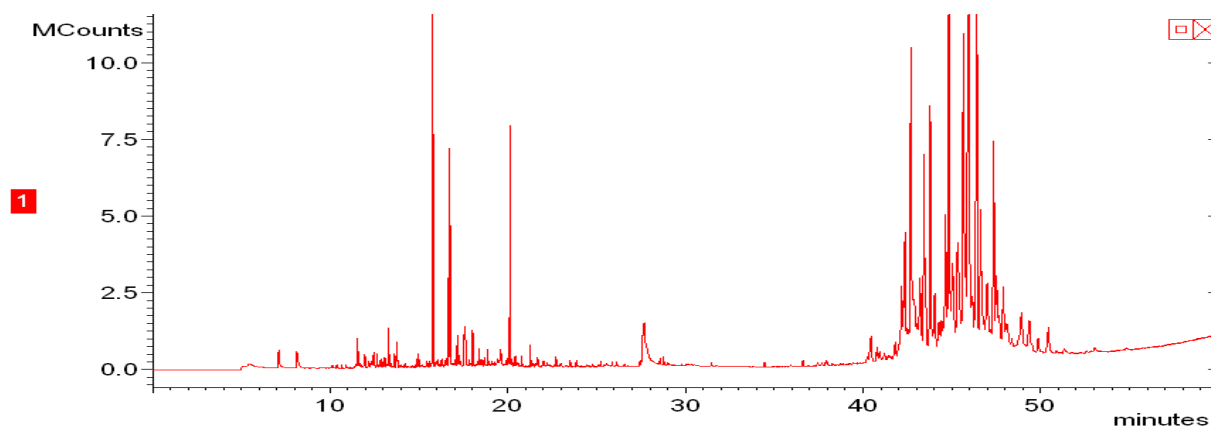
tenure. *B. excelsa*, chromatogram exhibited a wide variety of compounds in the sesqui- and monoterpene fraction *B. laxiflora* as well, but in quantitative terms the tenure of this compounds is rather modest in the last species (figure 78).

Concerning *B. penicillata* its triterpenoid fraction seems to be much richer than we initially suppose after HPLC analysis.

The same happened with *B. simaruba*, its richness of triterpenoid content of could be the cause of the difficulties in the resolution of some peaks in HPLC chromatograms (figure 79).

*B. simaruba* and *B. grandifolia* species exhibit a moderate variety of molecules in the volatile fraction of the resin.

### ♣ *B. penicillata*



### ♣ *B. simaruba*

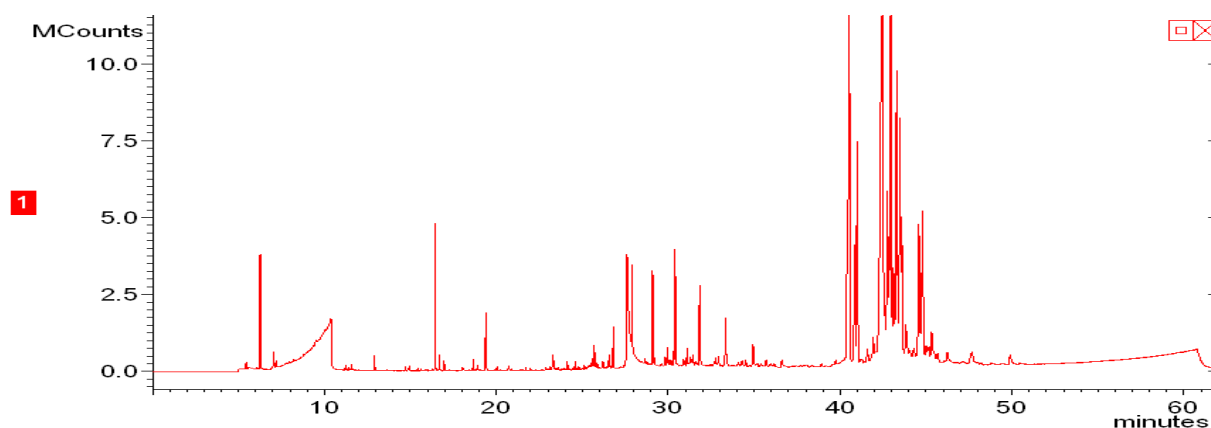
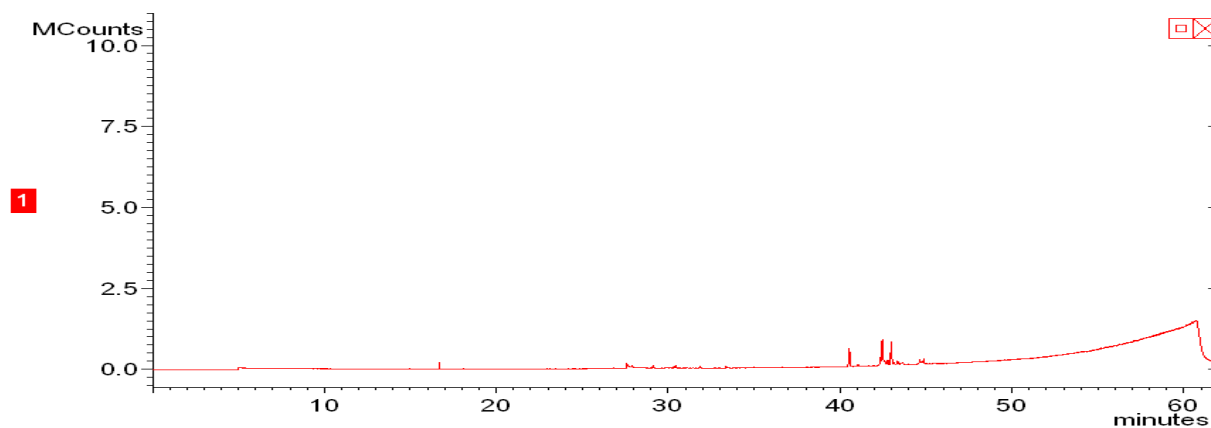


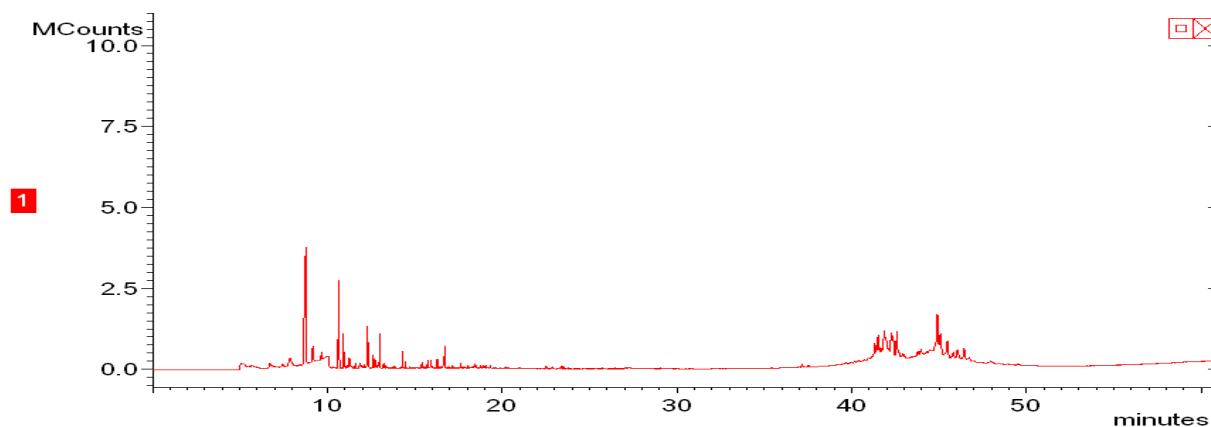
Fig 79 Global gas chromatograms for resin samples of certified botanical origin and for *B. penicillata* and *B. simaruba* resin sample

Concerning *B. grandifolia*, GC-MS was the only chromatographic technique that allows its study. Its triterpenic fraction can be judged as rather modest in quantitative terms, although triterpenoid tenure is varied in qualitative terms (figure 80).

### ♂ *B. grandifolia*



### ♂ *B. copallifera*



**Fig 80** Global gas chromatograms for resin samples of certified botanical origin and for A) *B. grandifolia* and B) *B. copallifera* resin sample

Finally and although *B. copallifera* was not part of the original study we would like to address a commentary on its composition: it seems to have very rich terpenoid tenure in qualitative terms (figure 80). Although their concentration is limited, volatile fraction (sesqui- and monoterpenoids) seems to include a number of molecules as well.

An in depth commentary on the composition of triterpenic fraction will be addressed in section 5.5 of this chapter.

## 5.5 Insight on triterpenic composition for samples of certificated origin

In this section we will present an insight into the identification of standard molecules in the triterpenic fractions of botanical certified resins. For this purpose a comment on chromatograms obtained under the protocol 2 conditions will be addressed.

In figure 81 the entire chromatogram of triterpenic of *B. bipinnata* is presented. As it can be seen only minor peaks are detected before 30 min, even more spectra from these peaks are related to secondary products of TMS reactions. Therefore for a better identification of compounds a partial TIC chromatogram between minutes 30 and 40 using gradient two, are presented in this section.

As it has been said complete account on identified triterpenoids and their retention time for each botanical studied species can be found in annex 4 (table 49).

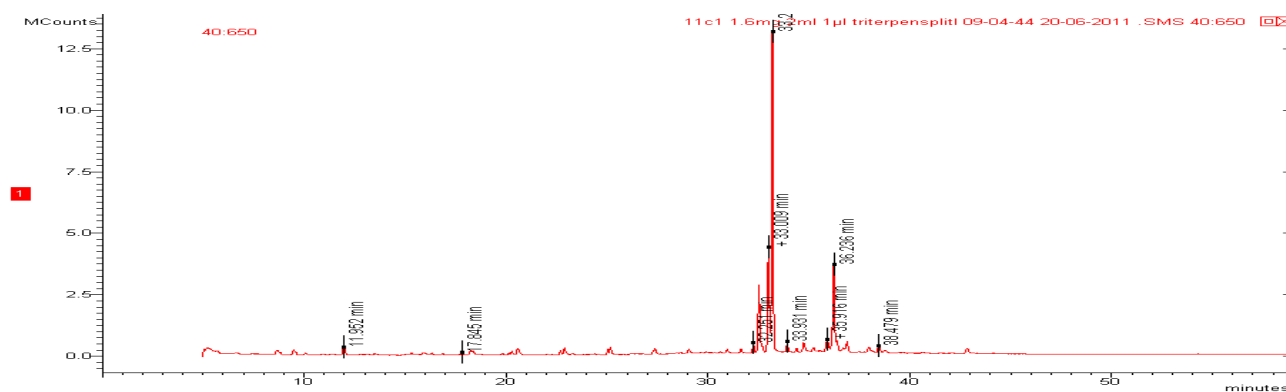


Fig 81 GC chromatogram of *B. bipinnata* sample 11c1

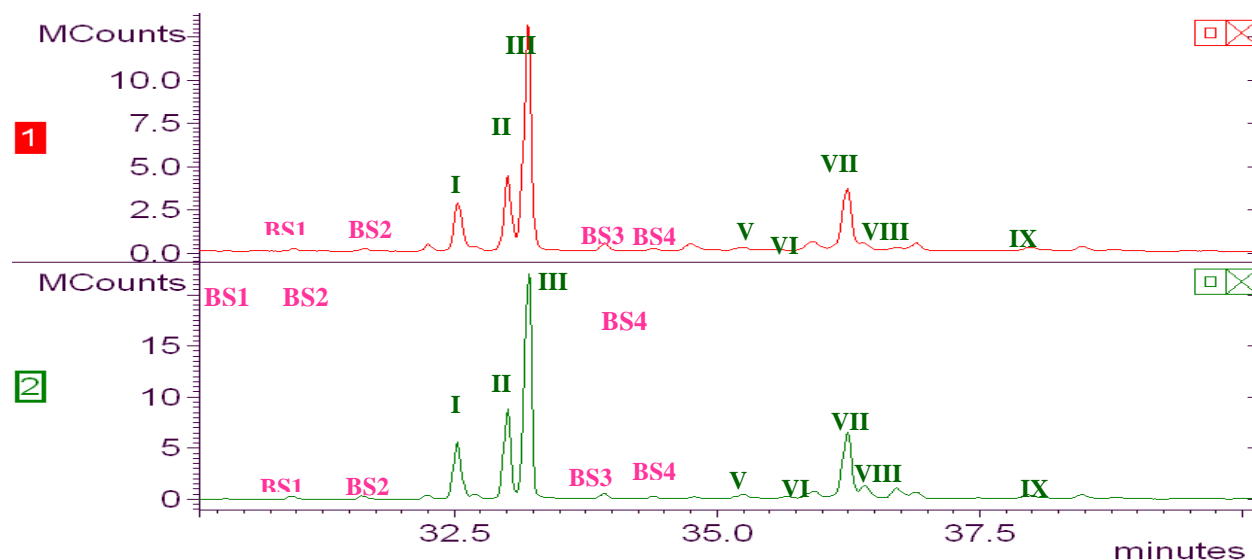
### 5.5.1 Comparison between *B. bipinnata* and *B. stenophylla* resins

A gas chromatogram of each of these two species is shown on figure 82. As it can be seen, triterpenic molecular composition of these resins is identical. In both chromatograms the nine triterpenic standard molecules were characterized. They are identified in the chromatograms with the previously assigned roman numbers

Four other triterpenic molecules were identified; these molecules are identified with a letter BS (for *bipinnata-stenophylla*), plus a number. Fragmentation patterns of these molecules were compared, and they are the same in both resins.

These results contribute to clarify and better understand the results obtained using the other analytical techniques. Furthermore IRTF spectroscopy and HPLC results of these two kinds of resins maybe explained considering on one side the differences in sesqui- and monoterpene composition, and in another side the small differences in the proportion of some triterpenic compounds (e.g. the biggest proportion of  $\beta$ -amyrone (**IV**) in *B. bipinnata* composition and the bigger proportion of lupeol (**VIII**) in *B. stenophylla*).

### 1) *B. bipinnata* 11c1 and 2) *B. stenophylla* 72d2

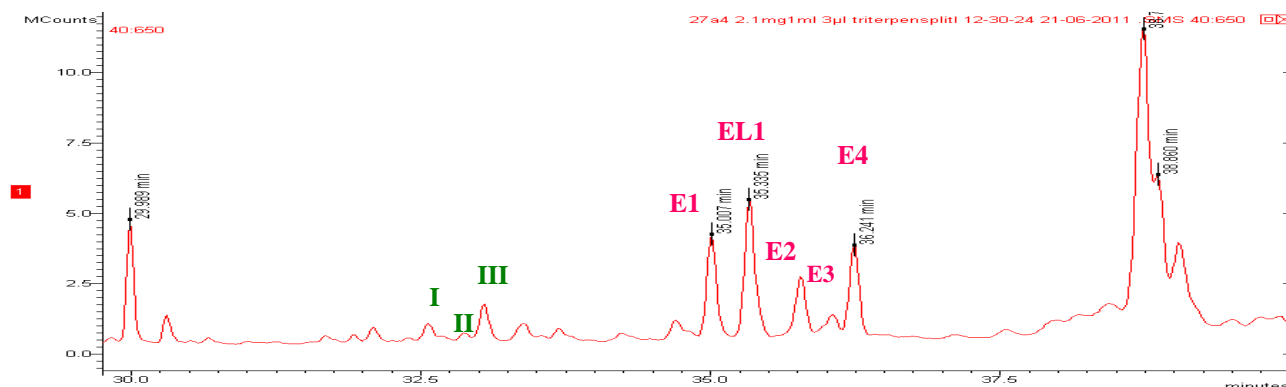


**Fig 82** Zoom into triterpenic zone of GC chromatogram of a sample of 1) *B. bipinnata* and 2) *B. stenophylla* resins. Identification of triterpenic compounds is as follows: (I) 3-*epi*- $\beta$ -amyrin  $\alpha$ -OTMS, (II) 3-*epi*- $\alpha$ -amyrin  $\alpha$ -OTMS, (III) 3-*epi*-lupeol  $\alpha$ -OTMS, (IV)  $\beta$ -amyrone, (V)  $\beta$ -amyrin  $\beta$ -OTMS, (VI)  $\alpha$ -amyrone, (VII)  $\alpha$ -amyrin  $\beta$ -OTMS, (VIII) lupeol  $\beta$ -OTMS, (IX) lupenone.

#### 5.5.2 *B. excelsa* triterpenic composition

Although only two out of the nine standard molecules were present: (I) 3-*epi*- $\alpha$ -amyrin, and (III) 3-*epi*-lupeol this sample is not as poor in triterpenes as one might suppose. In addition to these molecules other five triterpenes were detected. One of these markers was detected in *B. laxiflora* sample as well, in (figure 83) it is designed as EL1 (E for *excelsa*, L for *laxiflora* plus a number).

Molecules appearing exclusively in *B. excelsa* composition are identified with a letter “E” plus a progressive number. The determination of the exact structure of these compounds is beyond the scope of this research. Its study, depending on their specificity these molecules could be used as molecular markers for resins with this botanical origin.

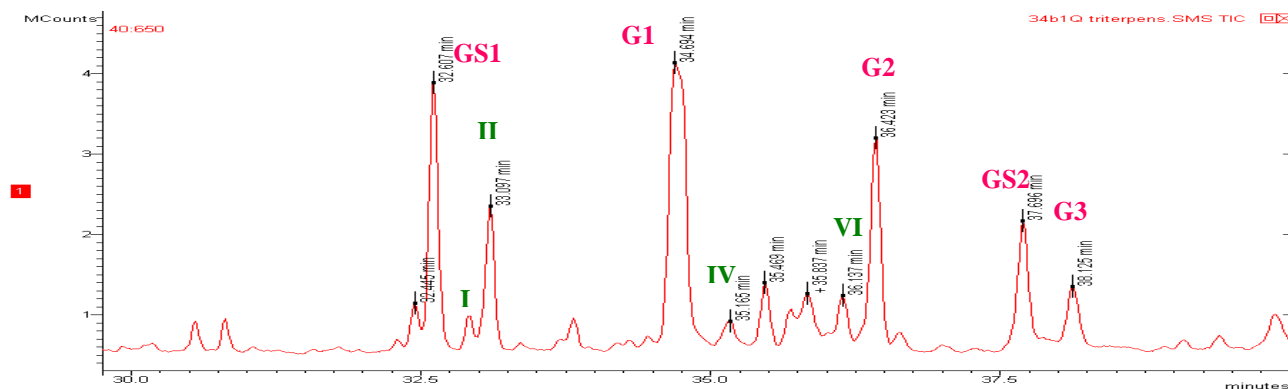


**Fig 83** Zoom into triterpenic zone of GC chromatogram of a sample of *B. excelsa* (27a4). Identification of triterpenic compounds is as follows: **(I)** 3-*epi*- $\beta$ -amyrin  $\alpha$ -OTMS, **(II)** 3-*epi*- $\alpha$ -amyrin  $\alpha$ -OTMS, **(III)** 3-*epi*-lupeol  $\alpha$ -OTMS.

### 5.5.3 *B. grandifolia* triterpenic composition

The GC-MS results allow us to confirm the triterpenic nature of this resin, and to have some insight on the compounds that are present in it. This is of great value considering that it was impossible to perform HPLC-UV/Vis analysis on this material.

In the resin from this species 4 compounds among the standard studied molecules were identified: **(I)** 3-*epi*- $\beta$ -amyrin and **(II)** 3-*epi*- $\alpha$ -amyrin, **(IV)**  $\beta$ -amyrone and **(VI)**  $\alpha$ -amyrone (figure 84). Along with these compounds other five triterpenoids were detected. Two of them GS1 and GS2 are also present in *B. simaruba* resin, G1 to G3 are encountered exclusively in *B. grandifolia* resin.



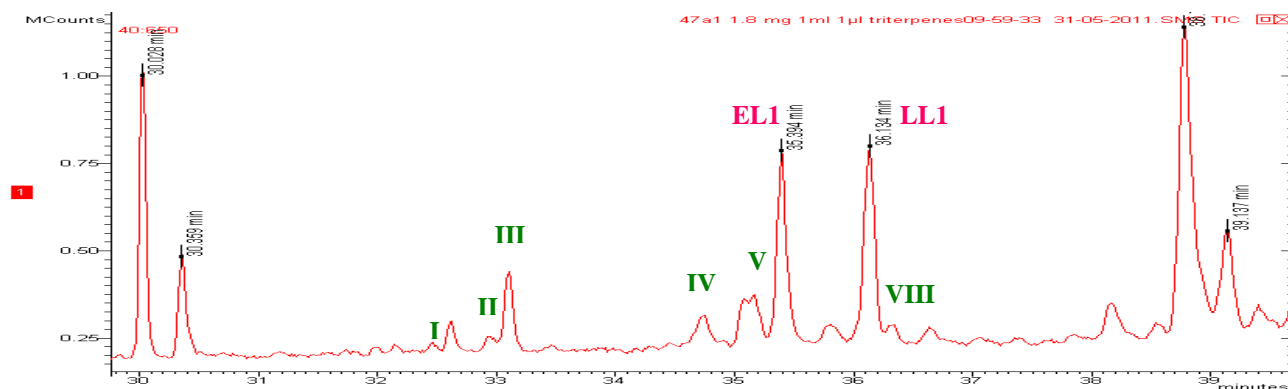
**Fig 84** Zoom into triterpenic zone of GC chromatogram of sample of *B. grandifolia* (34b1Q). Identification of triterpenic compounds is as follows: (I) 3-*epi*- $\beta$ -amyryn  $\alpha$ -OTMS, (II) 3-*epi*- $\alpha$ -amyryn  $\alpha$ -OTMS, (IV)  $\beta$ -amyrone (VI)  $\alpha$ -amyrone.

#### 5.5.4 *B. laxiflora* triterpenic composition

This was the species that confronted us to a more variable triterpenic profile in qualitative terms. Therefore in this section are presented the two major molecular profiles encountered.

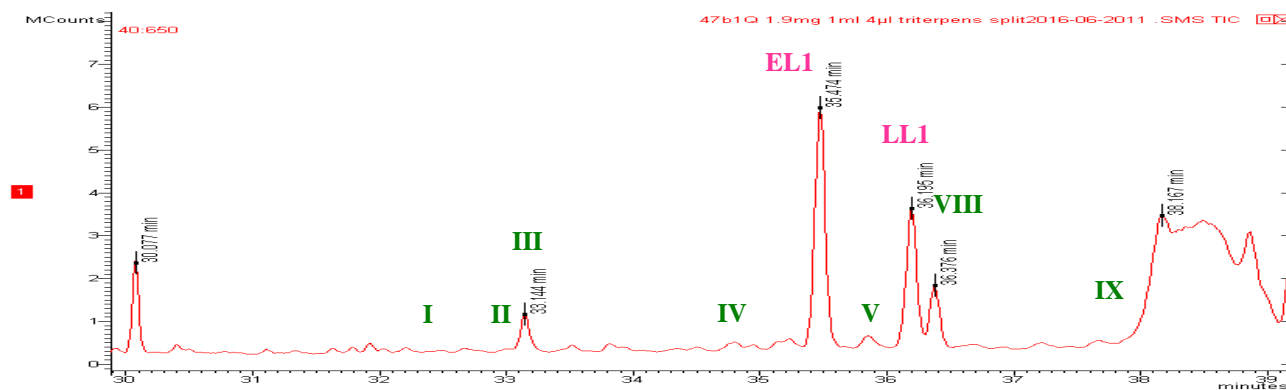
For the lot 1, seven out of the nine standard molecules were identified, the only absent compounds were two ursane squeeleton molecules (VII)  $\alpha$ -amyrine and (VI)  $\alpha$ -amyrone (figure 85).

Additionally two other triterpenoid molecules were detected, identified as EL1 entering as well in *B. excelsa* composition and L1 exclusive from *B. laxiflora* species.



**Fig 85** Zoom into triterpenic zone of GC chromatogram of sample of a *B. laxiflora* (47a1Q). Identification of triterpenic compounds is as follows: (I) 3-*epi*- $\beta$ -amyryn  $\alpha$ -OTMS, (II) 3-*epi*- $\alpha$ -amyryn  $\alpha$ -OTMS, (III) 3-*epi*-lupeol  $\alpha$ -OTMS, (IV)  $\beta$ -amyrone, (V)  $\beta$ -amyryn  $\beta$ -OTMS, (VIII) lupeol  $\beta$ -OTMS, (IX) lupenone.

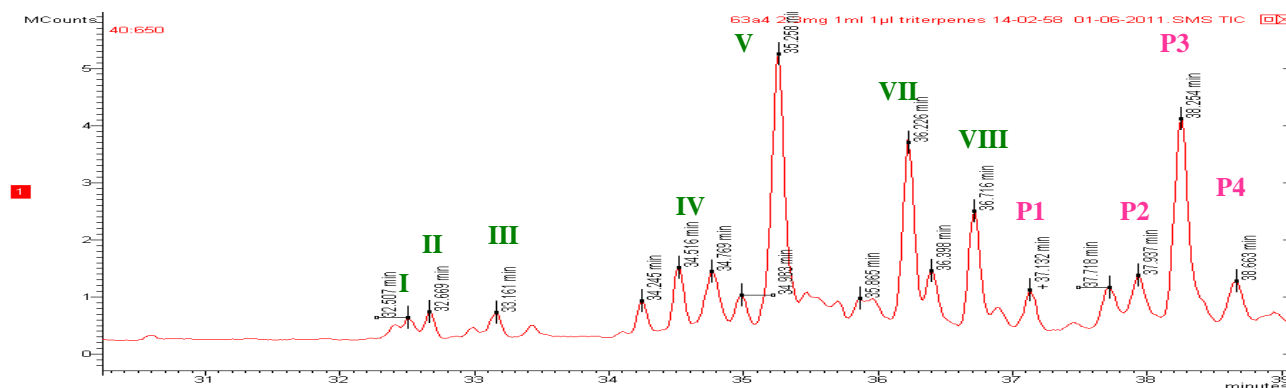
In the second lot molecular composition the same seven standard molecules along with the two markers, were identified. The difference between the two lots relies in the compound detected between minutes 38 and 39 (figure 86).



**Fig 86** Zoom into triterpenic zone of GC chromatogram of a sample of *B. laxiflora* (47b1Q). Identification of triterpenic compounds is as follows: (I) 3-*epi*- $\beta$ -amyryn  $\alpha$ -OTMS, (II) 3-*epi*- $\alpha$ -amyryn  $\alpha$ -OTMS, (III) 3-*epi*-lupeol  $\alpha$ -OTMS, (IV)  $\beta$ -amyryne, (V)  $\beta$ -amyryn  $\beta$ -OTMS, (VIII) lupeol  $\beta$ -OTMS, (IX) lupenone

### 5.5.5 *B. penicillata* triterpenic composition

This resin appears to be richer in triterpenoids than the other ones; in fact many important peaks were identified after 39 minutes. This is why we decided to present both chromatographic zones.



**Fig 87** Zoom into first triterpenic zone of GC chromatogram of a sample of *B. penicillata* (63a4). Identification of triterpenic compounds is as follows: (I) 3-*epi*- $\beta$ -amyryn  $\alpha$ -OTMS, (II) 3-*epi*- $\alpha$ -amyryn  $\alpha$ -OTMS, (III) 3-*epi*-lupeol  $\alpha$ -OTMS, (IV)  $\beta$ -amyryne, (V)  $\beta$ -amyryn  $\beta$ -OTMS, (VII)  $\alpha$ -amyryn  $\beta$ -OTMS, (VIII) lupeol.



In figure 87, from min 30 to 39 can be seen seven out of the nine standard molecules. The absent molecules were two ketons: (VI)  $\alpha$ -amyrone and (IX) lupenone. Additionally four markers were identified, marked as P1 to P4 in the chromatogram.

Figure 88 presents a partial chromatogram that runs from minute 38 to minute 50. From this zone three other molecules were chosen as markers (P5 to P7). Therefore molecules P1 and P2 can be seen at the beginning of the chromatogram.

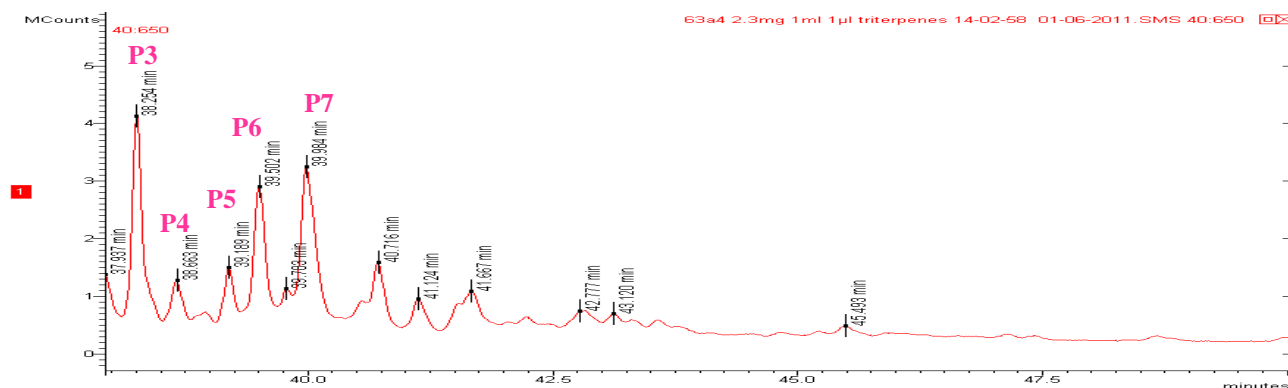


Fig 88 Zoom into second triterpenic zone of GC chromatogram of sample of *B. penicillata* (63a4).

### 5.5.6 *B. simaruba* triterpenic composition

As it can be seen on figure 89, eight out of the nine standard molecules studied were present in this sample, the only absent compound was lupenone, in contrast five other triterpenic compounds were detected, three exclusive for *B. simaruba* (S1-S3).

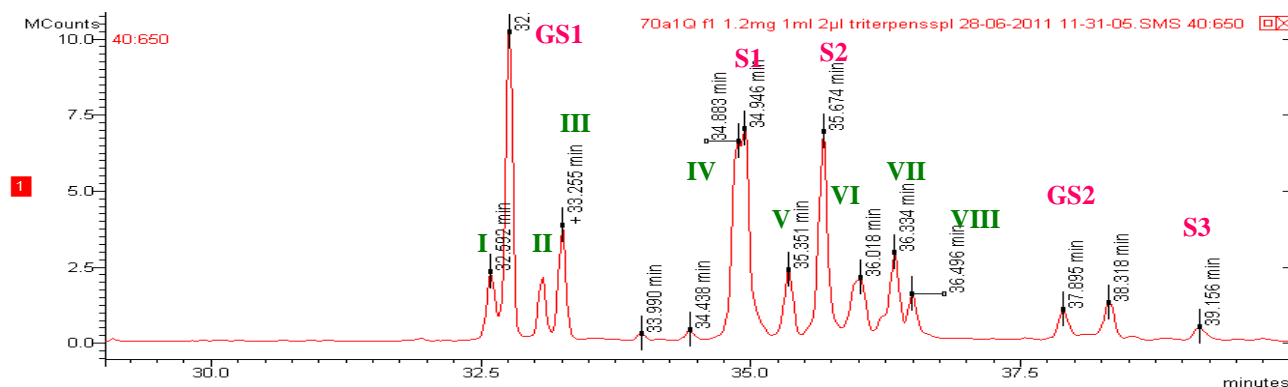
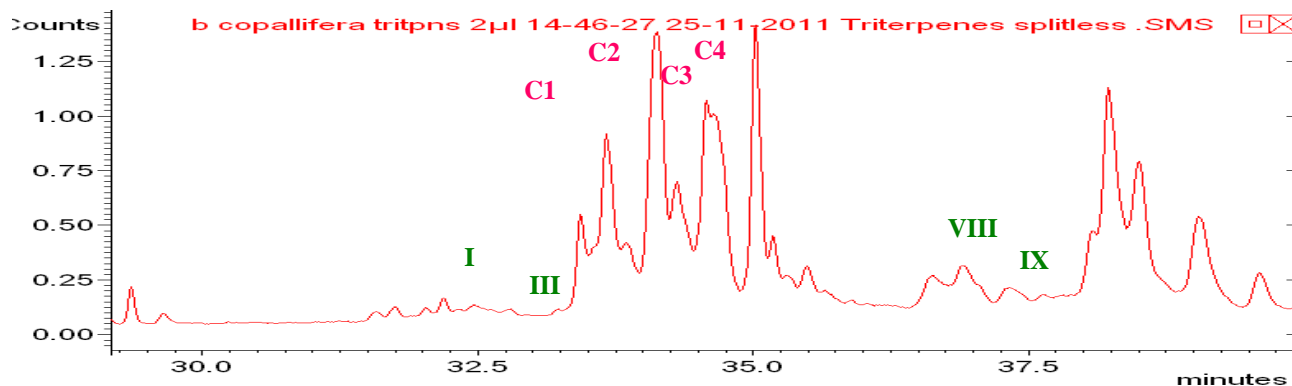


Fig 89 Zoom into triterpenic zone of GC chromatogram of a sample of *B. simaruba* (70a1Q). Identification of triterpenic compounds is as follows: (I) 3-*epi*- $\beta$ -amyrin  $\alpha$ -OTMS, (II) 3-*epi*- $\alpha$ -amyrin  $\alpha$ -OTMS, (III) 3-*epi*-lupeol  $\alpha$ -OTMS, (IV)  $\beta$ -amyrone, (V)  $\beta$ -amyrin  $\beta$ -OTMS, (VI)  $\alpha$ -amyrone, (VII)  $\alpha$ -amyrin  $\beta$ -OTMS, (VIII) lupeol.

### 5.5.7 *B. copallifera* triterpenic composition

As this sample was not part of the original set, in this chromatogram only four out of the standard molecules were detected: **(I)** 3-*epi*- $\beta$ -amyrin, **(III)** 3-*epi*-lupeol **(VIII)** lupeol and **(IX)** lupenone. Nevertheless this is not a resin poor in triterpenes, other five triterpenic molecules were characterized as markers (C1-C5).



**Fig 90 Zoom into triterpenic zone of GC chromatogram of the *B. copallifera* resin sample.** Identification of triterpenic compounds is as follows: **(I)** 3-*epi*- $\beta$ -amyrin  $\alpha$ -OTMS, **(II)** 3-*epi*- $\alpha$ -amyrin  $\alpha$ -OTMS, **(III)** 3-*epi*-lupeol  $\alpha$ -OTMS, **(IV)**  $\beta$ -amyrone, **(V)**  $\beta$ -amyrin  $\beta$ -OTMS, **(VI)**  $\alpha$ -amyrone, **(VII)**  $\alpha$ -amyrin  $\beta$ -OTMS, **(VIII)** lupeol, **(IX)** lupeol  $\beta$ -OTMS

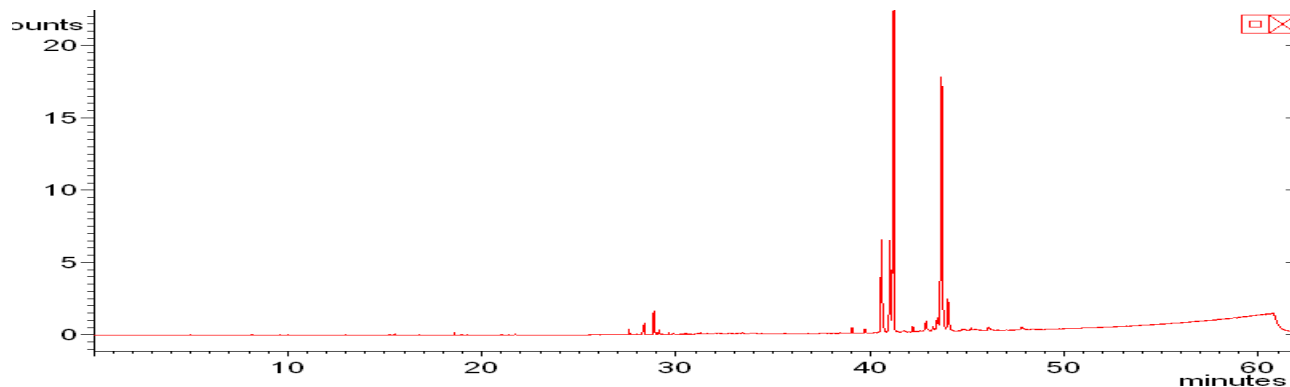
### 5.6 Study of archaeological samples

As we expected archaeological samples are rich in triterpenic compounds, these compounds were detected from 39 min of the chromatogram using protocol 1. The molecular composition of Aztec samples (26, 51, 52, 84, 140, 173 and TMT) can be correlated to that of *B. bipinnata* and *B. stenophylla* while the molecular composition of Chichen Itzá sample is completely different from that of Aztec and botanically certified resins, so we can conclude that its botanical origin is not within the studied species.

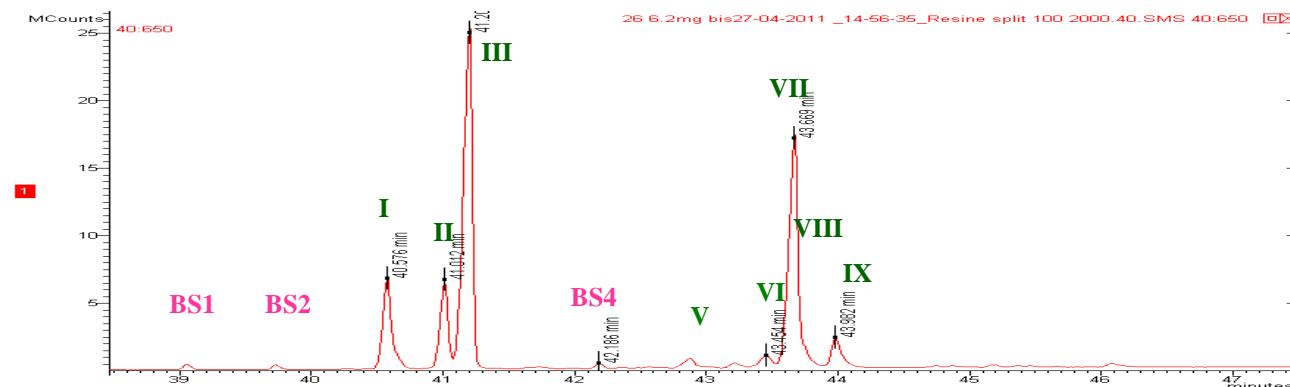
### 5.6.1 Molecular composition of archaeological sample 26

The complete chromatogram of this sample is presented in figure 91.

⊗ A)



⊗ B)

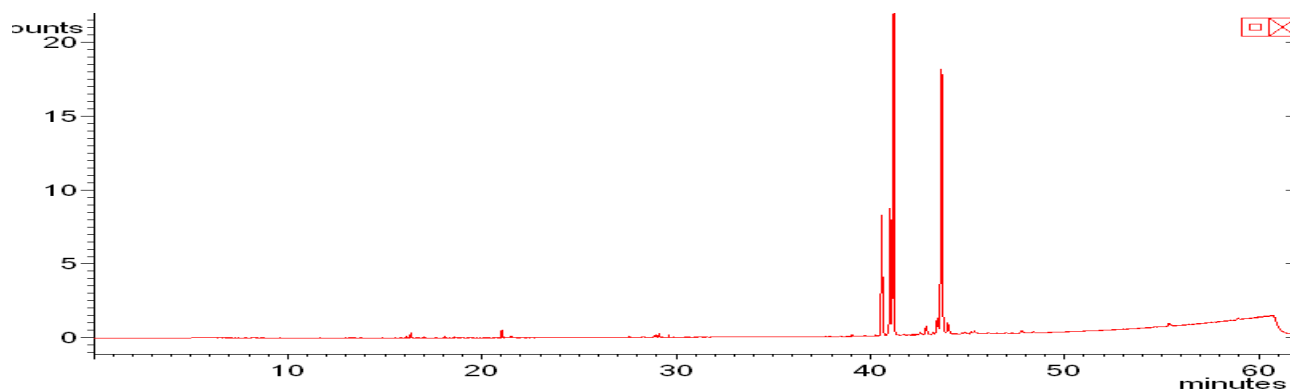


**Fig 91 A) complete GC chromatogram and B) Zoom into triterpenic zone of GC chromatogram of archaeological sample 26.** Identification of triterpenic compounds is as follows: (I) 3-*epi*- $\beta$ -amyrin  $\alpha$ -OTMS, (II) 3-*epi*- $\alpha$ -amyrin  $\alpha$ -OTMS, (III) 3-*epi*-lupeol  $\alpha$ -OTMS, (IV)  $\beta$ -amyrone, (V)  $\beta$ -amyryn  $\beta$ -OTMS, (VI)  $\alpha$ -amyrone, (VII)  $\alpha$ -amyryn  $\beta$ -OTMS, (VIII) lupeol  $\beta$ -OTMS, (IX) lupenone

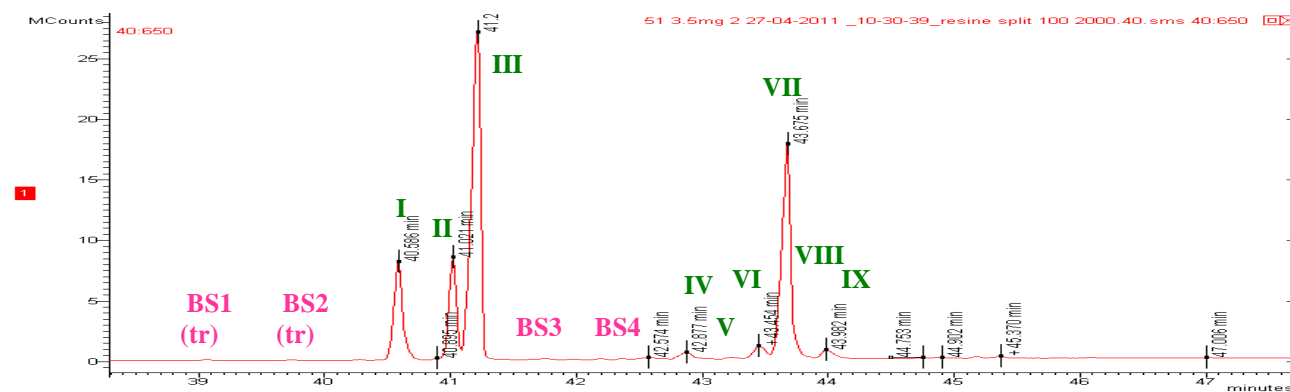
Regarding the zoom into triterpenic area of the chromatogram, the nine triterpenic standard molecules were detected, as well as the molecules markers for *B. stenophylla* and *B. bipinnata* BS1, BS2 and BS4. This allows us to conclude that the botanical origin for the resin on this sample is with no doubt comprised between *B. bipinnata* or *B. stenophylla* species.

### 5.6.2 Molecular composition of archaeological sample 51

Global chromatogram of this sample shows no important peaks before 38min (figure 92). **A**)



**B**)



**Fig 92 A) Complete chromatogram and B) zoom into triterpenic zone of archaeological sample 51.**

Identification of triterpenic compounds is as follows: **(I)** 3-*epi*- $\beta$ -amyirin  $\alpha$ -OTMS, **(II)** 3-*epi*- $\alpha$ -amyirin  $\alpha$ -OTMS, **(III)** 3-*epi*-lupeol  $\alpha$ -OTMS, **(IV)**  $\beta$ -amyrone, **(V)**  $\beta$ -amyirin  $\beta$ -OTMS, **(VI)**  $\alpha$ -amyrone, **(VII)**  $\alpha$ -amyirin  $\beta$ -OTMS, **(VIII)** lupeol  $\beta$ -OTMS, **(IX)** lupenone

In general terms, molecular composition of triterpenic fraction of this archaeological sample is quite close to that of sample 26, again all standard molecules are present plus the 4 markers for *B. bipinnata* and *B. stenophylla* resins.

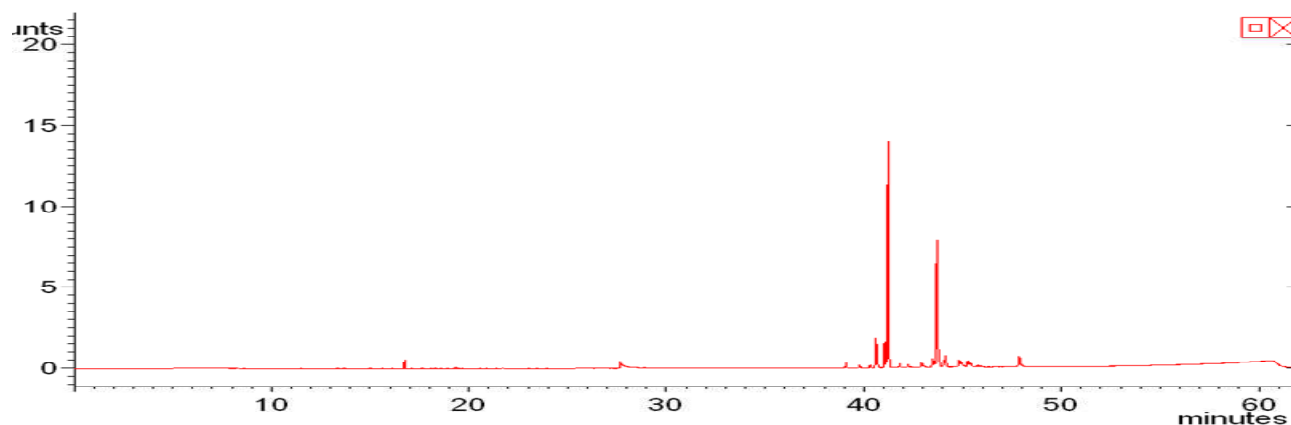
### 5.6.3 Molecular composition of archaeological sample 52

The global chromatogram of this sample is consistent with the former studied chromatograms. It shows no peaks before the 39 min.

The molecular composition of triterpenic fraction is close to that of samples 26 and 5: the nine standard triterpenic molecules were identified, plus the 4 markers for *B. bipinnata* and *B. stenophylla* (BS1 to BS4) resins.

NB. Although  $\beta$ -amyrin (V) is not marked and identified in the corresponding section of the chromatogram (figure 93 A and, B), some minor quantities of this compound were detected.

⊗ A)



⊗ B)

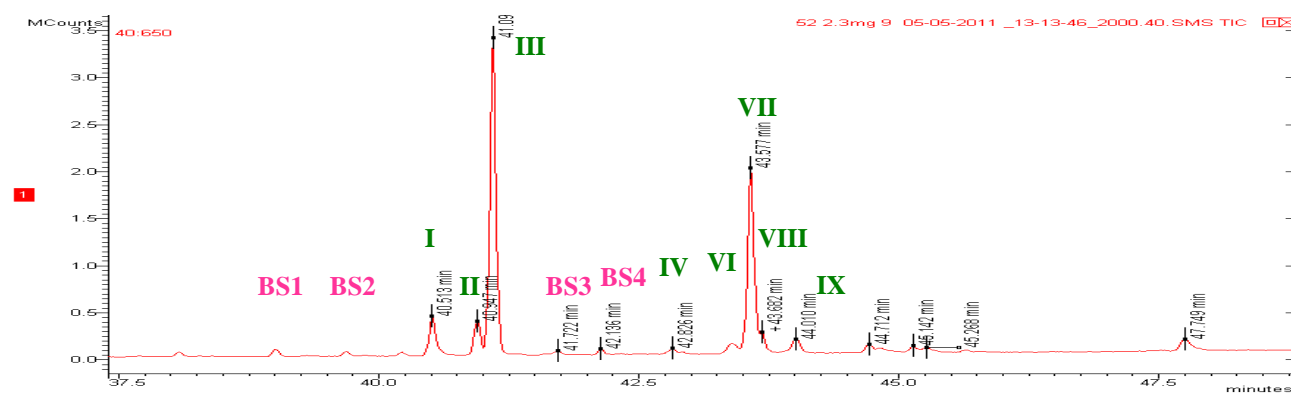


Fig 93 A) Complete chromatogram and B) zoom into triterpenic zone of archaeological sample 52.

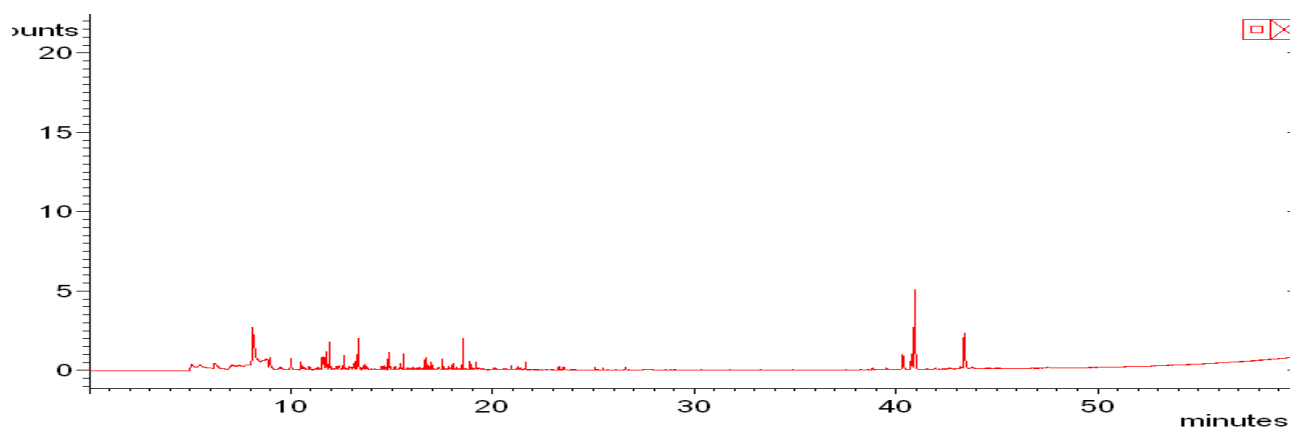
Identification of triterpenic compounds is as follows: (I) 3-*epi*- $\beta$ -amyrin  $\alpha$ -OTMS, (II) 3-*epi*- $\alpha$ -amyrin  $\alpha$ -OTMS, (III) 3-*epi*-lupeol  $\alpha$ -OTMS, (IV)  $\beta$ -amyrone, (V)  $\beta$ -amyrin  $\beta$ -OTMS, (VI)  $\alpha$ -amyrone, (VII)  $\alpha$ -amyrin  $\beta$ -OTMS, (VIII) lupeol  $\beta$ -OTMS, (IX) lupenone.

### 5.6.4 Molecular composition of archaeological sample 84

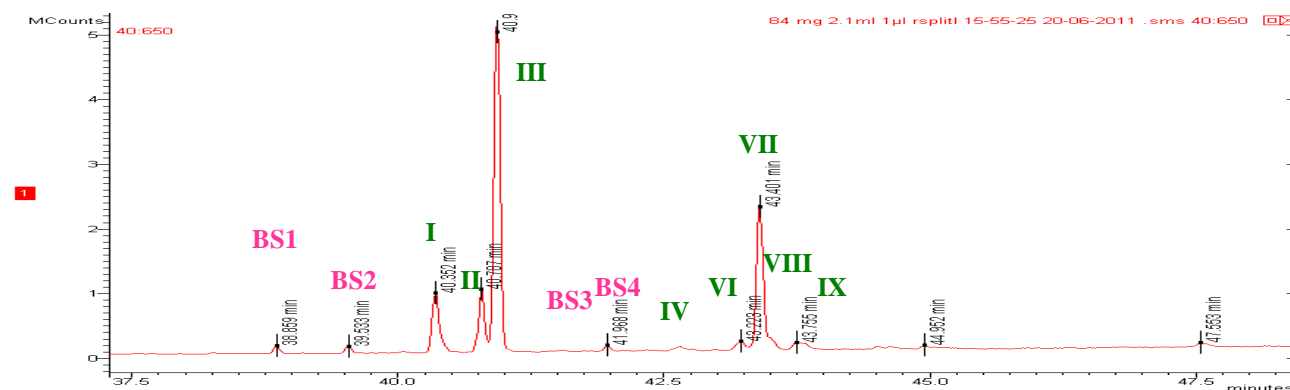
As it can be seen on figure 94A the molecular composition of this sample is complex, but its complexity is not related to the composition of the triterpenic fraction, as it is rather simple fraction.

Among triterpenes the nine studied standard molecules were detected, again some minor quantities of (V)  $\beta$ -amyrin were detected, along with the four *BS* molecular markers.

⊗ A)



⊗ B)



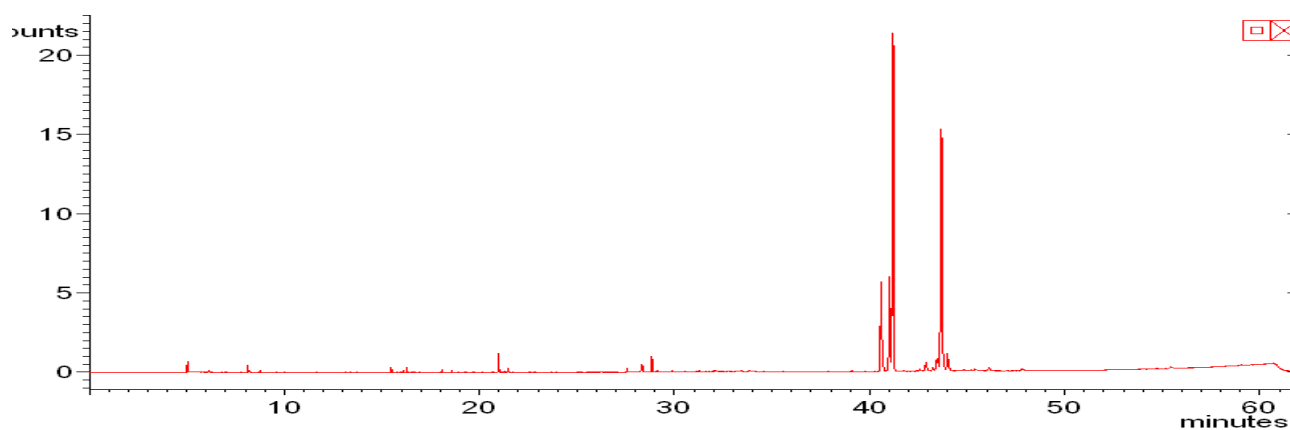
**Fig 94** A) Complete chromatogram and B) zoom into triterpenic zone of archaeological sample 84.

Identification of triterpenic compounds is as follows: (I) 3-*epi*- $\beta$ -amyrin  $\alpha$ -OTMS, (II) 3-*epi*- $\alpha$ -amyrin  $\alpha$ -OTMS, (III) 3-*epi*-lupeol  $\alpha$ -OTMS, (IV)  $\beta$ -amyrone, (V)  $\beta$ -amyrin  $\beta$ -OTMS, (VI)  $\alpha$ -amyrone, (VII)  $\alpha$ -amyrin  $\beta$ -OTMS, (VIII) lupeol  $\beta$ -OTMS, (IX) lupenone.

### 5.6.5 Molecular composition of archaeological sample 173

The molecular composition of this sample is quite close to that of samples 26, 51 and 52. The nine studied standard molecules were detected, concerning the markers for *B. bipinnata* and *B. stenophylla*, BS3 was absent from the molecular composition of this sample (figure 95)

⊗ A)



⊗ B)

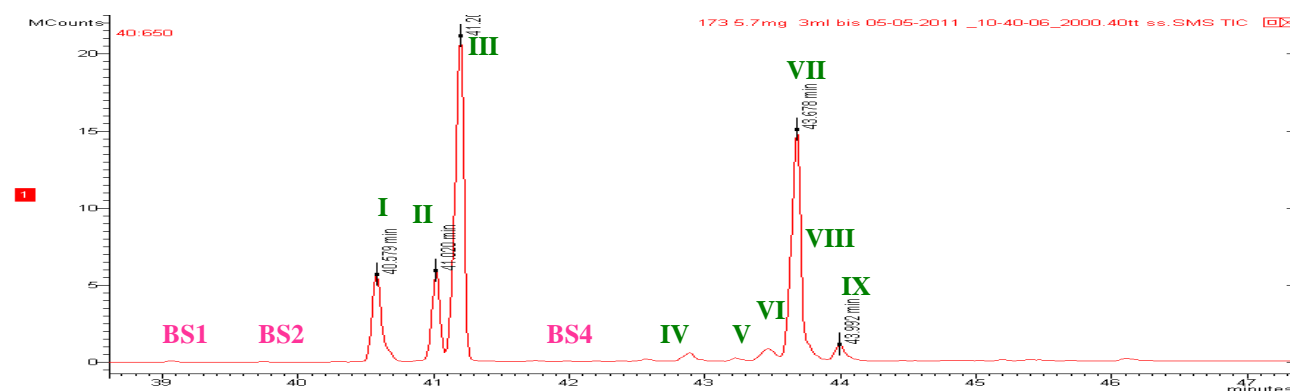


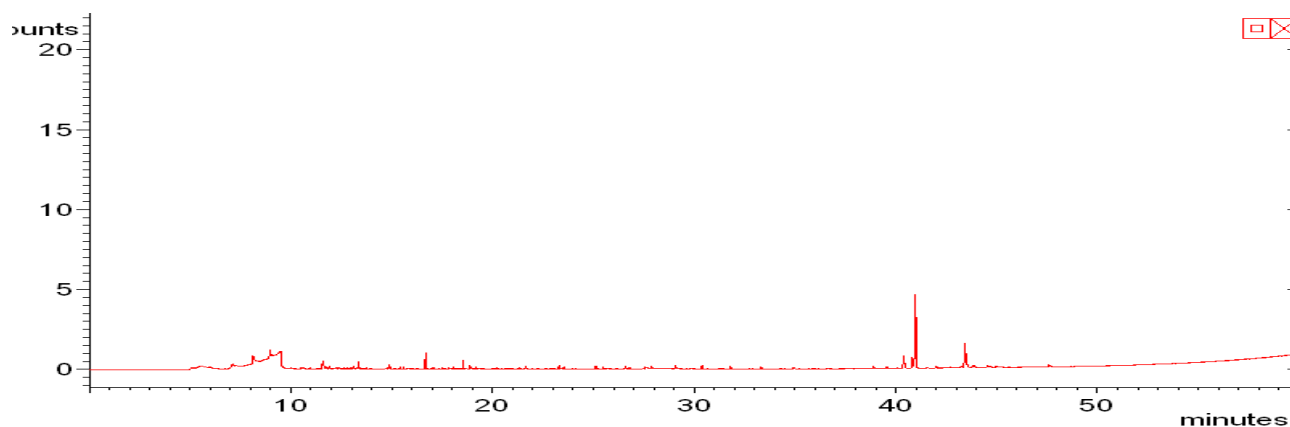
Fig 95 A) Complete chromatogram and B) zoom into triterpenic zone of archaeological sample 173.

Identification of triterpenic compounds is as follows: (I) 3-*epi*- $\beta$ -amyirin  $\alpha$ -OTMS, (II) 3-*epi*- $\alpha$ -amyirin  $\alpha$ -OTMS, (III) 3-*epi*-lupeol  $\alpha$ -OTMS, (IV)  $\beta$ -amyrone, (V)  $\beta$ -amyirin  $\beta$ -OTMS, (VI)  $\alpha$ -amyrone, (VII)  $\alpha$ -amyirin  $\beta$ -OTMS, (VIII) lupeol  $\beta$ -OTMS, (IX) lupenone.

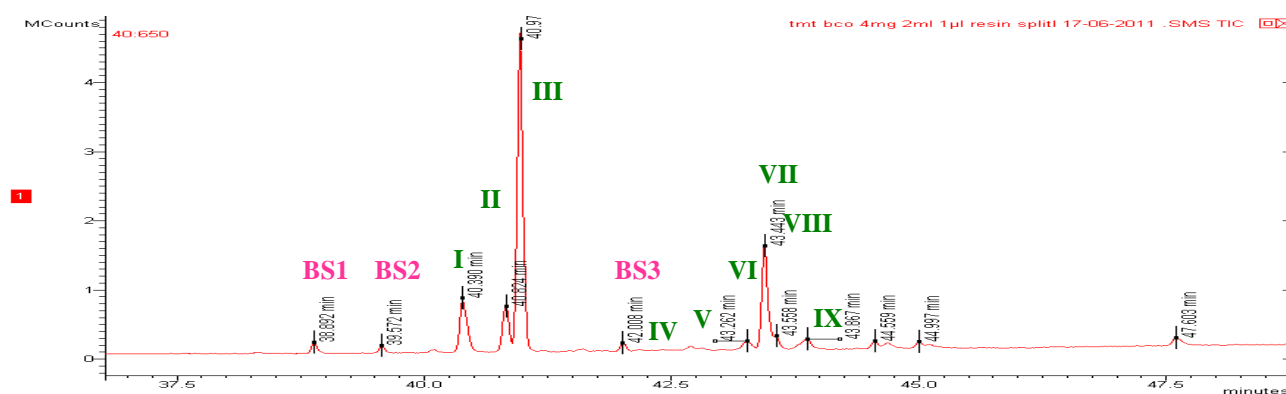
### 5.6.7 Molecular composition of archaeological sample TMT

As it can be seen on figure 96 A) many minor peaks corresponding to non triterpenic compounds were detected between 7 and 38 min. In the triterpenic fraction the nine studied standard molecules were detected, three of the four *BS* molecular markers were found with the absence of BS4 (figure 96 B).

A)



B)



**Fig 96 A) Complete chromatogram and B) zoom into triterpenic zone of archaeological sample TMT.** Identification of triterpenic compounds is as follows: **(I)** 3-*epi*- $\beta$ -amyryn  $\alpha$ -OTMS, **(II)** 3-*epi*- $\alpha$ -amyryn  $\alpha$ -OTMS, **(III)** 3-*epi*-lupeol  $\alpha$ -OTMS, **(IV)**  $\beta$ -amyryne, **(V)**  $\beta$ -amyryn  $\beta$ -OTMS, **(VI)**  $\alpha$ -amyryne, **(VII)**  $\alpha$ -amyryn  $\beta$ -OTMS, **(VIII)** lupeol  $\beta$ -OTMS, **(IX)** lupenone.

### 5.6.8 Molecular composition of archaeological sample 140

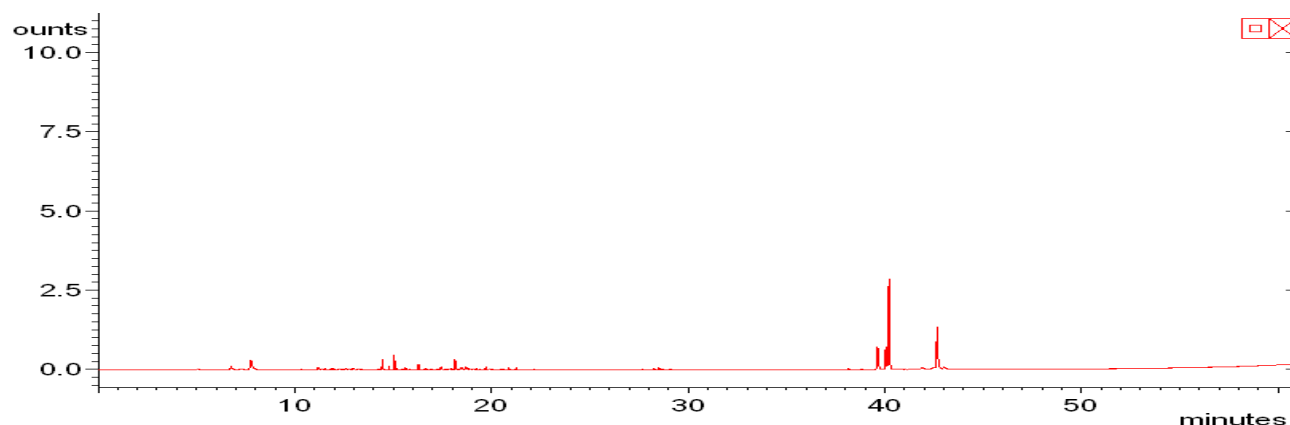
As it can be seen on figure 97A many peaks corresponding to non triterpenic compounds were detected between 6.7 and 23min.

As their fragmentation patterns are different their nature certainly differs a more detailed informations about them is beyond the scope of this work owing to time restriction.

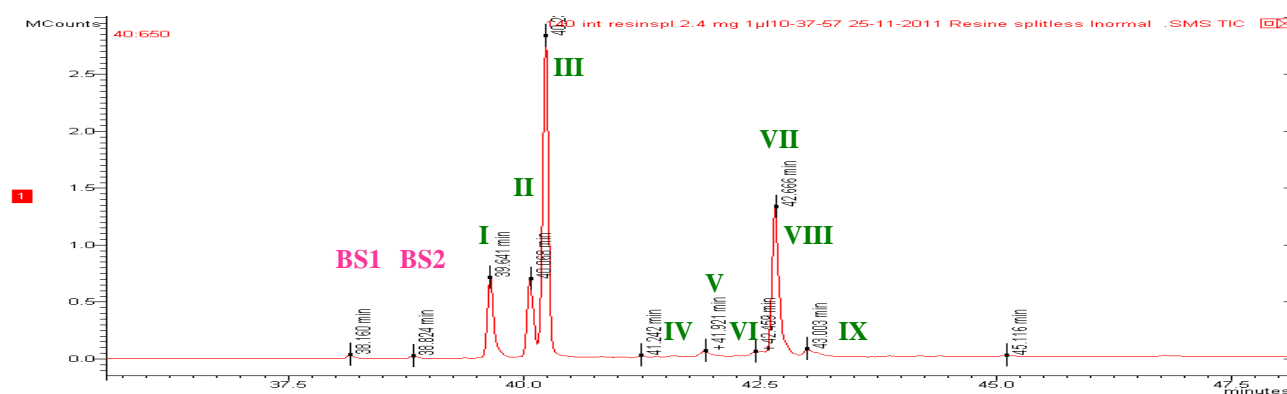
In the triterpenic fraction of this sample the nine studied standard molecules were detected, two of the four *BS* molecular markers were found: BS1 and BS2.



A)



B)



**Fig 97 A) Complete chromatogram and B) zoom into triterpenic zone of archaeological sample M1.** Identification of triterpenic compounds is as follows: **(I)** 3-*epi*- $\beta$ -amyrin  $\alpha$ -OTMS, **(II)** 3-*epi*- $\alpha$ -amyrin  $\alpha$ -OTMS, **(III)** 3-*epi*-lupeol  $\alpha$ -OTMS, **(IV)**  $\beta$ -amyrone, **(V)**  $\beta$ -amyrin  $\beta$ -OTMS, **(VI)**  $\alpha$ -amyrone, **(VII)**  $\alpha$ -amyrin  $\beta$ -OTMS, **(VIII)** lupeol  $\beta$ -OTMS, **(IX)** lupenone.

### 5.6.9 Molecular composition of archaeological sample from Chichén Itzá

As it can be seen on figure 98 A, the molecular composition of this sample differs from that of the other archaeological samples, this is consistent with our findings by HPLC-Uv/Vis.

As the fragmentation patterns from the peaks detected between 10 and 27min are different one from another their nature certainly differs, a more detailed information about their molecular structure is beyond the scope of this work owing to time and equipment restrictions.

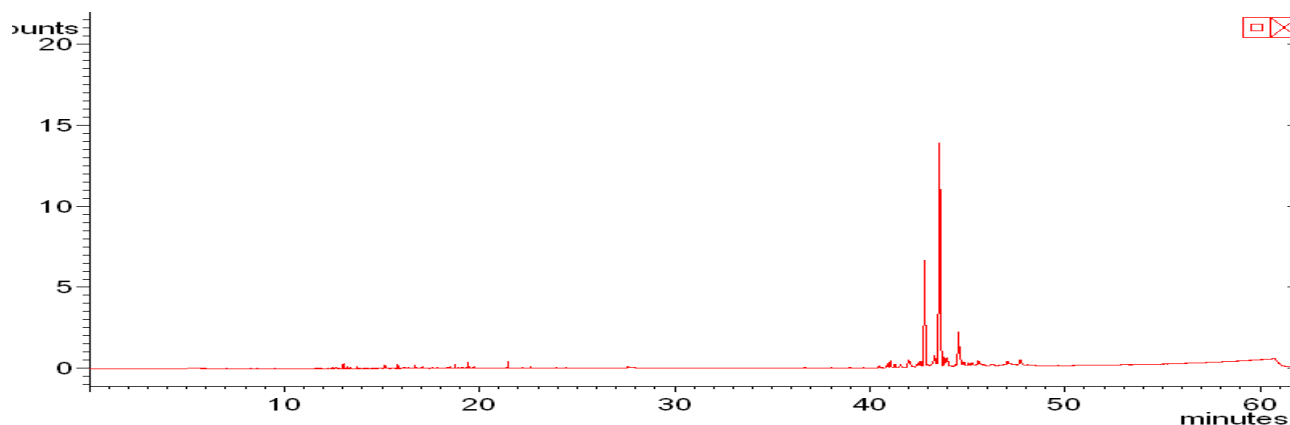
Also the triterpenic fraction of this sample differs greatly compared to that of the other archaeological samples: the relative proportion of 3-*epi*- $\alpha$ -amyrin, 3-*epi*- $\beta$ -amyrin, and 3-*epi*-

lupeol are considerable inferior compared to their proportion in the Aztec archaeological samples.

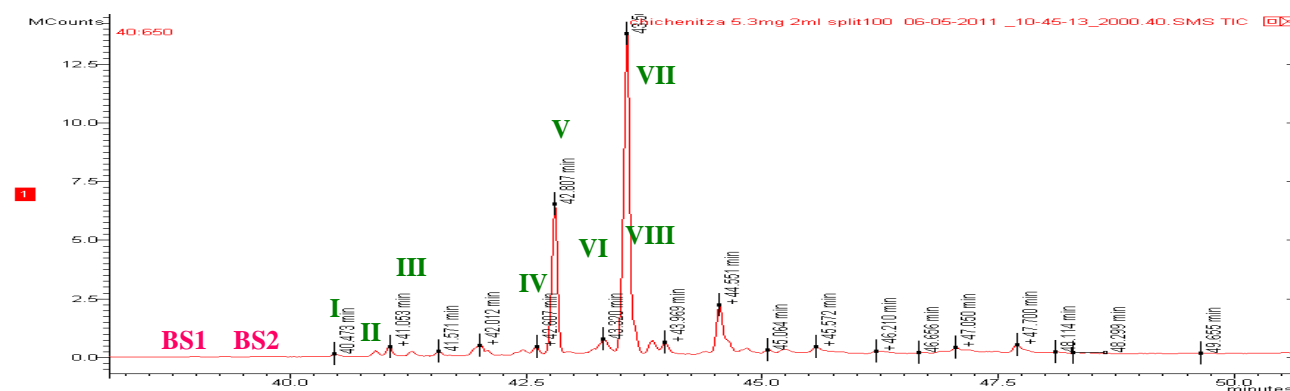
Concerning the proportions of  $\beta$ -amyrone and  $\alpha$ -amyrin, they are considerably more important in this sample than in the other archaeological ones.

Finally two markers BS1 and BS2 were detected in this sample.

⊗ A)



⊗ B)



**Fig 98 A) Complete chromatogram and B) zoom into triterpenic zone of archaeological sample Chichén Itzá**

Identification of triterpenic compounds is as follows: **(I)** 3-*epi*- $\beta$ -amyrin  $\alpha$ -OTMS, **(II)** 3-*epi*- $\alpha$ -amyrin  $\alpha$ -OTMS, **(III)** 3-*epi*-lupeol  $\alpha$ -OTMS, **(IV)**  $\beta$ -amyrone, **(V)**  $\beta$ -amyrin  $\beta$ -OTMS, **(VI)**  $\alpha$ -amyrone, **(VII)**  $\alpha$ -amyrin  $\beta$ -OTMS, **(VIII)** lupeol  $\beta$ -OTMS.

The abundance of secondary products visible in GC-MS and the high number of unidentified peaks is not surprising if we consider that this material is in fact a fifteen century resin and the fact that oxidation phenomena are quite active in this kind of molecularly complex materials.

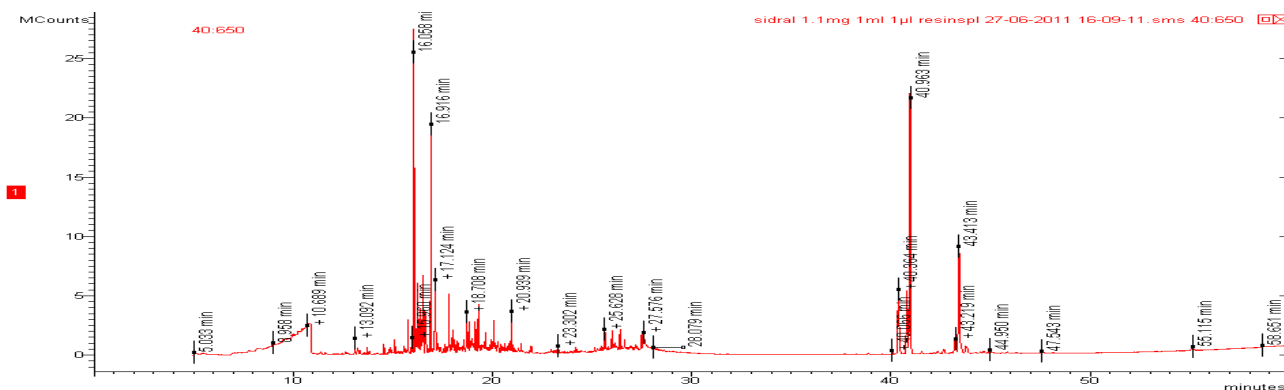
## 5.7 Study of commercial samples

In this section we will present the chromatograms of some selected commercial samples, the choice of studying them was determined in part by the results obtained by FTIR and HPLC-UV/Vis and because of their representatively considering the other commercial resins.

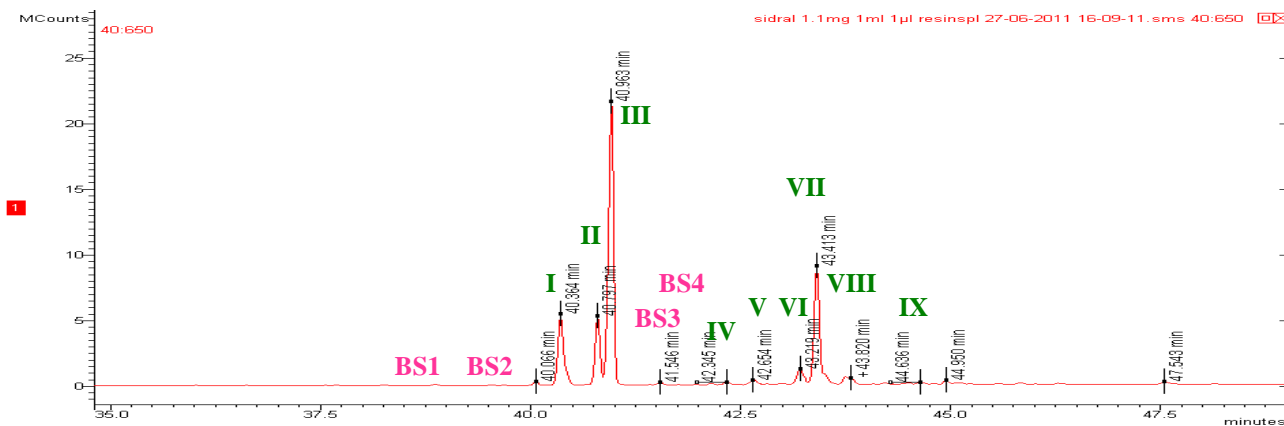
### 5.7.1 Molecular composition of Sidral

As can be seen on figure 99 A, the global chromatogram of Sidral exhibits an important amount of peaks between 13 and 30 min.

⊗ A)



⊗ B)



**Fig 99 A) Complete chromatogram and B) zoom into triterpenic zone of commercial sample Sidral.**

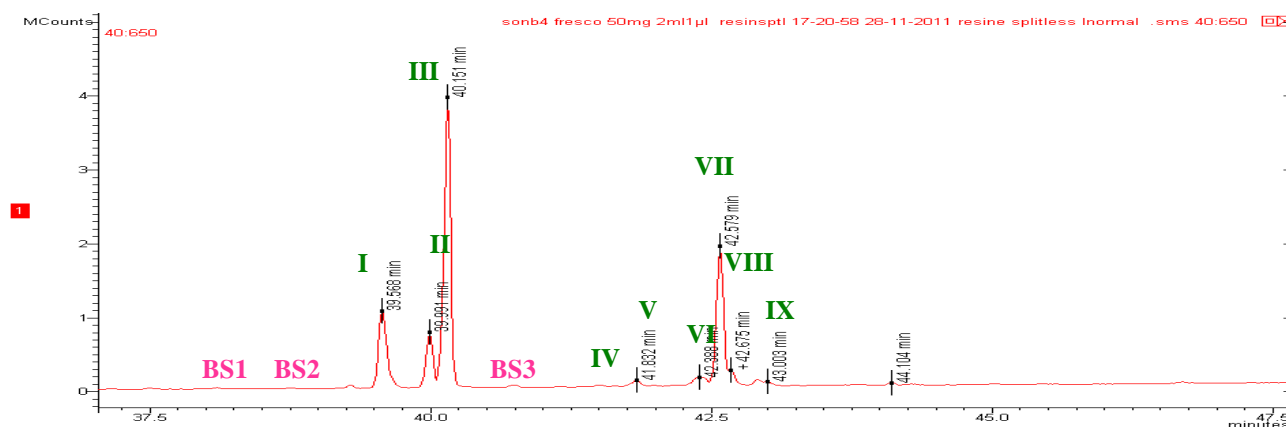
Identification of triterpenic compounds is as follows: (I) 3-*epi*- $\beta$ -amyryn  $\alpha$ -OTMS, (II) 3-*epi*- $\alpha$ -amyryn  $\alpha$ -OTMS, (III) 3-*epi*-lupeol  $\alpha$ -OTMS, (IV)  $\beta$ -amyryne, (V)  $\beta$ -amyryn  $\beta$ -OTMS, (VI)  $\alpha$ -amyryne, (VII)  $\alpha$ -amyryn  $\beta$ -OTMS, (VIII) lupenone, (IX) lupeol  $\beta$ -OTMS

Those peaks can be attributed in many cases to mono- and sesquiterpenoids; nevertheless for the proper study of these compounds a specific protocol of extraction of essential oils should have been conducted. Again this type of study is beyond the scope of this research.

The triterpenoid fraction of Sidral is identical to that of *B. bipinnata* and *B. stenophylla*, the nine identified standard molecules plus the four markers BS are present. Therefore its botanical origin is without doubt among these two species.

### 5.7.2 Molecular composition of commercial sample SONB4

According to the obtained GC chromatogram, this sample has a very similar molecular composition to that of Sidral with only minor difference: the absence of BS4 (figure 100). Considering that this sample is a fresh sample and that BS4 was detected in many of the archaeological resins one might hypothesized that this compound was never part of the composition of this sample.



**Fig 100 Zoom into triterpenic zone of commercial sample SONB4.** Identification of triterpenic compounds is as follows: (I) 3-*epi*- $\beta$ -amyrin  $\alpha$ -OTMS, (II) 3-*epi*- $\alpha$ -amyrin  $\alpha$ -OTMS, (III) 3-*epi*-lupeol  $\alpha$ -OTMS, (IV)  $\beta$ -amyrone, (V)  $\beta$ -amyrin  $\beta$ -OTMS, (VI)  $\alpha$ -amyrone, (VII)  $\alpha$ -amyrin  $\beta$ -OTMS, (VIII) lupeol  $\beta$ -OTMS, (IX) lupenone.

### 5.7.3 Comparison between molecular composition of ATZJ2 and SONB4

In figure 101 are presented the complete chromatograms of sample ATZJ2 and SONB4. Both samples were analyzed using the same gradient, and triterpenic zone of ATZJ2 is empty, not a single triterpenoid from the standard molecules was the chromatogram detected, neither any BS markers.

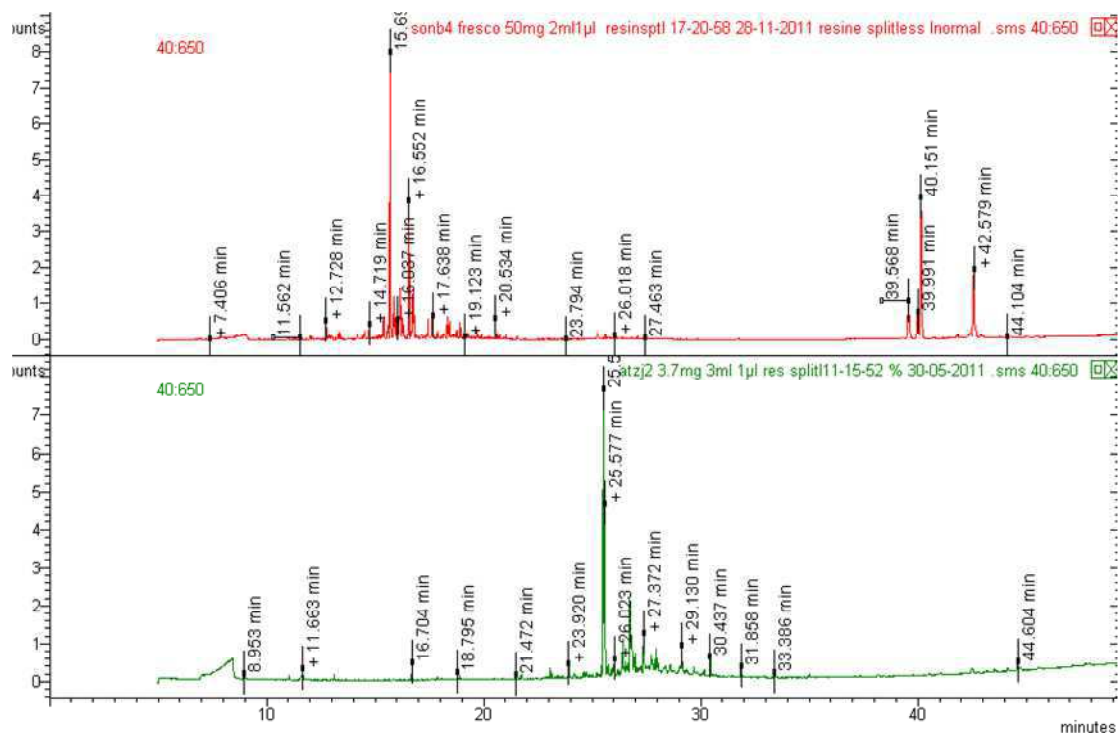


Fig 101 Global Chromatograms for SONB4 and ATZJ2

### 5.7.4 Molecular composition Oaxc2

The chromatogram showed on figure 102 confirms the absence of triterpenoids that we assumed from the study of the HPLC chromatogram for this sample.

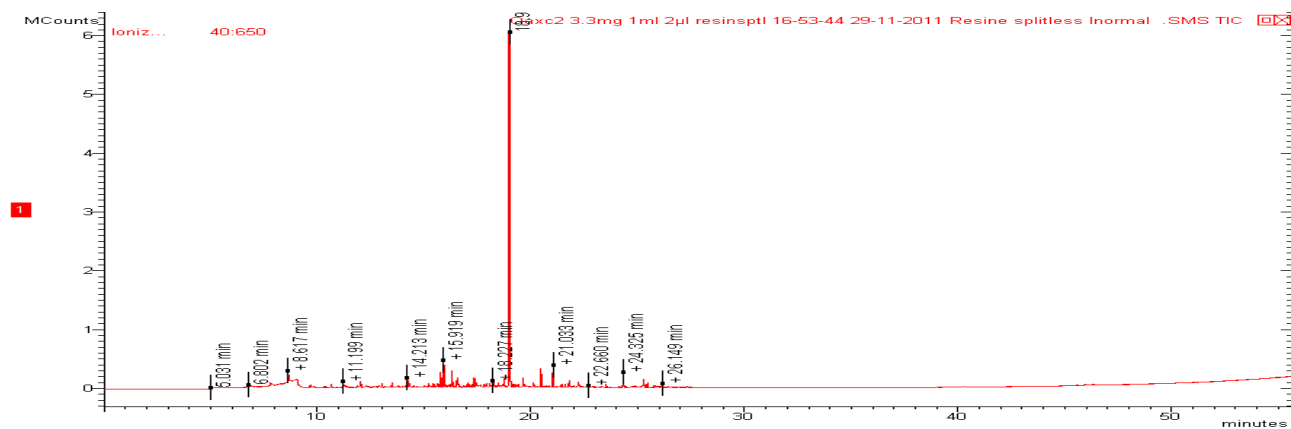


Fig 102 Global Chromatogram for Oaxc2

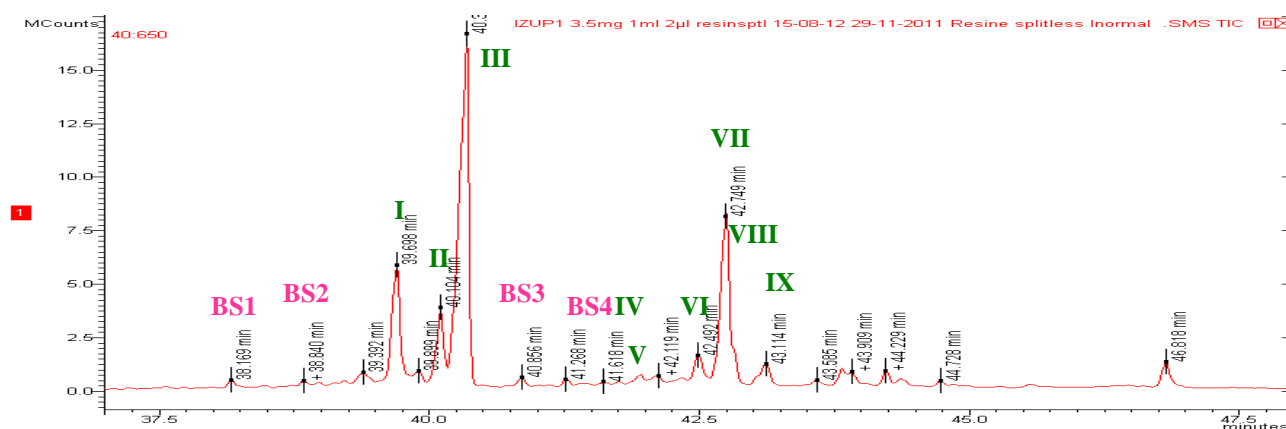
### 5.7.5 Molecular composition IZUP1 and SONR1

These samples correspond to two different kinds of copals a red one and a “piedra” one. The physical aspect of both samples differs a lot from white copals; nevertheless their molecular composition is close to that of SONB4.

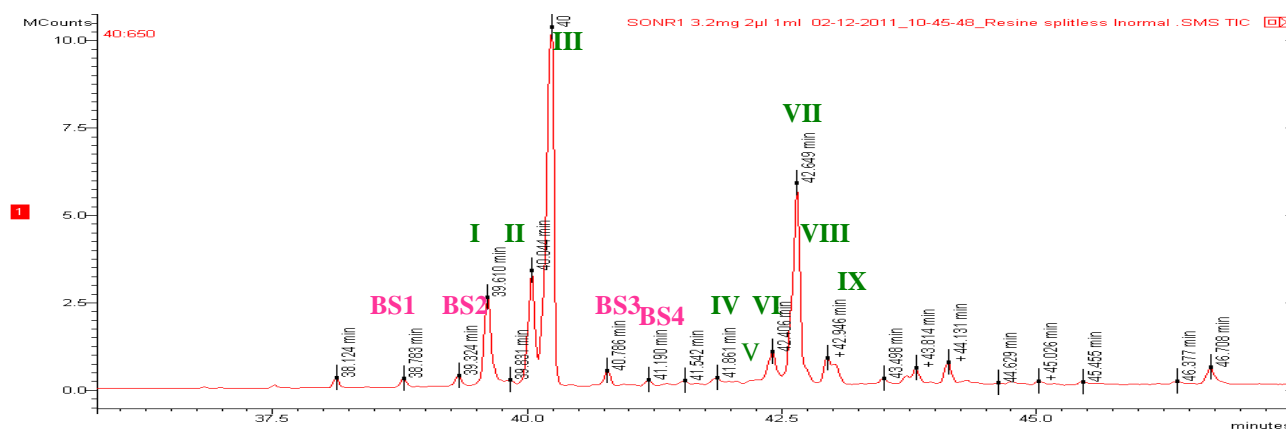
As it can be seen on 103 A and B chromatograms, the nine standard triterpenic compounds were identified on them, as well as the four molecular markers for *B. bipinnata* and *B. stenophylla* species.

These data strongly suggest that these two resins have a common origin and it can be correlated to the above mentioned species.

⊗ A)



⊗ B)



**Fig 103 Zoom into triterpenic zones of the chromatograms for A) IZUP1 and B) SONR1**

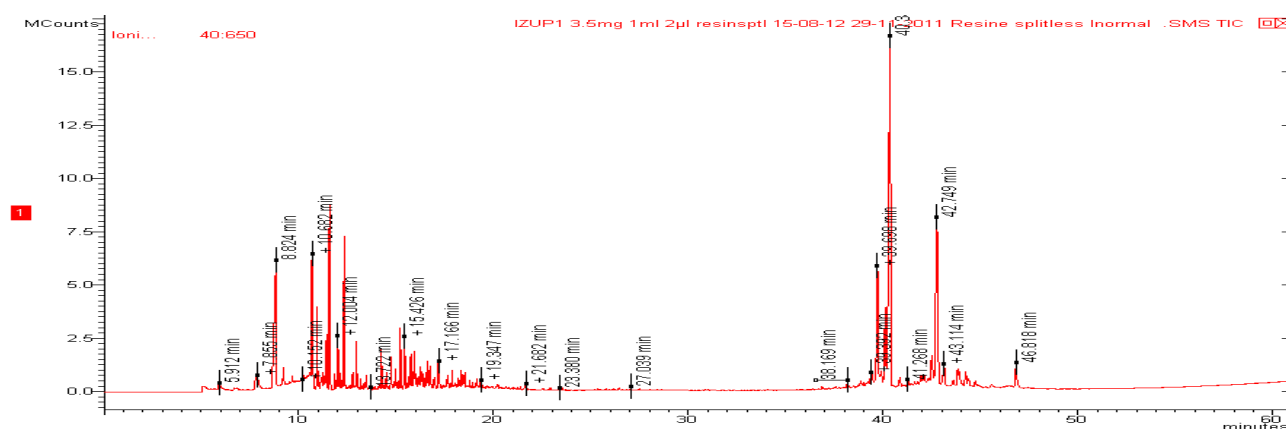
Identification of triterpenic compounds is as follows: **(I)** 3-*epi*- $\beta$ -amyrin  $\alpha$ -OTMS, **(II)** 3-*epi*- $\alpha$ -amyrin  $\alpha$ -OTMS, **(III)** 3-*epi*-lupeol  $\alpha$ -OTMS, **(IV)**  $\beta$ -amyrone, **(V)**  $\beta$ -amyrin  $\beta$ -OTMS, **(VI)**  $\alpha$ -amyrone, **(VII)**  $\alpha$ -amyrin  $\beta$ -OTMS, **(VIII)** lupeol  $\beta$ -OTMS, **(IX)** lupenone.

Concerning the volatile fraction of these two samples differences can be inferred from their global chromatogram presented here in figure 104, SONR1 the sesquiterpens  $\alpha$ -pinene and azulene, as well as limonene derivatives were detected. In IZUP1  $\alpha$ -pinene and myrtenol were detected. All the identifications were performed using NIST library 2011 version.

Considering the derivatization process that samples were subjected to, the complete characterization of volatile fraction is not possible, being light molecules some of them might have been volatilized.

Therefore an accurate procedure for the study of these molecules should be followed for their study.

⊗ A)



⊗ B)

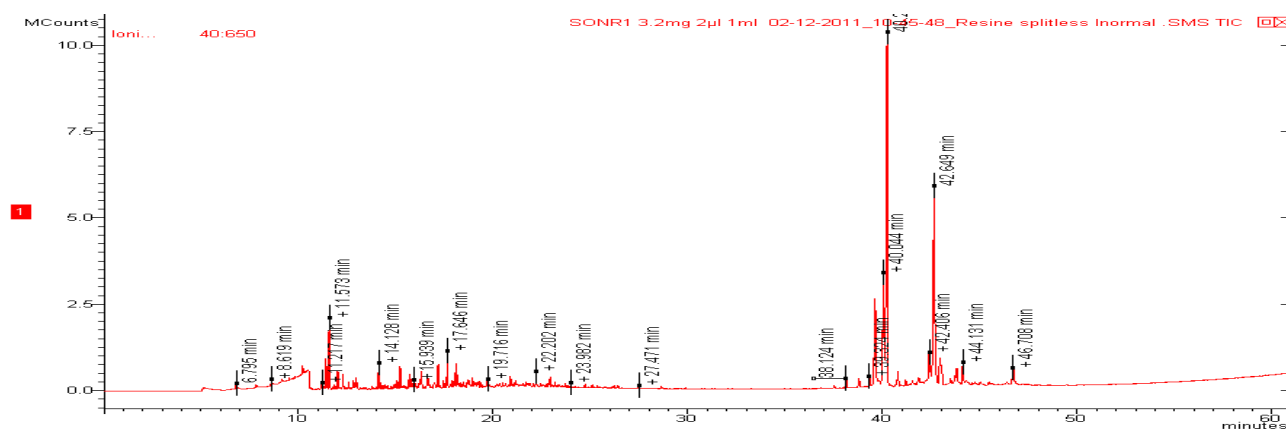


Fig 104 Global chromatograms for A) IZUP1 and B) SONR1

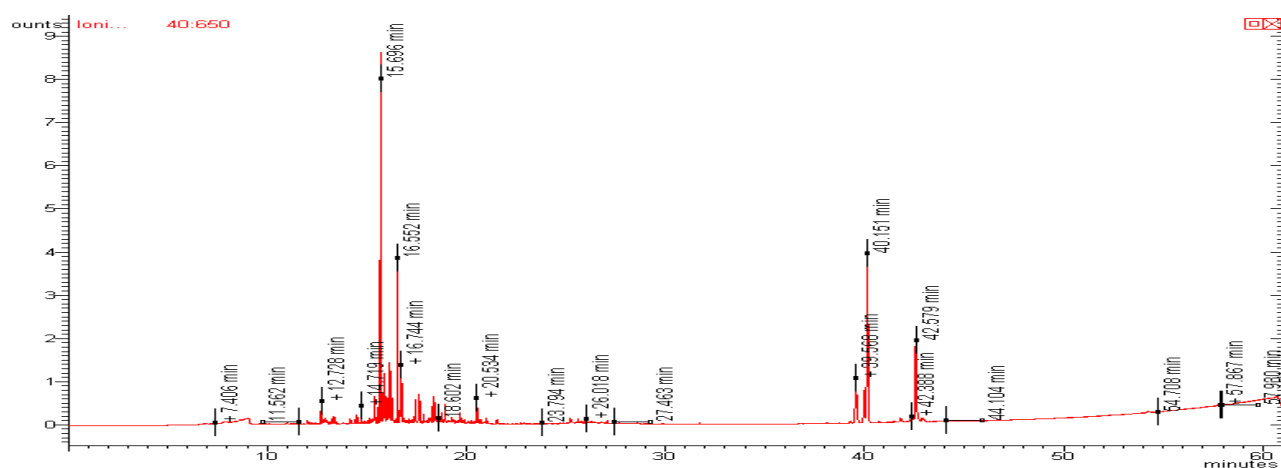
## 5.8 Comparison of partial analysis from the surface and the inner part of the samples

In this section we will report some results of comparing in one side the chromatograms of a fresh resins and the same resin aged under natural light from September to December 2011, and in the other side a chromatogram from the material obtained from the surface of TMT archaeological sample and the inner part of a piece of this resin sample.

### 5.8.1 Comparison between SONB4 fresh and naturally aged sample compositions

The ageing of the sample was conducted according to the procedure described below.

#### A) fresh SONB4



#### B) aged SONB4

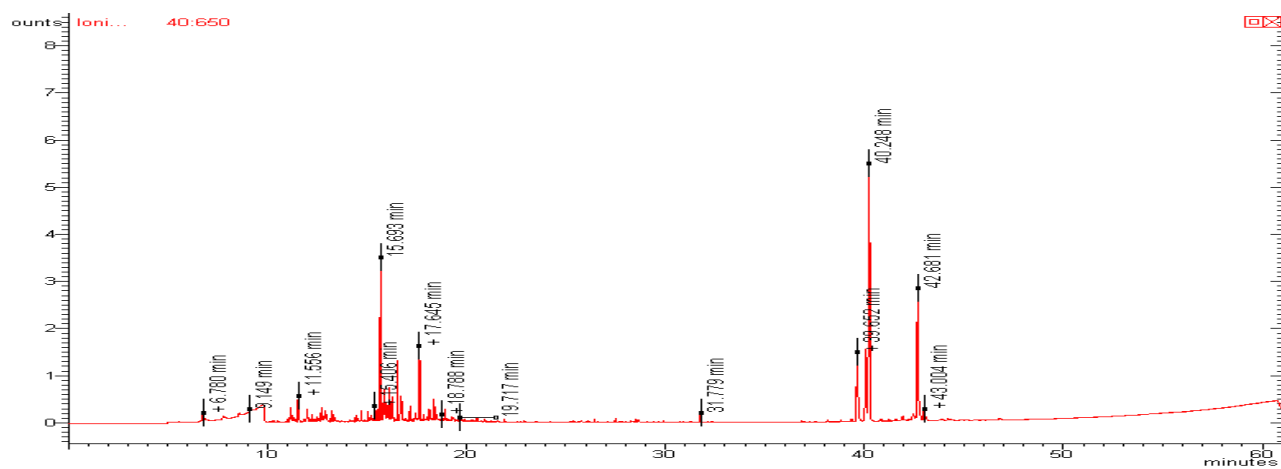
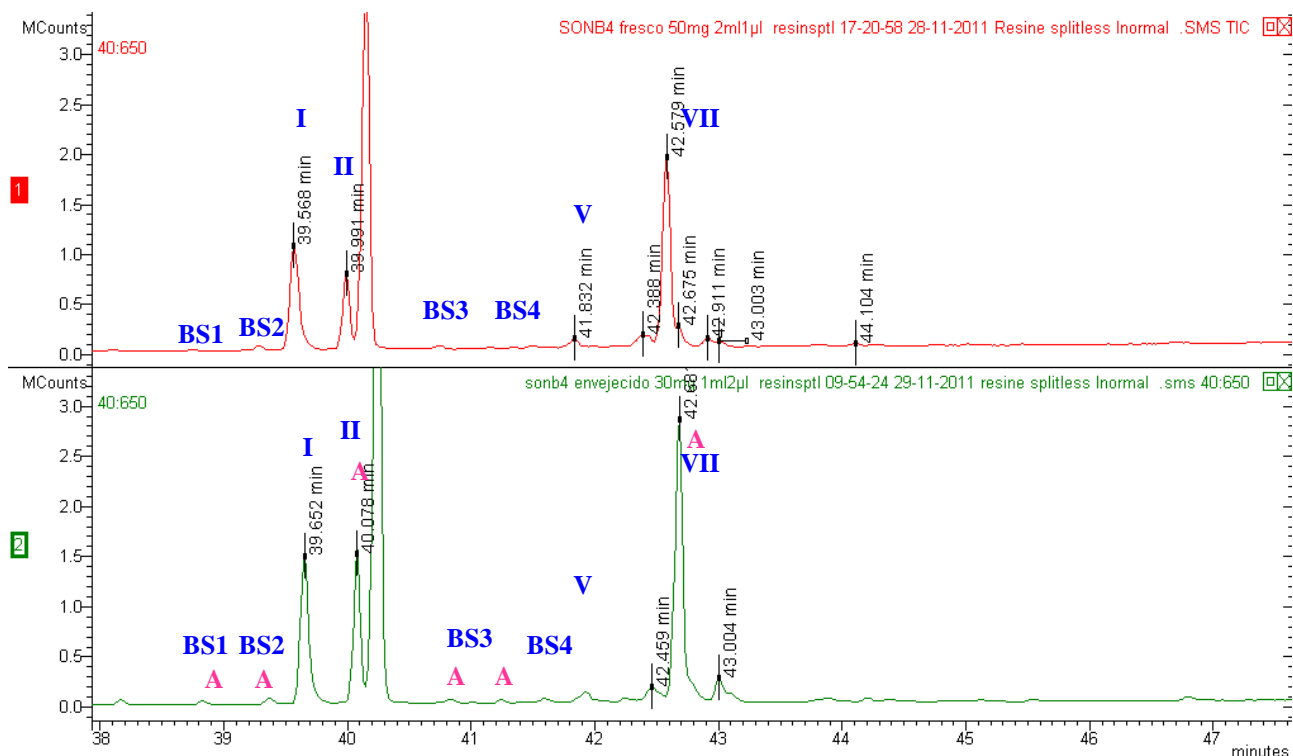


Fig 105 Global chromatograms for A) SONB4 resin and B) SONB4 aged resin





**Fig 106 Zoom into triterpenic zones of SONB4 resin and SONB4 aged resin.** Identification of triterpenic compounds is as follows: (I) 3-*epi*- $\beta$ -amyrin  $\alpha$ -OTMS, (II) 3-*epi*- $\alpha$ -amyrin  $\alpha$ -OTMS, (III) 3-*epi*-lupeol  $\alpha$ -OTMS, (IV)  $\beta$ -amyron, (V)  $\beta$ -amyrin  $\beta$ -OTMS, (VI)  $\alpha$ -amyron, (VII)  $\alpha$ -amyrin  $\beta$ -OTMS, (VIII) lupeol  $\beta$ -OTMS, (IX) lupenone.

A sample of 30 g of commercial copal was exposed to natural light behind a window facing south, during three months (September-December). The material subjected to GC-MS analysis was taken from the surface of this sample in a deep not exceeding 3 mm. As it can be seen on figure 105 A, the first impact of ageing in a copal is the lost of a big proportion of its non triterpenic compounds. Concerning the triterpenic fraction changes in proportion of triterpenes occur as well: (II) 3-*epi*- $\alpha$ -amyrin, (VII)  $\alpha$ -amyrin show an augmentation in their proportions. The same happens with BS3 and BS4. All these molecules are marked with an “A” from augmentation in the chromatogram (figure 106).

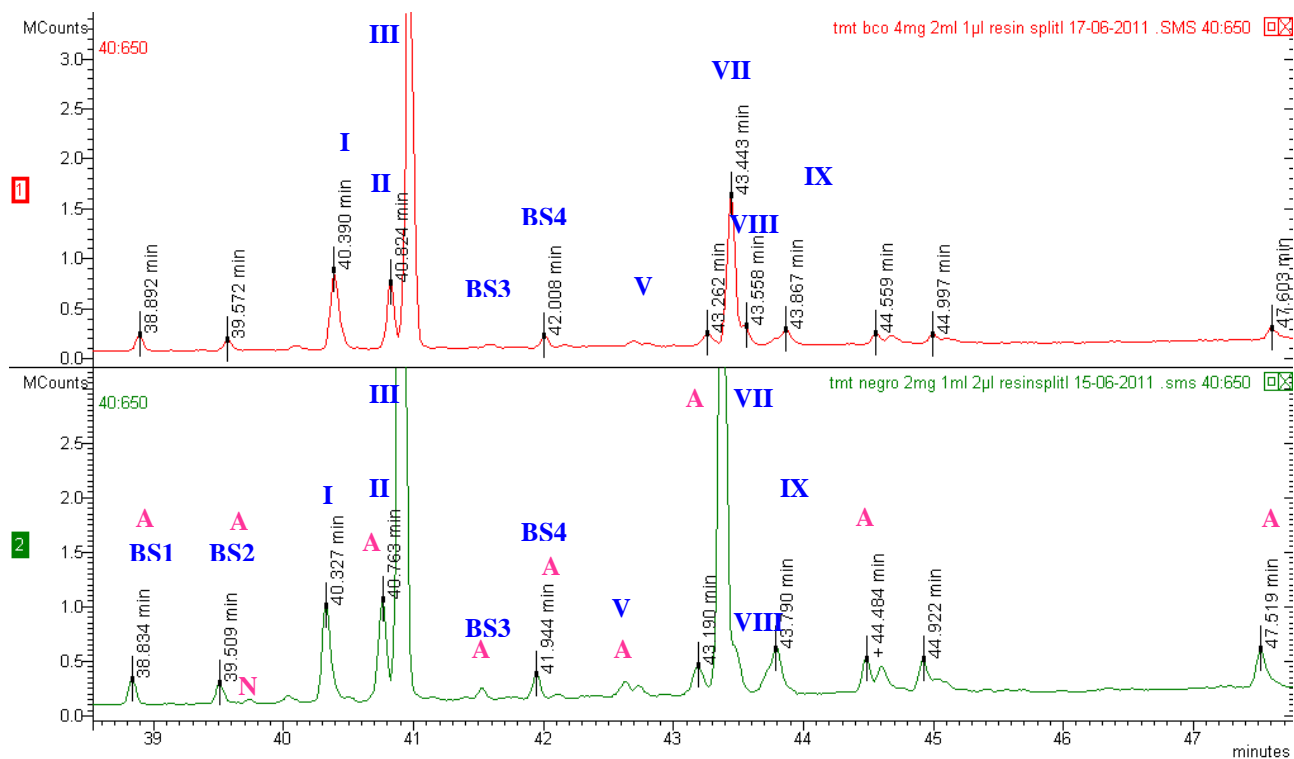
These findings are in accordance to those from De la Cruz, 2005. Her team analyzed both fresh and aged resins, and they found that ratio  $\beta$ -amyrin/ $\alpha$ -amyrin peak area ratios were of around 0.41 in fresh resins while it dropped to values between 0.30 and 0.15 in light and heat aged samples.

Although ratios were not measured in the present study the results of our experiences and those from De la Cruz-Cañizares suggest that  $\beta$ -amyrin is affected to a greater extent by heat and light than  $\alpha$ -amyrin.

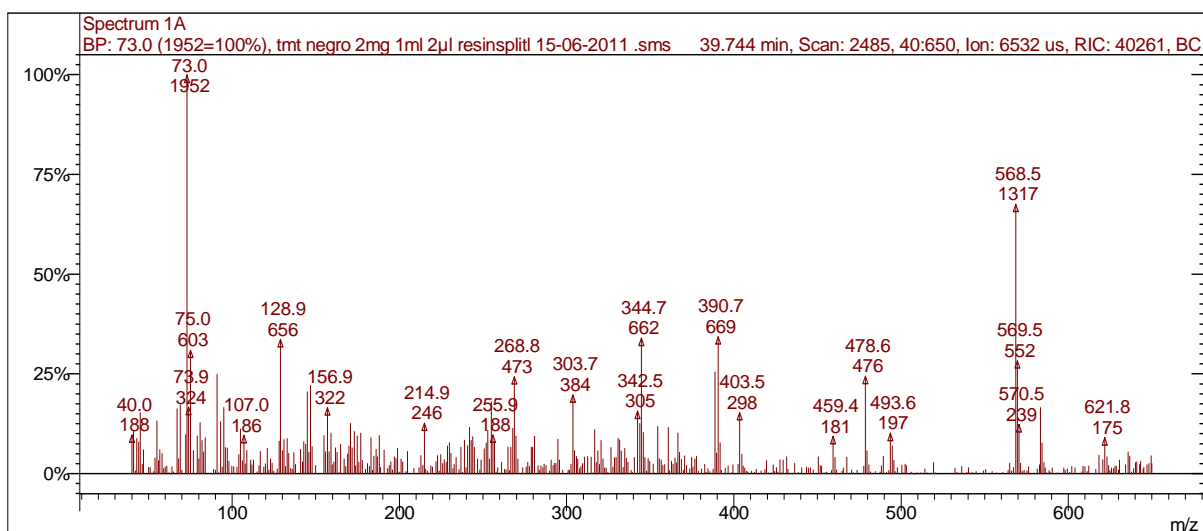
### 5.8.2 Molecular composition variation between external and internal part of an archaeological sample TMT

The chromatograms of both the inner part and the surface of TMT are presented here, some differences can be remarked, as in the case of the intentionally aged sample, some peaks exhibit an augmentation into their proportions, this is the case for: (II) 3-*epi*- $\alpha$ -amyrin, (III) 3-*epi*-lupeol, (V)  $\beta$ -amyrin, BS1, BS2, BS3, BS4, but the most spectacular change is the one occurred in (VII)  $\alpha$ -amyrin proportion that doubles its size. All these molecules are marked with an “A” from augmentation in the chromatogram (figure 107). As in the case of artificially aged samples  $\alpha$ -amyrin seems to be then less affected by natural ageing. The ageing of archaeological samples occurred under a temperature that can be estimated around 20°C, a no light exposure.

The major difference between SONB4 and the surface of TMT resin is the detection of a compound at 39.78min, it is marked in the chromatogram as “N” and its mass spectra is presented in figure 108.



**Fig 107 Zoom into triterpene zone of chromatograms of TMT resin in the inner part and from the surface.** Identification of triterpene compounds is as follows: (I) 3-*epi*- $\beta$ -amyryn  $\alpha$ -OTMS, (II) 3-*epi*- $\alpha$ -amyryn  $\alpha$ -OTMS, (III) 3-*epi*-lupeol  $\alpha$ -OTMS, (IV)  $\beta$ -amyryne, (V)  $\beta$ -amyryn  $\beta$ -OTMS, (VI)  $\alpha$ -amyryne, (VII)  $\alpha$ -amyryn  $\beta$ -OTMS, (VIII) lupeol  $\beta$ -OTMS, (IX) lupenone.



**Fig 108 Mass fragmentation for the "N" compound, peak detected at 39.78 min from resin TMT surface.**

## 5.9 Conclusions

This chapter evidences that the molecular composition of each botanically certified resin varies according to the species to what they belong.

Some species like *B. laxiflora* seem to be more variable than others as *B. penicillata*, *B. stenophylla* and *B. bipinnata*.

The superiority in sensibility of GC-MS technique allowed us to discover a far more complex composition of the triterpenic fraction of *B. penicillata* and *B. simaruba* than we were expecting based upon HPLC-UV/Vis chromatograms.

Also it allowed the study of terpenoid fraction of *B. grandifolia*. These analyses are important because it allowed us to identify (I) 3-*epi*- $\beta$ -amyrin, (II) 3-*epi*- $\alpha$ -amyrin, (IV)  $\beta$ -amyrone and (VI)  $\alpha$ -amyrone, and therefore to confirm the triterpenic nature of this resin.

Concerning the case of *B. bipinnata* and *B. stenophylla*, this technique allowed us to establish beyond any doubt, that the triterpenic fraction of both resins is identical. This fact explains the results obtained by FTIR and HPLC techniques.

Another great advantage of using GC-MS for the analysis of botanically certified resins was the possibility of detection of compounds that could be used as markers for each different botanical species. The structural characterization of these compounds by accurate techniques as NMR will certainly contribute to differentiate these resins in other commercial and archaeological samples. In the case of Aztec resins, GC-MS permitted to correlate its origin to *B. bipinnata* and *B. stenophylla*.

As the only difference in composition of these resins is found within the non-triterpenic compounds, the chemical distinction between these two origins in aged samples is impossible using chromatographic techniques.

Concerning Maya sample from Chichén Itzá, we could only confirm the results obtained by HPLC-UV/Vis: its composition differs from the molecular profile of all studied certified resins. Its botanical origin certainly belongs to a species that was not studied in this research. Regarding the presence of BS1 and BS2 within this sample and considering the results of ageing experiences two conclusions can be assumed: the first one is considering this sample as a mixture of resins, which would not be surprising as Case, 2003 and Van Gemert, 2007 documented anthropomorphically mixed resins in Maya culture. The second possibility for this

finding is that BS1 and BS2 are actually molecules formed fast upon oxidation. This would explain the augmentation on their proportions in more aged resins.

Regarding the study of commercial samples it provides important information: the aspect, color and the place of acquisition of the resin have no correlation to its chemical composition, and therefore its botanical origin: a “piedra” copal bought in Puebla region (IZUP1), a white copal from Mexico City market of Sonora (SONB4) and a red copal (SONR1) also bought in Mexico City exhibit a very close triterpenic molecular composition. The composition of the three commercial resins can be correlated to a botanical origin within *B. bipinnata* and *B. stenophylla* species.

As these samples were bought in more or less distant regions their botanical origin may reveal that the exploitation of this species along Mexican territory is more or less prevalent.

The botanical origin from some other commercial resins that were studied remains unknown; this is the case for a red copal bought in Oaxaca region (Oaxc2) and a yellow copal bought in Mexico City (ATZJ2). Its molecular composition from the fragmentation patterns of their molecules is neither triterpenic nor diterpenic.

The evaluation of changes induced by ageing shows in the short term that the non terpenic molecules are highly affected. In the long term triterpenic fraction is modified: the formation of an unknown compound that we designed as “N” was appreciated as well as changes in the proportions of many triterpenes, the most spectacular change was that in the proportion of  $\alpha$ -amyrin whose peak doubled its size in the case of the more degraded resin.

It is hoped that this research will stimulate further investigations towards a better characterization of the molecular composition of Mexican *Bursera* resins.

# General Conclusion & Perspectives

## General Conclusion

In this research three types of samples of Mexican copals were studied: botanically certified archaeological samples and commercial. Here we present a recapitulative table of the botanical origin found for archaeological and commercial samples.

Type of Sample	Number of studied samples	Botanical origin <i>B. bipinnata</i> / <i>B. stenophylla</i>	Other botanical origin
Commercial Samples	33	22	11
Aztec Samples	7	7	0
Maya Samples	1	0	1

**Table 23 Recapitulative of botanical origin for archaeological and commercial samples studied**

Two analytical approaches were used in this study: a spectrometric one, based on FTIR and a separative one based on HPLC and GC-MS chromatography. Each approach had advantages and afforded valuable information.

From FTIR and HPLC data a maximum of information was extracted with the aid of modern statistical techniques as PCA and LDA. The use of multivariate statistical tools allowed building mathematical models for the classification and the prediction of the botanical origin of unknown samples of resin. According to LDA results the performance of the two models was evaluated and the value of positive recognition was of 95.2% for the model created with FTIR data, and 95% of correct recognition in the fitting matrix for the model created with HPLC-UV/Vis data.

These models were used for the identification not only of fresh commercial resins but also for archaeological resins. The changes induced by ageing into these samples that altered their composition do not seem to prevent the use of these models for their classification.

In the case of archaeological Aztec samples its relation to *B. stenophylla* or *B. bipinnata* species is clear, and confirmed by the results obtained with the three analytical tools. The uncertainty

between these two possible origins arisen from the fact that triterpenic composition of both resins is identical. Only some molecular differences occur on the essential oil and/or gum fractions, which tend to disappear from aged resins, this fact was confirmed by the results obtained by the chromatographic analytical techniques.

Concerning the Maya resin sample we were able to discard its membership to any of the studied resins. Nevertheless a doubt persists about its composition, as it may be constituted of a mixture of two or more resins. Further studies should be performed on resins from *Bursera* spp. endemic of Yucatan peninsula, then in order to clear out this point.

Although spectroscopic techniques are considered to be less sensitive than separative techniques, their hyphenation to multivariate statistical techniques seems to overcome its alleged limitations. It was the case at least for this study were as we mentioned above the performance of the discrimination model slightly overcome the model created with HPLC-UV/Vis data in the validation matrix.

Furthermore this performance in discrimination was achieved using only eleven variables for FTIR (band positions in the spectra) versus twentytwo variables in HPLC (relative area of the peaks in the chromatograms).

Also FTIR has the advantage of being a fast, less expensive tool with a higher sensitivity as in our experiences only 2 to 3 $\mu$ g were needed, regardless of the nature of the sample (botanical origin, age).

When a greater sensitivity in the discrimination of two closely related species was needed the deconvolution of selected spectral zones seems to be a good option. In this study the bands between 1200 and 1300  $\text{cm}^{-1}$  were deconvoluted allowing the discrimination of different botanical origins.



An advantage of chromatographic techniques over spectroscopic techniques is the fact that they can contribute with an overview of the molecular composition of the sample, from the chromatograms the number and the kind of compounds present in these samples was determined. When standards were available the identification and even the concentration of some triterpenic compounds was calculated.

The HPLC-UV/Vis-PCA model was in fact the only of the three techniques able to discriminate between the origin of fresh samples of *B. bipinnata* and *B. stenophylla* resins. The advantage of constructing a model considering both triterpenic and non triterpenic compounds increases the sensibility of the model in this aspect.

HPLC-UV/Vis also was the only analytical tool that documented the presence of molecules that could correspond to saponines or to degradation compounds in archeological samples.

Finally GC-MS was the only tool from what information on particular compounds present in the resins could be obtained.

Its sensibility towards the detection of different triterpenoids exceeds largely the performance of HPLC-UV/Vis, as the limitations of UV/Vis capabilities into the discrimination of closely related structures are well known.

The characterization of botanically certified resins by GC-MS allowed us to find molecular markers for each botanical originated species, that hopefully will be useful in the future for the study of commercial and archaeological resins.

Finally the results of the characterization of commercial samples revealed that the origins of some commercialized resins in Mexico are *B. bipinnata* and *B. stenophylla* species regardless of the appearance and the presentation of the copals.

In the other hand, we were unable to determinate the provenance of some other commercial resins with close aspect to those of *Bursera* spp., but which botanical origin seems not to be even in the same Genus, as they are neither triterpenic nor diterpenic resins. It is possible then that these commercial resins are either pure or a mixture of resinous materials, coming from *Rhus* spp., *Liquidambar styraciflua*, *Myroxylon balsamum* and/or *Bursera*. spp.

## Perspectives

The results on the molecular characterization of resins from certified botanical origin open the possibility of applying these results to the analysis of archeological organic materials found in censers, or other type of recipients, to the adhesives used in mosaics or in dental incrustations, to figurines molded in resins and generally speaking to organic materials assimilate to copal. We hope that these results will be applicable not only to Aztec archeological sites and objects, but to the numerous sites from cultures that were located in the middle and the south of Mexican current territory like the Teotihuacans, the Xochicalcans or the Toltecs.

Additionally the determination of the botanical origin of commercial and archaeological samples, using protocols involving PCA and LDA coupled to classical analytical techniques open the possibility of applying similar protocols to two types of resins:

- A) The first one constituted by certified resins from Mexican origin. As we said in the second chapter of this work, the great diversity of *Busera* spp. in Pacific coast lead us to select a number of species for our study, so as a continuation of the present work, some other species may be studied. A special emphasis could be put selecting samples from trees of *Busera* spp. present in Yucatan peninsula, in order to find the botanical origin of Maya sample.
- B) The second possibility is applying this same methodology to samples from other botanical origins like mastic, dammar, oliban, etc.

The advantages of using FTIR into patrimony objects are undeniable, as this technique is considered as non destructive, it is fast and generally speaking inexpensive compared to other techniques. This tool could be very useful specifically in the assessment of botanical origin for

commercial samples used in art works or in conservation treatments. The possibility of evaluate the preservation state of a commercial sample is a plus.

Concerning molecular profiling of copal composition a very interesting job on the isolation and the structural characterization of compounds present in both fresh and aged resin is to be done.

In the case of molecules that seem to be present only in one species, molecular characterization is really important as they could be use as molecular markers.

Structural characterization of the oxidized products of original compounds may lead important information on degradation pathways that will ease conservator's job.

Finally an inventory of molecules that compose volatile fraction of Mexican copal could be very valuable for perfume industrial uses, as these species seem to have a very rich tenure on sesqui- and monoterpenic compounds.

Coupling the information on volatile phase to the information on triterpenic fraction may allow building an extra efficient model for the classification of commercial resins.

Finally another intriguing question that remains open relies on the origin of commercial resins with such a different composition that no apparent relation to *Bursera* species could be established.

# Materials and Methods

## Materials and Methods

### FTIR methodology

The analyzed samples being natural, hard and elastic resins were analyzed, in solid phase. They were prepared as a potassium bromide pellet. The solid samples were crushed in a homogeneous way in an agate mortar with anhydrous potassium bromide (in a proportion of 1/20) transparent to the infrared radiations in the zone ranging between 4.000 and 400  $\text{cm}^{-1}$ . The powder was then compressed under a pressure of 10  $\text{t}/\text{cm}^2$  with a manual press, to form thin pellets of translucent aspect.

The pellet was then analyzed, the air being taken as reference. The ratio of the sample to potassium bromide is important; little sample is needed (around 2 or 3 mg) of sample with 200 mg of KBr. Contributions due to moist in the alkali halide (Uvasol, Merck) were avoided, by keeping it desiccated and warm prior to use.

### Analytical conditions for HPLC study

For the HPLC study, both standards and global resins were solved in methanol (analytical grade, Merck), the protocol consist in solving a variable amount of crude resin (depending on its botanical origin (refer to table 11) in 2 mL of this solvent, then the solution was sonicated during 10 min. After centrifugation, the supernatant was injected into HPLC system. Each sample was injected in triplicate.

The identification of commercial and archaeological resins was achieved by using a reverse phase column with an elution gradient. The type of column used in this type of research is essential, taking as antecedent the results obtained by our team. Indeed, previous works (Mathe,

2004), showed that for resins, a column in reverse phase C18 led to satisfactory separations and resolutions of the compounds. This study was thus carried out using a column with non-polar stationary phase Merck LiChrocart Purostar 5  $\mu\text{m}$  100 RP-18e 250 mm x 4 mm (Merck, Darmstadt, Germany).

LC-PDA analysis is carried out in a Waters liquid chromatography consisting of a high-pressure ternary pump Waters 600, a vacuum degasser, a high pressure manual injector valve (20  $\mu\text{L}$  injection loop) and a photodiode array detection (PDA) system Waters 2996. The system is controlled by Empower 2 software. The LC separation is performed at 35° C with a mobile phase consisting of a binary elution composed of methanol analytical grade (Merck) (A) and bidistilled water (B) containing 0.01% trifluoroacetic acid (TFA), pH = 3 (Acros Organics). Chromatography is carried out for 35 min at a continuous flow-rate of 1 mL/min. The gradient program is presented in table 24. The chromatograms are acquired at 210 nm. Identification of original triterpenoids was based on the co-injection of samples with reference molecules.

<b>Time (min)</b>	0	10	15	35
<b>% Metanol</b>	85	95	100	100
<b>% H<sub>2</sub>O-TFA</b>	15	5	0	0

Flow : 1 mL.min<sup>-1</sup>

Temperature of the column = 35 °C

**Table 24 HPLC Gradient 1, employed for the study of the terpenic compounds in fresh resins**

For the study of archeological resins gradient 2 was used (table 25).

<b>Time (min)</b>	0	10	15	45
<b>% Metanol</b>	85	95	100	100
<b>% H<sub>2</sub>O-TFA</b>	15	5	0	0

Flow : 1 mL.min<sup>-1</sup>

Temperature of the column = 35 °C

**Table 25 HPLC Gradient 2 employed for the study of the terpenic compounds in archaeological resins**

NB: This gradient was also used to analyze some samples once an automatic injector was adapted to the HPLC instrumentation.

### General methodology for the selective extraction of triterpens by SPE

For SPE Chromabond C-18EC cartridges were chosen. Selection was based upon adsorbents affinity to triterpen molecules. The volume of the cartouche was defined by the volume of the sample and the quantity of analyte present in the crude resin. In the present case for the analysis of commercial resins a 6 mL cartridges was selected, while a 1 mL was chosen for archaeological samples.

Methanol used in this protocol was analytic grade (Merck).

For the 6 mL cartridges SPE protocol steps were as follows

- 5) Conditioning. For this stage column was conditioned prior to use by drawing 2 times 3 mL of methanol, followed by the same volume of distilled water.
- 6) Deposit of the sample. A prepared volume of 2 mL of a solution with a concentration of 2 mg/mL of resin solved in methanol was loaded onto and drawn through the column
- 7) Washing of the adsorbent was performed with 3 mL of a mixture methanol-water (5:95, v/v). The cover of the manifold was then removed and the cover was wiped with a tissue, to remove drops of washing solution.
- 8) Elution. Triterpenoids were then eluted from the column with 2 x 2 mL of methanol.

For 1 mL cartridges SPE protocol steps were as follows

- 1) Conditioning. For this stage column was conditioned prior to use by drawing 2 times 300  $\mu$ L of methanol, followed by the same volume of distilled water.
- 2) Deposit of the sample. A prepared volume of 200  $\mu$ L of a solution with a concentration of 2 mg/mL of resin solved in methanol was loaded onto and drawn through the column
- 3) Washing of the adsorbent was performed with 300  $\mu$ L of a mixture methanol-water (5:95, v/v). The cover of the manifold was then removed and the cover was wiped with a tissue, to remove drops of washing solution.



- 4) Elution. Triterpenoids were then eluted from the column with 2 x 200  $\mu$ L of methanol.

After this procedure the eluate collected was analysed by means of HPLC.

### GC- MS Materials and Methods

GC-MS was carried out in a Varian Saturn 3900 gas chromatography, with a Varian injector 1177 coupled with a Varian 2100 T ion trap mass spectrometer (Varian Walnut Creek, USA). The gas chromatograph was equipped with a 30 m length, and 0,25 mm internal diameter fused silica capillary column coated with 0.25  $\mu$ m film of poly (5% phenyl, 95% dimethylsiloxane): CP-Sil 8 CB Low Bleed/MS (Varian). The MS electron multiplier voltage was set at 1400 V and an ionization time of 25000  $\mu$ s was used, running in electronic impact (EI) with transfer line, ion trap and manifold temperatures of 300°C, 200°C and 50°C respectively. The mass spectrometer was set to scan masses ranging between 40 and 650  $m/z$  with an ionizing voltage of 70 eV. Samples were injected (1  $\mu$ L) with no splitting ratio. The injector temperature was set to 250°C. A continuous flow rate of 1 mL/min of chromatographic grade helium was used. Temperature gradient employed for the global study of the resins is shown in table 26.

Temperature (°C)	Increase of Temperature (°C/min)	Hold	Total time (min)
50	-	2	10
250	8	0	27
350	3	0	60
T <sub>trap</sub> = 200°C	T <sub>transfer line</sub> = 300°C	T <sub>injector</sub> = 250°C	Splitless

**Table 26 Gardient 1, GC-MS temperature gradient for the global analysis of resins**

For a better resolution of the compounds in the triterpenic zone, a second gradient was used. It starts at 190° C during 2 min, then it increases to 265° C with 3° C/min, then the rise continues with 10° C/min to reach 285° C and finally it passes to 300°C with 0.5° C/min. The total duration of the analysis is approximately 1h (table 27).

Temperature (°C)	Increase of Temperature (°C/min)	Hold	Total time (min)
190	-	2	2
265	3	0	27
285	10	0	29
300	0,5	0	59
T <sub>trap</sub> = 200°C	T <sub>transfer line</sub> = 300°C	T <sub>injector</sub> = 250°C	Splitless

**Table 27 Gradient 2, optimal gradient for the analysis of triterpenoids GC-MS**

### Preparation of samples: off-line derivatization

The derivatization procedure was based on a previous methodology for the analysis of diterpenoid resins developed in our laboratory (Mathe, 2003): a sample of raw resin was crushed, then solved in 0.5mL of pyridine, then it was trimethylsilylated with 0.45 mL of HMDS and 0.3mL of TMSCl. The reaction was conducted at room temperature for 30 min and then the solution was dried with a stream of nitrogen. The residue was immediately dissolved in 2 mL of diethyl ether and filtered on a membrane filter. Then the sample was injected into GC-MS system.

# Bibliographical References

- Acevedo-Ramos R. *et al.* Identificación de barnices en pintura de caballete por cromatografía en placa fina (TLC) y espectroscopia infraroja (FTIR). *Conserva* **9** (2003) 97-119
- Acevedo-Rosas *et al.* Especies de plantas vasculares descritas de las barrancas aledañas a la ciudad de Guadalajara y de Río Blanco, Jalisco, México. *Polibotánica*. **26** (2008) 1-38
- Akihisa T. *et al.* Antitubercular activity and inhibitory effect on Epstein-Barr virus activation of sesterols and polyisoprenepolyols from an edible mushroom *Hypsizygus marmoreus*. *Biological and Pharmaceutical Bulletin* **28** (2005) 117-119
- Akouhi F. *et al.* Gas chromatographic- mass spectrometric characterisation of triterpene alcohols and monomethylsterols in developing *Olea europaea* fruits. *Food Chemistry* **116** (2009) 345-350
- Allouche Y. *et al.* Triterpenic Content and Chemometric Analysis of Virgin Olive Oils from Forty Olive Cultivars. *Journal of Agricultural and Food Chemistry* **57** (2009) 3604- 3610
- Alonso-Olvera A. *et al.* Informe de las actividades de conservación y restauración de la colección de bienes arqueológicos del Proyecto Templo Mayor-Séptima Temporada. Julio-Diciembre 2008. Coordinación Nacional de Conservación del Patrimonio Cultural, ENSRyM Manuel Castillo Negrete, Museo de Templo Mayor, INAH; México. (Unpublished Material)
- Al-Rehaily A *et al.* Pharmacological studies of various extracts and the major constituent, lupeol, obtained from hexane extract of *Teclea nobilis* in rodents. *Natural Products*. **7** (2001) 76-82
- Andreotti A. *et al.* Combined GC/MS analytical procedure for the characterization of glycerolipid, waxy, resinous, and proteinaceous materials in a unique paint microsample. *Analytical chemistry* **78** (2006) 4490-4500
- Andrews E. *et al.* 1980. Excavations at Dzibilchaltún, Yucatán. Middle American research institut, Tulane University, United States.
- Andrisano V. *et al.* HPLC analysis of licorice triterpenoids -applications to the quality control of pharmaceuticals. *Journal of Pharmaceutical and Biomedical Analysis* **13** (1995) 597-605
- Archier P. and Vieillescazes C. Characterization of various geographical origin incense based on chemical criteria, *Analysis*, **28** (2000) 233-237
- Armanino C. *et al.* Modelling aroma of 3 Italian red wines by head space-mass spectrometry and potential functions. *Analytica chimica acta* **614** (2008) 134-142
- Arrabal C. *et al.* Differentiation among five Spanish *Pinus pinaster* provenances based on its oleoresin terpenic composition. *Biochemical Systematics and Ecology* **33** (2005) 1007-1016
- Aveni. A. *et al.* Myth, environment and the orientation of the Templo Mayor of Tenochtitlan. *American Antiquity* **53** (1988) 287-309
- Awadh N. *et al.* Chemical composition and biological activities of essential oils from the oleogum resins of three endemic Soqotraen *Boswellia* species. *Records of natural products* **1** (2008) 6-12

- Bakkali F *et al.* Biological effects of essential oils-A review. *Food and chemical toxicology* **46** (2008) 446-475
- Barreto C. 2009. Minería de datos aplicada a la mejora de procesos de extrusión de elastómeros. Ph. D. thesis in Engineering projects and innovation. Polytechnic University of Valencia, Spain
- Bartle K. and Myers P. History of gas chromatography. *Trends in analytical chemistry* **21** (2002) 547-557
- Becerra J. and Venable L. Nuclear ribosomal DNA phylogeny and its implications for evolutionary trends in mexican *Bursera* (Burceraceae). *American Journal of Botany*. **86** (1999) 1047-1057
- Beddows P. *et al.* Los cenotes de la península de Yucatán. *Arqueología Mexicana* **83** (2007) 32-35
- Beck C. Science and technology in science of conservation, preprints of the IIC Washington congress (1984) 104
- Bellamy L. 1954 The infra-red spectra of complex molecules. Editions John Wiley & Sons, Inc, New York, United States
- Bennett B. and Larter S. Quantitative Separation of Aliphatic and Aromatic Hydrocarbons Using Silver Ion-Silica Solid-Phase Extraction. *Analytical Chemistry* **72** (2000) 1039-1044
- Bellot-Gurlet L. 2010. De la source aux techniques. Méthodologies d'analyses élémentaires et structurales et physico-chimie de matériaux du patrimoine culturel. HdR Thesis. Université Pierre et Marie Curie (Paris 6), France
- Bernal I. 1950 Compendio de arte mesoamericano. Enciclopedia Mexicana de Arte, Mexico City, Mexico
- Berns R. and de la Rié R. The Effect of the Refractive Index of a Varnish on the Appearance of Oil Paintings. *Studies in Conservation* **48** (2003) 251
- Binet M. *et al.* Thermo-oxidation of polyterpenes: influence of the physical state. *European Polymer Journal* **36** (2000) 2133-2142
- Bonaduce I. *et al.* GC-MS characterization of plant gums in samples from painted works of art. *Journal of Chromatography A* **1175** (2007) 275-282
- Bowen-Forbes C. *et al.* Ursolic acid analogues: non phenolic functional food components in Jamaican raspberry fruits. *Food chemistry* **116** (2009) 633-637
- Buchele B. and Simmet T. Analysis of 12 different pentacyclic triterpenic acids from frankincense in human plasma by high-performance liquid chromatography and photodiode array detection, *Journal of Chromatography B* **795** (2003) 355- 362
- Buchele B. *et al.* Analysis of pentacyclic triterpenic acids from frankincense gum resins and related phytopharmaceuticals by high-performance liquid chromatography. Identification of lupeolic acid, a novel pentacyclic triterpene. *Journal of Chromatography B* **791** (2003) 21-30
- Bucio L. *et al.* Incrustation of precious stones in dental apatite. *Zeitschrift für Kristallographie Supplement* **23** (2006) 569-574
- Bullock, A. Further notes on the genus *Bursera*. *Kew Bulletin*. (1937) 447-458; and

(1938) 163-168.

Burger P. 2008. Caractérisation moléculaire de résines végétales archéologiques et actuelles: Étude de résines de dipterocarpaceae. Thesis in Chemistry. University of Strasbourg, France.

Burger P. *et al.* Taxonomic characterization of fresh Dipterocarpaceae resins by gas chromatography–mass spectrometry (GC–MS): providing clues for identification of unknown archaeological resins. *Archaeological and anthropological sciences* **3** (2011) 185-200

Campos-Osorno M. and Salazar-Martinez L. 2006. Proceso de Exrtacción de copal en una comunidad de la Sierra de Huautla, Morelos. Thesis in Agroecological engineering. Autonomous University of Chapingo, Mexico.

Cano O. Chichén Itzá, Yucatan. *Arqueología Mexicana* **53** (2002) 80-87

Cappitelli F. *et al.* (Eds) 2006. Macromolecules in Cultural Heritage, WileyVCH, Weinheim, UK.

Carrasco D. 1999. City of Sacrifice. The Aztec empire and the role of violence in civilization. Boston, Beacon Press, United States

Carrasco D. Centro y periferia en el Templo Mayor. *Arqueología Mexicana* **6** (1999) 42-51

Carreon-Blaine E. Reseña de las ofrendas del Templo Mayor de Tenochtitlan de Leonardo Lopez-Lujan. *Anales del Instituto de Investigaciones Esteticas. UNAM.* **15** (1994) 225-230

Cartoni G. *et al.* GC-MS characterization and identification of natural terpenic resins employed in works of art. *Annali di Chimica* **94** (2004) 767-782

Caruso F. 2010. Characterization of the varnishes from historical musical instruments. Ph.D. thesis in Chemistry. University of studies of Palermo, Italy.

Casale M. *et al.* Characterisation of table olive cultivar by NIR spectrscopy. *Food chemistry* **122** (2010) 1261-1265

Casale M. *et al.* Chemometrical strategies for feature selection and data compression applied to NIR and MIR spectra of extra virgin olive oils for cultivar identification. *Talanta* **80** (2010) 1832-1837 B.

Case Ryan J. *et al.* Chemistry and ethnobotany of commercial incense copals, copal blanco, copal oro, and copal negro, of North America. *Economic Botany* **57** (2003) 189-202

Cerrato C. *et al.* Optimisation of new head space mass spectrometry instruments. Discrimination of different georgraphical origin olive oils. *Journal of Chromatography A* **1076** (2005) 7-15

Charrié-Duhaut A. *et al.* The canopic jars of Rameses II: real use revealed by molecular study of organic residues. *Journal of Archaeological Science* **34** (2007) 957-967

Charters S. *et al.* Identification of an adhesive used to repair a roman jar *Archaeometry* **35** (1993) 91–101

Chen G. and Huang Y. Deconvolution method of the Nitrogen content in carbamates. *Chinese Chemical letters* **12** (2001) 365-368

- Chiavari G. *et al.* Characterisation of natural resins by pyrolysis - silylation. *Chromatographia* **55** (2002) 611-616
- Chiavari G. *et al.* Characterisation of varnishes used in violins by pyrolysis-gas chromatography/mass spectrometry. *Rapid Communications in Mass Spectrometry* **22** (2008) 3711-3718
- Chiavari G. *et al.* Pyrolysis gas chromatography mass spectrometry of natural resins used for artistic objects. *Chromatographia* **41** (1995) 273-281
- Cobos R. El cenote sagrado de Chichén Itzá, Yucatán. *Arqueología Mexicana* **83** (2007) 50-53
- Coelho D. *et al.* Chemical characterization of the lipophilic fraction of giant reed (*Arundo donax*) fibres used for pulp and paper manufacturing. *Industrial Crops and Products* **26** (2007) 229-236
- Coggings C. and Ladd J. 1992. Artifacts from the Cenote of Sacrifice, Chichen Itza, Yucatan: textiles, basketry, stone, bone, shell, ceramics, wood, copal, rubber, other organic materials, and mammalian remains. Peabody Museum of Archaeology & Ethnology, Harvard University, United States.
- Colombini M. *et al.* Two procedures for suppressing interference from inorganic pigments in the analysis by gas chromatography–mass spectrometry of proteinaceous binders in paintings. *Journal of chromatography A* **846** (1999) 101–111
- Colombini M. *et al.* Characterisation of the balm of an Egyptian mummy from the seventh century B.C. *Studies in conservation* **45** (2000) 19-29
- Colombini M. *et al.* GC-MS characterization of paint varnishes *Microchemical Journal* **67** (2000) 385–396
- Colombini M. *et al.* Ion chromatography characterization of polysaccharides in ancient wall paintings. *Journal of Chromatography A* **968** (2002) 79-88
- Colombini M. *et al.* The characterization of paints and waterproofing materials from the shipwrecks found at the archaeological site of the Etruscan and Roman harbour of Pisa (Italy). *Archaeometry* **45** (2003) 659-674
- Colombini M. and Modugno F. Characterisation of proteinaceous binders in artistic paintings by chromatographic techniques. *Journal of Separation Science* **27** (2004) 147–160
- Colombini M. *et al.* The Egyptian mummies in the ‘Museo di Anatomia’ of the University of Pisa: a chemical approach for the characterization of balms. *Science and Technology for Cultural Heritage* **13** (2004) 83–87
- Colombini M. *et al.* Characterisation of organic residues in pottery vessels of the Roman age from Antinoe (Egypt). *Microchemical Journal* **79** (2005) 83–90
- Colombini M. *et al.* Direct exposure electron ionization mass spectrometry and gas chromatography/mass spectrometry techniques to study organic coatings on archaeological amphorae. *Journal of Mass Spectrometry* **40** (2005) 675–687
- Colombini M. *et al.* Chemical study of triterpenoid resinous materials in archaeological findings by means of direct exposure electron ionisation mass spectrometry and gas chromatography/mass spectrometry *Rapid Communications in Mass Spectrometry* **20** (2006) 1787–1800

- Colombini M. *et al.* 2009. Organic mass spectrometry in art and archaeology. Wiley. West Sussex, UK.
- Connan J. *et al.* Use and trade of bitumen in antiquity and prehistory: molecular archaeology reveals secrets of past civilizations *Philosophical Transactions: Biological Sciences* **354** (1999) 33–50
- Connan J. and Nissenbaum A. Conifer tar on the keel and hull planking of the Ma'agan Mikhael ship (Israel, 5th century BC): identification and comparison with natural products and artefacts employed in boat construction. *Journal of Archaeological Science* **30** (2003) 709–719
- Contel J. Tlaloc, el cerro, la olla y el chalchihuitl. Una interpretación de la lamina 25 del codice Borbonico. *Itinerarios* **8** (2008) 153-183
- Cordell G. Phytochemistry and traditional medicine. A revolution in process. *Phytochemistry Letters* **4** (2011) 391–398
- Cosio M. *et al.* Geographical origin and authentication of extra virgin olive oils by an electronic nose in combination with artificial neural networks. *Analytica Chimica Acta* **567** (2006) 202-210
- Cosio M. *et al.* (Evaluation of different storage conditions of extra virgin olive oils with an innovative recognition tool built by means of electronic nose and electronic tongue. *Food Chemistry* **101** (2007) 485 - 491
- Cruz M. and Badiano 1991. J. Códice de la Cruz-Badiano: Libellus de medicinalibus indorum herbis. FCE, Mexico city, Mexico
- Cruz-León A. Antecedentes y actualidad del aprovechamiento del copal en la sierra de Huautla, Morelos. *Revista de geografía agrícola* **37** (2006) 97-116
- Culioli G. *et al.* A lupane triterpene from frankincense (*Boswellia* sp., Burseraceae), *Phytochemistry* **62** (2003) 537-541
- De la Cruz-Canizares J. *et al.* Study of Burceraceae resins used in binding media and varnishes from artworks by gas chromatography-mass spectrometry and pyrolysis-gas chromatography-mass spectrometry. *Journal of Chromatography A* **1093** (2005) 177-194
- De la Rié R. The Influence of Varnishes on the Appearance of Paintings. *Studies in Conservation* **32** (1987) 1-13
- De la Rié E. Photochemical and thermal degradation of films of dammar resin. *Studies in Conservation* **33** (1988) 53-70
- De la Rié R. Old Master Paintings: A Study of the Varnish Problem. *Analytical Chemistry* **61** (1989) 1228-1240 A
- De la Rié R. and Shedrinsky A. The chemistry of ketone resins and the synthesis of a derivative with increased stability and flexibility. *Studies in Conservation* **34** (1989) 9-19
- De la Rié R. and McGlinchey. Stabilized Dammar Picture Varnish. *Studies in Conservation* **34** (1989) 137-146
- Degano I. and Colombini M. Multi-analytical techniques for the study of pre-Columbian mummies and related funerary materials. *Journal of Archaeological Science* **36** (2009) 1783-1790



- Díaz del Castillo B. 2004. Historia verdadera de la conquista de la Nva. España. Sepan cuantos. 5. Ed. Porrúa. Mexico city, Mexico
- Dietemann P. 2003. Towards more stable natural resin varnishes for paintings. PhD. thesis in Natural sciences. Swiss federal institute of technology (ETH), Switzerland
- Dietemann P. *et al.* Aging and yellowing of triterpenoid resins varnishes-Influence of aging conditions and resin composition. *Journal of cultural heritage* **10** (2009) 30-40
- Dillon-Gorham L. and Bryant V. Pollen, phytoliths, and other microscopic plant remains in underwater archaeology. *International Journal of Nautical Archaeology* (2001) **30** 282–298
- Doménech-Carbó M. *et al.* Study of the influencing effect of pigments on the photoageing of terpenoid resins used as pictorial media. *Journal of Chromatography A* **1121** (2006) 248-258
- Doménech-Carbó M. Novel analytical techniques for characterising binding media and protective coatings in art works. *Analytica chimica acta* **621** (2008) 109-139
- Doménech-Carbó M. *et al.* Study of ageing of ketone resins used as picture varnishes by FTIR spectroscopy, UV–Vis spectrophotometry, atomic force microscopy and scanning electron microscopy X-ray microanalysis. *Annals of bioanalytical chemistry* **391** (2008) 1351–1359
- Doménech-Carbó M. *et al.* Study of ageing of ketone resins used as picture varnishes by pyrolysis–silylation–gas chromatography–mass spectrometry. *Journal of Analytical and Applied Pyrolysis* **85** (2009) 470–479
- Dzubak P. *et al.* Review Pharmacological activities of natural triterpenoids and their therapeutic implications. *Natural Products* **23** (2006) 394-411
- Echard J.P. and Lavéfrine B. Review on ancient musical stringed musical instruments varnishes and implementation of an analytical strategy. *Journal of Cultural Heritage* **9** (2008) 420-429
- Edwards H. and Falk M. Fourier-transform Raman spectroscopic study of unsaturated and saturated waxes. *Spectrochimica acta part A: molecular spectroscopy* **53** (1997) 2685- 2694
- Eisenreich W. *et al.* Deoxycelulose phosphate pathway to terpenoids. *Trends Plant Science* **6** (2001) 78–84
- Etzold E. and Lichtenber-Kraag B. Determination of the botanical origin of honey by Fourier infrared spectroscopy: an approach for routine analysis. *European Food Research Technology* **1** (2008) 579-586
- Evans D. *et al.* Determination of the authenticity of orange juice by discriminant analysis of near infrared spectra. *Journal of Near Infrared spectroscopy* **1** (1993) 33-44
- Evershed R. *et al.* Archaeological frankincense *Nature* **390** (1997) 667–668
- Evershed R. 2000. Biomolecular analysis by organic mass spectrometry, in *Modern Analytical Methods in Art and Archaeology*, E. Ciliberto and G. Spoto (Eds), Wiley Interscience, New York, USA
- Evershed R. *et al.* Archaeology: formulation of a Roman cosmetic *Nature* **432** (2004) 35–36

- Faust B. Mayan environmental successes and failures in the Yucatan Peninsula. *Environmental Science and Policy* **4** (2001) 153-169
- Feist M. *et al* Thermal investigations of amber and copal. *Thermochimica Acta* **458** (2007) 162-170
- Fernandes J. *et al*. Pentacyclic triterpenes from Chrysobalanaceae species: cytotoxicity on multidrug resistant and sensitive leukemia cell lines. *Cancer Letters* **190** (2001) 165-169.
- Ferré L. Selection of components in principal component analysis: a comparison of methods. *Computational Statistics and Data Analysis* **19** (1995) 669-682
- Fresquet J. Lopez Terrada M. Plantas mexicanas en Europa en el siglo XVI. *Arqueología Mexicana* **39** (1999) 38-43
- Frisvad J. *et al*. The use of secondary metabolite profiling in chemotaxonomy of filamentous fungi. *Mycological Research* **112** (2008) 231-240
- Fronde J. Amber Facts and Fancies. *Economic Botany* **22** (1968) 371-382
- Fronde J. X-Ray Diffraction Study of Some Fossil and Modern Resins *Science* **155** (1967) 1411-1413
- Fronde J. X-Ray Diffraction Study of Fossil Elemis. *Nature* **215** (1967 a) 1360 – 1361
- Gallareta T. Los cenotes de la península de Yucatán. *Arqueología Mexicana* **83** (2007) 36-43
- Gan-Peng L. *et al*. Three new triterpenoids from *Dracocephalum forrestii*. *Helvetica Chimica Acta* **89** (2006) 3018-3022
- García A. Modelización por técnicas no paramétricas del proceso de mezclas de gomas para extrusión. Thesis of a Research work. University de La Rioja. Spain (2002)
- García-Hernández C. 2000. Producción de resina en una población de copal santo (*B. bipinnata* [Moc & Sessé ex DC] Eng de Teotlaco, Mixteca poblana. Thesis in Forestal Engineering. Autonomous University of Chapingo, Mexico
- Garnier N. *et al*. Characterization of the archaeological beeswax by electron ionization and electrospray ionization mass spectrometry. *Analytical Chemistry* **74** (2002) 4868-4877
- Gautier G. and Colombini M. GC-MS identification of proteins in wall painting samples: A fast clean-up procedure to remove copper-based pigment interferences. *Talanta* **73** (2007) 95-102
- Gonzalez A. *et al*. A review of non-chromatographic methods for speciation analysis. *Analytica chemical acta* **636** (2009) 129-157
- Gregorio-Martinez A. 2005. Uso y aprovechamiento del copal (*B. bipinnata* [Moc & Sessé ex DC] Eng. En el municipio de Sn. Juan Quiotepec, Ixtlan, Oaxaca. Thesis in Natural Renewable Resources Autonomous University of Chapingo. Mexico
- Guizar-Nolazco E. and Sanchez-Vélez A. 1991. Guía para el reconocimiento de los principales árboles del alto Balsas. Universidad Autónoma Chapingo. Chapingo, Mexico.
- Hamm S. *et al* Headspace solid phase microextraction for screening for the presence of

- resins in Egyptian archaeological samples. *Journal of Separation Science* **27** (2004) 235–243
- Hamm S. *et al.* A chemical investigation by headspace SPME and GC-MS of volatile and semi-volatile terpenes in various olibanum samples. *Phytochemistry* **66** (2005) 1499-1514
- Hegnauer R. Phytochemistry and plant taxonomy an essay on the chemotaxonomy of higher plants. *Phytochemistry* **25** (1986) 1519-1535
- Hernández F. 1959. Historia natural de la Nueva España. Obras Completas, National Autonomous University of Mexico
- Hernández-Vazquez L. *et al.* Valuable medicinal plants and resins: commercial phytochemicals with bioactive properties. *Industrial Crops and Products* **31** (2010) 476-480
- Heyden D. 1980 Comunicación no verbal en el ritual prehispánico. Cuadernos de Trabajo. INAH, Mexico City, Mexico
- Horie C. 1987. Materials for Conservation, Organic Consolidants, Adhesives and Coatings, Butterworth Heinemann, Oxford, UK
- Hovanessian M. 2005. Différenciation de substances naturelles par diverses techniques analytiques: spectroscopie IRTE, CLHP / uv-visible / fluorimétrie et CPG /SM. Application à l'étude d'échantillons officinaux et archéologiques. PhD. thesis in organic and analytical chemistry. University of Avignon, France.
- Hubschmann H. 2008. Handbook of GC/MS. Wiley. West Sussex, UK
- Ikeda Y. *et al.* Ursolic acid promotes the release of macrophage migration inhibitory factor via ERK2 activation in resting mouse macrophages. *Biochemical pharmacology* **70** (2005) 1492-1505
- Inés-Pedrebón L. 2005. Posibilidades plásticas del polímero acrílico Paraloid b-72 utilizado como aglutinante pictórico. PhD Thesis in Painting and restoration. Universidad Complutense de Madrid, Spain
- Jaeger S. *et al.* Pentacyclic triterpene distribution in various plants - rich sources for a new group of multi-potent plant extracts. *Molecules* **14** (2009) 2016-2031
- Janicsak G. *et al.* Gas chromatographic method for routine determination of oleanolic and ursolic acids in medicinal plants. *Chromatographia* **58** (2003) 295-299
- Johnson, M. The genus *Bursera* in Sonora, Mexico and Arizona, U.S.A. *Desert Plants* **10** (1992) 126-143
- Jimenez-Badillo D. Una aplicación de la teoría de gráficas en arqueología (primera parte). *Sociedad Matemática Mexicana* **60** (2009) 1-8
- Jing Y. *et al.* Boswellic acid acetate induces differentiation and apoptosis in leukemia cell lines. *Leukemia Research* **23** (1999) 43-50
- Kasahara M. *et al.* Chloroplast avoidance movement reduces photodamage in plants. *Nature* **420** (2002) 829 – 832
- Kpoviessi D. *et al.* Cytotoxic activities of sterols and triterpenes identified by GC- MS in *Justicia anselliana* (NEES) T. anders active fractions and allelopathic effects on cowpea (*Vigna unguiculata* (L.) Walp) plant. *Journal de la Societe Ouest-Africaine de*

*Chimie* **13** (2008) 59-67

Lachlan G. 1992. Discriminant analysis and statistical pattern recognition. Wiley. New York, USA

Lambert J. *et al.* Resin from Africa and South America: Criteria for distinguishing between fossilized and recent resin based on NMR spectroscopy. *ACS Symposium Series* (Amber, Resinite, and Fossil Resins) **617** (1995), 193-202

Landa D. 2011. Relación de las cosas de Yucatán. Red ediciones, Mexico, Mexico

Langenheim. J.H. 2003. Plant resin, Chemistry, evolution, ecology, ethnobotany. Timber press, Cambridge, United Kingdom

Laszlo P. 2007. Copal, Benjoin, Colophane. Ed. Le Pommier. Paris, France

Lattuati-Derieux and Regert M. Les composés organiques volatils des biens culturels dans les musées, les archives et en contexte archéologique. *Technè Hors série* (2008) 86-95

Le Guerin M. *et al.* Physico Chemical analysis of five hard bitumens: Identification of chemical species and molecular organisation before and artificial ageing. *Fuel* **89** (2010) 3330-3339

Lehmann H. Une statue aztèque en résine. *Journal de la Société des Américanistes*. **37** (1948) 269-274

Liu H. *et al.* Solid-phase extraction of ursolic acid from herb using beta-cyclodextrin-based molecularly imprinted microspheres. *Journal of separation science* **31** (2008) 3573-80

Lona Naoli V. El copal en las ofrendas del Templo Mayor. *Arqueología Mexicana* **12** (2004) 66-71

Lona Naoli V. Objects made of copal resin: a radiological analysis. *Boletín de la Sociedad Geológica Mexicana* **64** (2012) 207-213

López C. 2002. Aplicaciones del copal mexicano como aglutinante pictórico. Ph.D. Thesis project. National University of Mexico, Mexico

López-Austin A. 2001. La magia, la religión y la cosmovisión. Historia antigua de México. Vol. 4. UNAM-Porrúa-INAH, Mexico city, Mexico

Lopez-Lopez A. *et al.* Sterols, fatty alcohol and triterpenic alcohol changes during ripe table olive processing. *Food Chemistry* **117** (2009) 127-134

López-Luján L. 1997. Llover a cantaros: El culto a los dioses de la lluvia y el principio de disyuncion en la tradicion religiosa mesoamericana. In: Antonio Garrido Aranda (coord.) Pensar América. Cosmovision mesoamericana y andina. Obra Social y Cultural Cajasur-Ayuntamiento de Montilla, Cordoba, Spain

López-Luján L. Aguas petrificadas, las ofrendas a Tlaloc enterradas en el Templo Mayor de Tenochtitlan. *Arqueología Mexicana* **96** (2009) 62-65

López-Luján L. and Chavez X. 2010. Al pie del Templo Mayor: excavaciones en busca de los soberanos Mexicas. In Moctezuma II: tiempo y destino de un gobernante, López-Luján L. and McEwan C., coordinators, INAH, Mexico

López-Luján L. 1993. Las ofrendas del Templo Mayor de Tenochtitlan. Instituto

Nacional de Antropología e Historia, Mexico

Lucejko J. *et al.* Wood tar and wood resinous extracts as ingredients of Egyptian embalming materials: a GC/MS study. ICOM. Interim meeting. October 2010. Pisa. Italy

Lytovchenko A. *et al.* Application of GC- MS for the detection of lipophilic compounds in diverse plant tissues. *Plant Methods* **5** (2008) 1-11

Magaloni D. *et al.* Los pintores de Bonampak. In: Martha J. Macri and McHarque Jan, Editors, Eighth Palenque Round Table. 1993, Pre-Columbian Art Research Institute, San Francisco 159-168 (1996)

Magar V. and Menar P. 1995. Investigación para la interpretación y la conservación de un disco de mosaico de turquesa. Thesis en Restauration. National Institute of Conservation, Restauration y Museography Manuel del Castillo Negrete, Mexico

Marinach C. *et al.* Identification of binding media in works of art by gas chromatography-mass spectrometry. *Journal of cultural heritage* **5** (2004) 231- 240

Martínez Cortes F. 1974. Pegamentos, Gomas y Resinas en el México Prehispánico (Sticky- Materials, Gums and Resins in Prehispanic Mexico). SEP-Setentas No. 124, Mexico City, Mexico

Martos-López. Los cenotes en la actualidad: entre la veneración y la explotación. *Arqueología Mexicana* **83** (2007) 66-70

Masmoudi H. *et al.* The evaluation of cosmetic and pharmaceutical emulsions aging process using classical techniques and a new method: FTIR. *International Journal of Pharmaceutics* **280** (2005) 117-131

Mathe C. *et al.* Characterization of archaeological frankincense by gas chromatography-mass spectrometry. *Journal of Chromatography A* **1023** (2004) 277–285

Mathe C. *et al.* High-performance liquid chromatographic analysis of triterpenoids in commercial frankincense, *Chromatographia* **60** (2004) 493–499

Matos-Moctezuma E. 1988. The great temple of the Aztecs. Treasures of Tenochtitlan. Thames and Hudson, London, United Kingdom

Matos Moctezuma E. 1982. El Templo Mayor: excavaciones y estudios. Instituto Nacional de Antropología e Historia, Mexico city, Mexico

Matos- Moctezuma E. and López-Lujan L. La Diosa Tlaltecuhltli de la Casa de las Ajaracas y el Rey Ahuizotl. *Arqueología Mexicana* **83** (2007) 23-29

Matos-Moctezuma E. De conservaciones y restauraciones, *Arqueología Mexicana* **108** (2011) 24-27

Mazza P. *et al.* A new Palaeolithic discovery: tar-hafted stone tools in a European id-Pleistocene bone-bearing bed. *Journal of Archaeological Science* **33** (2006) 1310–1318

McVaugh R. and Rzedowski. J. Synopsis of the genus *Bursera* L. in western Mexico, with notes on the material of *Bursera* collected by sesse & Mocifio. *Kew Bulletin* **18** (1965) 317-382

Mills J. The gas chromatographic examination of paint media. Part I: Fatty acid composition and identification of dried oil films *Studies in Conservation* **11** (1966) 92–107

- Mills J. and White R. Natural resins of art and archaeology: their sources, chemistry, and identification. *Studies in conservation* **22** (1977) 12-31
- Mills J. and White R. 1987. The organic chemistry of the museum objects, Butterwoths, London, UK
- Miyashiro Y. *et al.* Effects of triterpenoids and flavonoids isolated from *Alnus firma* on HIV-1 viral enzymes. *Archives on Pharmacological Reserach* **7** (2007) 820-826
- Modugno F. *et al.* Aromatic resin characterisation by gas chromatography-mass spectrometry: Raw and archaeological materials. *Journal of Chromatography A* **85** (2006) 164-173
- Montúfar A. 2007. Los Copales Mexicanos y la resina sagrada del Templo Mayor de Tenochtitlan. Instituto Nacional De Antropología e Historia Mexico city, Mexico
- Mooney H. and W. A. Emboden, JR. The relationship of terpene composition, morphology and distribution of populationsof *Bursera microphylla* (Burseraceae). *Brittonia* **20** (1968) 44-51
- Moreno Y. *et al.* A NIR-FT-Raman study of fossilized resins from the Dominican Republic, Mexico and Madagascar. *Asian Chemistry Letters* **5** (2001) 117-123
- Morkhade D. *et al.* Gum copal and gum damar: novel matrix forming materials for sustained drug delivery. *Indian Journal of Pharmaceutical Sciences* **68** (2006) 53-58
- Morley S. 1972. La civilización Maya. Sección de Obras de Antropología. FCE. Mexico City, Mexico
- Moya-Moreno *et al.* Analytical evaluation of polyunsaturated fatty acids degradation during thermal oxidation of edible oils by Fourier transform infrared spectroscopy. *Talanta* **50** (1999) 269-275
- Nissenbaum A. Molecular archaeology: organic geochemistry of Egyptian mummies. *Journal of Archaeological Science* **19** (1992) 1-6
- Nowik W. Application de la chromatographie en phase liquide à l'identification des colorants naturels des textiles anciens. *Analisis* **24** (1996) 37-40
- Obregón-Rodríguez C. 2001. La zona del altiplano central en el posclásico: La etapa de la triple alianza», *Historia antigua de México*, vol. 3, Mexico, UNAM/ Porrúa/ INAH, Mexico city, Mexico
- O'Connell M. *et al.* Betulin and lupeol in bark from four white-barked birches. *Phytochemistry* **27** (1988) 2175-2176
- O'Hara S. and Metcalfe. The climate in Mexico since the Aztec period. *Quaternary International* **44**(1997) 25-31
- Orska-Gawrys J. *et al.* Identification of natural dyes in archeological Coptic textiles by liquid chromatography with diode array detection. *Journal of Chromatography A* **989** (2003) 239-248
- Orta M. *et al.* Microstructure and adhesive properties of copal composite in dental incrustations. *Materials Research Society Symposium Proceedings* (2005), 874 (Structure and Mechanical Behavior of Biological Materials) 179-184
- Orta-Amaro M. 2007. Copal: Microestructura, composicion y algunas propiedades relevantes. Thesis for Engineer in chemistry degree. National Polytechnic Institute.

## Mexico

Ortiz de Montellano B. 1983 Aztec health and medicine and nutrition. Rutgers university press

Osete-Cortina L. and Doménech-Carbo M., Analytical Characterization of diterpenoid resins present in pictorial varnishes using pyrolysis-gas chromatography-mass spectrometry with on line trimethylsilylation, *Journal of Chromatography A*, **1065** (2005) 265-278

Papageorgiou V. *et al.* Gas chromatographic-mass spectroscopic analysis of the acidic triterpenic fraction of mastic gum. *Journal of Chromatography A* **769** (1997) 263–273

Pastorova I. *et al.* Analytical study of free and ester bound benzoic and cinnamic acids of gum benzoin resins by GC-MS and HPLC-frit FAB-MS. *Phytochemical Analysis* **8** (1997) 63–73

Pedroza L. Cenotes y cuevas inundadas de la península de Yucatán: de los primeros pobladores a la Guerra de las Castas. *Arqueología Mexicana* **105** (2010) 48-52

Peng W. *et al.* Determination of chemical components of extractives from *Santalum album* leaves by means of Py-GC/ MS. *Huanan Ligong Daxue Xuebao, Ziran Kexueban* **36** (2008) 38-44

Pennington, T. and Sarukhan. J. 1998. Arboles tropicales de Mexico. 2a. ed. Universidad Nacional Autonoma de México y Fondo de Cultura Económica. Mexico

Peraza-Sánchez S. *et al.* A new triterpene from the resin of *B. Simaruba*. *Journal of Natural Products* **58** (1995) 271-274

Peris-Vicente J. *et al.* Characterization of waxes used in pictorial artworks according to their relative amount of fatty acids and hydrocarbons by gas chromatography. *Journal of Chromatography A* **1101** (2006) 254–260

Peris-Vicente P. 2008. Estudio analítico de materiales empleados en barnices, aglutinantes y consolidantes en obras de arte mediante métodos cromatográficos y espectrométricos. PhD. thesis in Chemistry. Universidad de Valencia, Spain.

Pisha E. *et al.* Discovery of betulinic acid as a selective inhibitor of human melanoma that functions by induction of apoptosis. *Natural medicine* **1** (1995) 1046- 1051

Pitthard V. and Finch P. GC-MS analysis of monosaccharide mixtures as their diethylthioacetal derivatives: Application to plant gums used in art works. *Chromatographia* **53** (2001) 317–321

Plutowska B. and Wardencki W. Determination of volatile fatty acid ethyl esters in raw spirits using solid phase microextraction and gas chromatography. *Analytica chimica acta* **613** (2008) 64-73

Pompa y Padilla J. El embellecimiento dentario en la época prehispánica en *Arqueología mexicana*. **14** (1995) 62-65

Portilla L. y Garibay A.M. 1984. La vision de los vencidos. UNAM. Mexico City, Mexico

Proefke M. *et al.* Probing the mysteries of ancient Egypt: chemical analysis of a Roman period Egyptian mummy. *Analytical Chemistry* **64** (2008) 105-111

Purata, S. 2008. Uso y manejo de los copales aromáticos: resinas y aceites. Editorial

- CONABIO/RAICES. Mexico city, Mexico
- Rahman S. H. Saleem M. Beneficial effects of lupeol triterpene: A review of preclinical studies. *Life sciences* **88** (2011) 285-293
- Raisa-Mangas M. *et al.* Gas chromatography/ mass spectrometry characterization of the apolar extract from *Clusia minor* L. leaves *Latin American Journal of Pharmacy* **27** (2008) 747-751
- Regert M. and Rolando C. Identification of archaeological adhesives using Direct Inlet Electron Ionization Mass Spectrometry. *Analytical Chemistry* **74** (2002) 965–975
- Regert M. *et al.* Adhesive production and pottery function during the Iron Age at the site of Grand Aunay (Sarthe, France) *Archaeometry* **45** (2003) 101–120
- Regert M. *et al.* Characterisation of wax works of art by gas chromatographic procedures. *Journal of Chromatography A* **1091** (2005) 124–136
- Regert M. *et al.* Reconstructing ancient Yemeni commercial routes during the Middle-Ages using structural characterisation of terpenoid resins. *Archaeometry* **50** (2008) 668-695
- Renfrew C. El proyecto Templo Mayor. *Arqueología Mexicana* **31**( 1998) 6-12
- Rezzi S. *et al.* Composition of *Pinus nigra ssp.* From Corsica. *Industrial Crops and Products* **21** (2005) 71-79
- Ribechini E *et al.* Gas chromatographic and mass spectrometric investigations of organic residues from Roman glass unguentaria. *Journal of Chromatography A* **1183** (2008) 158–169
- Ribechini E. *et al.* Direct exposure-(chemical ionization)-mass spectrometry for a rapid characterization of raw and archaeological diterpenoid resinous substances *Microchimica Acta* **162** (2008) 405–413
- Ribechini E. *et al.* An integrated analytical approach for characterizing an organic residue from an archaeological glass bottle recovered in Pompeii (Naples, Italy), *Talanta* **74** (2008)555–561
- Ribechini E. Py-GC-MS, GC/MS and FTIR investigations on LATE Roman-egyptian adhesives from opus sectile: New insightd into ancient recipes and technoogies. *Analytica chemical acta* **638** (2009) 79-87
- Riley L. Contributions to the flora of Sinaloa. *Kew Bulletin Miscelanous Information* **4** (1923) 163-175
- Robles Camacho J. *et al.* (2010) El Adhesivo utilizado para pegar las teselas de la máscara de Malinaltepec, in La máscara de Malinaltepec, S. Martínez del Campo Lanz, ed. INAH, 189- 197, Mexico City, Mexico
- Rojas-Sandoval C. Cementerios acuáticos mayas. *Arqueología Mexicana* **83** (2007) 58-63
- Romanik G. *et al.* Techniques of preparing plant material for chromatographic separation and analysis. *Journal of biochemical and biophysical methods* **70** (2007) 253-261
- Ruvalcaba-Sil, J. L. *et al.* (2010) Estudio no destructivo in situ de la máscara de Malinatepec, in La máscara de Malinaltepec, S. Martínez del Campo Lanz, éd. INAH,



Mexico city, Mexico

Rzendowski J. and Kruse H. Algunas tendencias evolutivas en *Bursera* (Burseraceae). *Taxon* **28** (1979) 103-116

Rzendowski J. and Palacios-Chavez R. La presencia de *Commiphora* (Burseraceae) en México. *Taxon* **34** (1985) 207-210

Rzedowski, I. and Guevara-Fefer F. Burseraceae. *Flora del Bajío y de Regiones Adyacentes* **3** (1992) 1-46

Rzedowski, J. and Calderon de Rzedowski G. Burseraceae. *Flotade Veracruz* **94** (1996 b) 1-37

Rzedowski, I. *et al.* Las especies de *Bursera* (Burseraceae) en la cuenca superior del río Papaloapan (Mexico). *Acta Botánica Mexicana* **66** (2004) 23-151

Rzendowski J. *et al.* Inventario del conocimiento taxonómico de la diversidad y del endemismo de las especies mexicanas de *Bursera* (Burseraceae) *Acta Botanica Mexicana* **70** (2005) 85-111

Sahagún F.B. 2006. Historia general de las cosas de Nueva España. Colección: Sepan cuantos.300. Ed.Porrúa. Mexico city, Mexico

Saleem M. *et al.* Lupeol, a triterpene, inhibits early responses of tumor promotion induced by benzoyl peroxide in murine skin. *Pharmacological Research* **43** (2001) 127-134

Scalarone D. *et al.* Ageing behavior and analytical pyrolysis characterization of diterpenic resins used as art materials: Manila copal and sandarac. *Journal of Analytical Applied Pyrolysis* **115** (2003) 68-69

Scalarone D. *et al.* Ageing behaviour and analytical pyrolysis characterization of diterpenic resins used as art materials: manila copal and sandarac. *Journal of analytical and applied pyrolysis*. **68** (2003) 115-136

Scalarone D. *et al.* Direct-temperature mass spectrometric detection of volatile terpenoids and natural terpenoid polymers in fresh and artificially aged resins. *Journal of Mass Spectrometry* **38** (2003) 607-617

Schieffer G. Use of solid-phase extraction for improving HPLC assays of triterpene glycosides in gotu kola (*Centella asiatica*), parthenolide in feverfew (*Tanacetum parthenium*), and valerenic acids in valerian (*Valeriana officinalis*). *Journal of Liquid Chromatography & Related Technologies* **28** (2005) 581-592

Schulz H. and Baranska M. Identification and quantification of valuable plant substances by infrared and Raman spectroscopy. *Vibrational spectroscopy* **43** (2007) 13-25

Serpico M. 2000. White, Resins, amber and bitumen, in *Ancient Egyptian Materials and Technology*, P. Nicholson and I. Shaw (Eds), Cambridge University Press, Cambridge, U.K.

Serpico M. and White R. The botanical identity and transport of incense during the Egyptian New Kingdom, *Antiquity* **74** (2000) 884-897

Siddique H. and Saleem M. Beneficial health effects of lupeol triterpene: A review of preclinical studies. *Life science* **88** (2011) 285-293

- Silva J. *et al.* Analysis of the hexane extracts from seven oleoresins of Protium species. *Journal of Essential Oil Research* **21** (2009) 305-308
- Smith M. and Montiel L. The archeological study of empires and imperialism in pre-hispanic central Mexico. *Journal of Anthropological archeology* **20** (2001) 245-248
- Soustelle J. 1956 La vida cotidiana de los aztecas. Fondo de cultura económica, Mexico City, Mexico
- Stacey R. and Cartwright R. Chemical Characterization of Ancient Mesoamerican Copal Resins: Preliminary Results. *Archaeometry* **48** (2006) 323-340
- Stacey R.J. and Cartwright R. (2009) Construction, modification and repair of Mexican mosaics: evidence from adhesives. Holding it all together. Ancient and modern approaches to joining, repair and consolidation. Archetype, London, United Kingdom
- Szostek B. *et al.* Investigation of natural dyes occurring in historical Coptic textiles by high-performance liquid chromatography with UV-Vis and mass spectrometric detection. *Journal of Chromatography A* **1012** (2003) 179-192
- Tapondjou L.A. *et al.* In Vivo anti-nociceptive and anti-inflammatory effect of the two triterpenes, ursolic acid and 23-hydroxyursolic acid, from *Cussonia bancoensis*. *Archives of Pharmacal Research* **26** (2003) 143-146
- Tapp H. *et al.* FTIR spectroscopy and Multivariate Analysis can distinguish the geographical origin of extra virgin olive oils. *Journal of Agricultural Food Chemistry* **51** (2003) 6110-6115.
- Tchapla A. *et al.* Characterization of embalming materials of a mummy of the Ptolemaic era. Comparison with balms from mummies of different eras. *Journal of Separation Science* **27** (2004) 217-234
- Tchapla *et al.* Contribution à la connaissance des substances organiques utilisées en Égypte ancienne. Encyclopédie religieuse de l'Univers végétal. Croyances phytoreligieuses de l'Égypte ancienne. *OrMonsp* **X** (1999) 445-487
- Terradez M. Principal component analysis. University Oberta de Catalunya (2000). web: [http://www.uoc.edu/in3/emath/docs/Componentes\\_principales](http://www.uoc.edu/in3/emath/docs/Componentes_principales). 1 Marzo 2009
- Theodorakopoulos, C. and Zafiropulos, V., Uncovering of scalar oxidation within naturally aged varnish layers. *Journal of Cultural Heritage* (Suppl. 1) **4** (2003) 216-222
- Toledo Manzur, C. A. 1982. El genero *Bursera* (Burseraceae) en el estado de Guerrero. Tesis. Facultad de Ciencias. Universidad Nacional Autónoma de Mexico, Mexico.
- Trojanowicz M. Modern chemical analysis in archeometry. *Annals of bioanalytical chemistry* **391** (2008) 915-918
- Van Bergen P. *et al* Chemical evidence for archaeological frankincense: boswellic acids and their derivatives in solvent soluble and insoluble fractions of resin-like materials. *Tetrahedron Letters* **38** (1997) 8409-8412
- Van der Berg K. *et al* Cis-1,4-poly-b-myrcene; the structure of the polymeric fraction of mastic resin (*Pistacia lentiscus*) elucidated *Tetrahedron Letters* **39** (1998) 2654-2648

- Van der Doelen G. *et al.* Analysis of fresh triterpenoid resins and aged triterpenoid varnishes by high-performance liquid chromatography–atmospheric pressure chemical ionisation (tandem) mass spectrometry. *Journal of chromatography A* **809** (1988) 21-37
- Van der Doelen G. and Boon J. Artificial ageing of varnish triterpenoids in solution, *Journal of Photochemistry and Photobiology A: Chemistry* **134** (2000) 45–57
- Van der Doelen G.A. 1999 Molecular studies of fresh and aged triterpenoid varnishes. Ph.D. Thesis in chemistry. University of Amsterdam, Holland
- Van Gemert J. and Armitage, R. Characterization of copal incense from Mesoamerica: Identification of residues by GC-MS. Abstracts of Papers, 233rd ACS National Meeting, Chicago, IL, United States, March 25-29, 2007
- Van Keulen M. and Keijzer A. Qualitative effects of knowledge rules and user feedback in Probabilistic Data Integration. *VLDB Journal* **18** (2009) 1191-121
- Vandenabeele P. *et al.* Raman spectroscopy of different types of Mexican copal resins. *Spectrochimica Acta A* **59** (2003) 2221-2229
- Vandenabeele P. *et al.* Raman spectroscopic analysis of the Maya wall paintings in Ek'Balam, Mexico. *Spectrochimica acta part A* **61**(2005) 2349-2356
- Vandenabeele P. *et al.* A decade of Raman spectroscopy in art and archeology. *Chemical reviews* **107** (2007) 675-686
- Vandenabeele P. *et al.* Raman spectroscopic analysis of Mexican natural artists' materials. *Spectrochimica Acta A* **68** (2007) 1085–1088
- Velazquez-Castro A. *et al.* (2010) Análisis tecnológico de la máscara y el collar de Malinatepec, in La máscara de Malinatepec, S. Martínez del Campo Lanz, ed. INAH, Mexico city, Mexico
- Venegas M. 1944. Noticia de la California y de su conquista espiritual y temporal. 3v. Ed. Layac, Mexico, Mexico
- Victoria-Lona N. El copal en las ofrendas del Templo Mayor. *Arqueología Mexicana*. **64** (2004) 66-71
- Victoria-Lona N., Objects made of copal resin: a radiological analysis. *Boletín de la sociedad geológica Mexicana*. **64** (2012) 207-213
- Vieillescazes C. and Coen S. Caractérisation de quelques résines utilisées en Egypte ancienne. *Studies in Conservation* **38** (1993) 255–264
- Viveros D. Interest ceremonial plants in two indigenous communities of the centro-montaña region of Guerrero State, Mexico. A territorial approach. *Revista Brasileira de Agroecologia* **2** (2007) 475-478
- Wang F. *et al.* Triterpenoids from the resin of *styrax tonkinensis* and their antiproliferative and differentiation effects in human leukemia HL-60 Cells. *Journal of Natural Products* **69** (2006) 807-810
- Weeks A. and Simpson B. Molecular phylogenetic analysis of *Commiphora* (Burseraceae) yields insight on the evolution and historical biogeography of an "impossible" genus. *Molecular Phylogenetics and Evolution* **42** (2006) 62-79
- Whistler R. 1993. Exudate gums. In: Industrial gums: Polysaccharides and their derivatives, ed. 3. Academic press, New York, United States

- White R. The characterisation of proteinaceous binders in art objects. *National Gallery Technical Bulletin* **8** (1984) 5–14
- Zhang P. *et al.* Efficient synthesis of morolic acid and related triterpenes starting from betulin. *Tetrahedron* **65** (2009) 4304-4309
- Zhao W. *et al* Boswellic acid acetate induces differentiation and apoptosis in highly metastatic melanome and fibrosarcome cells. *Cancer Detection and Prevention* **27** (2003) 67-75
- Zhu L. and Xing Y. Infrared absorption spectrum representation of amber and its imitation. *Baoshi He Baoshixue Zazhi* **10** (2008) 33-36
- Zuco V. *et al* Selective cytotoxicity of betulinic acid on tumor cell lines, but not on normal cells *Cancer Letters* **175** (2002) 17 -25
- Zumbuhl S. *et al.* A graphite-assisted laser desorption/ionization study of light-induced aging in triterpene dammar and mastic varnishes. *Analytical chemistry* **70** (1988) 707-715

# Annexes

*B. bipinnata*, *B. excelsa* and *B. grandifolia*

Identification	Species	A.S.	Date of collection	Height (Ft)	North Latitude	West Lenght
R11a1	<i>B. Bipinnata</i>	S	9/08/2010	2182	25°7'21.42"	107°11'57.42"
R11b1	<i>B. Bipinnata</i>	S	9/08/2010	2182	25°7'21.42"	107°11'57.42"
R11b2	<i>B. Bipinnata</i>	S	25/08/2010	2182	25°7'21.42"	107°11'57.42"
R11b3	<i>B. Bipinnata</i>	S	7/09/2010	2182	25°7'21.42"	107°11'57.42"
R11c1	<i>B. Bipinnata</i>	S	9/08/2010	2182	25°7'21.42"	107°11'57.42"
R11c2	<i>B. Bipinnata</i>	S	25/08/2010	2182	25°7'21.42"	107°11'57.42"
R11c3	<i>B. Bipinnata</i>	S	7/09/2010	2182	25°7'21.42"	107°11'57.42"
R11d1	<i>B. Bipinnata</i>	S	25/08/2010	2182	25°7'21.42"	107°11'57.42"
R11d2	<i>B. Bipinnata</i>	S	7/09/2010	2182	25°7'21.42"	107°11'57.42"
R11d3	<i>B. Bipinnata</i>	S	7/09/2010	2182	25°7'21.42"	107°11'57.42"
R11e1	<i>B. Bipinnata</i>	S	25/08/2010	2182	25°7'21.42"	107°11'57.42"
R27a1	<i>B. excelsa</i>	LS	29/08/2009	702	24°50'37.62"	107°2'28.76"
R27a2	<i>B. excelsa</i>	S	29/08/2009	702	24°50'37.62"	107°2'28.76"
R27a2	<i>B. excelsa</i>	LS	23/07/2010	702	24°50'37.62"	107°2'28.76"
R27a3	<i>B. excelsa</i>	LS	29/08/2009	702	24°50'37.62"	107°2'28.76"
R27a4	<i>B. excelsa</i>	L	5/09/2009	702	24°50'37.62"	107°2'28.76"
R34a1	<i>B. grandifolia</i>	S	5/09/2009	515	24°45'36.06"	107°11'51.48"
R34b1	<i>B. grandifolia</i>	LS	23/07/2010	580	24°45'37.92"	107°11'20.22"
R34c2	<i>B. grandifolia</i>	LS	23/07/2010	580	24°45'37.92"	107°11'20.22"
R34c3	<i>B. grandifolia</i>	LS	23/07/2010	580	24°45'37.92"	107°11'20.22"
R34c4	<i>B. grandifolia</i>	LS	23/07/2010	580	24°45'37.92"	107°11'20.22"
R34d1	<i>B. grandifolia</i>	LS	23/07/2010	580	24°45'37.92"	107°11'20.22"
R34d2	<i>B. grandifolia</i>	LS	10/06/2010	580	24°45'37.92"	107°11'20.22"

Aggregation state (A.S) (S = solid, L = liquid, LS = very viscous liquid)

Table 28 Table of certified copals *B. bipinnata*, *B. excelsa* and *B. grandifolia* with GPS position of originating tree and date of collection

*B. laxiflora* y *B. penicillata*

Identification	Species	A.S	Date of collection	Height (Ft)	North Latitude	West Lenght
R47a1	<i>B. laxiflora</i>	L	5/09/2009	515	24°45'36.06"	107°11'51.48"
R47a2	<i>B. laxiflora</i>	L	5/09/2009	515	24°45'36.06"	107°11'51.48"
R47b1	<i>B. laxiflora</i>	LS	29/08/2009	515	24°45'36.06"	107°11'51.48"
R47b2	<i>B. laxiflora</i>	LS	29/08/2009	515	24°45'36.06"	107°11'51.48"
R47b3	<i>B. laxiflora</i>	LS	29/08/2009	515	24°45'36.06"	107°11'51.48"
R47b4	<i>B. laxiflora</i>	L	5/09/2009	515	24°45'36.06"	107°11'51.48"
R47b5	<i>B. laxiflora</i>	L	5/09/2009	515	24°45'36.06"	107°11'51.48"
R47b6	<i>B. laxiflora</i>	L	5/09/2009	515	24°45'36.06"	107°11'51.48"
R47c1	<i>B. laxiflora</i>	S3	12/09/2009	UA	UA	UA
R47d1	<i>B. laxiflora</i>	L	19/09/2009	UA	UA	UA
R47e1	<i>B. laxiflora</i>	L	10/07/2010	580	24°45'37.92"	107°11'20.22"
R47f1	<i>B. laxiflora</i>	L	10/07/2010	580	24°45'37.92"	107°11'20.22"
R63a1	<i>B. penicillata</i>	S4	29/08/2009	751.5	24°46'8.64"	107°9'28.26"
R63a2	<i>B. penicillata</i>	S5	29/08/2009	751.5	24°46'8.64"	107°9'28.26"
R63a3	<i>B. penicillata</i>	LS6	29/08/2009	751.5	24°46'8.64"	107°9'28.26"
R63a4	<i>B. penicillata</i>	S6	29/08/2009	751.5	24°46'8.64"	107°9'28.26"

Aggregation state (A.S) (S = solid, L = liquid, LS = very viscous liquid  
 UA Unavailable information

Table 29 Table of *B. laxiflora* y *B. penicillata* certified copals, with GPS position of originating tree and date of collection

*B. simaruba*, *B. stenophylla*

Identification	Species	A.S	Date of collection	Height (Ft)	North Latitude	West Lenght
R70a1	<i>B. simaruba</i>	L	29/08/2009	685	24°51'27.60"	107°1'7.02"
R70a2	<i>B. simaruba</i>	S	23/07/2010	685	24°51'27.60"	107°1'7.02"
R70b1	<i>B. simaruba</i>	L	10/07/2010	571	24°51'25.98"	107°0'8.16"
R70b2	<i>B. simaruba</i>	S	10/07/2010	571	24°51'25.98"	107°0'8.16"
R70b3	<i>B. simaruba</i>	S	10/07/2010	571	24°51'25.98"	107°0'8.16"
R70b4	<i>B. simaruba</i>	LS	10/07/2010	571	24°51'25.98"	107°0'8.16"
R70b5	<i>B. simaruba</i>	S	10/07/2010	571	24°51'25.98"	107°0'8.16"
R70c1	<i>B. simaruba</i>	S	10/07/2010	571	24°51'25.98"	107°0'8.16"
R70c2	<i>B. simaruba</i>	S	10/07/2010	571	24°51'25.98"	107°0'8.16"
R70c3	<i>B. simaruba</i>	LS	10/07/2010	571	24°51'25.98"	107°0'8.16"
R70d1	<i>B. simaruba</i>	S	23/07/2010	571	24°51'25.98"	107°0'8.16"
R70d2	<i>B. simaruba</i>	S	10/07/2010	571	24°51'25.98"	107°0'8.16"
R72a1	<i>B. stenophylla</i>	S	12/09/2009	276	26°41'26.4"	108°19'58.7"
R72a2	<i>B. stenophylla</i>	L	19/09/2009	276	26°41'26.4"	108°19'58.7"
R72b1	<i>B. stenophylla</i>	S	12/09/2009	276	26°41'26.4"	108°19'58.7"
R72b2	<i>B. stenophylla</i>	L	19/09/2009	276	26°41'26.4"	108°19'58.7"
R72c1	<i>B. stenophylla</i>	S	12/09/2009	276	26°41'26.4"	108°19'58.7"
R72c2	<i>B. stenophylla</i>	L	19/09/2009	276	26°41'26.4"	108°19'58.7"
R72d1	<i>B. stenophylla</i>	S	12/09/2009	276	26°41'26.4"	108°19'58.7"
R72d2	<i>B. stenophylla</i>	S	19/09/2009	276	26°41'26.4"	108°19'58.7"

**Table 30 Table of *B. simaruba*, *B. stenophylla***  
**Certified copals, with GPS position of originating tree and date of collection**  
**Aggregation state (A.S) (S = solid, L = liquid, LS = very viscous liquid)**



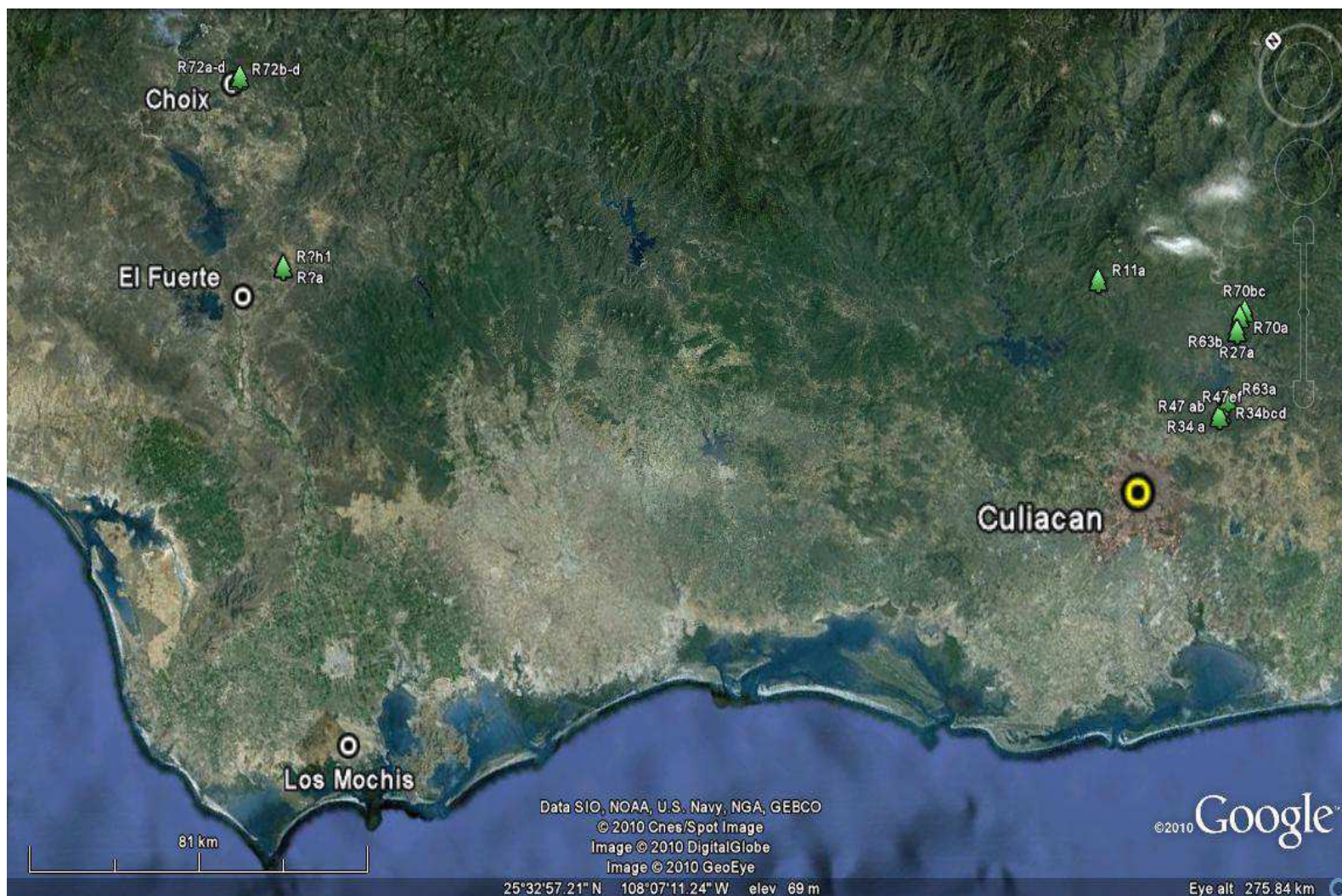


Fig 109 Map of the GPS position of originating trees for certified resins

### Commercial Samples



<p><b>Sidral</b> Scale 1 cm photo: 1.2 cm</p>	<p><b>ATZJ2</b> Scale 1 cm photo: 3 cm</p>	<p><b>IZUP1</b> Scale 1cm photo: 15 cm</p>	<p><b>IZUR1</b> Scale 1cm photo: 2.5 cm</p>
---	--	--	---



<p><b>CHOB1</b> Scale 1cm photo: 4 cm</p>	<p><b>ATZM1</b> Scale 1cm photo: 6 cm</p>	<p><b>Incienso</b> Scale 1cm photo: 1 cm</p>	<p><b>CHOR1</b> Scale 1cm photo: 2 cm</p>
---	---	--	---

Table 31 Pictures of some commercial samples

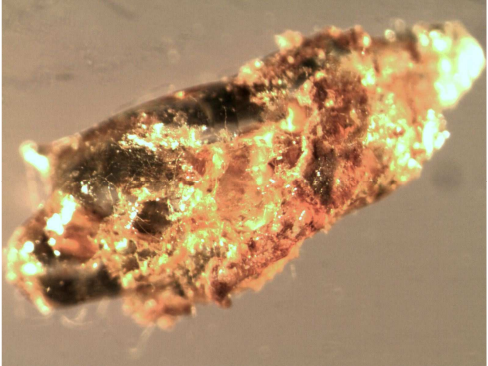

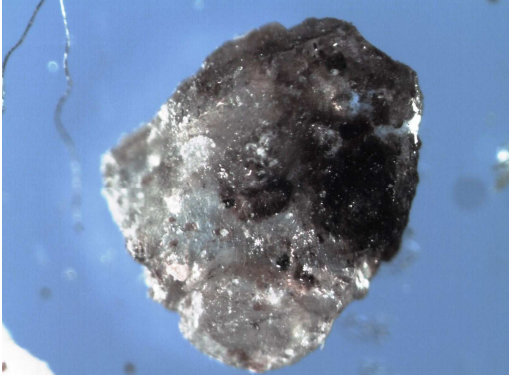
SAMPLE	PICTURE
11a1 (20 X)	
11b3 (20 X)	
11c2 (16 X)	

Table 32. Selected pictures of optical microscopic study of certified origin samples from *B. bipinnata* species

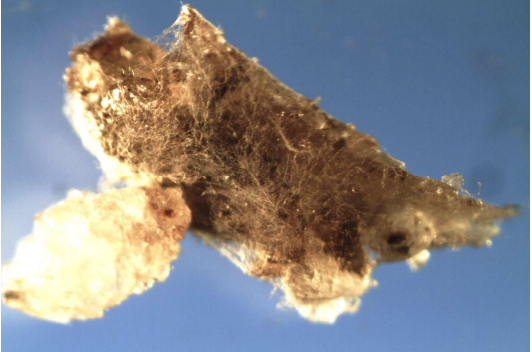
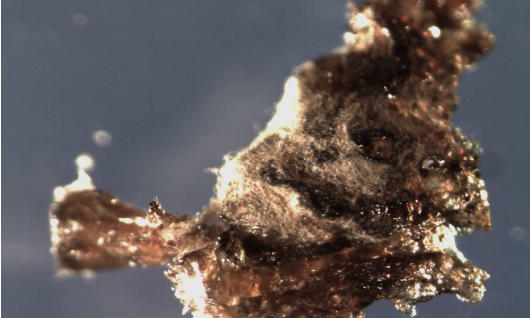

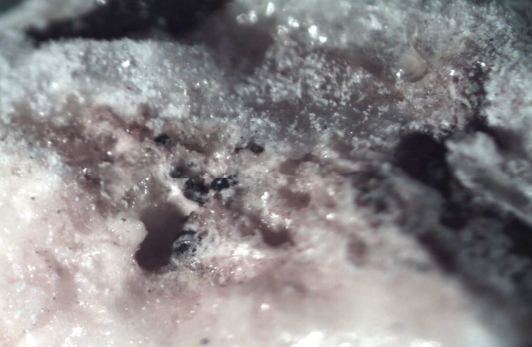
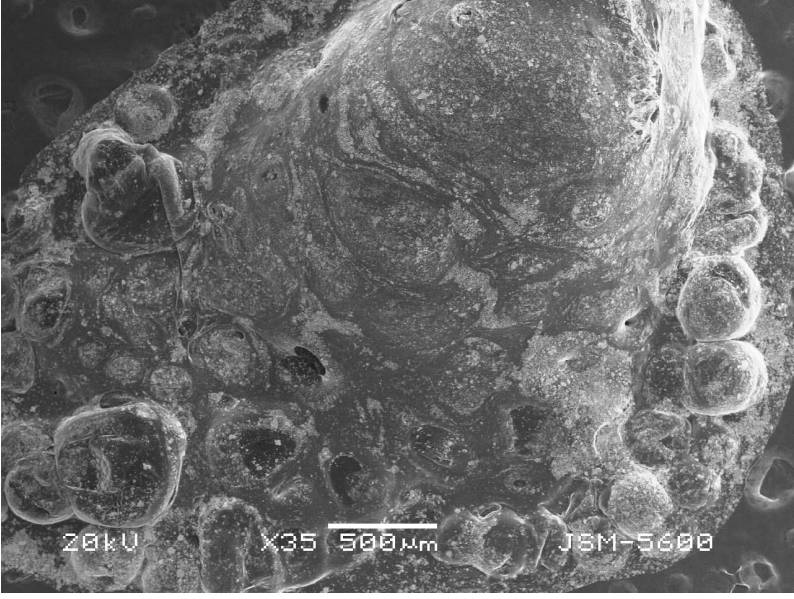
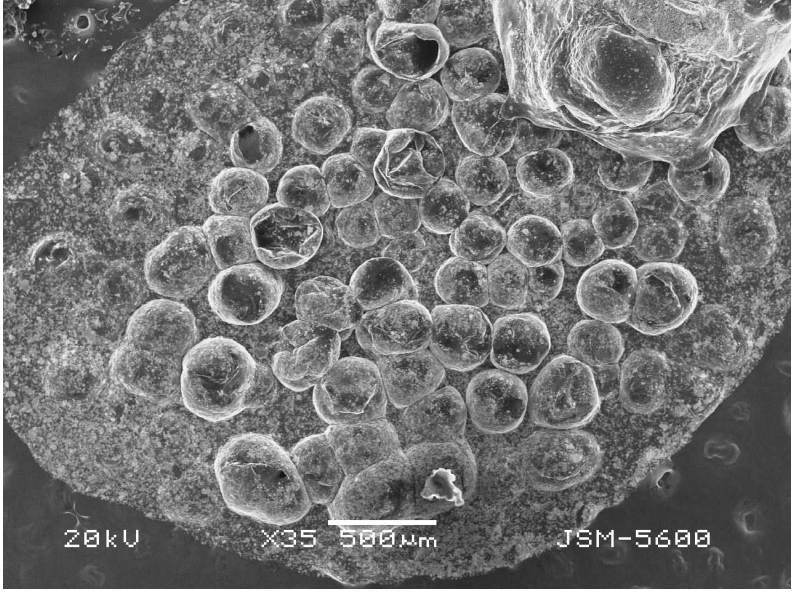
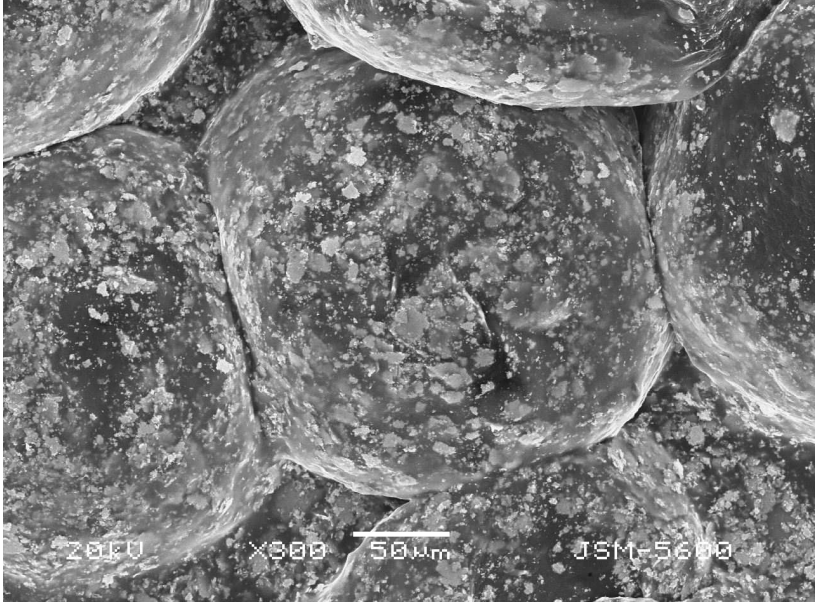
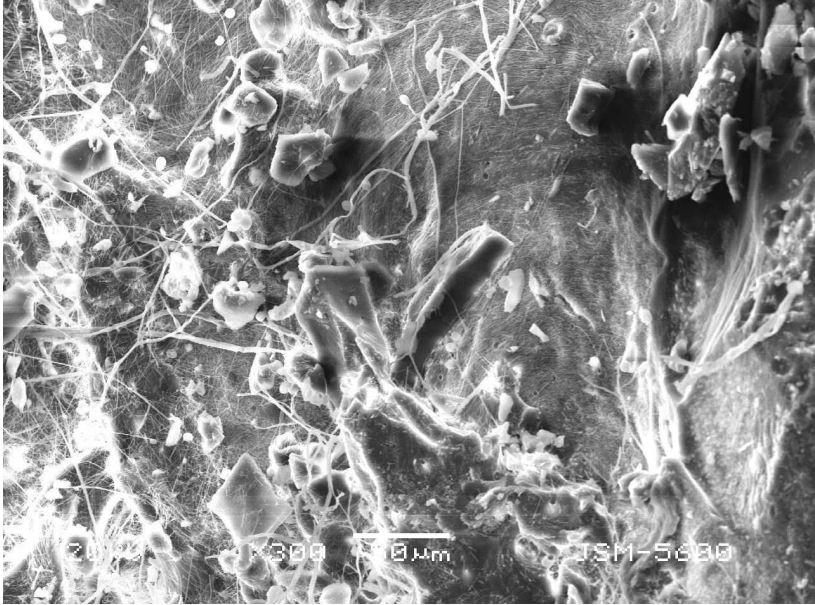
SAMPLE	PICTURE	
11c3 (16 X)		
11d1 (1.8 X)		
11d3 (12.5 X)		
M1 (16 X)		

Table 33. Selected pictures of optical microscopic study of certified origin samples from *B. bipinnata* species, and from archeological sample M1

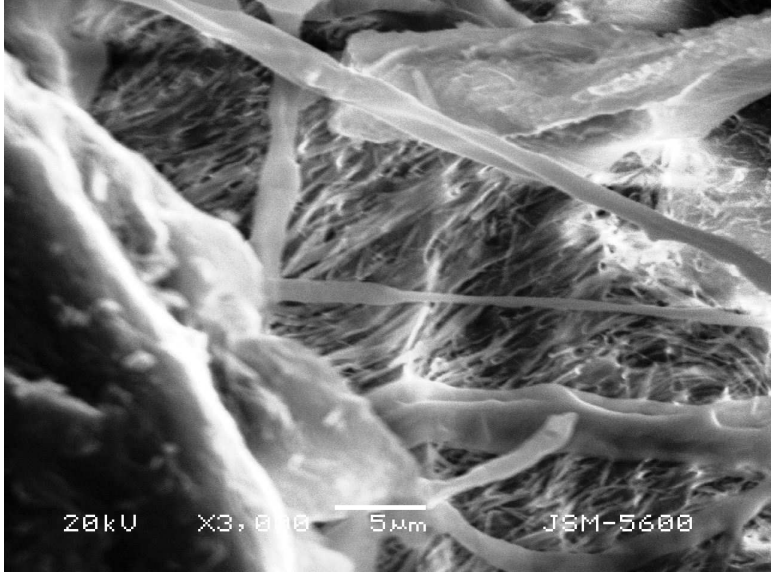
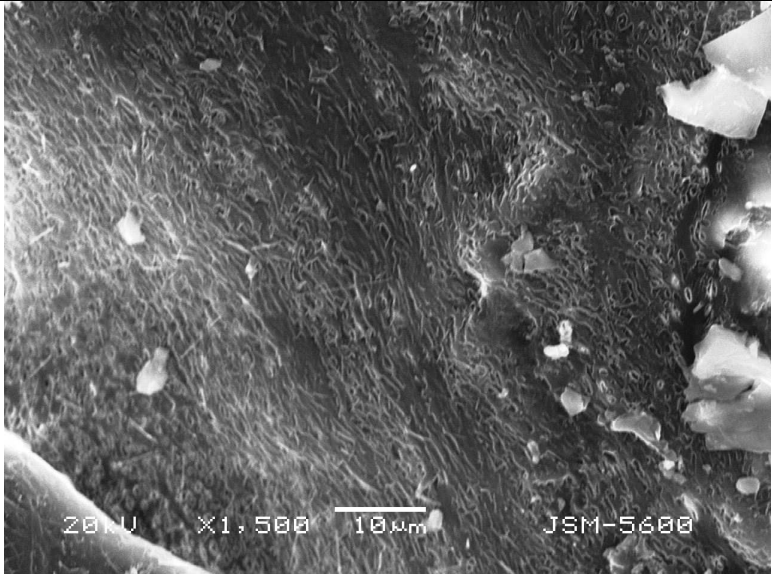
## Electronical microscopic study

SAMPLE	PICTURE
<p><b>11b3</b> <b>(35 X)</b></p>	
<p><b>11c2</b> <b>(35 X)</b></p>	

**Table 34** Selected pictures of electronic microscopic study of certified origin samples from *B. Bipinnata* species



SAMPLE	PICTURE
<b>11c2</b> <b>(300 X)</b>	
<b>11c3</b> <b>(35 X)</b>	

**Table 35** Selected pictures of electronic microscopic study of certified origin samples from *B. bipinnata* species

SAMPLE	PICTURE
<p><b>11c3</b> <b>(300 X)</b></p>	
<p><b>11c3</b> <b>(1500 X)</b></p>	

**Table 36** Selected pictures of electronic microscopic study of certified origin samples from *B. Bipinnata* species



**Pictures of an example of light aged copal**

<b>Sidral (Commercial sample ) Before light ageing</b>	
<b>After light ageing</b>	

**Table 37 Picture of Sidral sample before and after light ageing**

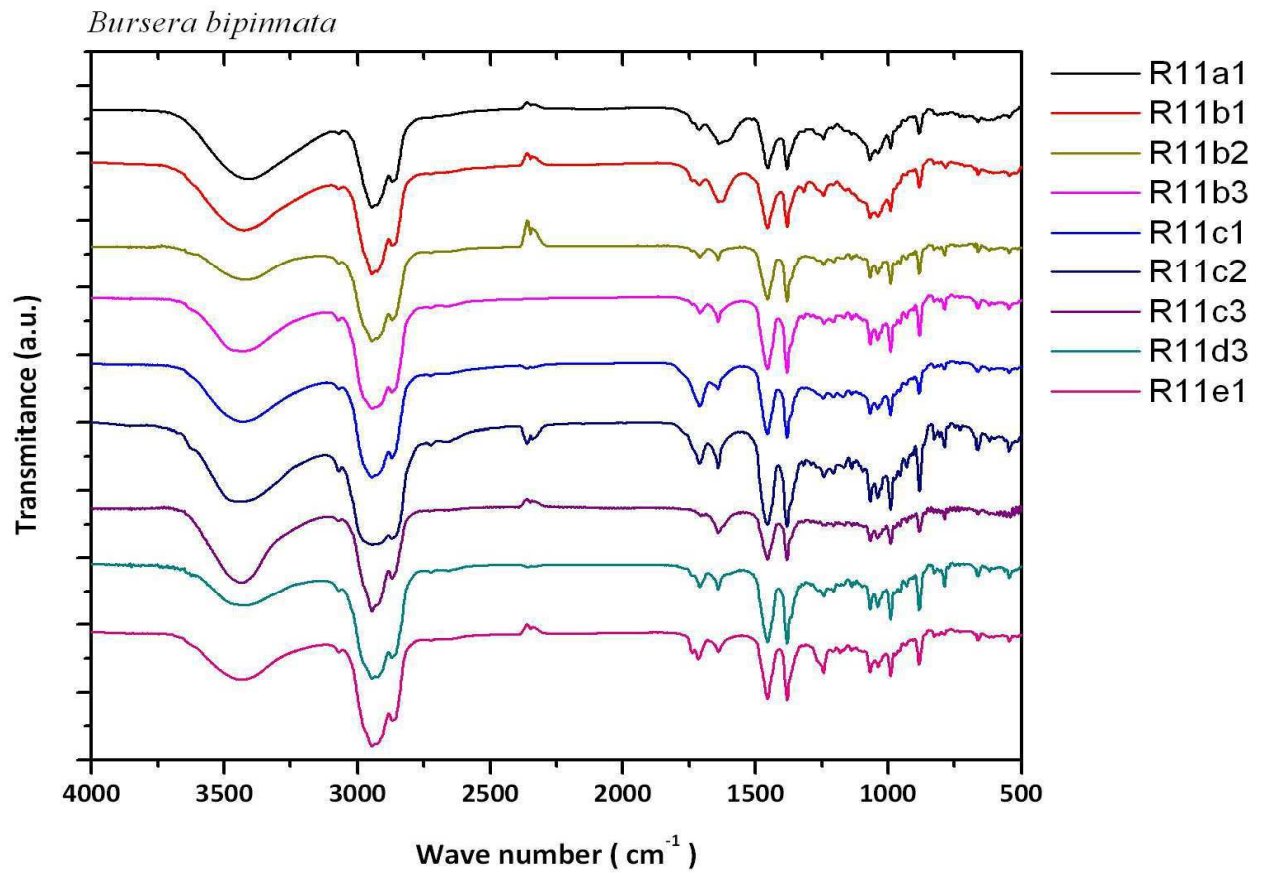


### Differences between *B. Bipinata* and *B. Stenophylla*

<p><i>Bursera bipinnata</i></p> <p>It has bipinnate to tripinnate leaves. The amount of leaflets and foliolulos (up to a hundred) per leaf, the distance between foliolulos is small and they are touching, and the end of the leaf, it has up to seven pairs of undivided leaflets.</p>	
<p><i>Bursera stenophylla</i></p> <p>Leaflets and foliolulos a does not exceed 10. The distance between leaflets and foliolulos is larger than in <i>B. bipinnata</i> and seldom touched each other. At the end of each leaf there are few pairs (two or three) of leaflets which are not divided into foliolulos</p>	

**Table 38** Botanical differences between *B. bipinnata* and *B. stenophylla*

## Comparative of Spectra for botanical certified resins

Fig 110 FTIR spectra of *B. bipinnata* samples

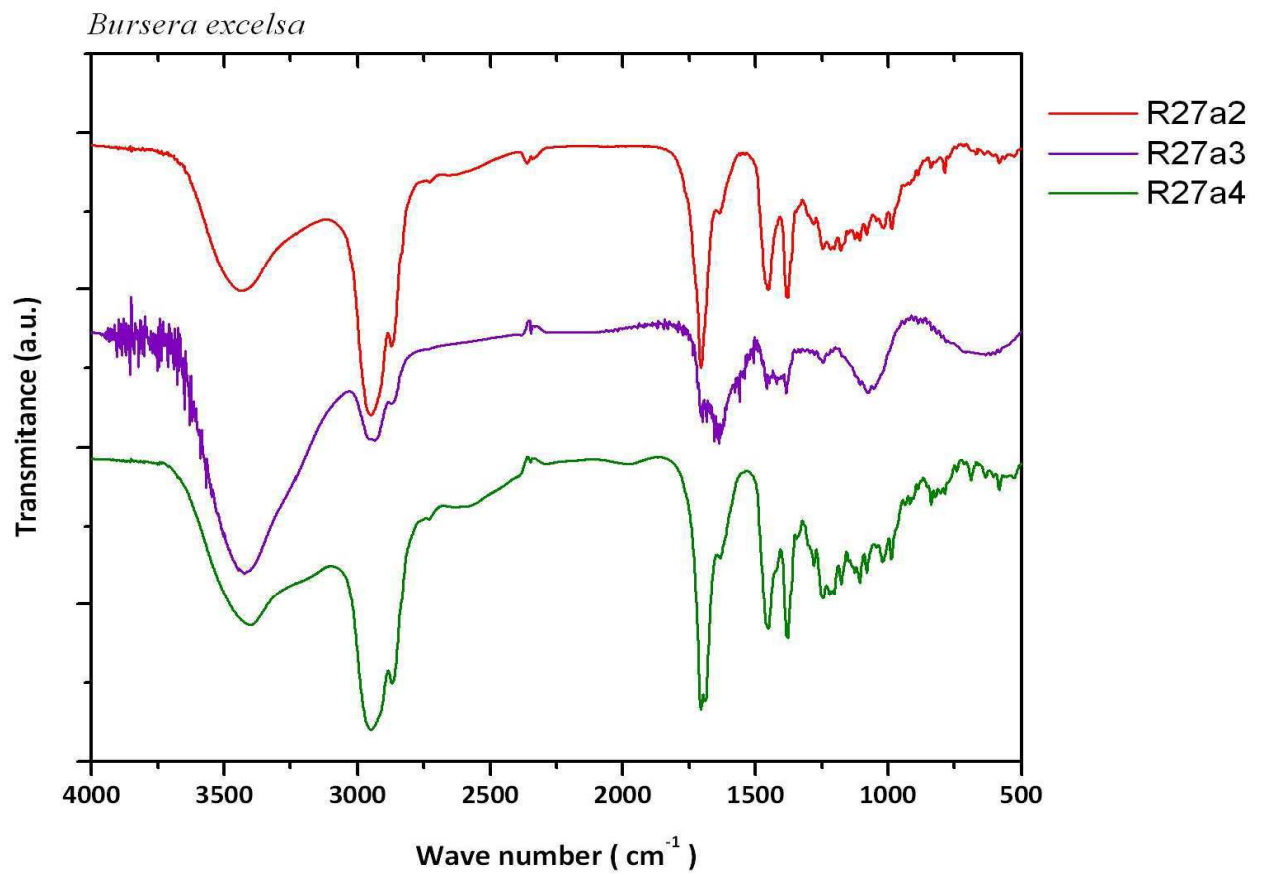


Fig 111 FTIR spectra of *B. excelsa* sample

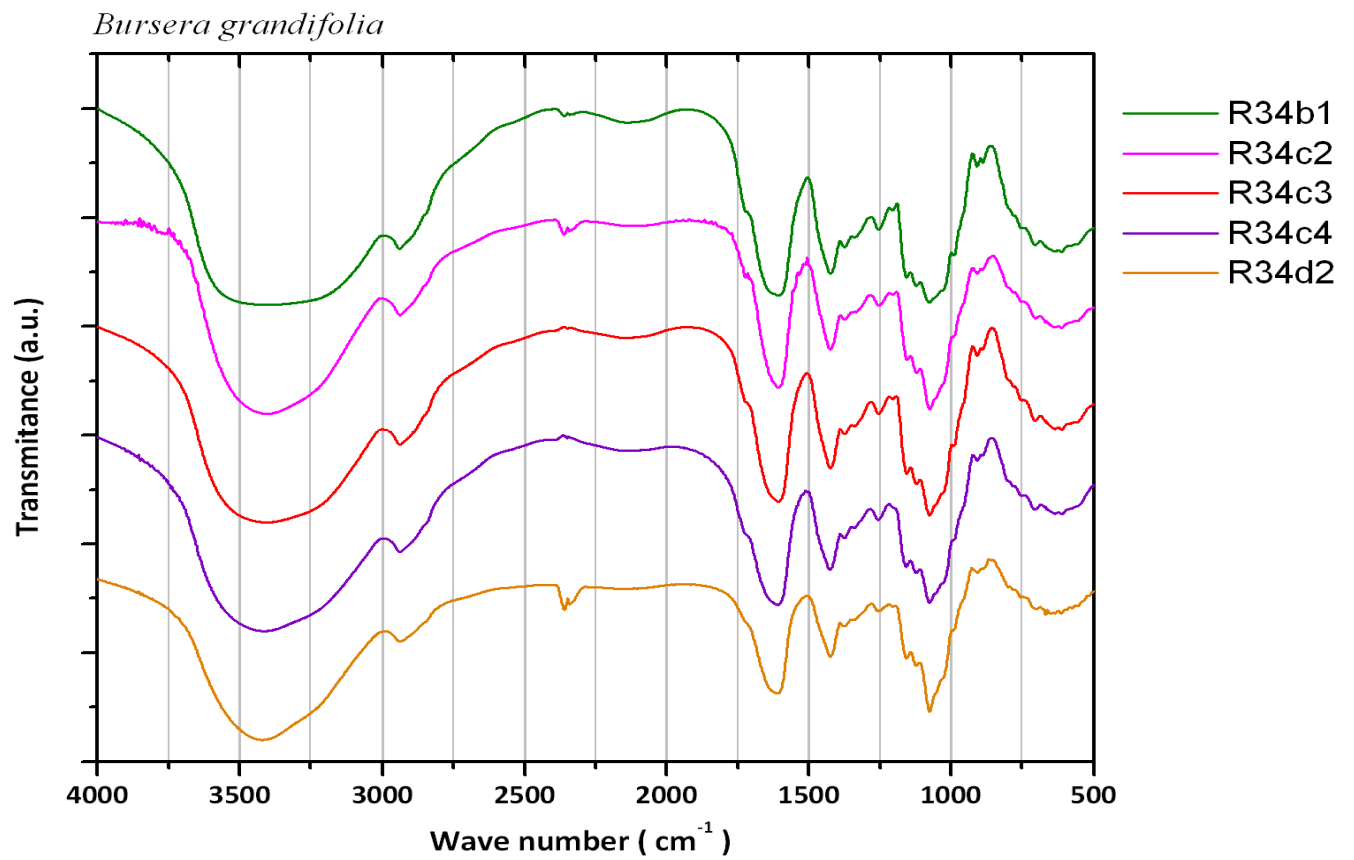


Fig 112 FTIR spectra of *B. grandifolia* samples

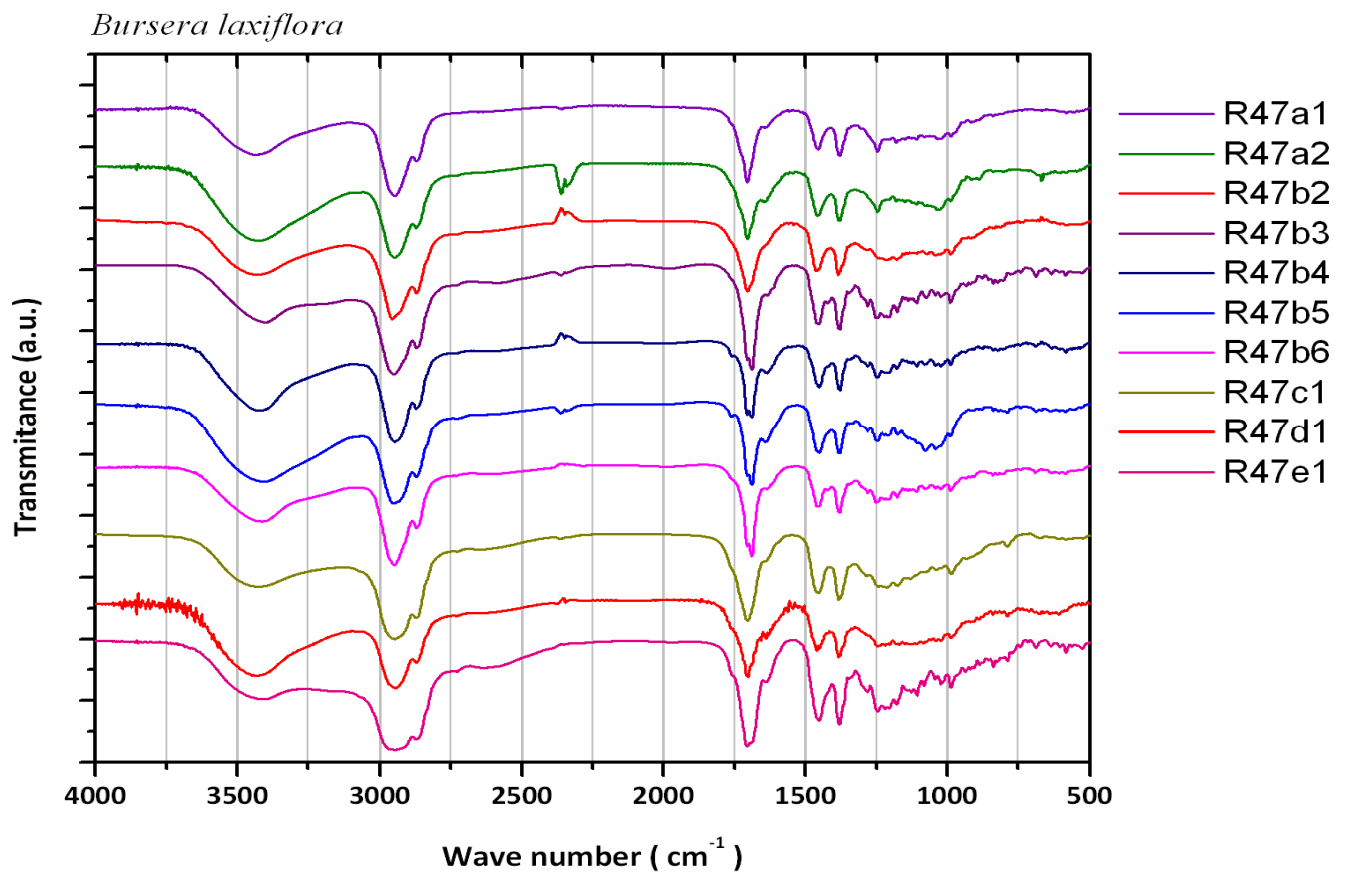


Fig 113 FTIR spectra of *B. laxiflora* samples

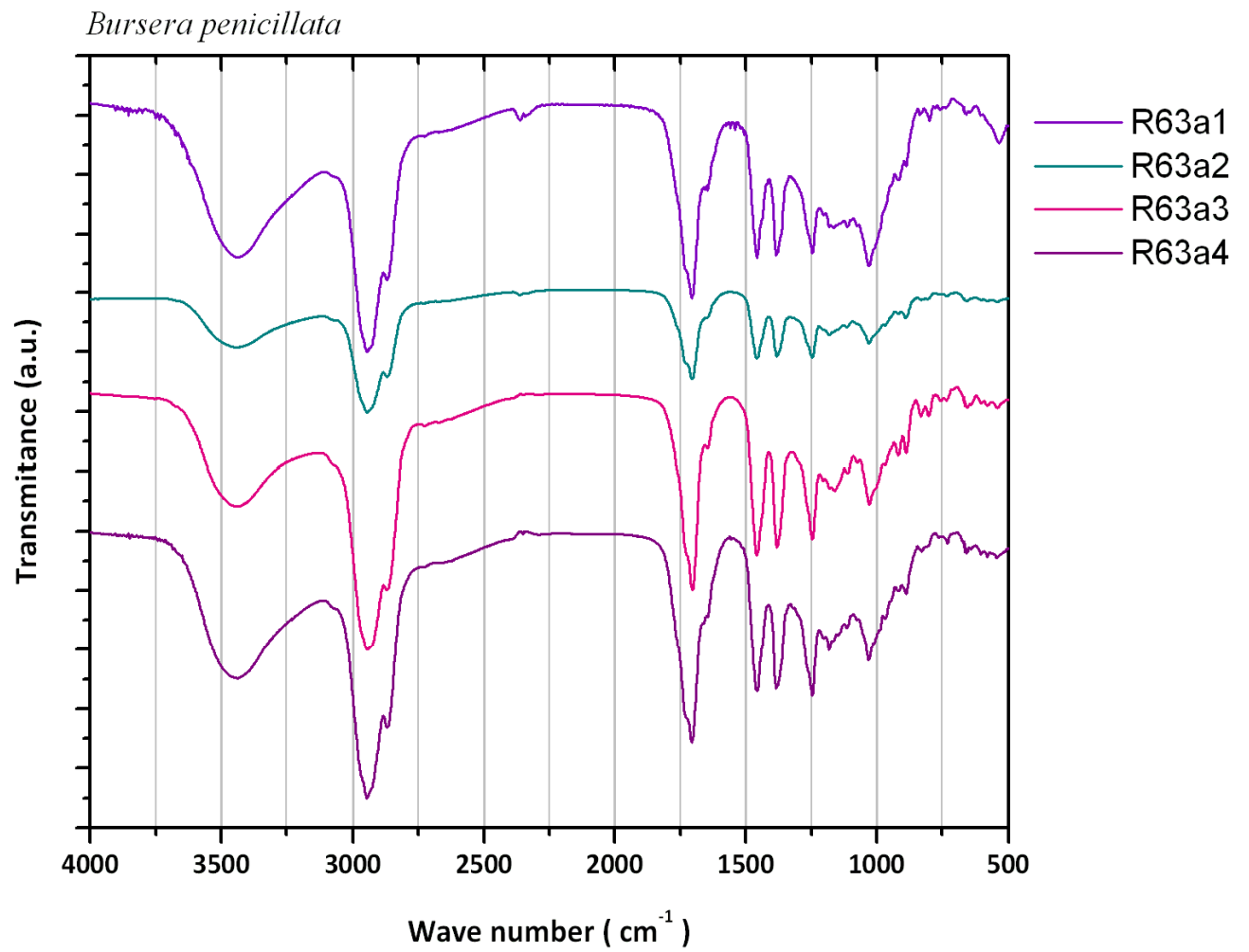


Fig 114 FTIR spectra of *B. penicillata* samples

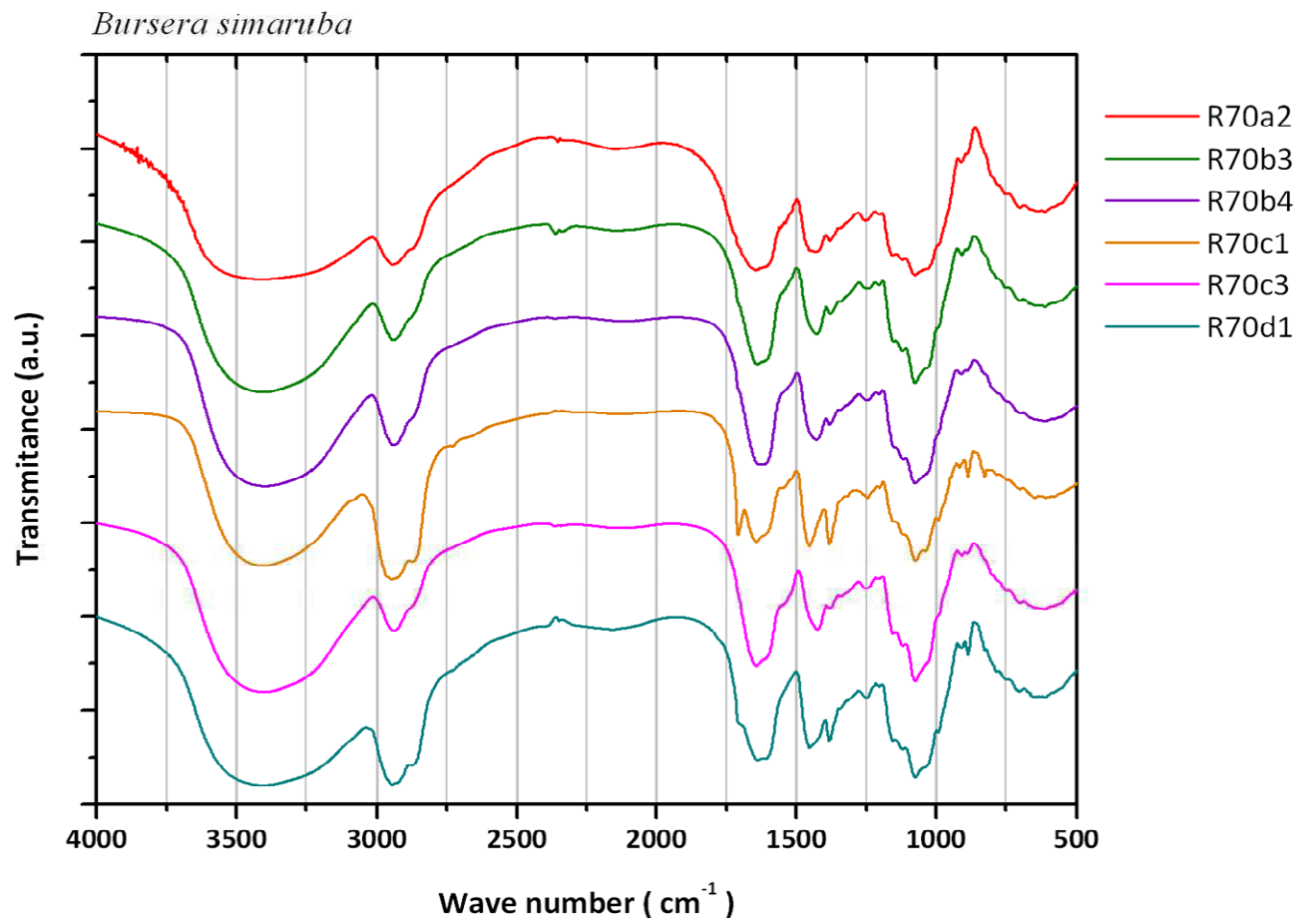


Fig 115 FTIR spectra of *B. simaruba* samples

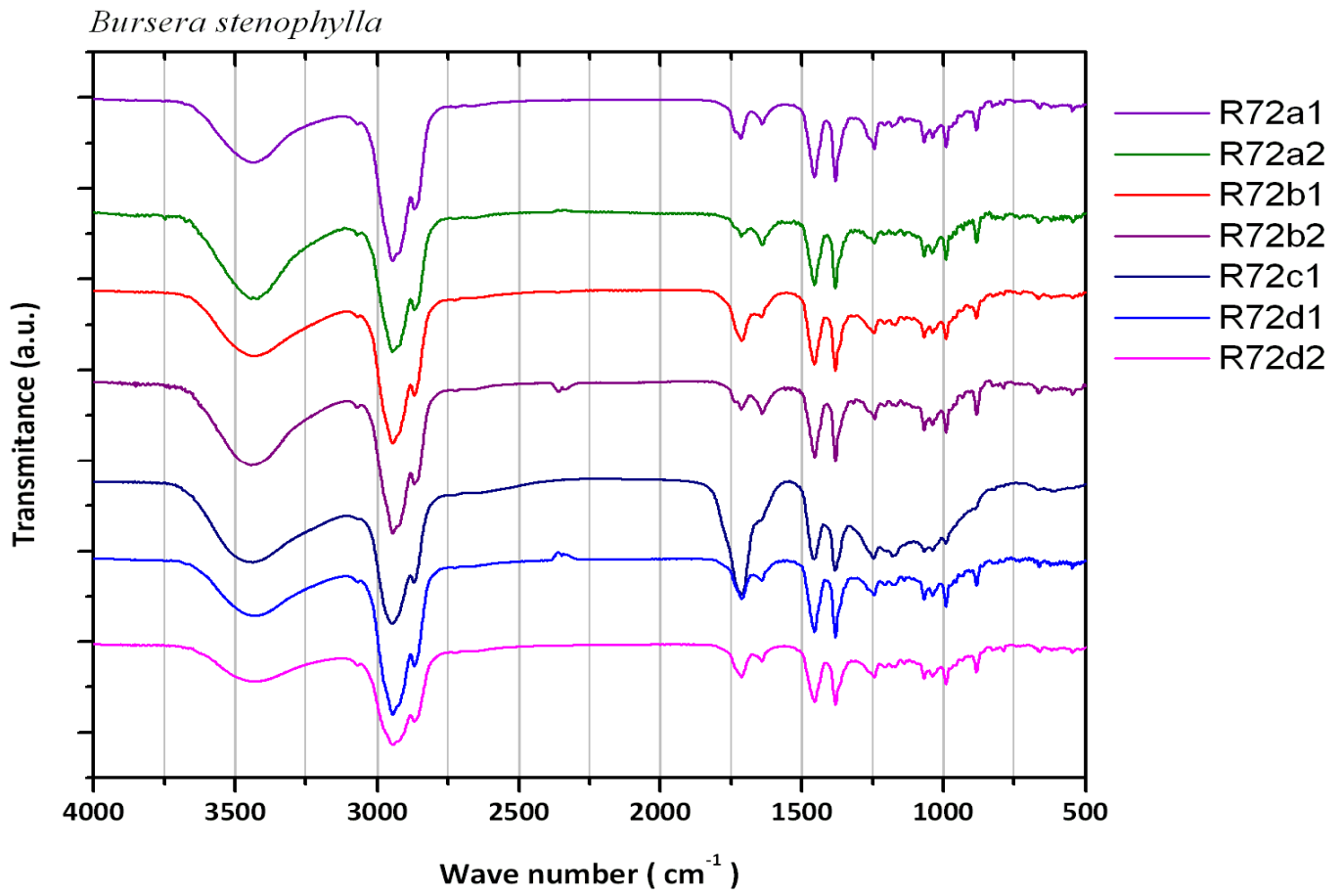


Fig 116 FTIR spectra of *B. stenophylla* samples



## FTIR Data &amp; PCA

11e1	3446.99	2946.6	1717.61	1640.6	1454.62	1379.47	1243.78	1068.22	883.04	667.92	547.69
R27a2	3431.73	2950.27	1706.01	1638.38	1454.26	1381.23	1214.34	1082.4	885.39	673.78	582.38
R27a3	3424.41	2946.33	1703.38	1630.04	1457.58	1384.7	1225.93	1076.24	883.07	671.38	585.5
R27a4	3403.89	2948.41	1705.88	1634.48	1451.62	1377.92	1220.55	1080.69	886.75	687.35	584.45
27a1Q	3430.89	2948.06	1705.96	1634.05	1455.74	1377.69	1218.88	1082.4	886.23	673.78	587.41
34b1	3419.75	2939.77	1640.75	1609.53	1423.37	1335.75	1255.09	1074.48	907.82	667.76	612.48
34c2	3405.36	2938.46	1631.35	1605.53	1424.38	1335.75	1253.81	1074.65	906.69	669.69	612.85
34c3	3404.93	2938.62	1636.22	1606.18	1424.14	1335.75	1255.05	1075.02	907.72	645.17	612.64
34c4	3417.64	2938.76	1635.84	1607.35	1425.37	1339.84	1256.37	1075.1	906.69	645.17	612.64
34d2	3417.85	2939.51	1633.04	1610.75	1423.37	1339.84	1258.1	1075.09	906.69	669.69	612.48
34a1Q	3436.25	2939.96	1635.14	1616.53	1427.42	1339.29	1254.03	1073.64	906.69	669.98	612.48
R63a1	3438.91	2947.02	1736.2	1706.11	1457.55	1384.48	1245.72	1030.25	890.35	662.75	536.27
R63a2	3440	2945.53	1732.12	1705.25	1457.78	1384.74	1246.75	1029.94	889.24	663.01	536.01
R63a3	3437.97	2949.83	1723.95	1704.18	1457.93	1384.82	1246.29	1028.58	887.54	661.73	544.16
R63a4	3436.61	2946.49	1736.2	1706.27	1456.67	1384.74	1246.31	1031.29	886.26	661.39	536.54
R63a1Q	3433.46	2944.74	1732.12	1703.19	1457.59	1384.82	1245.85	1029.42	887.37	660.27	543.58
R63b1Q	3433.47	2943.89	1732.12	1701.88	1457.81	1384.82	1245.61	1029.42	887.37	662.11	543.88
R72a1	3440.8	2953.91	1716.17	1639.95	1455.65	1380.7	1244.23	1067.92	882.92	669.69	546.99
R72a2	3442.6	2946.9	1714.54	1640	1455.37	1380.65	1243.33	1068.1	882.65	664.31	544.95
R72b1	3425.33	2945.74	1712.88	1638.13	1455.71	1381.29	1245.36	1068.01	882.82	665.42	547.81
R72b2	3443.62	2946.06	1714.46	1641.92	1454.9	1381.07	1243.46	1067.88	882.33	665.22	546.16
R72c1	3436.55	2947.63	1711.07	1650.39	1456.34	1380.79	1246.83	1067.58	886.32	606.32	551.36
R72c2	3447.64	2938.07	1700.86	1647.12	1458.08	1381.55	1253.96	1067.9	887.89	614.26	564.36
R72d1	3431.34	2946.03	1713.81	1641.13	1455.31	1383.82	1244.55	1068.09	882.83	612.54	547.33
R72d2	3429.56	2945.94	1713.96	1642.2	1455.02	1380.67	1244.32	1068.13	882.59	620.96	548.15
47b1Q	3406.57	2953.28	1709.83	1634.05	1454.6	1377.65	1249.94	1073.72	837.52	687.18	587.96
R47b2	3429.21	2956.3	1704.99	1633.17	1450.83	1376.91	1246.53	1078.32	837.23	687.72	584.82
R47b3	3399.58	2949.14	1705.14	1634.05	1453.89	1377.74	1249.23	1073.05	837.66	687.73	582.8
R47b4	3418.62	2947.44	1711.69	1634.02	1451.19	1377.61	1245.85	1074.23	833.14	688.54	585.16

R47b5	3411.3	2948.45	1703.51	1629.96	1453.21	1378.63	1249.35	1074.07	838.06	688.5	585.75
R47b6	3406.08	2958	1704.18	1642.22	1450.67	1377.68	1249.94	1078.54	838.9	688.14	584.39
R47c1	3427.36	2947.36	1704.52	1637.54	1454.18	1381.82	1245.78	1081.77	838.76	674.25	585.08
R47d1	3434.67	2941.65	1703.03	1638.52	1459.63	1382	1246.44	1083.69	839.73	677.53	582.61
47E 1	3417.29	2945.09	1705.98	1638.51	1453.19	1381.28	1245.64	1083.96	840	687.68	583.7
47f1	3432	2953.52	1706.58	1638.5	1450.25	1384.04	1246.57	1081.26	837.66	691.37	582.1

**Table 39 FTIR bands of certified resins used in PCA**

### FTIR Data & PCA

Bands	a	b	c	d	e	f	g	h	i	j	k
TMT	3433.16	2945.54	1708.92	1642.92	1455.24	1380.95	1243.17	1067.94	881.16	663.83	546.08
173	3432.43	2948.23	1709.12	1663.77	1454.84	1379.24	1244.42	1067.6	881.57	663.2	584.6
51	3432.15	2951.18	1706.53	1665.63	1454.9	1379.86	1247.25	1068.26	883.19	660.04	556.12
52	3432.88	2945.13	1706.64	1642.84	1456.01	1380.84	1243.8	1067.78	881.83	665.23	547.31
84	3435.27	2945.64	1712.2	1642.36	1454.91	1380.44	1242.82	1068.19	881.23	663.22	546.23
26	3417.97	2946.88	1708.81	1659.94	1454.48	1378.92	1244.88	1066.64	882.41	662.23	547.05
Chichen	3430.63	2950.89	1707.32	1654.94	1458.53	1384.31	1249.94	1078.32	883.73	665.6	581.87

**Table 40 FTIR bands of archaeological resins used in PCA**

FTIR Data & LDA

I.D.	a	b	c	d	e	f	g	h	i	j	k	Actual species	Fitting Matrix	Confusion Matrix
R11a1	3429.38	2945.91	1711.18	1638.47	1454.15	1380.3	1243.86	1039.24	883.1	663.19	546.35	<i>bipinnata</i>	<i>bipinnata</i>	<i>bipinnata</i>
R11b2	3425.46	2944.56	1710.98	1640.26	1455.55	1381.65	1242.56	1038.41	882.8	662.89	545.86	<i>bipinnata</i>	<i>bipinnata</i>	<i>bipinnata</i>
11b3	3429.63	2945.81	1708.9	1640.81	1455.95	1380.53	1242.22	1067.66	881.51	663.53	547.46	<i>bipinnata</i>	<i>stenophylla</i>	<i>stenophylla</i>
R11c2	3438.2	2945.17	1709.6	1641.7	1456.1	1381.83	1240.15	1038.02	881.19	665.81	546.38	<i>bipinnata</i>	<i>bipinnata</i>	<i>bipinnata</i>
R11c3	3445.21	2944.76	1712.02	1640.69	1455.8	1381.8	1222.27	1037.79	881.74	662.11	545.14	<i>bipinnata</i>	<i>bipinnata</i>	<i>bipinnata</i>
R11d1	3440.04	2944.76	1711.7	1639.33	1455.33	1381.46	1243.97	1037.41	883.13	664.08	543.24	<i>bipinnata</i>	<i>bipinnata</i>	<i>bipinnata</i>
R11d2	3438.74	2944.69	1709.68	1640.73	1455.71	1381.53	1240.07	1038.04	881.97	664.66	545.66	<i>bipinnata</i>	<i>bipinnata</i>	<i>bipinnata</i>
11e1	3446.99	2946.6	1717.61	1640.6	1454.62	1379.47	1243.78	1068.22	883.04	667.92	547.69	<i>bipinnata</i>	<i>stenophylla</i>	<i>stenophylla</i>
R27a2	3431.73	2950.27	1706.01	1638.38	1454.26	1381.23	1214.34	1082.4	885.39	673.78	582.38	<i>excelsa</i>	<i>excelsa</i>	<i>excelsa</i>
R27a3	3424.41	2946.33	1703.38	1630.04	1457.58	1384.7	1225.93	1076.24	883.07	671.38	585.5	<i>excelsa</i>	<i>excelsa</i>	<i>excelsa</i>
R27a4	3403.89	2948.41	1705.88	1634.48	1451.62	1377.92	1220.55	1080.69	886.75	687.35	584.45	<i>excelsa</i>	<i>excelsa</i>	<i>excelsa</i>
27a1Q	3430.89	2948.06	1705.96	1634.05	1455.74	1377.69	1218.88	1082.4	886.23	673.78	587.41	<i>excelsa</i>	<i>excelsa</i>	<i>excelsa</i>
34b1	3419.75	2939.77	1640.75	1609.53	1423.37	1335.75	1255.09	1074.48	907.82	667.76	612.48	<i>grandifolia</i>	<i>grandifolia</i>	<i>grandifolia</i>
34c2	3405.36	2938.46	1631.35	1605.53	1424.38	1335.75	1253.81	1074.65	906.69	669.69	612.85	<i>grandifolia</i>	<i>grandifolia</i>	<i>grandifolia</i>
34c3	3404.93	2938.62	1636.22	1606.18	1424.14	1335.75	1255.05	1075.02	907.72	645.17	612.64	<i>grandifolia</i>	<i>grandifolia</i>	<i>grandifolia</i>
34c4	3417.64	2938.76	1635.84	1607.35	1425.37	1339.84	1256.37	1075.1	906.69	645.17	612.64	<i>grandifolia</i>	<i>grandifolia</i>	<i>grandifolia</i>
34d2	3417.85	2939.51	1633.04	1610.75	1423.37	1339.84	1258.1	1075.09	906.69	669.69	612.48	<i>grandifolia</i>	<i>grandifolia</i>	<i>grandifolia</i>
34a1Q	3436.25	2939.96	1635.14	1616.53	1427.42	1339.29	1254.03	1073.64	906.69	669.98	612.48	<i>grandifolia</i>	<i>grandifolia</i>	<i>grandifolia</i>
R63a1	3438.91	2947.02	1736.2	1706.11	1457.55	1384.48	1245.72	1030.25	890.35	662.75	536.27	<i>penicillata</i>	<i>penicillata</i>	<i>penicillata</i>
R63a2	3440	2945.53	1732.12	1705.25	1457.78	1384.74	1246.75	1029.94	889.24	663.01	536.01	<i>penicillata</i>	<i>penicillata</i>	<i>penicillata</i>
R63a3	3437.97	2949.83	1723.95	1704.18	1457.93	1384.82	1246.29	1028.58	887.54	661.73	544.16	<i>penicillata</i>	<i>penicillata</i>	<i>penicillata</i>
R63a4	3436.61	2946.49	1736.2	1706.27	1456.67	1384.74	1246.31	1031.29	886.26	661.39	536.54	<i>penicillata</i>	<i>penicillata</i>	<i>penicillata</i>
R63a1Q	3433.46	2944.74	1732.12	1703.19	1457.59	1384.82	1245.85	1029.42	887.37	660.27	543.58	<i>penicillata</i>	<i>penicillata</i>	<i>penicillata</i>
R63b1Q	3433.47	2943.89	1732.12	1701.88	1457.81	1384.82	1245.61	1029.42	887.37	662.11	543.88	<i>penicillata</i>	<i>penicillata</i>	<i>penicillata</i>
R72a1	3440.8	2953.91	1716.17	1639.95	1455.65	1380.7	1244.23	1067.92	882.92	669.69	546.99	<i>stenophylla</i>	<i>stenophylla</i>	<i>stenophylla</i>
R72a2	3442.6	2946.9	1714.54	1640	1455.37	1380.65	1243.33	1068.1	882.65	664.31	544.95	<i>stenophylla</i>	<i>stenophylla</i>	<i>stenophylla</i>
R72b1	3425.33	2945.74	1712.88	1638.13	1455.71	1381.29	1245.36	1068.01	882.82	665.42	547.81	<i>stenophylla</i>	<i>stenophylla</i>	<i>stenophylla</i>
R72b2	3443.62	2946.06	1714.46	1641.92	1454.9	1381.07	1243.46	1067.88	882.33	665.22	546.16	<i>stenophylla</i>	<i>stenophylla</i>	<i>stenophylla</i>

R72c1	3436.55	2947.63	1711.07	1650.39	1456.34	1380.79	1246.83	1067.58	886.32	606.32	551.36	<i>stenophylla</i>	<i>stenophylla</i>	<i>stenophylla</i>
R72c2	3447.64	2938.07	1700.86	1647.12	1458.08	1381.55	1253.96	1067.9	887.89	614.26	564.36	<i>stenophylla</i>	<i>stenophylla</i>	<i>stenophylla</i>
R72d1	3431.34	2946.03	1713.81	1641.13	1455.31	1383.82	1244.55	1068.09	882.83	612.54	547.33	<i>stenophylla</i>	<i>stenophylla</i>	<i>stenophylla</i>
R72d2	3429.56	2945.94	1713.96	1642.2	1455.02	1380.67	1244.32	1068.13	882.59	620.96	548.15	<i>stenophylla</i>	<i>stenophylla</i>	<i>stenophylla</i>
47b1Q	3406.57	2953.28	1709.83	1634.05	1454.6	1377.65	1249.94	1073.72	837.52	687.18	587.96	<i>laxiflora</i>	<i>laxiflora</i>	<i>laxiflora</i>
R47b2	3429.21	2956.3	1704.99	1633.17	1450.83	1376.91	1246.53	1078.32	837.23	687.72	584.82	<i>laxiflora</i>	<i>laxiflora</i>	<i>laxiflora</i>
R47b3	3399.58	2949.14	1705.14	1634.05	1453.89	1377.74	1249.23	1073.05	837.66	687.73	582.8	<i>laxiflora</i>	<i>laxiflora</i>	<i>laxiflora</i>
R47b4	3418.62	2947.44	1711.69	1634.02	1451.19	1377.61	1245.85	1074.23	833.14	688.54	585.16	<i>laxiflora</i>	<i>laxiflora</i>	<i>laxiflora</i>
R47b6	3411.3	2948.45	1703.51	1629.96	1453.21	1378.63	1249.35	1074.07	838.06	688.5	585.75	<i>laxiflora</i>	<i>laxiflora</i>	<i>laxiflora</i>
R47b5	3406.08	2958	1704.18	1642.22	1450.67	1377.68	1249.94	1078.54	838.9	688.14	584.39	<i>laxiflora</i>	<i>laxiflora</i>	<i>laxiflora</i>
R47c1	3427.36	2947.36	1704.52	1637.54	1454.18	1381.82	1245.78	1081.77	838.76	674.25	585.08	<i>laxiflora</i>	<i>laxiflora</i>	<i>laxiflora</i>
R47d1	3434.67	2941.65	1703.03	1638.52	1459.63	1382	1246.44	1083.69	839.73	677.53	582.61	<i>laxiflora</i>	<i>laxiflora</i>	<i>laxiflora</i>
47E 1	3417.29	2945.09	1705.98	1638.51	1453.19	1381.28	1245.64	1083.96	840	687.68	583.7	<i>laxiflora</i>	<i>laxiflora</i>	<i>laxiflora</i>
47f1	3432	2953.52	1706.58	1638.5	1450.25	1384.04	1246.57	1081.26	837.66	691.37	582.1	<i>laxiflora</i>	<i>laxiflora</i>	<i>laxiflora</i>

Table 41 LDA results of classification of FTIR data of certified resins

**FTIR Data of Selected Commercial Samples  
& PCA**

	<b>a</b>	<b>b</b>	<b>c</b>	<b>d</b>	<b>e</b>	<b>f</b>	<b>g</b>	<b>h</b>	<b>i</b>	<b>j</b>	<b>k</b>
IZUR1	3438.61	2946.77	1708.96	1641.57	1455.57	1380.24	1243.33	1067.63	881	663.75	546.79
ATZM1	3395.53	2945.8	1713.46	1641.59	1455.4	1379.85	1243.22	1067.67	881.1	663.98	547.32
CHOB1	3399.41	2945.39	1709.89	1642.73	1457.92	1379.86	1243.62	1067.64	881.2	663.8	546.91
ATZB1	3400.23	2945.68	1709.71	1642.22	1455.33	1380.43	1242.76	1067.55	880.7	664.12	547.2

Table 42 FTIR data used on PCA on selected commercial sampl

## PCA results for selected commercial resins

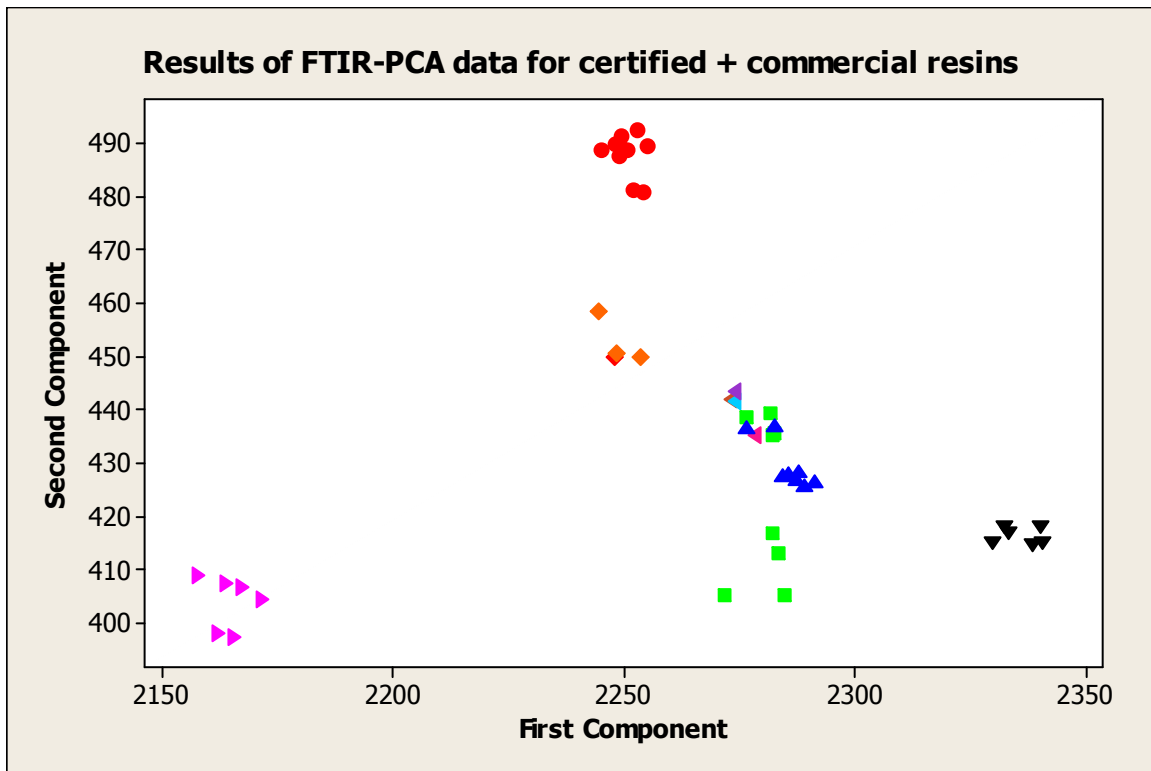


Fig 117 PCA: First two components for certified resins plus commercial samples: ◀ ATZM1, ◀ CHOB1, ◀ ATZB1, ◀ IZUR1. Symbols for certified resins are the same than the ones used along Chapter 3

## Principal Component Analysis (FTIR data)

Variables: a, b, k, c, d, e, f, g, h, i, j

### Eigenanalysis of the Covariance Matrix

Eigenvalue	2104.4	835.4	315.3	178.5	130.3	75.4	53.6	12.9	9.6
Proportion	0.565	0.224	0.085	0.048	0.035	0.020	0.014	0.003	0.003
Cumulative	0.565	0.790	0.874	0.922	0.957	0.977	0.992	0.995	0.998

Eigenvalue	6.5	1.4
Proportion	0.002	0.000
Cumulative	1.000	1.000

Variable	PC1	PC2	PC3	PC4	PC5	PC6	PC7	PC8
a	0.155	-0.151	0.177	-0.130	0.095	0.916	-0.216	-0.033
b	0.035	0.097	0.002	0.008	0.062	-0.028	0.080	-0.011
k	0.552	0.269	0.151	-0.000	0.189	-0.161	-0.043	0.256
c	0.481	-0.124	-0.603	0.466	0.253	0.094	0.133	-0.236
d	0.195	0.123	0.152	0.005	0.119	-0.023	-0.093	0.354
e	0.276	0.195	0.196	0.002	0.146	-0.032	-0.128	0.357
f	-0.055	-0.057	-0.117	0.318	-0.497	0.239	0.457	0.596
g	-0.264	0.281	0.368	0.274	0.507	0.142	0.576	-0.144
h	-0.059	-0.703	-0.062	-0.293	0.474	-0.131	0.203	0.352
i	-0.064	0.469	-0.526	-0.618	0.105	0.161	0.255	0.100
j	-0.495	0.176	-0.300	0.349	0.333	0.062	-0.505	0.339

Variable	PC9	PC10	PC11
a	0.093	-0.032	0.007
b	0.717	0.669	0.132
k	0.426	-0.538	-0.007
c	-0.135	0.092	0.010
d	-0.372	0.225	0.765
e	-0.320	0.431	-0.627
f	0.077	-0.056	-0.038
g	-0.073	-0.063	-0.008
h	0.065	-0.021	-0.036
i	-0.066	-0.015	-0.005
j	0.129	-0.100	-0.020

## Linear Discriminant Analysis: FTIR data

**Linear Method for Response: c1**  
**Variables: a, b, c, d, e, f, g, h, i, j, k**

Group	bipinnata	excelsa	grandifolia	laxiflora	penicillata	stenophylla
Count	8	4	6	10	6	8

**Summary of classification**

Put into Group	True Group					
	bipinnata	excelsa	grandifolia	laxiflora	penicillata	stenophylla
bipinnata	6	0	0	0	0	0
excelsa	0	4	0	0	0	0
grandifolia	0	0	6	0	0	0
laxiflora	0	0	0	10	0	0
penicillata	0	0	0	0	6	0
stenophylla	2	0	0	0	0	8
Total N	8	4	6	10	6	8
N correct	6	4	6	10	6	8
Proportion	0.750	1.000	1.000	1.000	1.000	1.000

Put into Group	stenophylla
bipinnata	0
excelsa	0
grandifolia	0
laxiflora	0
penicillata	0
stenophylla	8
Total N	8
N correct	8
Proportion	1.000

N = 42                      N Correct = 40                      Proportion Correct = 0.952

**Summary of Classification with Cross-validation**

Put into Group	True Group						
	bipinnata	excelsa	grandifolia	laxiflora	penicillata	stenophylla	stenophylla
bipinnata	6	0	0	0	0	0	0
excelsa	0	4	0	0	0	0	0
grandifolia	0	0	6	0	0	0	0
laxiflora	0	0	0	10	0	0	0
penicillata	0	0	0	0	6	0	0
stenophylla	2	0	0	0	0	0	8
Total N	8	4	6	10	6	6	8
N correct	6	4	6	10	6	6	8
Proportion	0.750	1.000	1.000	1.000	1.000	1.000	1.000

N = 42                      N Correct = 40                      Proportion Correct = 0.952

**Squared Distance Between Groups**

	bipinnata	excelsa	grandifolia	laxiflora	penicillata	stenophylla
bipinnata	0.00	488.90	2504.58	1600.45	757.95	
excelsa	488.90	0.00	2756.76	1834.44	1385.37	
grandifolia	2504.58	2756.76	0.00	4840.90	4827.41	
laxiflora	1600.45	1834.44	4840.90	0.00	2045.44	
penicillata	757.95	1385.37	4827.41	2045.44	0.00	
stenophylla	17.60	455.42	2539.15	1583.71	794.18	

stenophylla

bipinnata	17.60
excelsa	455.42
grandifolia	2539.15
laxiflora	1583.71
penicillata	794.18
stenophylla	0.00

#### Linear Discriminant Function for Groups

	bipinnata	excelsa	grandifolia	laxiflora	penicillata	stenophylla
Constant	-3620271	-3644189	-3544947	-3600516	-3641690	-3623754
a	-98	-99	-95	-99	-100	-98
b	752	754	748	750	750	752
c	659	662	648	657	663	659
d	-26	-27	-33	-19	-15	-26
e	1161	1162	1141	1163	1164	1162
f	1102	1110	1087	1100	1104	1103
g	-36	-40	-36	-35	-35	-35
h	-23	-22	-22	-22	-24	-23
i	900	905	909	869	896	900
j	45	46	45	45	46	45
k	570	579	569	575	572	570

Variable	Pooled		Means for Group			
	Mean	bipinnata	excelsa	grandifolia	laxiflora	penicillata
a	3428.3	3436.7	3422.7	3417.0	3418.3	3436.7
b	2946.2	2945.3	2948.3	2939.2	2950.0	2946.3
c	1701.8	1711.5	1705.3	1635.4	1705.9	1732.1
d	1643.9	1640.3	1634.2	1609.3	1636.1	1704.5
e	1450.8	1455.4	1454.8	1424.7	1453.2	1457.6
f	1375.0	1381.1	1380.4	1337.7	1379.5	1384.7
g	1244.0	1239.9	1219.9	1255.4	1247.5	1246.1
h	1062.8	1045.6	1080.4	1074.7	1078.3	1029.8
i	876.65	882.31	885.36	907.05	837.87	888.02
j	665.16	664.27	676.57	661.24	685.86	661.88
k	568.21	545.97	584.94	612.59	584.44	540.07

Variable	stenophylla
a	3437.2
b	2946.3
c	1712.2
d	1642.6
e	1455.8
f	1381.3
g	1245.8
h	1068.0
i	883.79
j	639.84
k	549.64

Variable	Pooled		StDev for Group			
	StDev	bipinnata	excelsa	grandifolia	laxiflora	penicillata
a	9.719	7.799	12.979	11.493	12.221	2.768
b	3.339	0.741	1.615	0.644	5.135	2.090
c	3.497	2.717	1.286	3.210	2.782	4.473
d	3.217	0.995	3.409	4.054	3.589	1.730
e	1.763	0.681	2.518	1.536	2.779	0.456
f	1.865	0.866	3.300	2.149	2.500	0.132
g	3.976	7.277	4.787	1.603	1.837	0.436
h	6.518	13.800	2.909	0.562	4.281	0.918



i	1.569	0.793	1.626	0.559	1.911	1.489
j	13.84	1.86	7.27	12.48	5.44	0.99
k	3.387	1.401	2.098	0.147	1.740	4.170

Variable	stenophylla
a	7.804
b	4.282
c	4.816
d	4.100
e	1.026
f	1.063
g	3.497
h	0.179
i	2.094
j	28.46
k	6.230

## Pooled Covariance Matrix

	a	b	c	d	e	f	g	h	i	j	k
a	94.458										
b	-3.644	11.146									
c	-0.847	3.504	12.228								
d	12.223	0.090	-1.951	10.349							
e	5.557	-3.309	-2.196	0.691	3.110						
f	7.541	-1.823	-1.437	1.240	1.191	3.480					
g	-8.709	-1.211	-3.711	-0.318	0.566	-0.199	15.811				
h	11.475	0.034	2.574	3.720	0.022	-0.396	3.161				
i	1.287	-1.204	-2.008	2.387	0.603	-0.110	1.488				
j	-0.179	15.841	15.176	-13.755	-6.490	-4.939	-8.496				
k	0.622	-3.364	-6.889	1.230	1.402	-0.780	5.218				
h	42.485										
i	1.528	2.460									
j	-0.150	-7.505	191.663								
k	1.200	1.635	-19.018	11.470							

## Covariance matrix for Group bipinnata

	a	b	c	d	e	f	g	h	i	j	k
a	60.825										
b	0.827	0.549									
c	12.568	1.110	7.383								
d	2.340	-0.081	-0.330	0.991							
e	0.057	-0.295	-1.082	0.524	0.464						
f	-0.562	-0.605	-1.464	0.257	0.420	0.751					
g	-24.440	1.979	0.839	-2.200	-1.916	-2.854	52.951				
h	11.937	8.048	15.584	3.000	-1.263	-9.359	27.973				
i	-0.373	0.125	1.235	-0.627	-0.443	-0.309	2.637				
j	7.185	0.794	2.928	0.631	-0.252	-0.816	6.037				
k	-1.511	0.767	0.768	0.479	-0.138	-0.774	2.131				
h	190.448										
i	-0.127	0.629									
j	12.405	0.135	3.452								
k	14.032	-0.258	1.106	1.963							

## Covariance matrix for Group excelsa

	a	b	c	d	e	f	g	h	i	j	k
a	168.451										
b	3.463	2.609									
c	-0.792	1.696	1.654								
d	8.044	5.500	3.672	11.624							

e	22.464	-2.372	-2.315	-4.951	6.339						
f	13.101	-2.153	-3.631	-4.901	5.615	10.891					
g	-20.160	-7.504	-5.274	-15.998	5.580	7.489	22.912				
h	7.289	3.897	3.631	8.481	-3.896	-7.455	-12.687				
i	-7.555	1.505	1.933	3.303	-3.328	-5.209	-4.653				
j	-86.564	2.195	4.132	4.455	-16.608	-14.602	-1.977				
k	2.429	-2.265	-0.516	-4.512	2.273	-1.732	4.924				
h	8.462										
i	3.910	2.645									
j	4.519	8.119	52.904								
k	-0.884	0.036	-2.646	4.403							

Covariance matrix for Group *grandifolia*

	a	b	c	d	e	f	g	h	i	j	k
a	132.085										
b	6.358	0.415									
c	9.045	0.889	10.306								
d	44.268	2.307	1.556	16.435							
e	11.696	0.232	-0.711	3.816	2.359						
f	14.934	0.479	-1.731	4.682	1.444	4.619					
g	-0.315	0.115	-0.219	-0.173	-1.110	2.013	2.571				
h	-4.742	-0.228	-0.237	-1.747	-0.602	-0.018	0.586				
i	-1.849	0.018	1.382	-0.596	-0.405	-0.844	-0.146				
j	55.736	4.623	-8.361	25.312	-0.122	-0.053	-2.916				
k	-1.222	-0.085	-0.258	-0.443	-0.017	-0.139	-0.099				
h	0.316										
i	0.032	0.312									
j	-3.879	-1.838	155.639								
k	0.024	-0.017	-0.404	0.022							

Covariance matrix for Group *laxiflora*

	a	b	c	d	e	f	g	h	i	j	k
a	149.361										
b	-16.532	26.370									
c	-5.826	1.392	7.737								
d	9.009	1.444	-2.090	12.883							
e	5.414	-10.294	-2.441	0.127	7.721						
f	19.608	-5.446	-1.830	4.191	1.742	6.252					
g	-17.630	4.503	-0.488	-1.161	-0.184	-2.462	3.376				
h	36.899	-7.002	-5.075	10.530	2.967	8.183	-5.084				
i	2.123	-1.558	-4.087	3.157	2.357	2.125	0.312				
j	-27.064	14.710	5.687	-4.343	-10.401	-4.619	3.441				
k	-7.805	2.229	2.064	-2.858	-0.294	-2.450	1.210				
h	18.326										
i	5.104	3.653									
j	-10.659	-3.887	29.545								
k	-3.861	-0.918	0.126	3.027							

Covariance matrix for Group *penicillata*

	a	b	c	d	e	f	g	h	i	j	k
a	7.664										
b	3.273	4.367									
c	-0.345	-5.026	20.008								
d	3.636	1.628	3.281	2.994							
e	0.070	0.062	-1.339	-0.448	0.208						
f	-0.198	-0.045	-0.343	-0.152	0.011	0.017					
g	0.785	0.301	-0.449	0.359	-0.020	0.011	0.190				
h	0.446	-0.459	3.577	1.071	-0.371	-0.055	0.057				
i	2.586	0.258	1.249	0.852	0.290	-0.150	-0.014				
j	1.996	0.218	0.555	0.587	0.126	-0.070	0.112				

k -7.993 -0.100 -12.664 -6.260 0.972 0.380 -0.781  
h 0.844  
i -0.065 2.218  
j 0.105 1.047 0.988  
k -3.062 -2.863 -2.310 17.390

**Covariance matrix for Group stenophylla**

	a	b	c	d	e	f	g	h	i	j	k
a	60.908										
b	-6.673	18.335									
c	-15.310	17.350	23.195								
d	11.273	-6.480	-12.045	16.809							
e	3.530	-2.681	-4.618	2.582	1.052						
f	-2.005	-1.155	-0.535	-0.402	0.018	1.129					
g	10.622	-11.078	-16.558	8.783	3.481	0.342	12.231				
h	-0.419	-0.048	0.235	-0.560	-0.075	0.050	-0.202				
i	6.972	-5.157	-9.013	7.247	2.020	-0.046	6.723				
j	22.551	57.362	71.613	-86.198	-12.638	-12.301	-51.306				
k	20.285	-19.831	-29.402	16.241	6.071	0.483	21.667				
h	0.032										
i	-0.227	4.386									
j	1.285	-36.650	809.708								
k	-0.351	11.888	-96.000	38.810							

**Summary of Classified Observations**

Observation	True Group	Pred Group	X-val Group	Group	Squared Distanc
1	bipinnata	bipinnata	bipinnata	bipinnata	3.74
				excelsa	516.72
				grandifolia	2445.71
				laxiflora	1675.11
				penicillata	777.04
				stenophylla	25.45
2	bipinnata	bipinnata	bipinnata	bipinnata	3.84
				excelsa	499.58
				grandifolia	2582.15
				laxiflora	1635.64
				penicillata	714.84
				stenophylla	26.44
3**	bipinnata	stenophylla	stenophylla	bipinnata	18.14
				excelsa	470.23
				grandifolia	2504.77
				laxiflora	1464.65
				penicillata	805.26
				stenophylla	12.09
4	bipinnata	bipinnata	bipinnata	bipinnata	3.50
				excelsa	519.39
				grandifolia	2570.24
				laxiflora	1531.40
				penicillata	716.92
				stenophylla	30.26
5	bipinnata	bipinnata	bipinnata	bipinnata	23.47
				excelsa	411.93
				grandifolia	2527.60
				laxiflora	1652.14
				penicillata	806.80
				stenophylla	54.89
6	bipinnata	bipinnata	bipinnata	bipinnata	7.48
				excelsa	586.53
				grandifolia	2488.51
				laxiflora	1723.26

				penicillata	779.46
				stenophylla	33.50
7	bipinnata	bipinnata	bipinnata	bipinnata	2.15
				excelsa	528.74
				grandifolia	2506.12
				laxiflora	1597.83
				penicillata	748.58
8**	bipinnata	stenophylla	stenophylla	stenophylla	29.32
				bipinnata	17.59
				excelsa	457.97
				grandifolia	2491.42
				laxiflora	1603.47
				penicillata	794.66
9	excelsa	excelsa	excelsa	stenophylla	8.80
				bipinnata	488.64
				excelsa	4.27
				grandifolia	2785.81
				laxiflora	1837.11
				penicillata	1354.42
10	excelsa	excelsa	excelsa	stenophylla	455.27
				bipinnata	485.64
				excelsa	13.91
				grandifolia	2929.44
				laxiflora	1749.18
				penicillata	1420.00
				stenophylla	449.81
11	excelsa	excelsa	excelsa	bipinnata	514.98
				excelsa	9.78
				grandifolia	2672.25
				laxiflora	1915.41
				penicillata	1372.92
				stenophylla	485.32
12	excelsa	excelsa	excelsa	bipinnata	500.10
				excelsa	5.83
				grandifolia	2673.31
				laxiflora	1869.86
				penicillata	1427.94
				stenophylla	465.05
13	grandifolia	grandifolia	grandifolia	bipinnata	2525.94
				excelsa	2766.63
				grandifolia	5.63
				laxiflora	4922.13
				penicillata	4816.86
				stenophylla	2561.58
14	grandifolia	grandifolia	grandifolia	bipinnata	2664.15
				excelsa	2912.64
				grandifolia	7.14
				laxiflora	4986.62
				penicillata	5063.21
				stenophylla	2703.93
15	grandifolia	grandifolia	grandifolia	bipinnata	2585.04
				excelsa	2837.89
				grandifolia	5.78
				laxiflora	4982.65
				penicillata	4969.31
				stenophylla	2614.24
16	grandifolia	grandifolia	grandifolia	bipinnata	2443.60
				excelsa	2685.56
				grandifolia	4.69
				laxiflora	4793.93
				penicillata	4811.34
				stenophylla	2470.23
17	grandifolia	grandifolia	grandifolia	bipinnata	2514.73
				excelsa	2772.01
				grandifolia	5.24
				laxiflora	4813.48

				penicillata	4814.36
				stenophylla	2551.20
18	grandifolia	grandifolia	grandifolia	bipinnata	2335.26
				excelsa	2607.09
				grandifolia	12.79
				laxiflora	4587.84
				penicillata	4530.65
				stenophylla	2374.99
19	penicillata	penicillata	penicillata	bipinnata	794.74
				excelsa	1444.53
				grandifolia	4908.85
				laxiflora	2258.01
				penicillata	6.66
				stenophylla	829.84
20	penicillata	penicillata	penicillata	bipinnata	751.86
				excelsa	1453.89
				grandifolia	4787.86
				laxiflora	2147.82
				penicillata	4.68
				stenophylla	790.97
21	penicillata	penicillata	penicillata	bipinnata	699.40
				excelsa	1298.42
				grandifolia	4647.36
				laxiflora	1907.58
				penicillata	10.71
				stenophylla	736.19
22	penicillata	penicillata	penicillata	bipinnata	827.24
				excelsa	1514.47
				grandifolia	5002.92
				laxiflora	2031.99
				penicillata	5.43
				stenophylla	862.89
23	penicillata	penicillata	penicillata	bipinnata	764.01
				excelsa	1332.26
				grandifolia	4843.82
				laxiflora	1984.92
				penicillata	3.03
				stenophylla	799.07
24	penicillata	penicillata	penicillata	bipinnata	745.12
				excelsa	1303.32
				grandifolia	4808.30
				laxiflora	1976.96
				penicillata	4.14
				stenophylla	780.78
25	stenophylla	stenophylla	stenophylla	bipinnata	28.45
				excelsa	420.85
				grandifolia	2632.25
				laxiflora	1629.72
				penicillata	822.12
				stenophylla	12.05
26	stenophylla	stenophylla	stenophylla	bipinnata	13.94
				excelsa	492.16
				grandifolia	2502.83
				laxiflora	1603.80
				penicillata	824.21
				stenophylla	5.34
27	stenophylla	stenophylla	stenophylla	bipinnata	19.15
				excelsa	420.84
				grandifolia	2566.75
				laxiflora	1580.08
				penicillata	811.86
				stenophylla	7.18
28	stenophylla	stenophylla	stenophylla	bipinnata	12.74
				excelsa	480.83
				grandifolia	2521.50
				laxiflora	1547.97

				penicillata	777.27
				stenophylla	5.59
29	stenophylla	stenophylla	stenophylla	bipinnata	38.20
				excelsa	502.88
				grandifolia	2615.86
				laxiflora	1643.38
				penicillata	722.19
				stenophylla	11.70
30	stenophylla	stenophylla	stenophylla	bipinnata	45.52
				excelsa	424.98
				grandifolia	2328.96
				laxiflora	1601.17
				penicillata	817.33
				stenophylla	24.44
31	stenophylla	stenophylla	stenophylla	bipinnata	37.42
				excelsa	484.04
				grandifolia	2652.67
				laxiflora	1605.34
				penicillata	851.42
				stenophylla	10.23
32	stenophylla	stenophylla	stenophylla	bipinnata	27.57
				excelsa	498.92
				grandifolia	2574.56
				laxiflora	1540.34
				penicillata	809.22
				stenophylla	5.63
33	laxiflora	laxiflora	laxiflora	bipinnata	1650.38
				excelsa	1809.04
				grandifolia	5061.22
				laxiflora	15.58
				penicillata	2042.74
				stenophylla	1629.46
34	laxiflora	laxiflora	laxiflora	bipinnata	1598.09
				excelsa	1860.00
				grandifolia	4599.83
				laxiflora	15.49
				penicillata	2176.46
				stenophylla	1581.25
35	laxiflora	laxiflora	laxiflora	bipinnata	1606.25
				excelsa	1880.00
				grandifolia	4879.66
				laxiflora	6.67
				penicillata	2033.21
				stenophylla	1595.37
36	laxiflora	laxiflora	laxiflora	bipinnata	1871.09
				excelsa	2138.12
				grandifolia	5143.70
				laxiflora	20.87
				penicillata	2272.57
				stenophylla	1862.62
37	laxiflora	laxiflora	laxiflora	bipinnata	1545.88
				excelsa	1777.10
				grandifolia	4649.66
				laxiflora	5.70
				penicillata	2096.74
				stenophylla	1533.61
38	laxiflora	laxiflora	laxiflora	bipinnata	1639.98
				excelsa	1879.67
				grandifolia	4889.19
				laxiflora	13.85
				penicillata	1984.07
				stenophylla	1620.14
39	laxiflora	laxiflora	laxiflora	bipinnata	1569.03
				excelsa	1784.18
				grandifolia	4812.66
				laxiflora	3.09

40	laxiflora	laxiflora	laxiflora	penicillata	2032.48
				stenophylla	1547.47
				bipinnata	1540.31
				excelsa	1827.71
				grandifolia	4888.51
				laxiflora	18.37
41	laxiflora	laxiflora	laxiflora	penicillata	1981.14
				stenophylla	1522.13
				bipinnata	1522.43
				excelsa	1718.17
				grandifolia	4766.76
				laxiflora	9.23
42	laxiflora	laxiflora	laxiflora	penicillata	1926.17
				stenophylla	1504.00
				bipinnata	1585.27
				excelsa	1794.67
				grandifolia	4842.02
				laxiflora	15.39
				penicillata	2033.01
				stenophylla	1565.24

Observation	X-val	Probability	
		Pred	X-val
1	5.39	1.00	1.00
	511.09	0.00	0.00
	2404.38	0.00	0.00
	1682.40	0.00	0.00
	760.02	0.00	0.00
	25.92	0.00	0.00
2	5.55	1.00	1.00
	487.55	0.00	0.00
	2568.66	0.00	0.00
	1603.59	0.00	0.00
	708.54	0.00	0.00
	27.12	0.00	0.00
3**	54.33	0.05	0.00
	457.18	0.00	0.00
	2441.31	0.00	0.00
	1675.85	0.00	0.00
	860.83	0.00	0.00
	14.65	0.95	1.00
4	4.99	1.00	1.00
	514.99	0.00	0.00
	2540.35	0.00	0.00
	1526.16	0.00	0.00
	709.23	0.00	0.00
	31.68	0.00	0.00
5	116.95	1.00	1.00
	487.12	0.00	0.00
	2522.83	0.00	0.00
	1777.31	0.00	0.00
	942.71	0.00	0.00
	165.13	0.00	0.00
6	12.46	1.00	1.00
	682.04	0.00	0.00
	2420.13	0.00	0.00
	1847.18	0.00	0.00
	766.31	0.00	0.00
	38.10	0.00	0.00
7	2.93	1.00	1.00
	528.65	0.00	0.00
	2436.62	0.00	0.00
	1553.44	0.00	0.00
	728.22	0.00	0.00
	30.10	0.00	0.00

8**	50.61	0.01	0.00
	448.36	0.00	0.00
	2422.55	0.00	0.00
	1566.36	0.00	0.00
	824.12	0.00	0.00
	9.90	0.99	1.00
9	475.24	0.00	0.00
	8.76	1.00	1.00
	2720.30	0.00	0.00
	1786.59	0.00	0.00
	1324.41	0.00	0.00
	442.81	0.00	0.00
10	474.25	0.00	0.00
	49.59	1.00	1.00
	3494.53	0.00	0.00
	1795.14	0.00	0.00
	1424.29	0.00	0.00
	438.60	0.00	0.00
11	518.83	0.00	0.00
	26.48	1.00	1.00
	2676.83	0.00	0.00
	1978.41	0.00	0.00
	1334.88	0.00	0.00
	494.06	0.00	0.00
12	489.54	0.00	0.00
	12.84	1.00	1.00
	2668.22	0.00	0.00
	1837.45	0.00	0.00
	1415.15	0.00	0.00
	454.88	0.00	0.00
13	2463.04	0.00	0.00
	2692.17	0.00	0.00
	9.71	1.00	1.00
	4860.69	0.00	0.00
	4683.30	0.00	0.00
	2498.29	0.00	0.00
14	2885.58	0.00	0.00
	3114.25	0.00	0.00
	13.11	1.00	1.00
	5096.49	0.00	0.00
	5549.96	0.00	0.00
	2943.02	0.00	0.00
15	2587.86	0.00	0.00
	2834.84	0.00	0.00
	10.01	1.00	1.00
	5062.61	0.00	0.00
	5050.08	0.00	0.00
	2607.22	0.00	0.00
16	2406.15	0.00	0.00
	2653.44	0.00	0.00
	7.78	1.00	1.00
	4677.93	0.00	0.00
	4678.94	0.00	0.00
	2441.23	0.00	0.00
17	2447.21	0.00	0.00
	2699.14	0.00	0.00
	8.89	1.00	1.00
	4684.60	0.00	0.00
	4681.22	0.00	0.00
	2483.27	0.00	0.00
18	2616.41	0.00	0.00
	2799.29	0.00	0.00
	31.22	1.00	1.00
	5275.74	0.00	0.00
	5543.73	0.00	0.00
	2632.63	0.00	0.00



19	792.32	0.00	0.00
	1449.51	0.00	0.00
	4853.32	0.00	0.00
	2695.78	0.00	0.00
	11.98	1.00	1.00
	825.44	0.00	0.00
20	730.99	0.00	0.00
	1464.94	0.00	0.00
	4666.53	0.00	0.00
	2198.19	0.00	0.00
	7.77	1.00	1.00
	769.02	0.00	0.00
21	708.81	0.00	0.00
	1335.59	0.00	0.00
	4879.54	0.00	0.00
	2058.27	0.00	0.00
	23.31	1.00	1.00
	743.91	0.00	0.00
22	859.50	0.00	0.00
	1651.45	0.00	0.00
	5187.87	0.00	0.00
	1976.18	0.00	0.00
	9.29	1.00	1.00
	893.30	0.00	0.00
23	743.53	0.00	0.00
	1317.86	0.00	0.00
	4712.68	0.00	0.00
	1959.57	0.00	0.00
	4.72	1.00	1.00
	777.44	0.00	0.00
24	725.13	0.00	0.00
	1324.18	0.00	0.00
	4676.84	0.00	0.00
	1960.95	0.00	0.00
	6.73	1.00	1.00
	759.90	0.00	0.00
25	34.21	0.00	0.01
	415.50	0.00	0.00
	2697.32	0.00	0.00
	1626.60	0.00	0.00
	819.27	0.00	0.00
	24.80	1.00	0.99
26	13.58	0.01	0.06
	494.94	0.00	0.00
	2442.23	0.00	0.00
	1565.26	0.00	0.00
	812.94	0.00	0.00
	8.16	0.99	0.94
27	19.38	0.00	0.02
	416.65	0.00	0.00
	2507.53	0.00	0.00
	1536.32	0.00	0.00
	795.48	0.00	0.00
	11.80	1.00	0.98
28	12.39	0.03	0.13
	476.49	0.00	0.00
	2452.82	0.00	0.00
	1513.49	0.00	0.00
	756.88	0.00	0.00
	8.63	0.97	0.87
29	49.95	0.00	0.00
	531.88	0.00	0.00
	2639.15	0.00	0.00
	1660.28	0.00	0.00
	746.75	0.00	0.00
	23.64	1.00	1.00

30	138.70	0.00	0.48
	414.42	0.00	0.00
	3452.78	0.00	0.00
	1617.18	0.00	0.00
	872.65	0.00	0.00
	138.57	1.00	0.52
31	46.69	0.00	0.00
	487.84	0.00	0.00
	2753.94	0.00	0.00
	1572.35	0.00	0.00
	879.76	0.00	0.00
	19.23	1.00	1.00
32	29.09	0.00	0.00
	507.75	0.00	0.00
	2518.88	0.00	0.00
	1510.93	0.00	0.00
	790.75	0.00	0.00
	8.71	1.00	1.00
33	1666.54	0.00	0.00
	1760.19	0.00	0.00
	5724.71	0.00	0.00
	36.02	1.00	1.00
	1988.40	0.00	0.00
	1638.54	0.00	0.00
34	1556.18	0.00	0.00
	1832.54	0.00	0.00
	5203.28	0.00	0.00
	35.60	1.00	1.00
	2424.41	0.00	0.00
	1539.77	0.00	0.00
35	1563.11	0.00	0.00
	1853.55	0.00	0.00
	4763.62	0.00	0.00
	10.09	1.00	1.00
	1977.03	0.00	0.00
	1554.23	0.00	0.00
36	3609.78	0.00	0.00
	4298.29	0.00	0.00
	7208.48	0.00	0.00
	70.35	1.00	1.00
	3505.50	0.00	0.00
	3704.69	0.00	0.00
37	1524.68	0.00	0.00
	1752.02	0.00	0.00
	4833.86	0.00	0.00
	8.30	1.00	1.00
	2068.08	0.00	0.00
	1508.95	0.00	0.00
38	1631.78	0.00	0.00
	1873.19	0.00	0.00
	4804.00	0.00	0.00
	29.05	1.00	1.00
	1958.54	0.00	0.00
	1608.28	0.00	0.00
39	1532.10	0.00	0.00
	1753.07	0.00	0.00
	4684.22	0.00	0.00
	4.10	1.00	1.00
	1976.83	0.00	0.00
	1513.59	0.00	0.00
40	1527.75	0.00	0.00
	1779.28	0.00	0.00
	4828.13	0.00	0.00
	50.91	1.00	1.00
	1962.65	0.00	0.00
	1512.19	0.00	0.00

41	1529.78	0.00	0.00
	1790.63	0.00	0.00
	4678.55	0.00	0.00
	15.48	1.00	1.00
	1999.67	0.00	0.00
	1514.32	0.00	0.00
42	1541.24	0.00	0.00
	1753.32	0.00	0.00
	4711.41	0.00	0.00
	35.18	1.00	1.00
	1976.66	0.00	0.00
	1521.89	0.00	0.00

## HPLC Data &amp; PCA

	A4	A3	A2	A1	B1	B2	B3	B4	B5	B6	B7	B8
11a1	0.0233	0.0067	0.0157	0.397	0	0	0	0.1517	0.0141	0	0.0037	0
11b2	0.0128	0.0012	0.0171	0.3851	0	0	0	0.0755	0.0104	0	0.0134	0
11b3	0.0169	0.0105	0.0406	0.3192	0	0	0	0.1048	0.0118	0	0.0136	0
11c1	0.0384	0.0341	0.0199	0.3219	0	0	0	0.0304	0.0338	0	0.0352	0
11c2	0.027	0.0368	0.0345	0.3498	0	0	0	0.0528	0.0058	0	0.0052	0
11c3	0.0189	0.0784	0.0452	0.2616	0	0	0	0.0759	0.0129	0	0.016	0
11d1	0.0055	0.0097	0.0152	0.3347	0	0	0	0.222	0.0309	0	0.0391	0
11d2	0.0187	0.0068	0.0255	0.2287	0	0	0	0.1536	0.0156	0	0.0062	0
11d3	0.011	0.0074	0.0172	0.4593	0	0	0	0.1409	0.0153	0	0.0032	0
11e1	0.009	0.0013	0.0149	0.2093	0	0	0	0.308	0.0092	0	0.0057	0
27a2	0	0.0626	0	0.3859	0.3068	0	0	0	0.0285	0.0285	0	0.0198
27a3	0	0.0071	0	0.0506	0.869	0	0	0	0.0136	0.0136	0	0.0076
27a4	0	0.0676	0	0.4568	0.158	0	0	0	0.0506	0.0506	0	0.0438
27a1Q	0	0.145	0	0.4333	0.2092	0	0	0	0.0208	0.0208	0	0.0086
47a1	0.0221	0.0391	0.1012	0.1194	0.3672	0.2217	0	0	0	0	0	0.0545
47a2	0.0378	0.0653	0.1766	0.1005	0.2543	0.1932	0	0	0	0	0	0.0574
47b2	0	0	0.1698	0.0947	0.4557	0.0663	0	0	0	0	0	0.0376
47b3	0	0	0.2187	0.0004	0.7047	0.0353	0	0	0	0	0	0.0196
47b4	0	0	0.2848	0.022	0.5264	0.0206	0	0	0	0	0	0.0664
47b5	0	0	0.2334	0.0283	0.5934	0.0613	0	0	0	0	0	0.0492
47b6	0	0	0.0491	0.016	0.1293	0.6986	0	0	0	0	0	0.061
47c1	0.1104	0.1402	0.1709	0.5217	0.0251	0	0	0	0	0	0	0
47ee1	0.0766	0.0365	0.1023	0.3304	0.3864	0.0166	0	0	0	0	0	0.0334
47f1	0.0386	0.094	0.0535	0.2543	0.3446	0.0596	0	0	0	0	0	0.0762
47a1Q	0.021	0.0253	0.153	0.0861	0.357	0.2069	0	0	0	0	0	0.0461
47b1Q	0	0	0.4468	0.0628	0.0893	0.0893	0	0	0	0	0	0.0708
63a1	0	0	0	0.2158	0.2558	0	0.1093	0.0662	0.2312	0	0	0
63a2	0	0	0	0.1685	0.2507	0	0.1249	0.0791	0.2201	0	0	0
63a3	0	0	0	0.2085	0.2043	0	0.0965	0.0553	0.1906	0	0	0
63a4	0	0	0	0.1916	0.1839	0	0.1004	0.0809	0.1695	0	0	0
63a1Q	0	0	0	0.2832	0.2694	0	0.0839	0.026	0.2118	0	0	0
63b1Q	0	0	0	0.3657	0.218	0	0.0876	0.0536	0.1955	0	0	0
72a1	0.105	0.0251	0.0114	0.1732	0	0	0	0.1363	0	0	0	0
72a2	0.0549	0.0292	0.0377	0.1481	0	0	0	0.1385	0	0	0	0
72b1	0.0917	0.0233	0.0301	0.1181	0	0	0	0.1105	0	0	0	0
72b2	0.0422	0.0378	0.0297	0.2469	0	0	0	0.2578	0	0	0	0
72c1	0.1024	0.0056	0.0156	0.1793	0	0	0	0.0278	0	0	0	0
72d1	0.0887	0.0225	0.0114	0.1967	0	0	0	0.0432	0	0	0	0
72d2	0.0899	0.0176	0.0172	0.2691	0	0	0	0.0277	0	0	0	0
72c2	0.1349	0.0315	0.0465	0.2876	0	0	0	0.063	0	0	0	0

**Table 43 HPLC data of peaks corresponding to non triterpenic compounds in botanical certified resins and archaeological resins used in PCA**

## HPLC Data &amp; PCA

	A4	A3	A2	A1	B1	B2	B3	B4	B5	B6	B7	B8
<b>51</b>	0.0475	0	0.0179	0.0146	0	0	0	0.0238	0	0	0.3021	0.0681
<b>52</b>	0.0191	0.0031	0.0054	0.1141	0	0	0	0.0479	0	0	0.0506	0.0336
<b>TMT</b>	0.266	0	0	0.0125	0	0	0	0.0552	0	0	0.0292	0.0187
<b>Chichén Itzá</b>	0.0905	0.0318	0.0227	0.0211	0.0201	0.0878	0	0.0184	0.0373	0	0.0522	0.0136
<b>26</b>	0.0792	0.0069	0.0048	0.0404	0	0	0	0.0169	0	0	0.0203	0.0469
<b>84</b>	0.0298	0	0	0.1056	0	0	0	0	0.0247	0	0.0102	0.0526
<b>173</b>	0.0723	0.0061	0	0.0065	0	0	0	0.002	0	0	0	0

**Table 44 HPLC data of peaks corresponding to non triterpenic compounds in botanical certified resins and archaeological resins used in PCA**

## HPLC Data &amp; PCA

	T3	Epi lupeol	lupeol	Epi $\beta$ amyrina	lupenone	Epi $\alpha$ amyrin	$\beta$ amyrin	$\alpha$ amyrin/ $\beta$ amyrona	$\alpha$ amyrona	T1
11a1	0	0.1433	0.0084	0.0075	0.06054	0.01501	0.06394	0.0801	0.009	0
11b2	0	0.1853	0.0081	0.0072	0.07902	0.01955	0.07931	0.0996	0.0065	0
11b3	0	0.1874	0.0102	0.0126	0.07763	0.02161	0.07785	0.0914	0.0038	0
11c1	0	0.1969	0.0138	0.0118	0.07692	0.02279	0.08119	0.0774	0.0055	0
11c2	0	0.1909	0.006	0.01	0.07642	0.02043	0.08088	0.1005	0.0029	0
11c3	0	0.1907	0.0104	0.0128	0.07899	0.02199	0.07922	0.093	0.0039	0
11d1	0	0.1186	0.0036	0.0066	0.05596	0.01364	0.06611	0.0669	0.0115	0
11d2	0	0.1873	0.0134	0.0119	0.0859	0.022	0.08975	0.1187	0.016	0
11d3	0	0.1089	0.007	0.0066	0.06017	0.01463	0.0625	0.0859	0	0
11ee1	0	0.1382	0.0061	0.0106	0.07508	0.01783	0.1055	0.0724	0.017	0
27a2	0.0199	0.0695	0.0588	0	0.01031	0	0.00944	0	0	0
27a3	0.0102	0.0157	0.0054	0	0.0059	0	0.00029	0	0.001	0
27a4	0.0506	0.062	0.0245	0	0.03374	0	0.00128	0	0.0004	0
27a1Q	0.0138	0.0757	0.0526	0	0.00834	0	0.01142	0	0.0004	0
47a1	0	0.0313	0.0051	0.008	0.01681	0	0.00338	0.0026	0.0076	0
47a2	0	0.0453	0.0333	0	0.01028	0	0.01306	0.0083	0.0047	0
47b2	0	0.0062	0.139	0.0066	0.00463	0.00966	0.002	0.0011	0.0066	0
47b3	0	0.0085	0.0073	0	0.00199	0	0.00284	0.0007	7E-05	0
47b4	0	0.0508	0.0083	0.0079	0.0075	0	0.00507	0	0.0002	0
47b5	0	0.0296	0.0021	0	0.00275	0	0	0	0	0
47b6	0	0.0404	0.002	0	0.00201	0	0	0	0.0016	0
47c1	0	0.0117	0.0114	0	0.00289	0.00055	0.00372	0	0.0014	0
47ee1	0	0.0006	0.0062	0	0.00098	0	0	0.0057	0.0044	0
47f1	0	0.0415	0.0103	0	0.00847	0	0.01116	0.0053	0.0025	0
47a1Q	0	0.0612	0.0271	0.0038	0.00522	0.00341	0.00136	0.0002	0.0022	0
47b1Q	0	0.1613	0.0302	0.0141	0.01434	0.00745	0.00419	0.0055	0.0039	0
63a1	0	0.0031	0.0026	0.0054	0.01488	0.00621	0.0082	0.0551	0.0264	0
63a2	0	0.0031	0.0025	0.0048	0.01672	0.00529	0.00716	0.0887	0.0284	0
63a3	0	0.0188	0.0387	0.0208	0.02135	0.01536	0.07256	0.0312	0.0261	0
63a4	0	0.0171	0.0366	0.046	0.0261	0.01477	0.01941	0.0755	0.0382	0

63a1Q	0	0.0061	0.0161	0.0181	0.01032	0.00831	0.00907	0.0317	0.026	0
63b1Q	0	0.0008	0.0016	0.0101	0.00453	0.00373	0.00228	0.0297	0.0267	0
72a1	0.0647	0.1593	0.02	0.0189	0.06751	0.02481	0.103	0.0612	0.0272	0.0022
	<b>T3</b>	<b>Epi lupeol</b>	<b>lupeol</b>	<b>Epi <math>\beta</math>amyrina</b>	<b>lupenone</b>	<b>Epi <math>\alpha</math>amyrin</b>	<b><math>\beta</math> amyrin</b>	<b><math>\alpha</math>amyrin/<math>\beta</math> amyrona</b>	<b><math>\alpha</math> amyrona</b>	<b>T1</b>
72a2	0.0271	0.2145	0.0141	0.0139	0.0838	0.02599	0.08323	0.1064	0.0113	0.0113
72b1	0.0216	0.226	0.022	0.0184	0.0778	0.03036	0.10866	0.0688	0.0263	0.0263
72b2	0.0315	0.0193	0.0112	0.0136	0.0819	0.02331	0.09656	0.0745	0.0169	0.0169
72c1	0.0013	0.272	0.0192	0.0041	0.09463	0.02175	0.12298	0.0986	0.0276	0.0072
72d1	0.0469	0.1998	0.025	0.0203	0.08103	0.03186	0.10288	0.0893	0.0203	0.0203
72d2	0.042	0.1926	0.0299	0.0134	0.07321	0.0272	0.08268	0.0857	0.0212	0.0107
72c2	0.0709	0.1926	0.0207	0.0137	0.05241	0.01822	0.05702	0.0633	0.0199	0.0089
51	0	0.1797	0.0199	0	0.06983	0.02434	0.06022	0.1034	0.0168	0.0347
52	0	0.3122	0.0314	0	0.09262	0.02435	0.05261	0.1528	0.0068	0.0041
TMT	0	0.2878	0.0206	0	0.08422	0.01833	0.05112	0.1563	0	0
Chichén Itzá	0	0.0328	0	0.0164	0.01759	0	0.14822	0.0255	0.1482	0.2321
26	0	0.2978	0.022	0.0126	0.10526	0.02753	0.07452	0.1858	0.0043	0.0521
84	0	0.3049	0.0215	0.0299	0.09856	0.02619	0.07091	0.1537	0.0036	0.0357
173	0	0.3344	0.0224	0	0.12263	0.03345	0.09979	0.2032	0.0184	0.0458

Table 45 HPLC data of peaks corresponding to non triterpenic compounds in botanical certified resins and archaeological resins used in PCA

## HPLC Data &amp; PCA

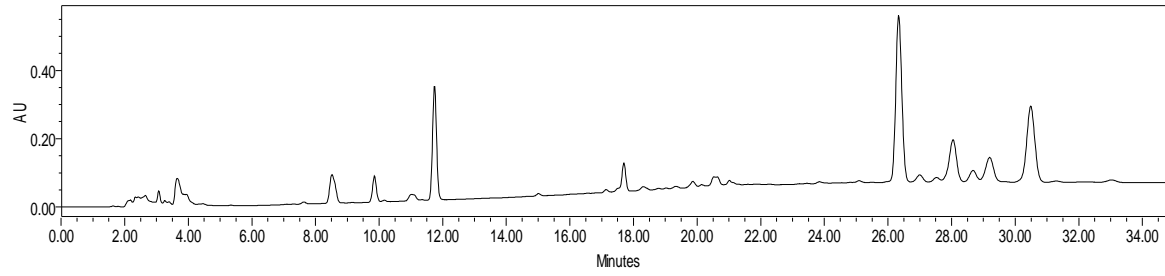
<b>I.D.</b>	<b>Actual Species</b>	<b>Fitting Matrix</b>	<b>Confusion Matrix</b>
11a1	<i>B. bipinnata</i>	<i>bipinnata</i>	<i>bipinnata</i>
11b2	<i>B. bipinnata</i>	<i>bipinnata</i>	<i>bipinnata</i>
11b3	<i>B. bipinnata</i>	<i>bipinnata</i>	<i>bipinnata</i>
11c1	<i>B. bipinnata</i>	<i>bipinnata</i>	<i>bipinnata</i>
11c2	<i>B. bipinnata</i>	<i>bipinnata</i>	<i>bipinnata</i>
11c3	<i>B. bipinnata</i>	<i>bipinnata</i>	<i>bipinnata</i>
11d1	<i>B. bipinnata</i>	<i>bipinnata</i>	<i>bipinnata</i>
11d2	<i>B. bipinnata</i>	<i>bipinnata</i>	<i>bipinnata</i>
11d3	<i>B. bipinnata</i>	<i>bipinnata</i>	<i>bipinnata</i>
11e1	<i>B. bipinnata</i>	<i>bipinnata</i>	<i>bipinnata</i>
27a2	<i>B. excelsa</i>	<i>excelsa</i>	<i>excelsa</i>
27a3	<i>B. excelsa</i>	<i>excelsa</i>	<i>laxiflora</i>
27a4	<i>B. excelsa</i>	<i>excelsa</i>	<i>excelsa</i>
27a1Q	<i>B. excelsa</i>	<i>excelsa</i>	<i>excelsa</i>
47a1	<i>B. laxiflora</i>	<i>laxiflora</i>	<i>laxiflora</i>
47a2	<i>B. laxiflora</i>	<i>laxiflora</i>	<i>laxiflora</i>
47b2	<i>B. laxiflora</i>	<i>laxiflora</i>	<i>laxiflora</i>
47b3	<i>B. laxiflora</i>	<i>laxiflora</i>	<i>laxiflora</i>
47b4	<i>B. laxiflora</i>	<i>laxiflora</i>	<i>laxiflora</i>
47b5	<i>B. laxiflora</i>	<i>laxiflora</i>	<i>laxiflora</i>
47b6	<i>B. laxiflora</i>	<i>laxiflora</i>	<i>laxiflora</i>
47c1	<i>B. laxiflora</i>	<i>laxiflora</i>	<i>laxiflora</i>
47e1	<i>B. laxiflora</i>	<i>laxiflora</i>	<i>laxiflora</i>
47f1	<i>B. laxiflora</i>	<i>laxiflora</i>	<i>laxiflora</i>
47a1Q	<i>B. laxiflora</i>	<i>laxiflora</i>	<i>laxiflora</i>
47b1Q	<i>B. laxiflora</i>	<i>laxiflora</i>	<i>laxiflora</i>
63a1	<i>B. penicillata</i>	<i>penicillata</i>	<i>penicillata</i>
63a2	<i>B. penicillata</i>	<i>penicillata</i>	<i>penicillata</i>
63a3	<i>B. penicillata</i>	<i>penicillata</i>	<i>penicillata</i>
63a4	<i>B. penicillata</i>	<i>penicillata</i>	<i>penicillata</i>
63a1Q	<i>B. penicillata</i>	<i>penicillata</i>	<i>penicillata</i>
63b1Q	<i>B. penicillata</i>	<i>penicillata</i>	<i>penicillata</i>
72a1	<i>B. stenophylla</i>	<i>stenophylla</i>	<i>stenophylla</i>
72a2	<i>B. stenophylla</i>	<i>stenophylla</i>	<i>bipinnata</i>
72b1	<i>B. stenophylla</i>	<i>stenophylla</i>	<i>stenophylla</i>
72b2	<i>B. stenophylla</i>	<i>stenophylla</i>	<i>stenophylla</i>
72c1	<i>B. stenophylla</i>	<i>stenophylla</i>	<i>stenophylla</i>
72d1	<i>B. stenophylla</i>	<i>stenophylla</i>	<i>stenophylla</i>
72d2	<i>B. stenophylla</i>	<i>stenophylla</i>	<i>stenophylla</i>
72c2	<i>B. stenophylla</i>	<i>stenophylla</i>	<i>stenophylla</i>

Table 46 LDA results with HPLC data for certified samples: fitting and confusion matrix

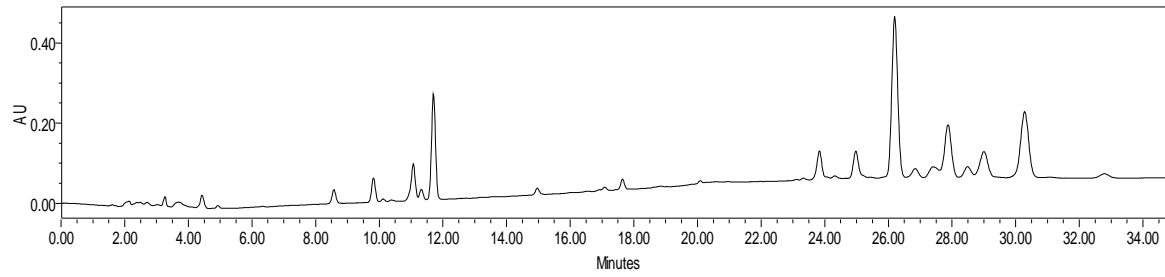


## Chromatograms of Commercial Samples

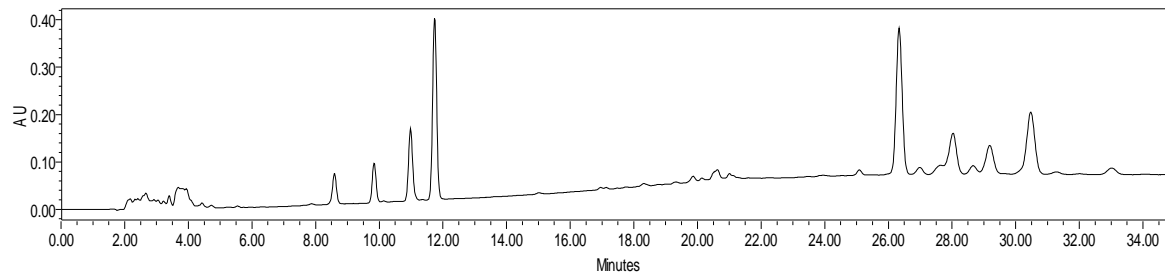
ATZB1 C= 1.75mg/mL



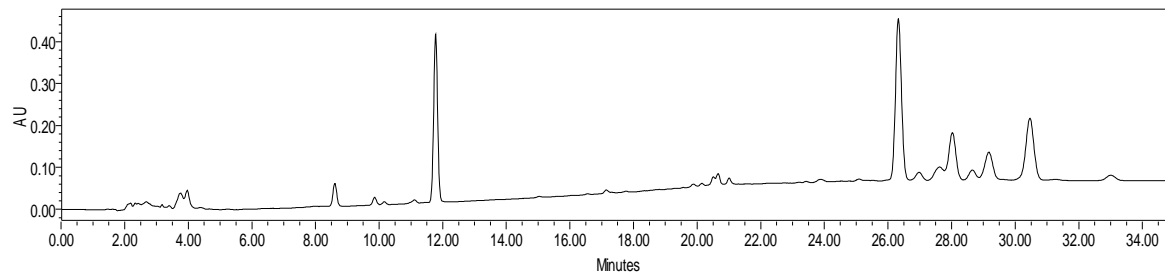
ATZM1 C= 1.75mg/mL



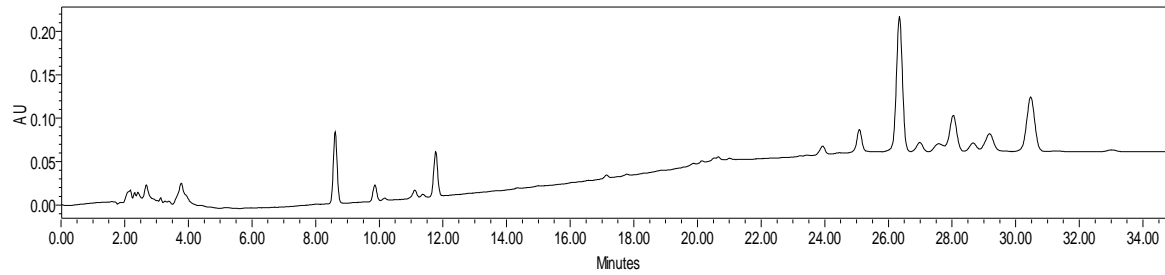
CHOB1 C= 3 mg/mL



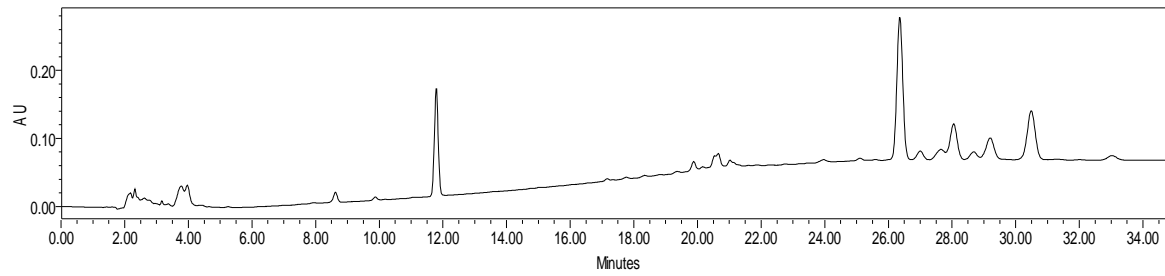
CHOB2 C= 3 mg/mL



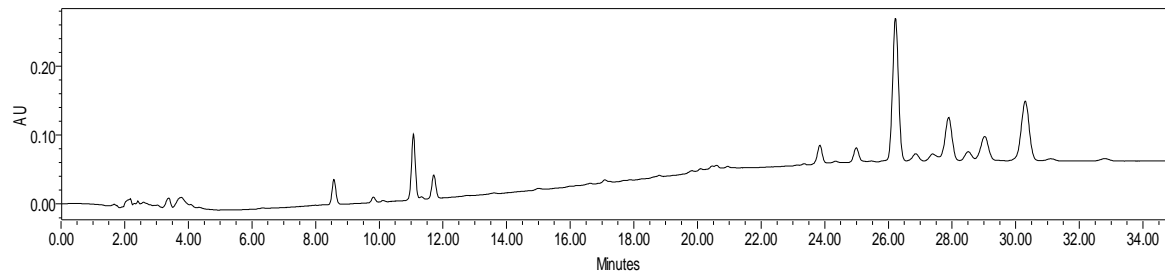
CHOB3 C= 2 mg/mL



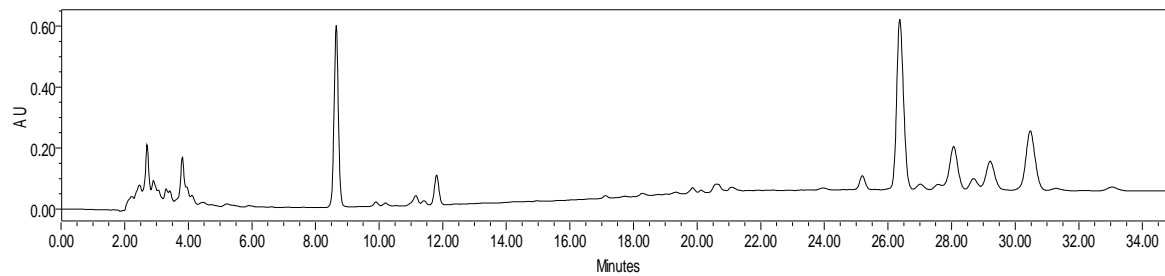
CHOB4 C= 3.5 mg/mL



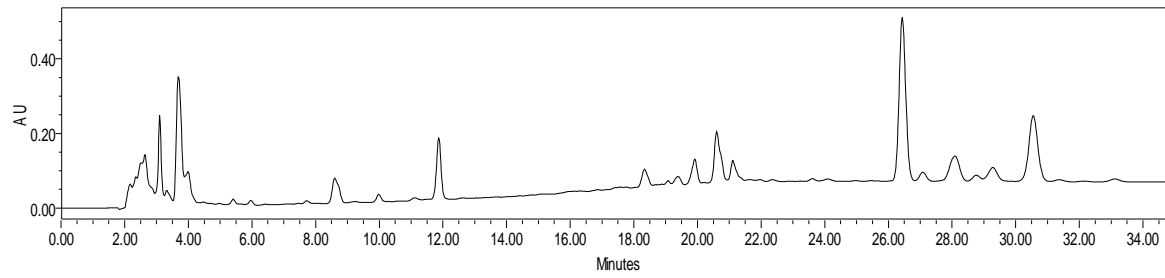
CHOM1 C= 2.5 mg/mL



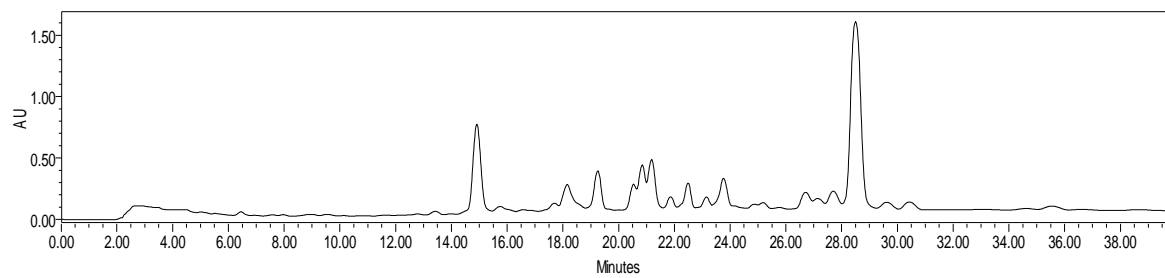
Sidral C= 2.4 mg/mL



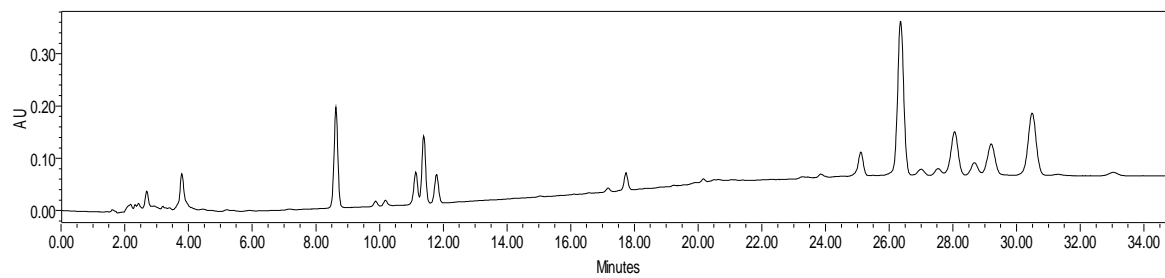
Huitzucó C= 2.8 mg/mL



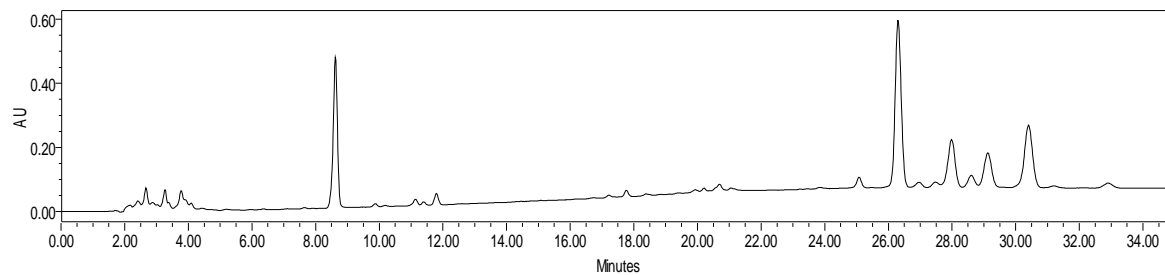
Incienso C= 14mg/mL



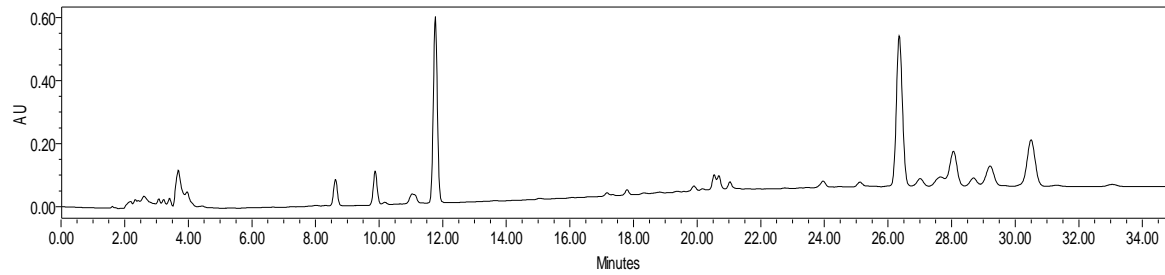
IZUB2 C= 2mg/mL



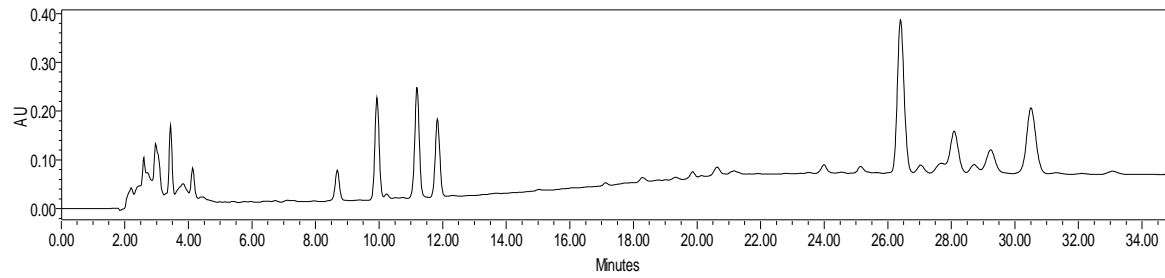
IZUM1 C= 3mg/mL



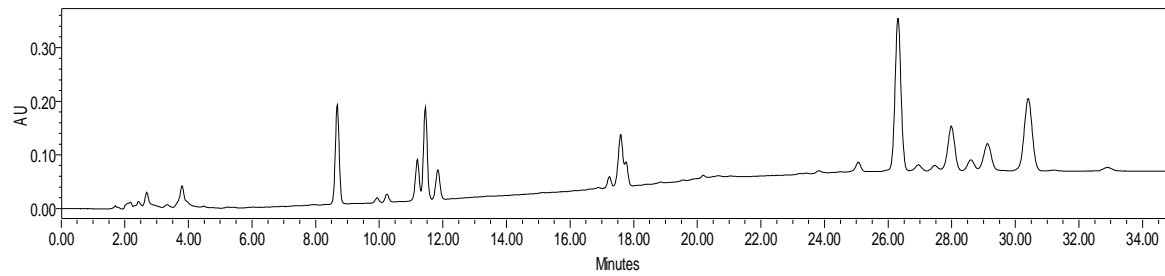
IZUP1 C= 5mg/mL



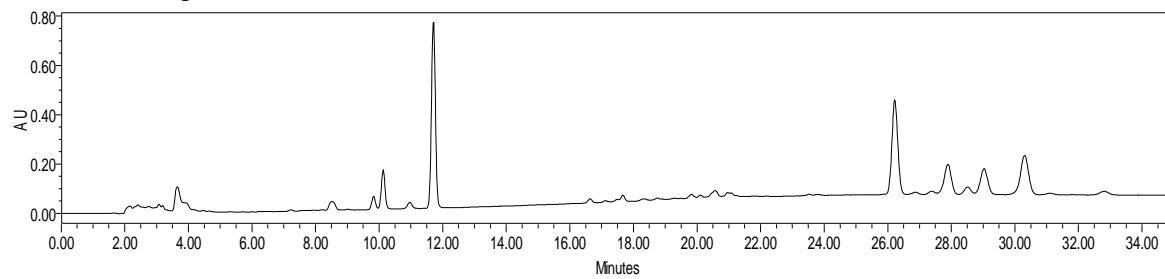
SONB2 C= 2.1mg/mL



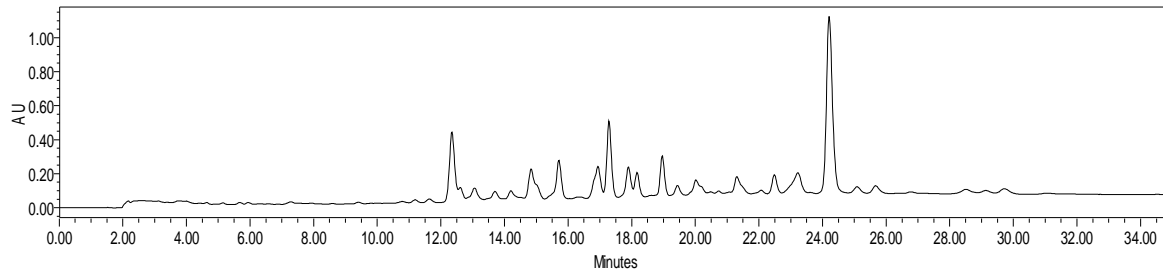
SONB3 C= 2mg/mL



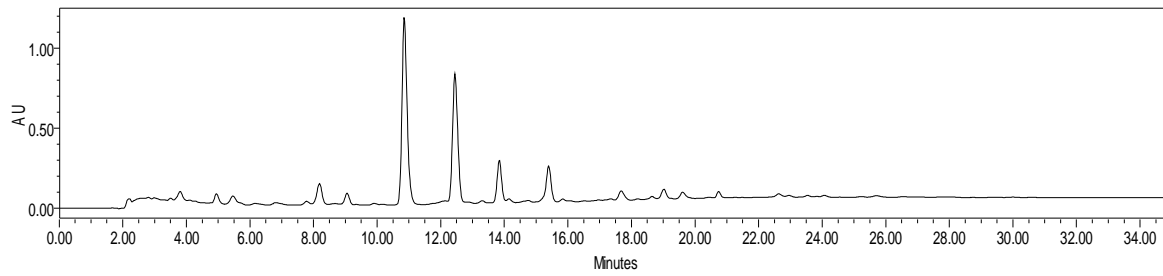
SONR1 C= 5mg/mL



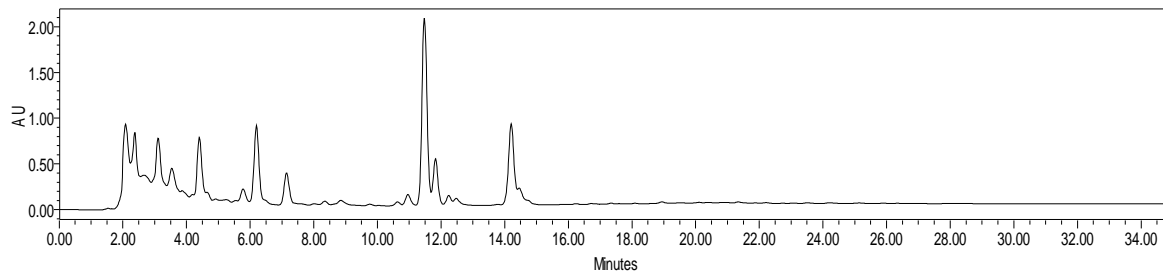
Oaxc1 C= 8mg/2mL



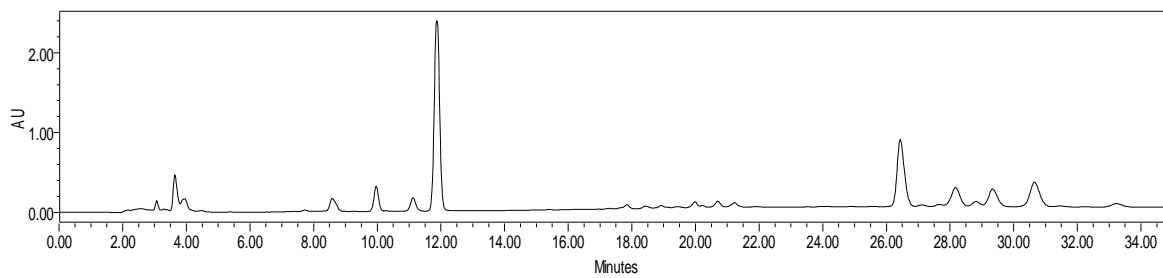
Oaxc2 C = 3.25 mg/mL



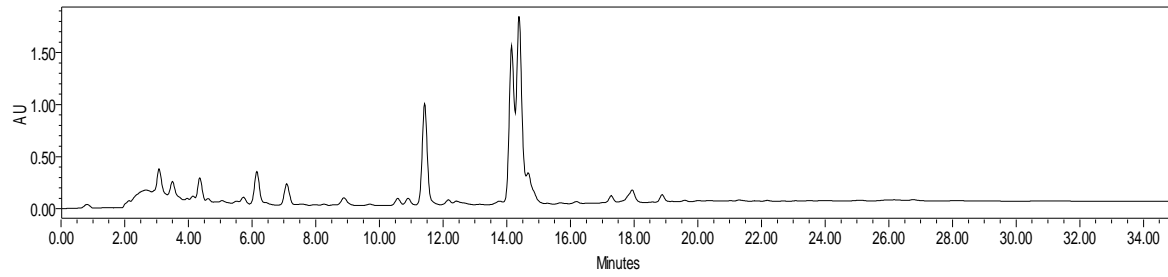
Oaxc3 C = 3mg/mL



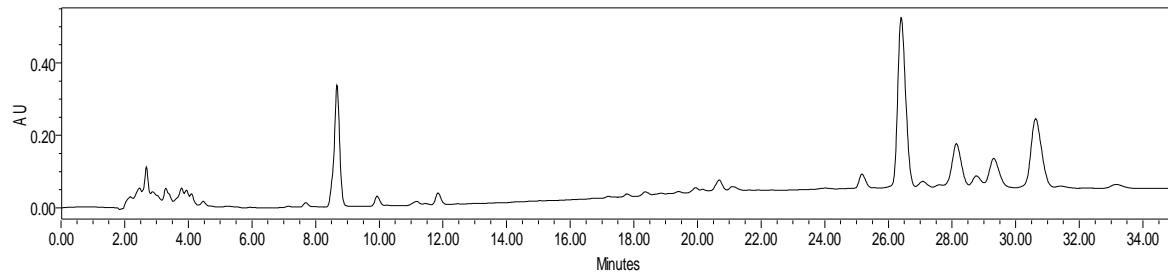
Colima L1 C = 4mg/mL



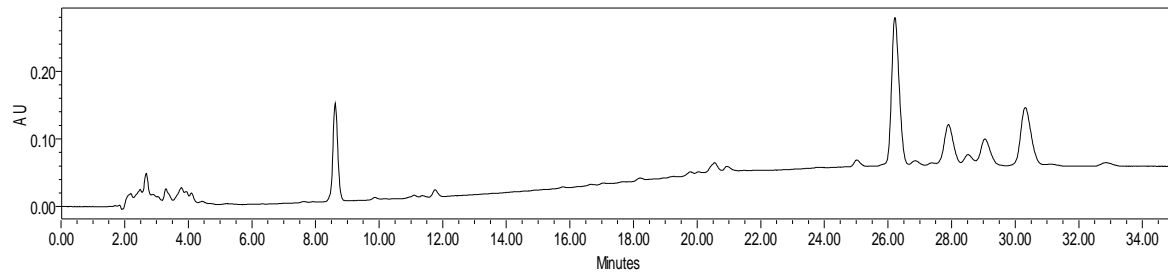
Colima L2 C = 8mg/mL



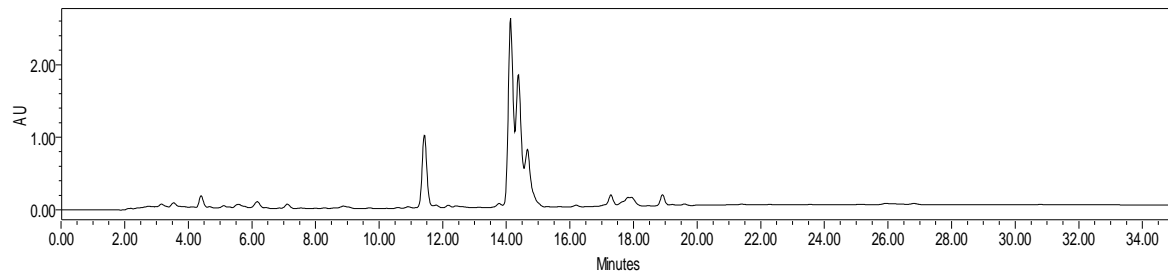
M6 C = 1.5mg/mL



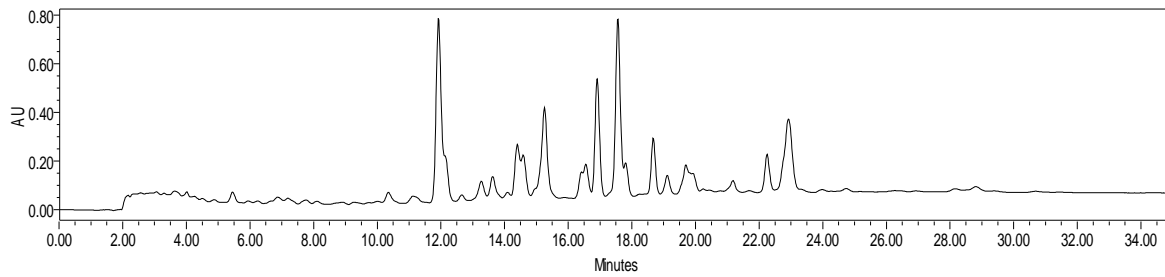
M6Q C = 1.5mg/mL



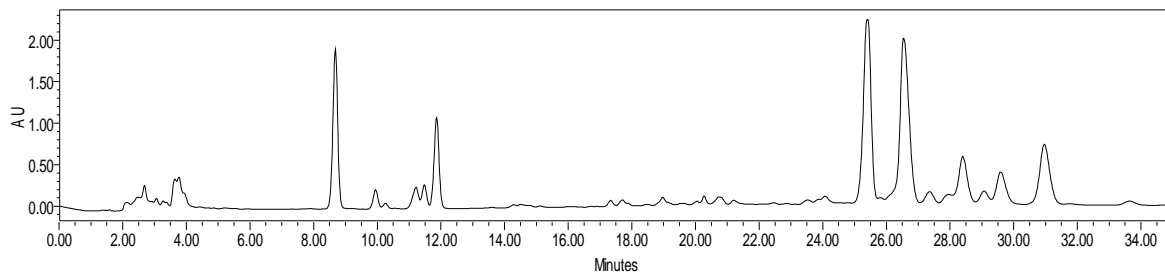
ATZB2 C = 3mg/mL



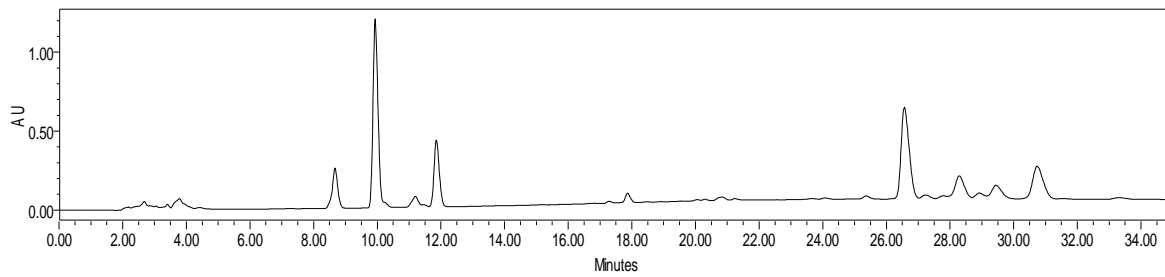
ATZJ2 C = 2.5mg/mL



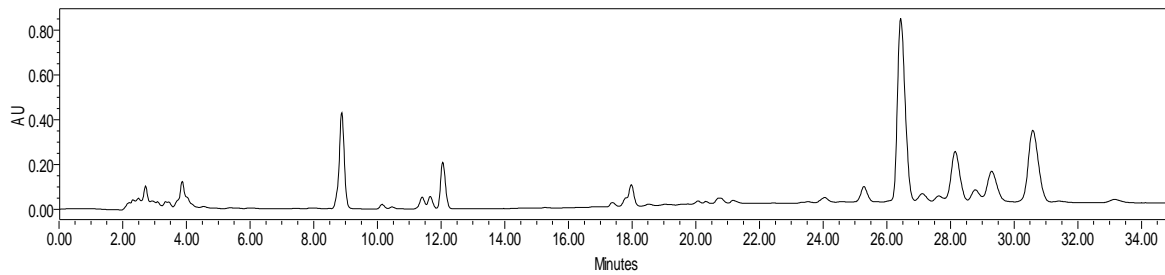
SONR2 C = 30 mg/mL



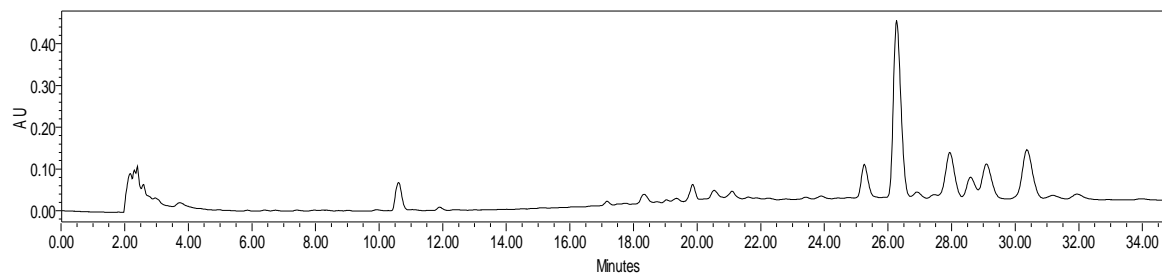
SONB4 C = 2.5mg/mL



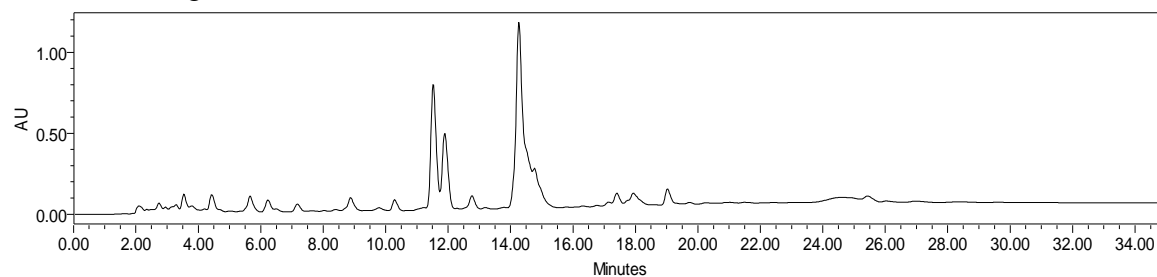
MEXB1 C = 2.5 mg/mL



MEXJ1 C= 3.5 mg/mL

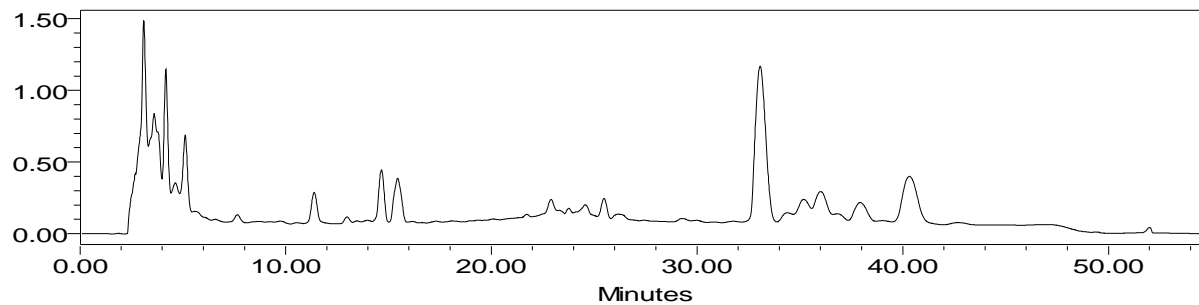


MEXM1 C= 3mg/mL

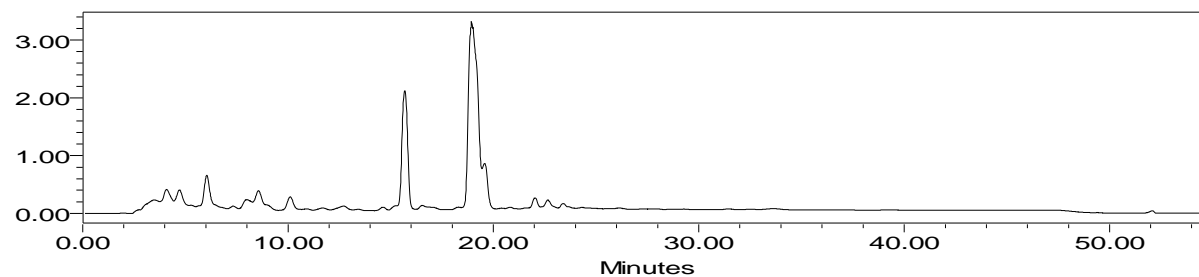


**Samples analyzed after the installation of the automatic injector under HPLC gradient number 2**

CHOR1 C= 12.5mg/ mL



IZUR1 C= 6mg/mL



**Fig 118 Chromatograms of commercial samples**



## Principal Component Analysis for HPLC data

Variables: A4, A3, A2, A1, B1, B2, B3, B4, B5, B6, B7, B8, etc

### Eigenanalysis of the Correlation Matrix

Eigenvalue	6.4080	3.2056	2.6222	1.9800	1.3123	1.2851	0.9155	0.8665
Proportion	0.291	0.146	0.119	0.090	0.060	0.058	0.042	0.039
Cumulative	0.291	0.437	0.556	0.646	0.706	0.764	0.806	0.845

Eigenvalue	0.8082	0.7062	0.6103	0.3526	0.2973	0.2435	0.1585	0.1040
Proportion	0.037	0.032	0.028	0.016	0.014	0.011	0.007	0.005
Cumulative	0.882	0.914	0.942	0.958	0.971	0.982	0.990	0.994

Eigenvalue	0.0634	0.0298	0.0162	0.0111	0.0030	0.0007		
Proportion	0.003	0.001	0.001	0.001	0.000	0.000		
Cumulative	0.997	0.999	0.999	1.000	1.000	1.000		

Variable	PC1	PC2	PC3	PC4	PC5	PC6	PC7
A4	0.195	-0.176	-0.005	-0.219	0.027	-0.094	0.636
A3	-0.092	-0.088	-0.374	-0.334	-0.087	0.097	0.062
A2	-0.209	-0.234	0.134	0.096	-0.101	-0.344	-0.104
A1	0.007	0.208	-0.481	-0.063	-0.177	0.136	-0.110
B1	-0.320	0.002	0.081	0.072	0.100	-0.070	0.105
B2	-0.161	-0.166	0.197	-0.020	-0.230	-0.093	-0.004
B3	-0.068	0.480	0.140	0.138	0.173	0.086	0.204
B4	0.201	0.185	-0.103	0.117	-0.403	-0.115	-0.381
B5	-0.070	0.498	0.104	0.086	0.171	0.148	0.150
B6	-0.117	-0.009	-0.357	-0.217	0.312	0.223	-0.148
B7	0.081	-0.131	0.190	-0.044	0.144	0.559	-0.307
B8	-0.198	-0.339	0.200	0.040	0.142	0.099	-0.132
T3	0.094	-0.014	-0.288	-0.252	0.200	-0.352	0.082
Epi lupeol	0.318	-0.238	-0.020	0.134	0.140	0.054	0.116
lupeol	-0.053	-0.080	-0.095	0.011	0.622	-0.230	-0.288
Epi $\beta$ amyrina	0.156	0.259	0.129	-0.003	0.182	-0.427	-0.214
lupenone	0.371	-0.108	-0.052	0.132	0.029	0.059	-0.028
Epi $\alpha$ amyryn	0.365	-0.039	-0.010	0.167	0.144	-0.089	-0.057
$\beta$ amyryn	0.355	-0.002	0.055	-0.175	-0.118	-0.078	-0.160
$\alpha$ amyryn/ $\beta$ amyrona	0.343	-0.030	0.067	0.204	0.112	0.176	0.156
$\alpha$ amyrona	0.096	0.217	0.314	-0.499	-0.007	-0.037	-0.064
T4	0.107	-0.007	0.322	-0.532	0.017	0.077	-0.090

Variable	PC8	PC9	PC10	PC11	PC12	PC13	PC14
A4	0.113	-0.048	0.317	0.208	-0.152	0.273	0.358
A3	0.289	0.338	0.090	-0.087	0.343	0.304	-0.509
A2	0.367	-0.088	0.148	-0.291	-0.465	-0.176	-0.242
A1	0.188	0.222	0.073	-0.086	-0.125	-0.316	0.416
B1	0.014	-0.458	-0.234	0.062	0.456	0.047	0.042
B2	-0.566	0.534	0.021	0.258	0.026	-0.138	-0.023
B3	-0.023	0.107	0.150	-0.017	-0.128	0.068	-0.267
B4	-0.102	-0.233	0.143	0.256	-0.203	0.540	-0.060
B5	-0.045	0.101	0.074	-0.062	-0.182	0.011	-0.157
B6	-0.349	-0.134	-0.269	-0.209	-0.292	0.181	0.090
B7	0.040	-0.158	0.582	0.064	0.159	-0.159	0.043
B8	-0.127	0.149	0.168	-0.316	-0.111	0.396	0.068
T3	-0.440	-0.278	0.374	-0.103	-0.000	-0.208	-0.251
Epi lupeol	-0.011	0.099	-0.164	-0.181	-0.131	-0.099	-0.040
lupeol	0.233	0.203	-0.045	0.569	-0.117	0.051	0.012
Epi $\beta$ amyrina	0.013	0.231	0.148	-0.424	0.344	0.194	0.366
lupenone	-0.058	0.005	-0.141	-0.083	0.009	0.041	-0.092
Epi $\alpha$ amyryn	-0.015	0.028	0.069	-0.004	0.159	-0.163	-0.191

$\beta$ amyrin	0.024	-0.046	-0.136	0.059	0.066	-0.119	-0.109
$\alpha$ amyrin/ $\beta$ amyrona	0.004	0.072	-0.160	-0.055	-0.050	0.164	-0.092
$\alpha$ amyrona	0.045	-0.028	-0.059	0.058	-0.141	-0.076	-0.041
T4	0.077	-0.006	-0.241	-0.076	-0.065	0.028	0.006

Variable	PC15	PC16	PC17	PC18	PC19	PC20	PC21
A4	-0.186	0.084	-0.149	-0.044	-0.033	0.002	0.029
A3	-0.105	-0.025	0.057	0.017	-0.021	-0.041	-0.008
A2	-0.243	-0.133	-0.173	0.062	0.056	-0.042	0.014
A1	0.308	0.010	-0.081	0.051	-0.001	0.078	0.101
B1	0.025	0.030	-0.011	0.042	-0.001	0.001	0.122
B2	-0.180	-0.109	-0.080	0.022	0.033	-0.016	0.058
B3	-0.009	0.087	-0.077	0.157	0.177	0.511	0.435
B4	0.009	-0.087	0.141	-0.128	-0.048	0.052	0.055
B5	-0.019	0.154	-0.016	-0.369	-0.055	-0.555	-0.231
B6	-0.444	-0.002	-0.173	0.058	-0.056	0.130	-0.076
B7	-0.223	-0.106	0.036	0.029	0.101	-0.044	0.046
B8	0.493	0.387	-0.057	0.040	-0.072	0.049	-0.039
T3	0.309	-0.116	0.080	0.005	0.152	-0.081	0.019
Epi lupeol	-0.113	0.091	0.716	-0.226	0.030	0.114	0.162
lupeol	0.080	-0.007	0.024	0.006	0.076	-0.063	0.051
Epi $\beta$ amyrina	-0.241	-0.120	0.043	0.033	0.088	-0.039	0.007
lupenone	0.010	0.038	-0.262	0.258	-0.164	-0.489	0.618
Epi $\alpha$ amyrin	-0.007	0.056	-0.335	-0.235	-0.597	0.349	-0.199
$\beta$ amyrin	-0.109	0.618	-0.212	0.019	0.510	0.040	-0.162
$\alpha$ amyrin/ $\beta$ amyrona	0.211	-0.473	-0.116	0.333	0.298	0.015	-0.404
$\alpha$ amyrona	0.036	0.086	0.277	0.526	-0.400	-0.025	-0.121
T4	0.217	-0.329	-0.184	-0.494	0.100	0.088	0.246

Variable	PC22
A4	0.134
A3	0.110
A2	0.256
A1	0.393
B1	0.601
B2	0.311
B3	0.019
B4	0.201
B5	0.227
B6	0.062
B7	0.110
B8	0.102
T3	0.010
Epi lupeol	0.255
lupeol	0.047
Epi $\beta$ amyrina	0.010
lupenone	0.001
Epi $\alpha$ amyrin	0.153
$\beta$ amyrin	0.116
$\alpha$ amyrin/ $\beta$ amyrona	0.226
$\alpha$ amyrona	0.128
T4	0.042

## Linear Discriminant Analysis

### Method for Response: C1

**Predictors:** A4, A3, A2, A1, B11, B12, P1, P2, B14, B15, E1, D1, T3, Epi lupeol, lupeol, Epi  $\beta$ amyrina, lupenone, Epi  $\alpha$ myrin,  $\beta$  amyryr,  $\alpha$ myryr/ $\beta$  amyryna,  $\alpha$  amyryne, T1

Group	bipinnata	excelsa	laxiflora	penicillata	stenophylla
Count	10	4	12	6	8

#### Summary of classification

Put into Group	True Group				
	bipinnata	excelsa	laxiflora	penicillata	stenophylla
bipinnata	10	0	0	0	0
excelsa	0	4	0	0	0
laxiflora	0	0	12	0	0
penicillata	0	0	0	6	0
stenophylla	0	0	0	0	8
Total N	10	4	12	6	8
N correct	10	4	12	6	8
Proportion	1.000	1.000	1.000	1.000	1.000

N = 40                      N Correct = 40                      Proportion Correct = 1.000  
Squared Distance Between Groups

	bipinnata	excelsa	laxiflora	penicillata	stenophylla
bipinnata	0.00	679.97	690.36	3279.80	180.25
excelsa	679.97	0.00	182.13	2992.85	929.53
laxiflora	690.36	182.13	0.00	3482.11	803.47
penicillata	3279.80	2992.85	3482.11	0.00	4278.58
stenophylla	180.25	929.53	803.47	4278.58	0.00

#### Summary of Classification with Cross-validation

Put into Group	True Group				
	bipinnata	excelsa	laxiflora	penicillata	stenophylla
bipinnata	10	0	0	0	1
excelsa	0	3	0	0	0
laxiflora	0	1	12	0	0
penicillata	0	0	0	6	0
stenophylla	0	0	0	0	7
Total N	10	4	12	6	8
N correct	10	3	12	6	7
Proportion	1.000	0.750	1.000	1.000	0.875

N = 40                      N Correct = 38                      Proportion Correct = 0.950

#### Squared Distance Between Groups

	bipinnata	excelsa	laxiflora	penicillata	stenophylla
bipinnata	0.00	321.39	376.81	1818.41	88.66
excelsa	321.39	0.00	135.50	1652.92	312.32
laxiflora	376.81	135.50	0.00	2197.02	253.57
penicillata	1818.41	1652.92	2197.02	0.00	2094.50
stenophylla	88.66	312.32	253.57	2094.50	0.00

## Linear Discriminant Function for Groups

	bipinnata	excelsa	laxiflora	penicillata	stenophylla
Constant	-16822	-16070	-15564	-21660	-15525
A4	20013	19668	20062	20707	19466
A3	34892	35207	34555	39224	33328
A2	32138	31765	31468	35532	30812
A1	33890	33107	32557	37709	32404
B11	32325	31830	31302	35886	30936
B12	32104	31595	31144	35615	30739
P1	28353	29885	28949	39002	26533
P2	31079	30164	29691	33595	29777
B14	44385	43042	41775	56848	41771
B15	67277	76938	73794	76835	62552
E1	24202	22004	22115	19525	23505
D1	34560	34580	35044	37742	33103
T3	2890	-493	-663	-1455	4154
Epi lupeol	28255	27326	26553	30939	27054
lupeol	17478	16931	16733	18599	16968
Epi $\beta$ amyrina	22028	22316	20346	38010	19361
lupenone	1399	-2927	-2211	-3716	2820
Epi $\alpha$ amyrin	187044	187676	186754	205004	177598
$\beta$ amyrin	37079	36046	35142	42496	35385
$\alpha$ amyrin/ $\beta$ amyrona	38749	37353	36849	41103	37090
$\alpha$ amyrona	77601	78781	77640	90278	74731
T1	-23910	-26593	-26212	-32395	-19759

Variable	Pooled Mean	Means for Group			
		bipinnata	excelsa	laxiflora	penicillata
A4	0.02994	0.01815	0.00000	0.02554	0.00000
A3	0.02670	0.01928	0.07057	0.03337	0.00000
A2	0.06514	0.02458	0.00000	0.18000	0.00000
A1	0.23205	0.32666	0.33166	0.13638	0.23889
B11	0.17896	0.00000	0.38575	0.35279	0.23035
B12	0.04173	0.00000	0.00000	0.13911	0.00000
P1	0.01506	0.00000	0.00000	0.00000	0.10042
P2	0.06204	0.13156	0.00000	0.00000	0.06019
B14	0.03731	0.01599	0.02837	0.00000	0.20313
B15	0.00284	0.00000	0.02837	0.00000	0.00000
E1	0.00353	0.01413	0.00000	0.00000	0.00000
D1	0.01630	0.00000	0.01997	0.04768	0.00000
T3	0.01001	0.00000	0.02364	0.00000	0.00000
Epi lupeol	0.09710	0.16474	0.05573	0.04070	0.00817
lupeol	0.01927	0.00870	0.03533	0.02352	0.01635
Epi $\beta$ amyrina	0.00899	0.00975	0.00000	0.00337	0.01753
lupenone	0.03922	0.07266	0.01457	0.00649	0.01565
Epi $\alpha$ amyrin	0.01169	0.01895	0.00000	0.00176	0.00894
$\beta$ amyrin	0.04328	0.07863	0.00561	0.00390	0.01978
$\alpha$ amyrin/ $\beta$ amyrona	0.04688	0.08861	0.00000	0.00244	0.05198
$\alpha$ amyrona	0.01139	0.00761	0.00043	0.00294	0.02862
T1	0.00259	0.00000	0.00000	0.00000	0.00000

Variable	stenophylla
A4	0.08870
A3	0.02406
A2	0.02495
A1	0.20237
B11	0.00000
B12	0.00000
P1	0.00000
P2	0.10061

B14	0.00000
B15	0.00000
E1	0.00000
D1	0.00000
T3	0.03825
Epi lupeol	0.18452
lupeol	0.02028
Epi $\beta$ amyrina	0.01453
lupenone	0.07654
Epi $\alpha$ amyrin	0.02544
$\beta$ amyrin	0.09463
$\alpha$ amyrin/ $\beta$ amyrona	0.08098
$\alpha$ amyrona	0.02133
T1	0.01297

Variable	Pooled StDev	StDev for Group			
		bipinnata	excelsa	laxiflora	penicillata
A4	0.02438	0.00965	0.00000	0.03576	0.00000
A3	0.03316	0.02425	0.05666	0.04563	0.00000
A2	0.06215	0.01143	0.00000	0.10988	0.00000
A1	0.1175	0.0776	0.1896	0.1564	0.0731
B11	0.1501	0.0000	0.3280	0.2046	0.0334
B12	0.1078	0.0000	0.0000	0.1923	0.0000
P1	0.005681	0.000000	0.000000	0.000000	0.015030
P2	0.05569	0.08410	0.00000	0.00000	0.02027
B14	0.01072	0.00913	0.01603	0.00000	0.02236
B15	0.004693	0.000000	0.016029	0.000000	0.000000
E1	0.006574	0.012964	0.000000	0.000000	0.000000
D1	0.01335	0.00000	0.01684	0.02213	0.00000
T3	0.01157	0.00000	0.01843	0.00000	0.00000
Epi lupeol	0.04514	0.03374	0.02725	0.04262	0.00776
lupeol	0.02365	0.00328	0.02490	0.03799	0.01737
Epi $\beta$ amyrina	0.006911	0.002550	0.000000	0.004751	0.015392
lupenone	0.009397	0.010002	0.012904	0.005135	0.007689
Epi $\alpha$ amyrin	0.003754	0.003441	0.000000	0.003354	0.004970
$\beta$ amyrin	0.01522	0.01287	0.00564	0.00421	0.02646
$\alpha$ amyrin/ $\beta$ amyrona	0.01457	0.01540	0.000000	0.00294	0.02554
$\alpha$ amyrona	0.004466	0.005673	0.000396	0.002537	0.004771
T1	0.003466	0.000000	0.000000	0.000000	0.000000

Variable	stenophylla
A4	0.02903
A3	0.00968
A2	0.01307
A1	0.0600
B11	0.0000
B12	0.0000
P1	0.000000
P2	0.07824
B14	0.00000
B15	0.000000
E1	0.000000
D1	0.00000
T3	0.02289
Epi lupeol	0.07423
lupeol	0.00584
Epi $\beta$ amyrina	0.005076
lupenone	0.012565
Epi $\alpha$ amyrin	0.004465
$\beta$ amyrin	0.02010
$\alpha$ amyrin/ $\beta$ amyrona	0.01664
$\alpha$ amyrona	0.005649
T1	0.007750

## Pooled Covariance Matrix

	A4	A3	A2	A1	B11
A4	0.0005946				
A3	0.0004495	0.0010995			
A2	-0.0004010	-0.0005057	0.0038624		
A1	0.0017711	0.0025658	-0.0016662	0.0138005	
B11	-0.0010635	-0.0026780	0.0000868	-0.0101369	0.0225355
B12	-0.0006434	-0.0006566	-0.0026873	-0.0033731	-0.0044839
P1	0.0000000	0.0000000	0.0000000	-0.0001190	0.0000097
P2	-0.0004561	-0.0001598	-0.0000639	-0.0007972	-0.0000443
B14	0.0000049	0.0000104	-0.0000093	0.0001722	-0.0002142
B15	0.0000000	0.0000088	-0.0000000	0.0001763	-0.0003108
E1	0.0000039	0.0000159	-0.0000039	-0.0000198	0.0000000
D1	-0.0001364	-0.0001085	0.0000830	-0.0004069	-0.0003345
T3	0.0000594	0.0000243	0.0000082	0.0003065	-0.0003037
Epi lupeol	0.0001145	-0.0000411	0.0010465	-0.0008726	-0.0018908
lupeol	-0.0000660	-0.0000159	0.0001252	0.0000399	-0.0004346
Epi $\beta$ amyryna	-0.0000203	-0.0000137	0.0001125	-0.0001549	-0.0000970
lupenone	-0.0000457	0.0000103	0.0000542	-0.0001968	-0.0003039
Epi $\alpha$ amyryn	-0.0000150	-0.0000062	0.0000522	-0.0001128	-0.0000478
$\beta$ amyryn	-0.0000177	0.0000283	-0.0000346	-0.0003848	-0.0001882
$\alpha$ amyryn/ $\beta$ amyryna	-0.0000281	0.0000071	0.0000185	-0.0002645	-0.0000559
$\alpha$ amyryne	0.0000176	-0.0000201	-0.0000303	-0.0001021	-0.0000439
T1	-0.0000152	0.0000029	0.0000027	-0.0000272	-0.0000000
P1	0.0000323				
P2	0.0000338	0.0031018			
B14	0.0000191	-0.0000202	0.0001149		
B15	-0.0000000	-0.0000000	0.0000220	0.0000220	
E1	0.0000000	-0.0000337	0.0000264	-0.0000000	0.0000432
D1	-0.0000000	-0.0000000	0.0000228	0.0000228	-0.0000000
T3	-0.0000000	-0.0000001	0.0000249	0.0000249	-0.0000000
Epi lupeol	-0.0000023	-0.0014620	-0.0000130	0.0000166	0.0000054
lupeol	-0.0000102	-0.0001070	-0.0000386	0.0000021	0.0000003
Epi $\beta$ amyryna	-0.0000099	0.0000105	-0.0000432	0.0000000	0.0000001
lupenone	0.0000065	-0.0000537	-0.0000018	0.0000172	-0.0000063
Epi $\alpha$ amyryn	-0.0000018	-0.0000484	-0.0000118	0.0000000	0.0000004
$\beta$ amyryn	-0.0000061	0.0000824	-0.0000436	-0.0000018	-0.0000075
$\alpha$ amyryn/ $\beta$ amyryna	0.0000465	-0.0001512	-0.0000125	0.0000000	-0.0000248
$\alpha$ amyryne	0.0000015	0.0000643	-0.0000097	-0.0000003	0.0000004
T1	-0.0000000	0.0000175	0.0000000	0.0000000	-0.0000000
T3	0.0001339				
Epi lupeol	-0.0000834	0.0020377			
lupeol	0.0000022	0.0000956	0.0005593		
Epi $\beta$ amyryna	0.0000134	0.0000551	0.0000515	0.0000478	
lupenone	-0.0000313	0.0001601	0.0000125	0.0000162	0.0000883
Epi $\alpha$ amyryn	-0.0000037	0.0000604	0.0000500	0.0000166	0.0000175
$\beta$ amyryn	-0.0000647	0.0001409	0.0000632	0.0000183	0.0000788
$\alpha$ amyryn/ $\beta$ amyryna	-0.0000486	0.0001880	-0.0000006	0.0000030	0.0000755
$\alpha$ amyryne	-0.0000023	0.0000246	0.0000232	0.0000101	0.0000078
T1	-0.0000108	-0.0000091	0.0000005	0.0000032	0.0000045
$\beta$ amyryn	0.0002318				
$\alpha$ amyryn/ $\beta$ amyryna	-0.0000008	0.0002123			
$\alpha$ amyryne	0.0000229	0.0000022	0.0000199		
T1	0.0000057	0.0000001	-0.0000010	0.0000120	

	Epi									
	B12	P1	P2	B14	B15	E1	D1	T3	lupeol	lupeol
A4										
A3										
A2										
A1										

B11	
B12	0.0116194
P1	0.0000000
P2	-0.0000000
B14	-0.0000000
B15	0.0000000
E1	0.0000000
D1	0.0004196
T3	-0.0000000
Epi lupeol	0.0002604
lupeol	-0.0003280
Epi $\beta$ amyrina	-0.0000343
lupenone	-0.0000039
Epi $\alpha$ myrin	-0.0000263
$\beta$ amyryn	-0.0000450
$\alpha$ myrin/ $\beta$ amyrona	-0.0000249
$\alpha$ amyrone	0.0000073
T1	-0.0000000
P1	
P2	
B14	
B15	
E1	
D1	0.0001782
T3	0.0000263
Epi lupeol	0.0001873
lupeol	-0.0000236
Epi $\beta$ amyrina	0.0000131
lupenone	0.0000381
Epi $\alpha$ myrin	0.0000012
$\beta$ amyryn	0.0000079
$\alpha$ myrin/ $\beta$ amyrona	0.0000075
$\alpha$ amyrone	0.0000021
T1	-0.0000000
T3	
Epi lupeol	
lupeol	
Epi $\beta$ amyrina	
lupenone	
Epi $\alpha$ myrin	0.0000141
$\beta$ amyryn	0.0000272
$\alpha$ myrin/ $\beta$ amyrona	0.0000105
$\alpha$ amyrone	0.0000025
T1	0.0000045
$\beta$ amyryn	
$\alpha$ myrin/ $\beta$ amyrona	
$\alpha$ amyrone	
T1	

Covariance matrix for Group bipinnata

	A4	A3	A2	A1	B11
A4	0.000093				
A3	0.000101	0.000588			
A2	0.000027	0.000197	0.000131		
A1	0.000010	-0.000412	-0.000254	0.006025	
B11	0.000000	0.000000	0.000000	0.000000	0.000000
B12	0.000000	0.000000	0.000000	0.000000	0.000000
P1	0.000000	0.000000	0.000000	0.000000	0.000000
P2	-0.000574	-0.001066	-0.000472	-0.002252	0.000000
B14	0.000019	0.000006	-0.000036	0.000035	0.000000
B15	0.000000	0.000000	0.000000	0.000000	0.000000

E1	0.000015	0.000062	-0.000015	-0.000077	0.000000
D1	0.000000	0.000000	0.000000	0.000000	0.000000
T3	0.000000	0.000000	0.000000	0.000000	0.000000
Epi lupeol	0.000210	0.000385	0.000241	-0.000952	0.000000
lupeol	0.000020	0.000021	0.000012	-0.000075	0.000000
Epi $\beta$ amyrina	0.000011	0.000032	0.000021	-0.000143	0.000000
lupenone	0.000034	0.000066	0.000058	-0.000471	0.000000
Epi $\alpha$ amyrin	0.000020	0.000040	0.000025	-0.000136	0.000000
$\beta$ amyryn	0.000003	-0.000002	0.000014	-0.000830	0.000000
$\alpha$ amyrin/ $\beta$ amyrona	0.000026	0.000039	0.000079	-0.000168	0.000000
$\alpha$ amyrone	-0.000016	-0.000057	-0.000027	-0.000300	0.000000
T1	0.000000	0.000000	0.000000	0.000000	0.000000
P2	0.007073				
B14	-0.000035	0.000083			
B15	0.000000	0.000000	0.000000		
E1	-0.000131	0.000103	0.000000	0.000168	
D1	0.000000	0.000000	0.000000	0.000000	0.000000
T3	0.000000	0.000000	0.000000	0.000000	0.000000
Epi lupeol	-0.001982	-0.000046	0.000000	0.000021	0.000000
lupeol	-0.000140	0.000006	0.000000	0.000001	0.000000
Epi $\beta$ amyrina	-0.000054	-0.000002	0.000000	0.000000	0.000000
lupenone	-0.000302	-0.000031	0.000000	-0.000024	0.000000
Epi $\alpha$ amyrin	-0.000168	-0.000004	0.000000	0.000001	0.000000
$\beta$ amyryn	0.000325	-0.000035	0.000000	-0.000029	0.000000
$\alpha$ amyrin/ $\beta$ amyrona	-0.000568	-0.000068	0.000000	-0.000096	0.000000
$\alpha$ amyrone	0.000346	0.000004	0.000000	0.000001	0.000000
T1	0.000000	0.000000	0.000000	0.000000	0.000000
lupeol	0.000011				
Epi $\beta$ amyrina	0.000006	0.000007			
lupenone	0.000021	0.000020	0.000100		
Epi $\alpha$ amyrin	0.000009	0.000008	0.000032	0.000012	
$\beta$ amyryn	0.000009	0.000019	0.000092	0.000023	0.000166
$\alpha$ amyrin/ $\beta$ amyrona	0.000024	0.000013	0.000107	0.000030	0.000038
$\alpha$ amyrone	-0.000000	0.000001	0.000008	-0.000002	0.000043
T1	0.000000	0.000000	0.000000	0.000000	0.000000
T1	0.000000				

	B12	P1	P2	B14	B15	E1	D1	T3	Epi lupeol
A4									
A3									
A2									
A1									
B11									
B12	0.000000								
P1	0.000000	0.000000							
P2	0.000000	0.000000							
B14	0.000000	0.000000							
B15	0.000000	0.000000							
E1	0.000000	0.000000							
D1	0.000000	0.000000							
T3	0.000000	0.000000							
Epi lupeol	0.000000	0.000000							
lupeol	0.000000	0.000000							
Epi $\beta$ amyrina	0.000000	0.000000							
lupenone	0.000000	0.000000							
Epi $\alpha$ amyrin	0.000000	0.000000							
$\beta$ amyryn	0.000000	0.000000							
$\alpha$ amyrin/ $\beta$ amyrona	0.000000	0.000000							
$\alpha$ amyrone	0.000000	0.000000							
T1	0.000000	0.000000							
P2									
B14									
B15									
E1									



D1		
T3	0.000000	
Epi lupeol	0.000000	0.001138
lupeol	0.000000	0.000075
Epi $\beta$ amyrina	0.000000	0.000062
lupenone	0.000000	0.000289
Epi $\alpha$ amyrin	0.000000	0.000109
$\beta$ amyrin	0.000000	0.000165
$\alpha$ amyrin/ $\beta$ amyrona	0.000000	0.000311
$\alpha$ amyrona	0.000000	-0.000027
T1	0.000000	0.000000
lupeol		
Epi $\beta$ amyrina		
lupenone		
Epi $\alpha$ amyrin		
$\beta$ amyrin		
$\alpha$ amyrin/ $\beta$ amyrona	0.000237	
$\alpha$ amyrona	-0.000005	0.000032
T1	0.000000	0.000000
T1		

Covariance matrix for Group excelsa

	A4	A3	A2	A1	B11
A4	0.000000				
A3	0.000000	0.003210			
A2	0.000000	0.000000	0.000000		
A1	0.000000	0.008194	0.000000	0.035967	
B11	0.000000	-0.014158	0.000000	-0.062173	0.107592
B12	0.000000	0.000000	0.000000	0.000000	0.000000
P1	0.000000	0.000000	0.000000	0.000000	0.000000
P2	0.000000	0.000000	0.000000	0.000000	0.000000
B14	0.000000	0.000102	0.000000	0.002057	-0.003626
B15	0.000000	0.000102	0.000000	0.002057	-0.003626
E1	0.000000	0.000000	0.000000	0.000000	0.000000
D1	0.000000	-0.000043	0.000000	0.001767	-0.003133
T3	0.000000	0.000025	0.000000	0.001987	-0.003543
Epi lupeol	0.000000	0.001298	0.000000	0.004936	-0.008461
lupeol	0.000000	0.001009	0.000000	0.003362	-0.005633
Epi $\beta$ amyrina	0.000000	0.000000	0.000000	0.000000	0.000000
lupenone	0.000000	0.000021	0.000000	0.001323	-0.002373
Epi $\alpha$ amyrin	0.000000	0.000000	0.000000	0.000000	0.000000
$\beta$ amyrin	0.000000	0.000251	0.000000	0.000584	-0.000971
$\alpha$ amyrin/ $\beta$ amyrona	0.000000	0.000000	0.000000	0.000000	0.000000
$\alpha$ amyrona	0.000000	-0.000011	0.000000	-0.000062	0.000104
T1	0.000000	0.000000	0.000000	0.000000	0.000000
P2	0.000000				
B14	0.000000	0.000257			
B15	0.000000	0.000257	0.000257		
E1	0.000000	0.000000	0.000000	0.000000	
D1	0.000000	0.000266	0.000266	0.000000	0.000283
T3	0.000000	0.000291	0.000291	0.000000	0.000307
Epi lupeol	0.000000	0.000194	0.000194	0.000000	0.000139
lupeol	0.000000	0.000025	0.000025	0.000000	-0.000029
Epi $\beta$ amyrina	0.000000	0.000000	0.000000	0.000000	0.000000
lupenone	0.000000	0.000200	0.000200	0.000000	0.000212
Epi $\alpha$ amyrin	0.000000	0.000000	0.000000	0.000000	0.000000
$\beta$ amyrin	0.000000	-0.000020	-0.000020	0.000000	-0.000035
$\alpha$ amyrin/ $\beta$ amyrona	0.000000	0.000000	0.000000	0.000000	0.000000
$\alpha$ amyrona	0.000000	-0.000003	-0.000003	0.000000	-0.000003
T1	0.000000	0.000000	0.000000	0.000000	0.000000
lupeol	0.000620				



A2	-0.001298	-0.001817	0.012074							
A1	0.005378	0.006174	-0.005193	0.024457						
B11	-0.003384	-0.004660	0.000276	-0.015401	0.041854					
B12	-0.002047	-0.002089	-0.008551	-0.010732	-0.014267					
P1	0.000000	0.000000	0.000000	0.000000	0.000000					
P2	0.000000	0.000000	0.000000	0.000000	0.000000					
B14	0.000000	0.000000	0.000000	0.000000	0.000000					
B15	0.000000	0.000000	0.000000	0.000000	0.000000					
E1	0.000000	0.000000	0.000000	0.000000	0.000000					
D1	-0.000434	-0.000334	0.000264	-0.001777	-0.000210					
T3	0.000000	0.000000	0.000000	0.000000	0.000000					
Epi lupeol	-0.000531	-0.000454	0.003202	-0.002078	-0.003626					
lupeol	-0.000286	-0.000324	0.000410	-0.000569	0.000334					
Epi $\beta$ amyrina	-0.000071	-0.000086	0.000345	-0.000232	-0.000140					
lupenone	-0.000036	0.000009	0.000168	-0.000139	-0.000256					
Epi $\alpha$ amyrin	-0.000037	-0.000049	0.000163	-0.000083	-0.000103					
$\beta$ amyrin	0.000022	0.000094	-0.000005	0.000073	-0.000142					
$\alpha$ amyrin/ $\beta$ amyrona	0.000024	0.000034	0.000012	0.000076	-0.000156					
$\alpha$ amyrona	0.000008	0.000007	-0.000049	0.000046	-0.000121					
T1	0.000000	0.000000	0.000000	0.000000	0.000000					
P2	0.000000									
B14	0.000000	0.000000								
B15	0.000000	0.000000	0.000000							
E1	0.000000	0.000000	0.000000	0.000000						
D1	0.000000	0.000000	0.000000	0.000000	0.000490					
T3	0.000000	0.000000	0.000000	0.000000	0.000000					
Epi lupeol	0.000000	0.000000	0.000000	0.000000	0.000558					
lupeol	0.000000	0.000000	0.000000	0.000000	-0.000067					
Epi $\beta$ amyrina	0.000000	0.000000	0.000000	0.000000	0.000042					
lupenone	0.000000	0.000000	0.000000	0.000000	0.000063					
Epi $\alpha$ amyrin	0.000000	0.000000	0.000000	0.000000	0.000004					
$\beta$ amyrin	0.000000	0.000000	0.000000	0.000000	0.000035					
$\alpha$ amyrin/ $\beta$ amyrona	0.000000	0.000000	0.000000	0.000000	0.000024					
$\alpha$ amyrona	0.000000	0.000000	0.000000	0.000000	0.000007					
T1	0.000000	0.000000	0.000000	0.000000	0.000000					
lupeol	0.001443									
Epi $\beta$ amyrina	0.000055	0.000023								
lupenone	0.000002	0.000017	0.000026							
Epi $\alpha$ amyrin	0.000106	0.000010	0.000003	0.000011						
$\beta$ amyrin	0.000001	-0.000001	0.000010	-0.000002	0.000018					
$\alpha$ amyrin/ $\beta$ amyrona	0.000002	0.000001	0.000007	0.000000	0.000008					
$\alpha$ amyrona	0.000049	0.000005	0.000007	0.000004	0.000002					
T1	0.000000	0.000000	0.000000	0.000000	0.000000					
T1	0.000000									

	B12	P1	P2	B14	B15	E1	D1	T3	Epi lupeol
A4									
A3									
A2									
A1									
B11									
B12	0.036971								
P1	0.000000	0.000000							
P2	0.000000	0.000000							
B14	0.000000	0.000000							
B15	0.000000	0.000000							
E1	0.000000	0.000000							
D1	0.001335	0.000000							
T3	0.000000	0.000000							
Epi lupeol	0.000829	0.000000							
lupeol	-0.001044	0.000000							
Epi $\beta$ amyrina	-0.000109	0.000000							
lupenone	-0.000012	0.000000							
Epi $\alpha$ amyrin	-0.000084	0.000000							

$\beta$ amyryn	-0.000143	0.000000
$\alpha$ amyryn/ $\beta$ amyrona	-0.000079	0.000000
$\alpha$ amyrone	0.000023	0.000000
T1	0.000000	0.000000
P2		
B14		
B15		
E1		
D1		
T3	0.000000	
Epi lupeol	0.000000	0.001816
lupeol	0.000000	-0.000113
Epi $\beta$ amyryna	0.000000	0.000142
lupenone	0.000000	0.000130
Epi $\alpha$ amyryn	0.000000	0.000056
$\beta$ amyryn	0.000000	0.000032
$\alpha$ amyryn/ $\beta$ amyrona	0.000000	0.000036
$\alpha$ amyrone	0.000000	0.000002
T1	0.000000	0.000000
lupeol		
Epi $\beta$ amyryna		
lupenone		
Epi $\alpha$ amyryn		
$\beta$ amyryn		
$\alpha$ amyryn/ $\beta$ amyrona	0.000009	
$\alpha$ amyrone	0.000004	0.000006
T1	0.000000	0.000000
T1		

Covariance matrix for Group penicillata

	A4	A3	A2	A1	B11
A4	0.000000				
A3	0.000000	0.000000			
A2	0.000000	0.000000	0.000000		
A1	0.000000	0.000000	0.000000	0.005339	
B11	0.000000	0.000000	0.000000	0.000226	0.001115
B12	0.000000	0.000000	0.000000	0.000000	0.000000
P1	0.000000	0.000000	0.000000	-0.000833	0.000068
P2	0.000000	0.000000	0.000000	-0.000928	-0.000310
B14	0.000000	0.000000	0.000000	-0.000091	0.000676
B15	0.000000	0.000000	0.000000	0.000000	0.000000
E1	0.000000	0.000000	0.000000	0.000000	0.000000
D1	0.000000	0.000000	0.000000	0.000000	0.000000
T3	0.000000	0.000000	0.000000	0.000000	0.000000
Epi lupeol	0.000000	0.000000	0.000000	-0.000258	-0.000183
lupeol	0.000000	0.000000	0.000000	-0.000445	-0.000396
Epi $\beta$ amyryna	0.000000	0.000000	0.000000	-0.000237	-0.000372
lupenone	0.000000	0.000000	0.000000	-0.000474	-0.000141
Epi $\alpha$ amyryn	0.000000	0.000000	0.000000	-0.000168	-0.000108
$\beta$ amyryn	0.000000	0.000000	0.000000	-0.000625	-0.000422
$\alpha$ amyryn/ $\beta$ amyrona	0.000000	0.000000	0.000000	-0.001374	-0.000049
$\alpha$ amyrone	0.000000	0.000000	0.000000	-0.000133	-0.000104
T1	0.000000	0.000000	0.000000	0.000000	0.000000
P2	0.000411				
B14	-0.000078	0.000500			
B15	0.000000	0.000000	0.000000		
E1	0.000000	0.000000	0.000000	0.000000	
D1	0.000000	0.000000	0.000000	0.000000	0.000000
T3	0.000000	0.000000	0.000000	0.000000	0.000000
Epi lupeol	0.000025	-0.000125	0.000000	0.000000	0.000000
lupeol	0.000014	-0.000295	0.000000	0.000000	0.000000

Epi βamyrina	0.000058	-0.000299	0.000000	0.000000	0.000000
lupenone	0.000092	-0.000078	0.000000	0.000000	0.000000
Epi αamyrin	0.000012	-0.000076	0.000000	0.000000	0.000000
β amyryn	-0.000019	-0.000230	0.000000	0.000000	0.000000
αamyrin/β amyrona	0.000429	0.000035	0.000000	0.000000	0.000000
α amyrone	0.000059	-0.000073	0.000000	0.000000	0.000000
T1	0.000000	0.000000	0.000000	0.000000	0.000000
lupeol	0.000302				
Epi βamyrina	0.000221	0.000237			
lupenone	0.000100	0.000078	0.000059		
Epi αamyrin	0.000085	0.000061	0.000031	0.000025	
β amyryn	0.000353	0.000118	0.000109	0.000102	0.000700
αamyrin/β amyrona	-0.000041	0.000050	0.000104	-0.000002	-0.000200
α amyrone	0.000040	0.000061	0.000024	0.000012	-0.000009
T1	0.000000	0.000000	0.000000	0.000000	0.000000
T1	0.000000				

	B12	P1	P2	B14	B15	E1	D1	T3	Epi lupeol
A4									
A3									
A2									
A1									
B11									
B12	0.000000								
P1	0.000000	0.000226							
P2	0.000000	0.000236							
B14	0.000000	0.000134							
B15	0.000000	0.000000							
E1	0.000000	0.000000							
D1	0.000000	0.000000							
T3	0.000000	0.000000							
Epi lupeol	0.000000	-0.000016							
lupeol	0.000000	-0.000071							
Epi βamyrina	0.000000	-0.000070							
lupenone	0.000000	0.000045							
Epi αamyrin	0.000000	-0.000012							
β amyryn	0.000000	-0.000043							
αamyrin/β amyrona	0.000000	0.000326							
α amyrone	0.000000	0.000010							
T1	0.000000	0.000000							
P2									
B14									
B15									
E1									
D1									
T3	0.000000								
Epi lupeol	0.000000	0.000060							
lupeol	0.000000	0.000133							
Epi βamyrina	0.000000	0.000094							
lupenone	0.000000	0.000049							
Epi αamyrin	0.000000	0.000038							
β amyryn	0.000000	0.000166							
αamyrin/β amyrona	0.000000	-0.000001							
α amyrone	0.000000	0.000018							
T1	0.000000	0.000000							
lupeol									
Epi βamyrina									
lupenone									
Epi αamyrin									
β amyryn									
αamyrin/β amyrona	0.000652								
α amyrone	0.000072	0.000023							
T1	0.000000	0.000000							
T1									



E1	0.000000	0.000000
D1	0.000000	0.000000
T3	0.000000	0.000000
Epi lupeol	0.000000	0.000000
lupeol	0.000000	0.000000
Epi βamyrina	0.000000	0.000000
lupenone	0.000000	0.000000
Epi αamyrin	0.000000	0.000000
β amyrin	0.000000	0.000000
αamyrin/β amyrona	0.000000	0.000000
α amyrone	0.000000	0.000000
T1	0.000000	0.000000
P2		
B14		
B15		
E1		
D1		
T3	0.000524	
Epi lupeol	-0.000483	0.005510
lupeol	0.000032	0.000207
Epi βamyrina	0.000067	-0.000094
lupenone	-0.000258	0.000149
Epi αamyrin	-0.000018	0.000046
β amyrin	-0.000307	0.000273
αamyrin/β amyrona	-0.000243	0.000485
α amyrone	-0.000011	0.000145
T1	-0.000054	-0.000045
lupeol		
Epi βamyrina		
lupenone		
Epi αamyrin		
β amyrin		
αamyrin/β amyrona	0.000277	
α amyrone	-0.000039	0.000032
T1	0.000000	-0.000005
T1		

Summary of Classified Observations

Observation	True Group	Pred Group	Group	Squared Distance	Probability
1	bipinnata	bipinnata	bipinnata	9.58	1.000
			excelsa	594.52	0.000
			laxiflora	609.03	0.000
			penicillata	3131.98	0.000
			stenophylla	195.92	0.000
2	bipinnata	bipinnata	bipinnata	13.06	1.000
			excelsa	793.79	0.000
			laxiflora	800.85	0.000
			penicillata	3461.00	0.000
			stenophylla	169.08	0.000
3	bipinnata	bipinnata	bipinnata	5.47	1.000
			excelsa	724.74	0.000
			laxiflora	727.66	0.000
			penicillata	3374.19	0.000
			stenophylla	177.45	0.000
4	bipinnata	bipinnata	bipinnata	17.33	1.000
			excelsa	721.63	0.000
			laxiflora	721.50	0.000
			penicillata	3205.85	0.000
			stenophylla	211.85	0.000
5	bipinnata	bipinnata	bipinnata	6.72	1.000
			excelsa	639.68	0.000
			laxiflora	642.05	0.000
			penicillata	3326.03	0.000
			stenophylla	174.77	0.000

6	bipinnata	bipinnata	bipinnata	15.87	1.000
			excelsa	592.48	0.000
			laxiflora	605.65	0.000
			penicillata	3295.23	0.000
			stenophylla	200.13	0.000
7	bipinnata	bipinnata	bipinnata	24.20	1.000
			excelsa	699.54	0.000
			laxiflora	721.15	0.000
			penicillata	3333.03	0.000
			stenophylla	230.17	0.000
8	bipinnata	bipinnata	bipinnata	23.03	1.000
			excelsa	806.73	0.000
			laxiflora	816.26	0.000
			penicillata	3328.04	0.000
			stenophylla	196.48	0.000
9	bipinnata	bipinnata	bipinnata	15.05	1.000
			excelsa	637.77	0.000
			laxiflora	650.43	0.000
			penicillata	3126.60	0.000
			stenophylla	224.07	0.000
10	bipinnata	bipinnata	bipinnata	19.62	1.000
			excelsa	738.73	0.000
			laxiflora	758.91	0.000
			penicillata	3366.01	0.000
			stenophylla	172.50	0.000
11	excelsa	excelsa	bipinnata	677.52	0.000
			excelsa	6.12	1.000
			laxiflora	196.31	0.000
			penicillata	2971.68	0.000
			stenophylla	933.70	0.000
12	excelsa	excelsa	bipinnata	663.79	0.000
			excelsa	22.88	1.000
			laxiflora	130.65	0.000
			penicillata	3080.60	0.000
			stenophylla	887.17	0.000
13	excelsa	excelsa	bipinnata	763.54	0.000
			excelsa	24.21	1.000
			laxiflora	252.91	0.000
			penicillata	3106.33	0.000
			stenophylla	1005.07	0.000
14	excelsa	excelsa	bipinnata	685.84	0.000
			excelsa	17.60	1.000
			laxiflora	219.47	0.000
			penicillata	2883.62	0.000
			stenophylla	962.99	0.000
15	laxiflora	laxiflora	bipinnata	647.56	0.000
			excelsa	185.45	0.000
			laxiflora	19.84	1.000
			penicillata	3331.43	0.000
			stenophylla	747.13	0.000
16	laxiflora	laxiflora	bipinnata	796.83	0.000
			excelsa	262.30	0.000
			laxiflora	22.20	1.000
			penicillata	3842.38	0.000
			stenophylla	829.55	0.000
17	laxiflora	laxiflora	bipinnata	740.29	0.000
			excelsa	208.64	0.000
			laxiflora	29.41	1.000
			penicillata	3539.44	0.000
			stenophylla	845.37	0.000
18	laxiflora	laxiflora	bipinnata	683.22	0.000
			excelsa	125.49	0.000
			laxiflora	20.85	1.000
			penicillata	3403.95	0.000
			stenophylla	817.16	0.000



19	laxiflora	laxiflora	bipinnata	749.41	0.000
			excelsa	206.85	0.000
			laxiflora	13.03	1.000
			penicillata	3480.88	0.000
			stenophylla	858.91	0.000
20	laxiflora	laxiflora	bipinnata	726.43	0.000
			excelsa	171.02	0.000
			laxiflora	7.87	1.000
			penicillata	3497.82	0.000
			stenophylla	861.08	0.000
21	laxiflora	laxiflora	bipinnata	733.54	0.000
			excelsa	219.16	0.000
			laxiflora	28.86	1.000
			penicillata	3499.05	0.000
			stenophylla	864.04	0.000
22	laxiflora	laxiflora	bipinnata	692.68	0.000
			excelsa	210.06	0.000
			laxiflora	24.98	1.000
			penicillata	3522.56	0.000
			stenophylla	794.44	0.000
23	laxiflora	laxiflora	bipinnata	664.79	0.000
			excelsa	205.58	0.000
			laxiflora	14.57	1.000
			penicillata	3474.88	0.000
			stenophylla	787.77	0.000
24	laxiflora	laxiflora	bipinnata	703.68	0.000
			excelsa	198.79	0.000
			laxiflora	24.50	1.000
			penicillata	3481.79	0.000
			stenophylla	841.85	0.000
25	laxiflora	laxiflora	bipinnata	679.24	0.000
			excelsa	166.21	0.000
			laxiflora	4.25	1.000
			penicillata	3469.94	0.000
			stenophylla	803.38	0.000
26	laxiflora	laxiflora	bipinnata	705.04	0.000
			excelsa	264.43	0.000
			laxiflora	28.08	1.000
			penicillata	3479.68	0.000
			stenophylla	829.45	0.000
27	penicillata	penicillata	bipinnata	3510.70	0.000
			excelsa	3241.47	0.000
			laxiflora	3737.60	0.000
			penicillata	12.34	1.000
			stenophylla	4523.74	0.000
28	penicillata	penicillata	bipinnata	3369.91	0.000
			excelsa	3072.05	0.000
			laxiflora	3554.10	0.000
			penicillata	20.38	1.000
			stenophylla	4354.81	0.000
29	penicillata	penicillata	bipinnata	3258.90	0.000
			excelsa	3008.12	0.000
			laxiflora	3503.23	0.000
			penicillata	23.43	1.000
			stenophylla	4268.27	0.000
30	penicillata	penicillata	bipinnata	3333.78	0.000
			excelsa	3022.46	0.000
			laxiflora	3519.46	0.000
			penicillata	26.56	1.000
			stenophylla	4346.97	0.000
31	penicillata	penicillata	bipinnata	3367.10	0.000
			excelsa	3077.09	0.000
			laxiflora	3574.71	0.000
			penicillata	17.65	1.000
			stenophylla	4384.71	0.000

32	penicillata	penicillata	bipinnata	2959.53	0.000
			excelsa	2657.05	0.000
			laxiflora	3124.70	0.000
			penicillata	20.75	1.000
			stenophylla	3914.10	0.000
33	stenophylla	stenophylla	bipinnata	218.52	0.000
			excelsa	930.93	0.000
			laxiflora	802.97	0.000
			penicillata	4246.54	0.000
			stenophylla	25.05	1.000
34	stenophylla	stenophylla	bipinnata	174.03	0.000
			excelsa	988.90	0.000
			laxiflora	891.55	0.000
			penicillata	4473.09	0.000
			stenophylla	26.40	1.000
35	stenophylla	stenophylla	bipinnata	235.41	0.000
			excelsa	901.11	0.000
			laxiflora	787.44	0.000
			penicillata	4241.23	0.000
			stenophylla	23.77	1.000
36	stenophylla	stenophylla	bipinnata	184.23	0.000
			excelsa	957.97	0.000
			laxiflora	794.27	0.000
			penicillata	4263.67	0.000
			stenophylla	27.83	1.000
37	stenophylla	stenophylla	bipinnata	169.20	0.000
			excelsa	903.52	0.000
			laxiflora	778.88	0.000
			penicillata	4229.78	0.000
			stenophylla	27.70	1.000
38	stenophylla	stenophylla	bipinnata	257.73	0.000
			excelsa	1085.03	0.000
			laxiflora	960.10	0.000
			penicillata	4430.28	0.000
			stenophylla	17.61	1.000
39	stenophylla	stenophylla	bipinnata	172.94	0.000
			excelsa	889.58	0.000
			laxiflora	759.44	0.000
			penicillata	4215.82	0.000
			stenophylla	10.72	1.000
40	stenophylla	stenophylla	bipinnata	219.62	0.000
			excelsa	968.90	0.000
			laxiflora	842.85	0.000
			penicillata	4317.96	0.000
			stenophylla	30.63	1.000

**Concentration of Standard Molecules**  
**Calculated from peak areas and correspondent equations from calibration**

<b>Sample</b>	<b>Lupeol</b>	<b>Lupenone</b>	<b><math>\beta</math>-amyrin</b>	<b><math>\alpha</math>-amyrone</b>
<b>11a1</b>	.03269	.20992	.21902	.02859
<b>11b2</b>	.02242	.28544	.203043	.014324
<b>11b3</b>	0.29493	1.8014	1.917769	0.14504
<b>11c1</b>	.07075	.32878	.33903	.02074
<b>11c2</b>	0.027865	0.320973	0.332013	0.00996
<b>11c3</b>	.199096	1.21896	1.177103	.0566
<b>11d1</b>	.2442	.09025	.109128	.016385
<b>11d2</b>	.339180	01/01/60	1.743341	.31403
<b>11d3</b>	.0403	.299999	.148078	.04568
<b>11e1</b>	.067099	.697966	.45539	.153278
<b>27a2</b>	0.57309	0.077511	0.07435	0.00197
<b>27a3</b>	0.02679	0.02466	0.00565	0.00207
<b>27a4</b>	0.07678	0.08585	0.00758	nd
<b>27a1Q</b>	0.61844	0.07561	0.10660	0.00134
<b>47a1</b>	0.00268	0.00961	0.00939	nd
<b>47a2</b>	1.08655	0.2633	0.32767	0.11788
<b>47b2</b>	0.01092	0.01553	0.001152	0.0098
<b>47b3</b>	0.047712	0.01378	0.00817	0.0052
<b>47b4</b>	0.00993	0.16302	0.4594	0.06
<b>47b5</b>	nd	0.00316	nd	nd
<b>47b6</b>	0.13038	0.58163	0.05887	0.0437
<b>47d1</b>	0.00023	0.0098	0.02506	0.003359
<b>47c1</b>	0.0153	0.005961	0.01463	0.001853
<b>47ee1</b>	0.02586	0.00147	nd	0.014554
<b>47f1</b>	0.22704	nd	nd	0.0266
<b>47a1Q</b>	0.14343	0.002012	0.009985	0.007235
<b>47b1Q</b>	0.23616	0.087744	0.02957	0.02192
<b>63a1</b>	0.00089	0.022623	0.01754	0.041073
<b>63a2</b>	0.00452	0.045533	0.024	0.077333
<b>63a3</b>	0.08219	0.93544	0.12598	0.02622
<b>63a4</b>	0.05625	0.126608	0.04404	0.102615
<b>63a1Q</b>	0.183031	0.092325	0.08407	0.23138
<b>63b1Q</b>	0.0022	0.012729	0.01163	0.084771
<b>72a1</b>	0.09719	0.26849	0.09716	0.104671
<b>72a2</b>	0.05368	0.270574	0.26394	0.03376
<b>72b1</b>	0.10936	0.315295	0.42913	0.102815
<b>72b2</b>	0.02281	0.155033	nd	0.029475
<b>72c1</b>	0.040643	0.173141	0.22273	0.047922

<b>72d1</b>	0.09587	0.254174	0.3162	0.060707
<b>72d2</b>	0.15084	0.297971	0.32914	0.08268
<b>72c2</b>	nd	0.297971	0.32914	0.08268

**Table 47** Concentration of standard molecules in botanically certified samples (mg/ ml), nd: not detected compound

<b>Sample</b>	<b>Lupeol</b>	<b>Lupenone</b>	<b><math>\beta</math>-amyrin</b>	<b><math>\alpha</math>-amyrone</b>
<b>51</b>	0.10886	0.03117343	0.26372	0.05157
<b>52</b>	0.093941	0.02269353	0.12908	0.0142
<b>TMT</b>	0.20691	0.06780833	0.39981	nd
<b>Chiché Itzá</b>	nd	0.00534969	0.45495	0.45813
<b>26</b>	0.090095	0.03553556	0.24685	0.01198
<b>84</b>	0.08038	0.03042943	0.21561	0.00876
<b>173</b>	0.1266	0.05654073	0.44673	0.08102

**Table 48** Concentration of standard molecules in archaeological samples (mg/ ml), nd: not detected compound

<b>Sample</b>	<b>Lupenone</b>
<b>70a2</b>	0.479132
<b>70b1</b>	0.266126
<b>70b2</b>	0.881291
<b>70b3</b>	0.162498
<b>70b4</b>	0.481117
<b>70b5</b>	0.570789
<b>70c1</b>	0.1384026
<b>70c2</b>	0.318933
<b>70c3</b>	0.27475
<b>70d1</b>	0.703219
<b>70d1fr</b>	0.593591
<b>70d2</b>	0.866119
<b>70a1Q</b>	0.684949

**Table 49** Concentration of lupenone in *B. simaruba* samples (mg/ ml)

Sample	Lupeol	lupenone	$\beta$ -amyrine	$\alpha$ -amyrone
ATZB1	0.0973	0.2369	0.1705	0.0264
ATZM1	0.0514	0.1907	0.1205	0.0022
CHOB1	0.0229	0.1366	0.1029	0.0093
CHOB2	0.0305	0.1638	0.1138	0.0037
CHOB3	0.0247	0.0656	0.0451	nd
CHOB4	0.0437	0.0847	0.0554	0.0001
CHOM1	0.0293	0.0985	0.0709	0.0044
CHOR1	0.3379	0.9553	0.6666	1.7143
Sidral	0.0331	0.2377	0.166	0.0121
Huitzuco	0.0387	0.1314	0.0729	0.0073
Incienso	0.0139	0.1154	nd	nd
IZUB2	0.0327	0.1304	0.1062	0.0085
IZUM1	0.0729	0.2512	0.1994	0.0118
IZUP1	0.0855	0.1989	0.1415	0.0093
IZUR1	0.1008	0.2747	0.1709	0.0134
SONB1	0.0647	0.7933	0.6092	1.2628
SONB2	0.0306	0.1477	0.0977	0.004
SONB3	0.0163	0.1149	0.0828	0.0008
SONR1	0.0724	0.2278	0.21	0.3081
OAXC1	0.0246	nd	0.041	0.0104
OAXC2	0.0312	0.0022	0.0062	0.0004
OAXC3	nd	0.0036	nd	nd
ColimaL1	0.1069	0.4973	0.4612	0.0532
ColimaL2	0.0216	0.0043	nd	nd
M6	0.0747	0.2695	0.1934	0.0121
M6Q	0.0228	0.1223	0.0876	0.0051
ATZB2	0.0191	0.0146	0.0074	nd
SONR2	0.4217	1.1326	0.8104	0.007
SONB4	0.0993	0.3235	0.2185	0.0121
MEXB1	0.1056	0.417	0.2902	0.014
MEXJ1	0.0587	0.2315	0.1846	0.0276
MEXM1	0.0818	0.0528	0.0142	0.0059

Table 50 Concentration of estandards in commercial samples (mg/ ml), nd: not detected compound

**Retention time of Standard molecules under gradient 2 (for the study of triterpenic fraction) in GC-MS,  
according to each studied species**

Species	Certified Sample ID	3- <i>epi</i> $\beta$ amyrin	3- <i>epi</i> - $\alpha$ amyrin	3- <i>epi</i> lupeol	$\beta$ -amyrone	$\beta$ - amyrin	$\alpha$ - amyrone	$\alpha$ -amyrin	lupeol	lupenone
		I	II	III	IV	V	VI	VII	VII	IX
<i>B. bipinnata</i>	11d2	32.53	33.01	33.21	34.74	35.24	35.86	36.23	36.71	37.89
<i>B. excelsa</i>	27a4	32.41 (trc)	32.85	33.01	-	-	-	-	-	-
<i>B. grandifolia</i>	34b1Q	32.43	32.92	-	35.26	-	36.125	-	-	-
<i>B. laxiflora</i>	47a1	32.46 (trc)	32.94	33.10	34.73	35.15	-	-	36.30	-
<i>B. laxiflora</i>	47b5	32.55	33.01	33.18	34.81	35.26	35.93	36.27	36.44	38.22
<i>B. penicillata</i>	63a4	32.50	33.01	33.16	35.52	35.26	-	36.24	36.71	-
<i>B. simaruba</i>	70a1Q	32.48	32.96	33.16	34.66	35.23	35.88	36.23	36.35	-
<i>B. stenophylla</i>	72a1	32.53	33.02	33.22	34.76	35.24	35.87	36.24	36.71	37.85
<i>B. copallifera</i>	15a1	-	32.79	-	-	-	-	-	36.61	37.35

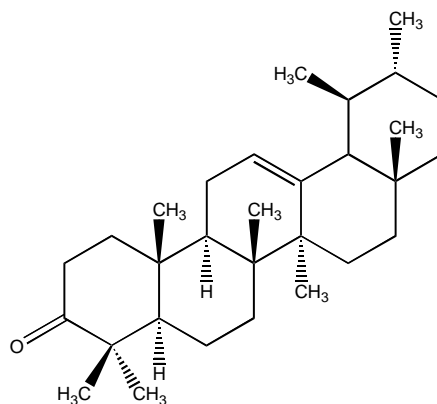
**Table 51 Retention times of standar molecules under gradient 2 for the study of triterpenic compounds.  
Absences of compounds are indicated as (-), concentration in traces as (trc)**

## Retention time of Standard molecules under gradient 1 for GC-MS, in archaeological samples.

Archaeological Sample	3-epi $\beta$ amyryn	3-epi- $\alpha$ amyryn	3-epi lupeol	$\beta$ -amyrone	$\beta$ - amyrone	$\alpha$ - amyrone	$\alpha$ -amyryn	lupeol	lupenone
<b>26</b>	40.61	41.01	41.19	42.86	43.21	-	43.67	43.67	-
<b>51</b>	40.58	41.02	41.18	42.55	42.87	43.40	43.65	43.65	-
<b>52</b>	40.51	40.95	41.10	42.48	42.80	43.34	43.39	43.39	43.85
<b>84</b>	40.68	41.12	41.31	42.61	42.90	43.47	43.86	43.86	44.78
<b>173</b>	40.58	41.01	41.19	42.57	42.87	43.41	43.69	43.69	44.77
<b>TMT</b>	40.40	40.82	40.96	42.68	43.05	43.27	43.44	43.76	-
<b>M1</b>	39.64	40.06	40.24	41.58	41.91	42.42	42.66	42.77	43.02
<b>Chichén Itzá</b>	40.50	40.93	41.09	42.51	42.82	43.31	43.56	43.761	-

Table 52 Retention times of standar molecules under gradient 1 for the study of archaeological samples.  
Absences of compounds are indicated as (-)

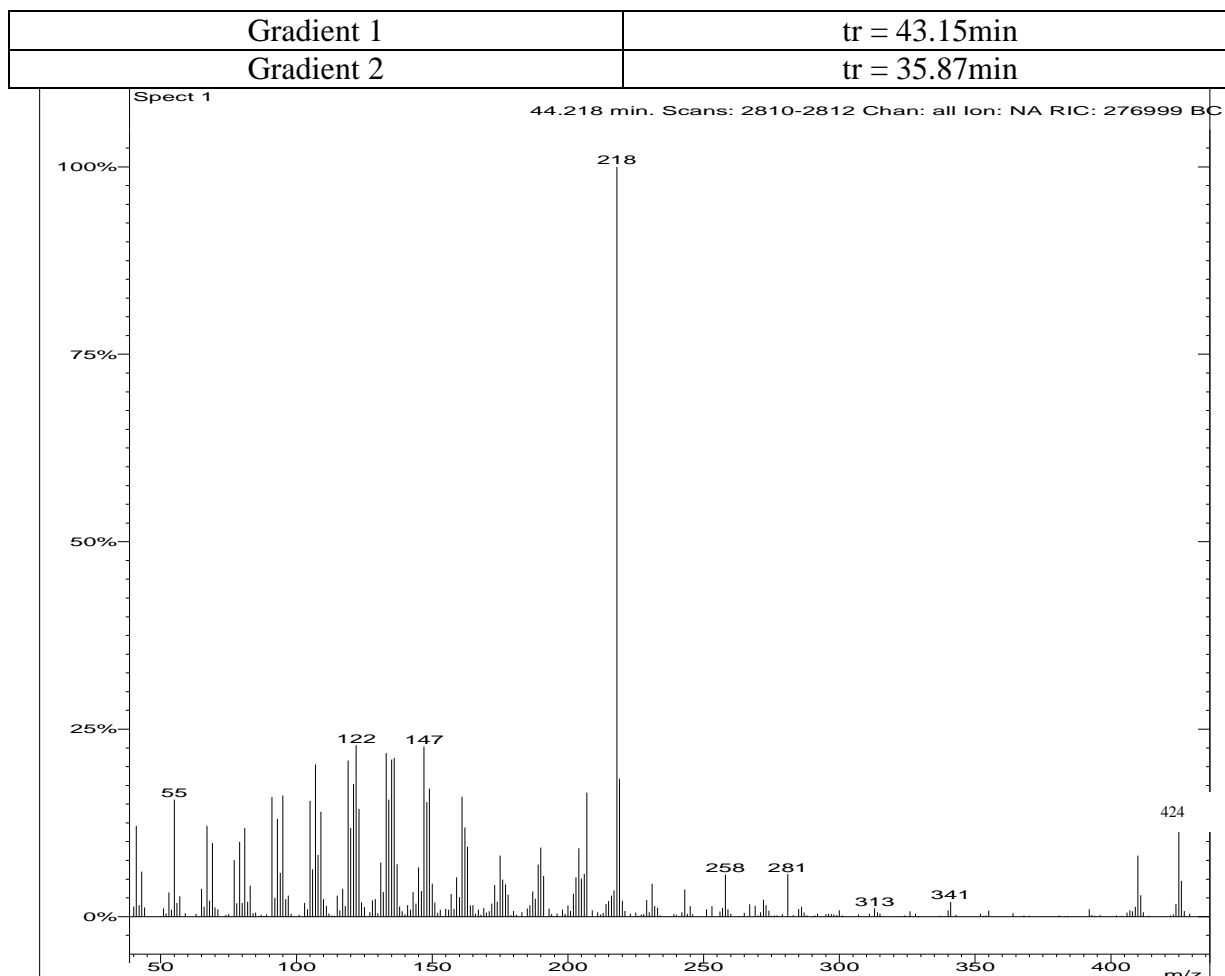
## Mass Spectra of Identified Triterpenoids in Mexican Copals



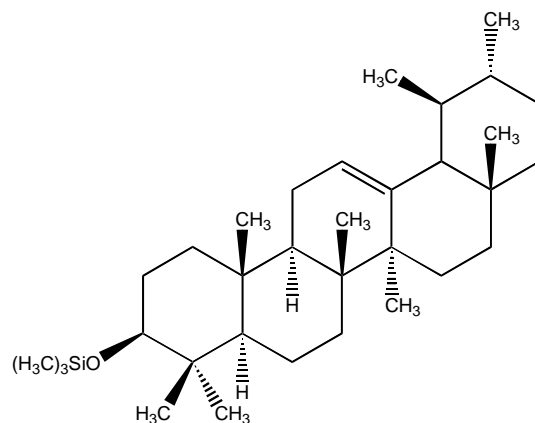
### $\alpha$ -Amyrenone

$C_{30}H_{48}O$   
424 g.mol<sup>-1</sup>

Commercial compound: BCP





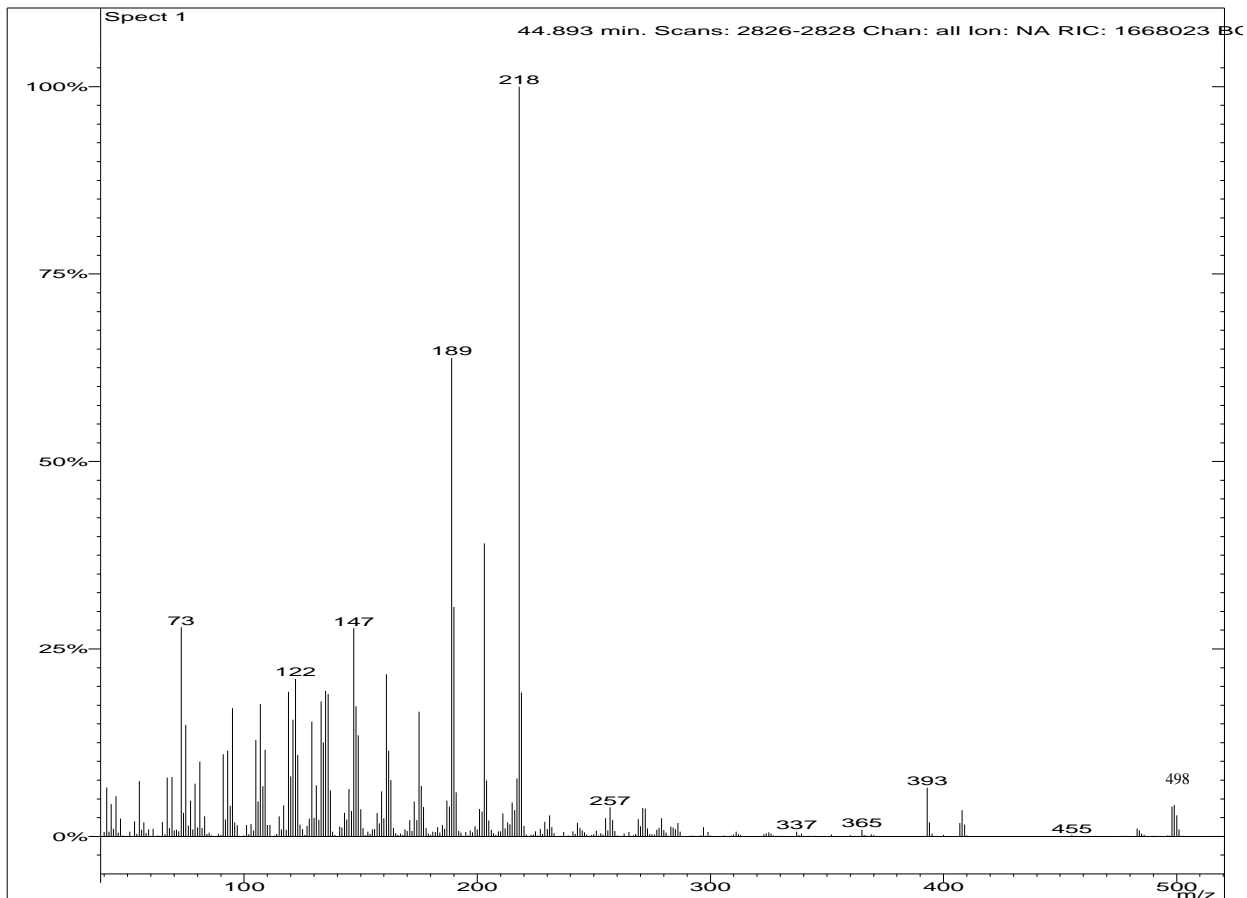


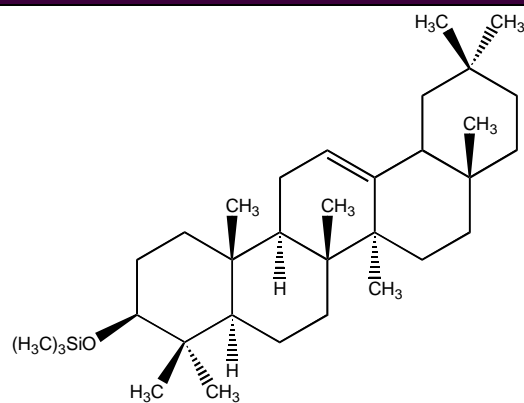
**$\alpha$ -Amyrine TMS**

$C_{33}H_{58}OSi$   
 498 g.mol<sup>-1</sup>

Commercial compound: Extrasynthèse

Gradient 1	tr = 43.58 min
Gradient 2	tr = 36.24 min



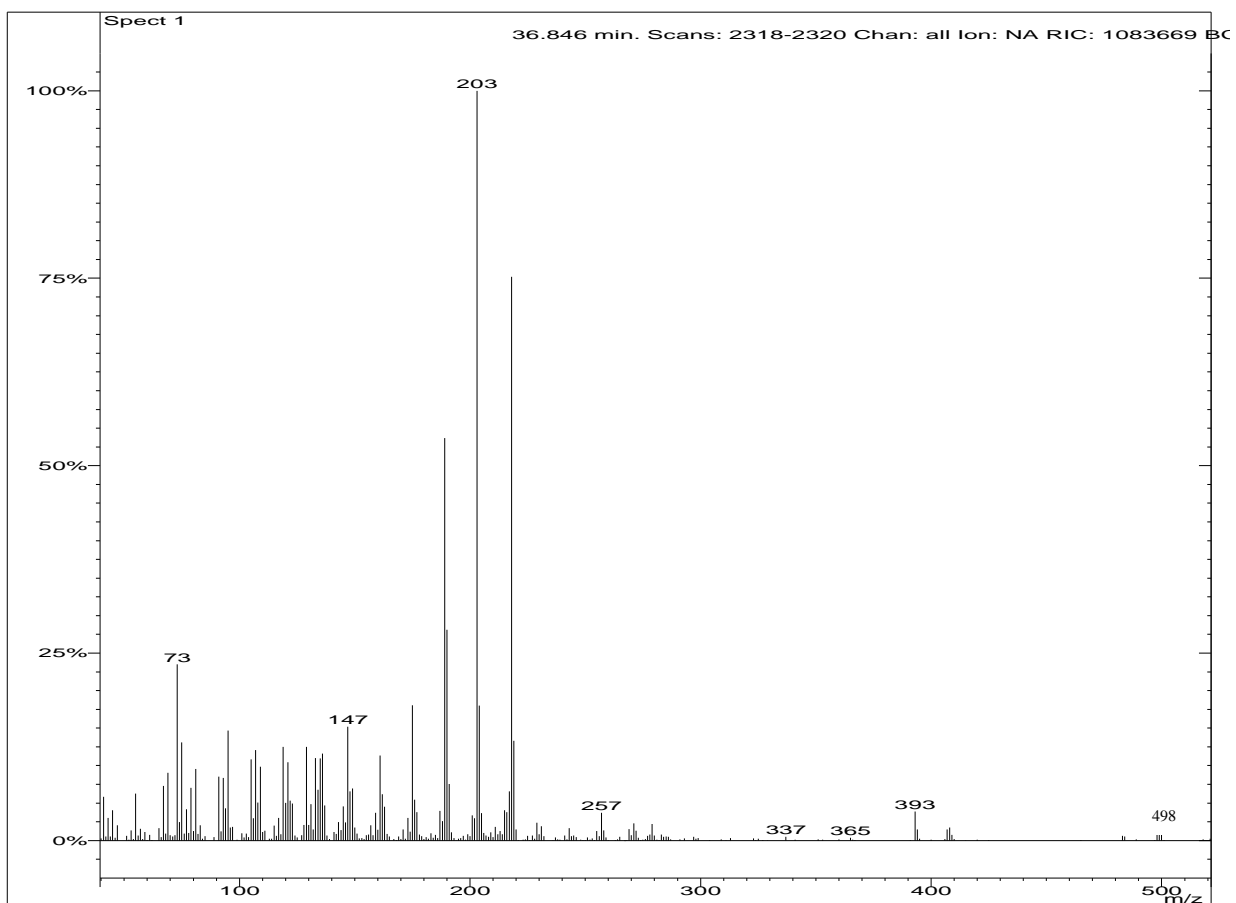


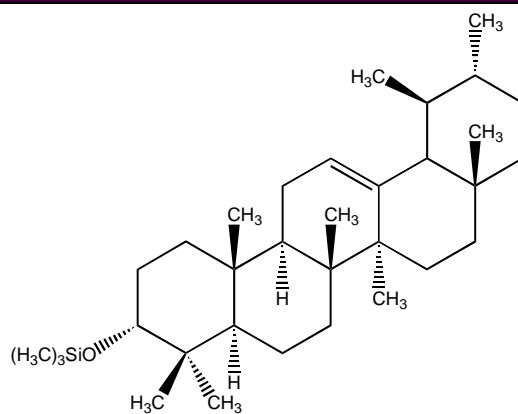
### $\beta$ -Amyrine TMS

$C_{33}H_{58}OSi$   
498 g.mol<sup>-1</sup>

Commercial compound: Extrasynthèse

Gradient 1	tr = 42.81 min
Gradient 2	tr = 35.24min





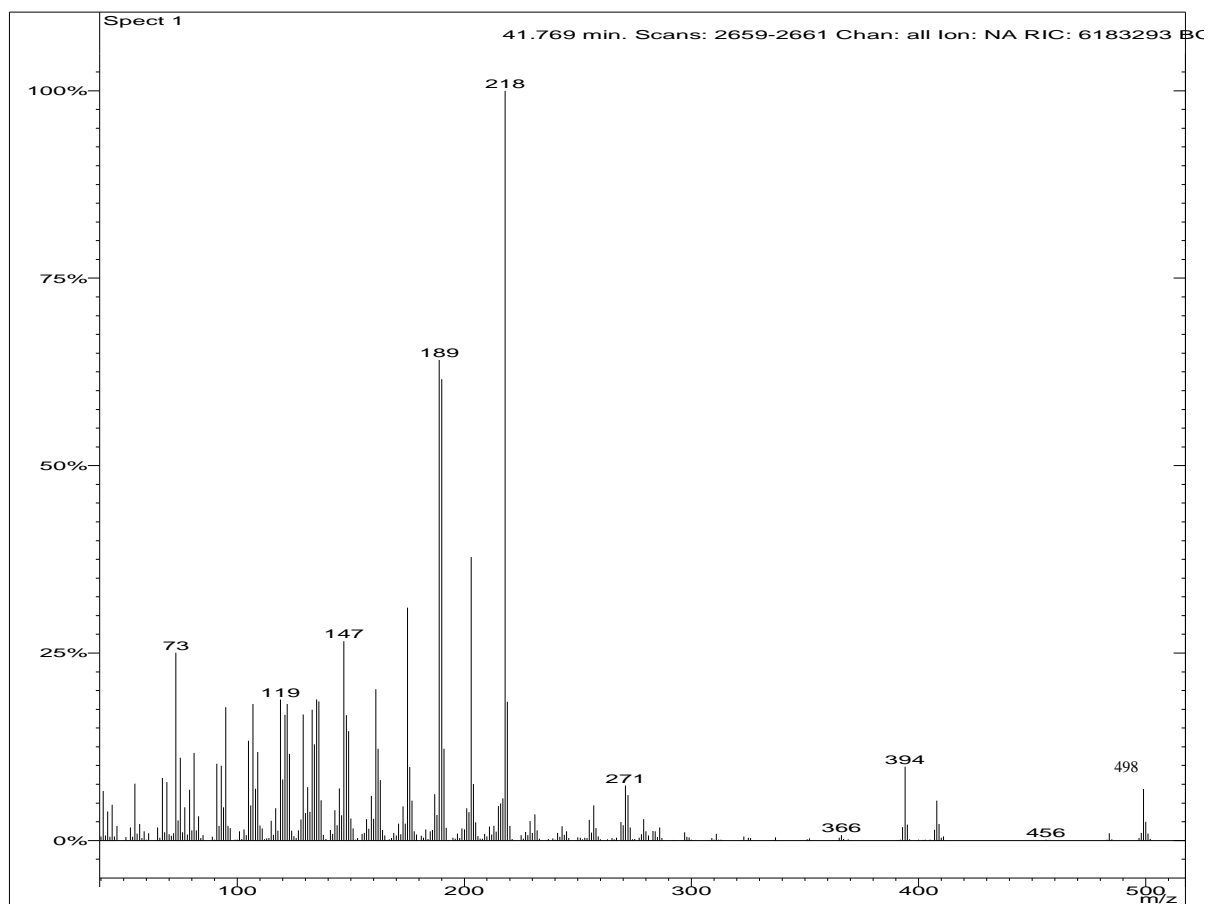
### 3-*epi*- $\alpha$ -amyrine TMS

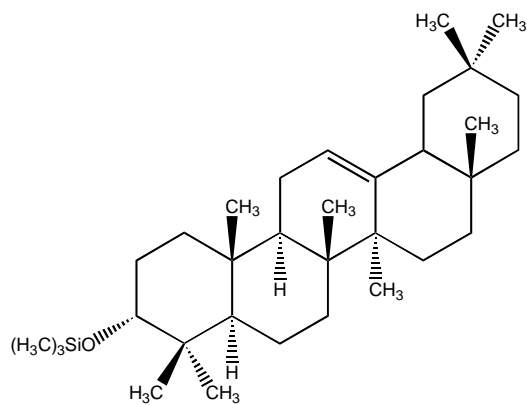
$C_{33}H_{58}OSi$

498 g.mol<sup>-1</sup>

Isolated compound

Gradient 1	tr = 40.96 min
Gradient 2	tr = 33.02 min





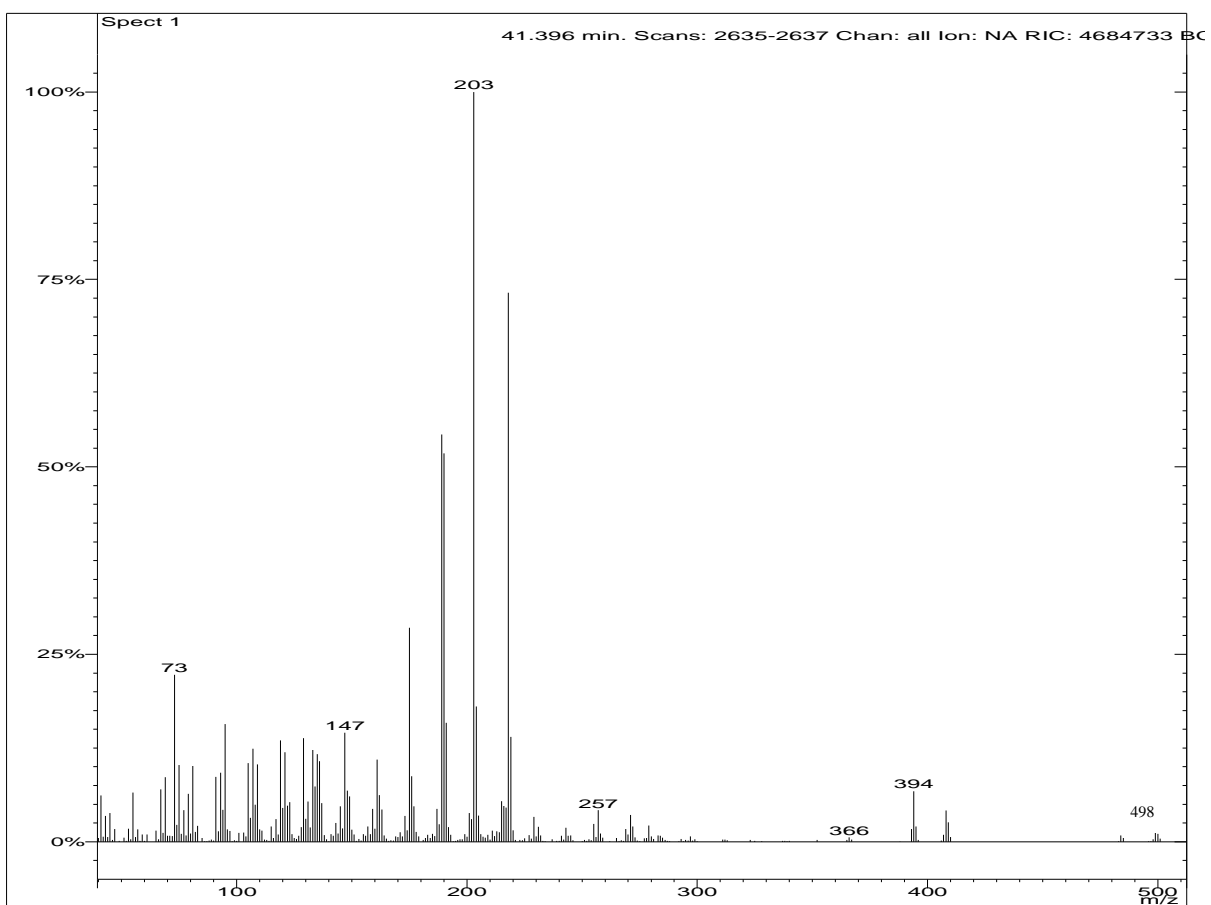
**3-*epi*- $\beta$ -amyrine**

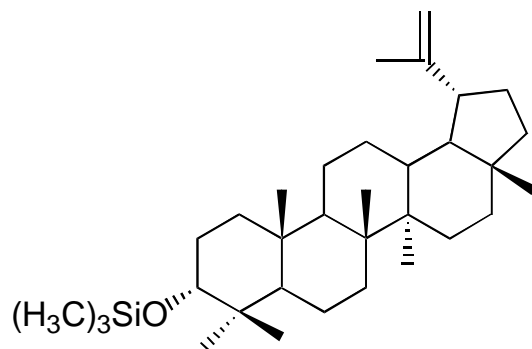
$\text{C}_{33}\text{H}_{58}\text{OSi}$

$498 \text{ g}\cdot\text{mol}^{-1}$

Isolated product

Gradient 1	tr = 40.50min
Gradient 2	tr = 32.53min

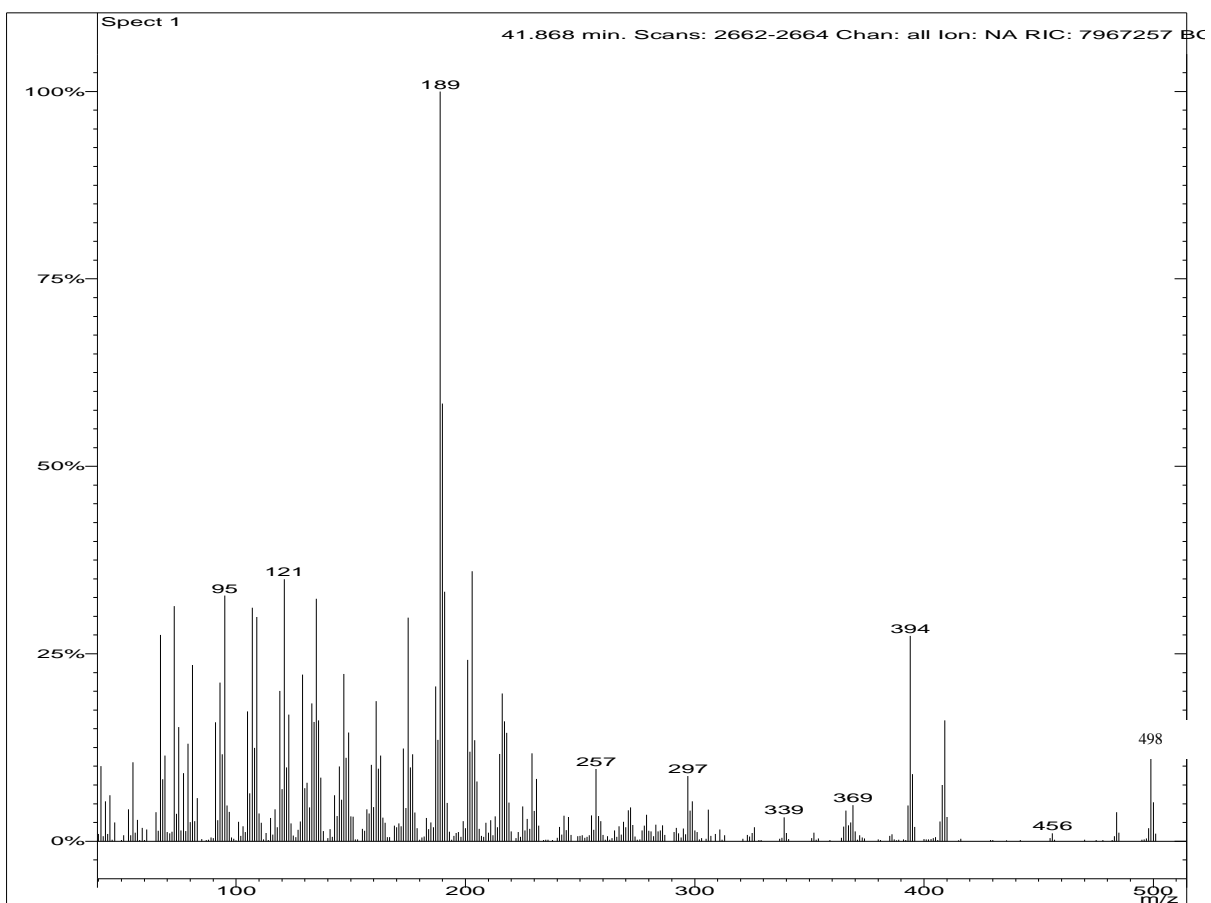


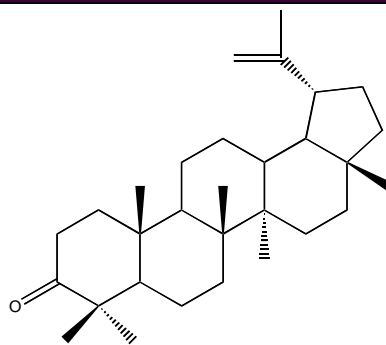


### 3-*epi*-lupeol TMS

$C_{33}H_{58}OSi$   
 $498 \text{ g}\cdot\text{mol}^{-1}$   
 Isolated product

Gradient 1	tr = 41.12 min
Gradient 2	tr = 33.22 min





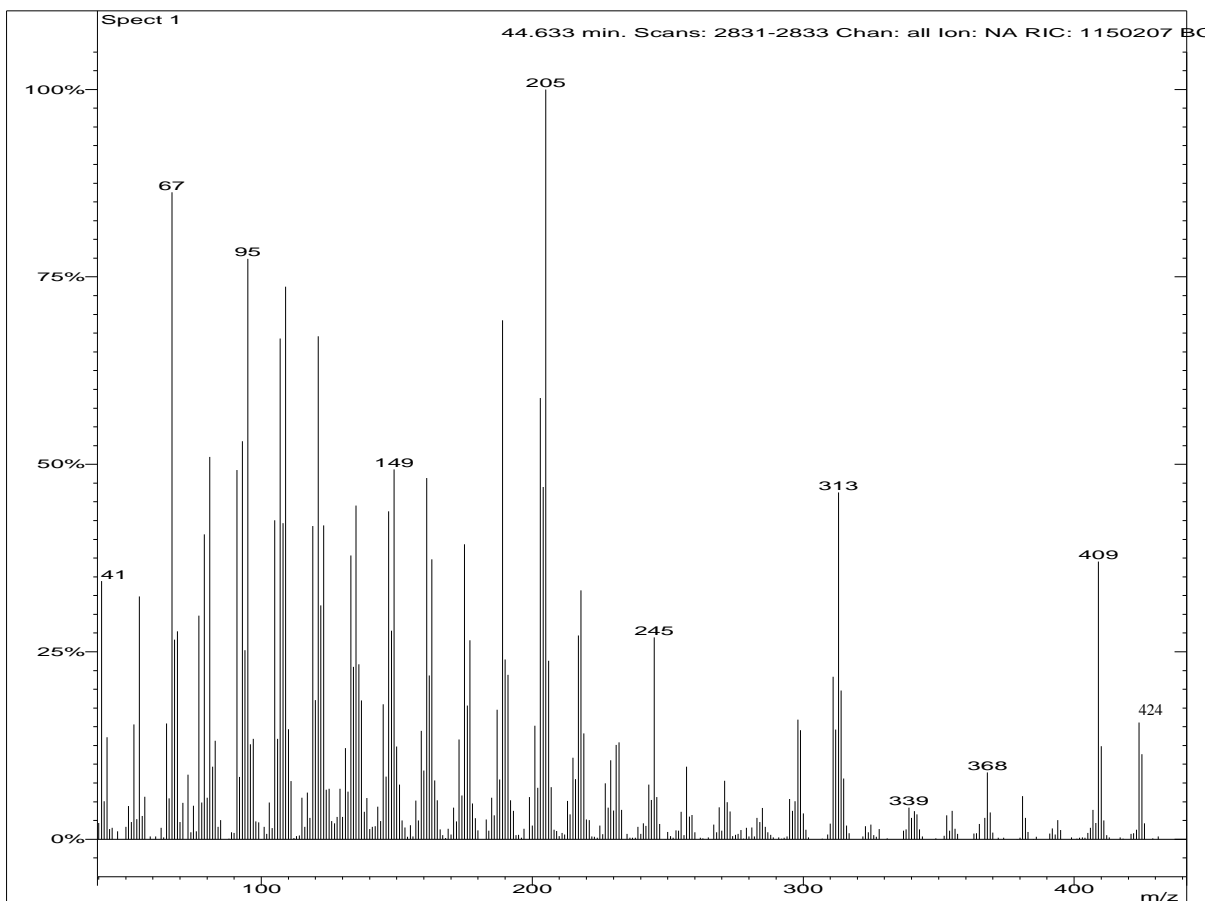
**Lupenone**

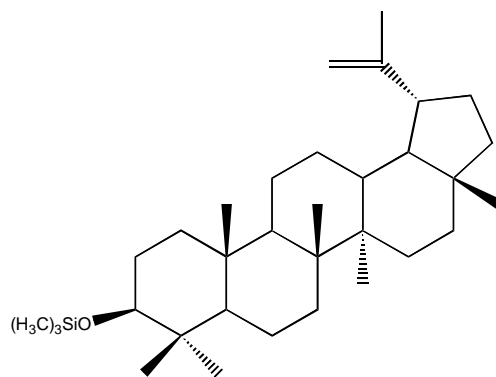
$C_{30}H_{48}O$

$424 \text{ g}\cdot\text{mol}^{-1}$

Commercial product : BCP intruments

Gradient 1	tr = 43.92 min
Gradient 2	tr = 37.85 min





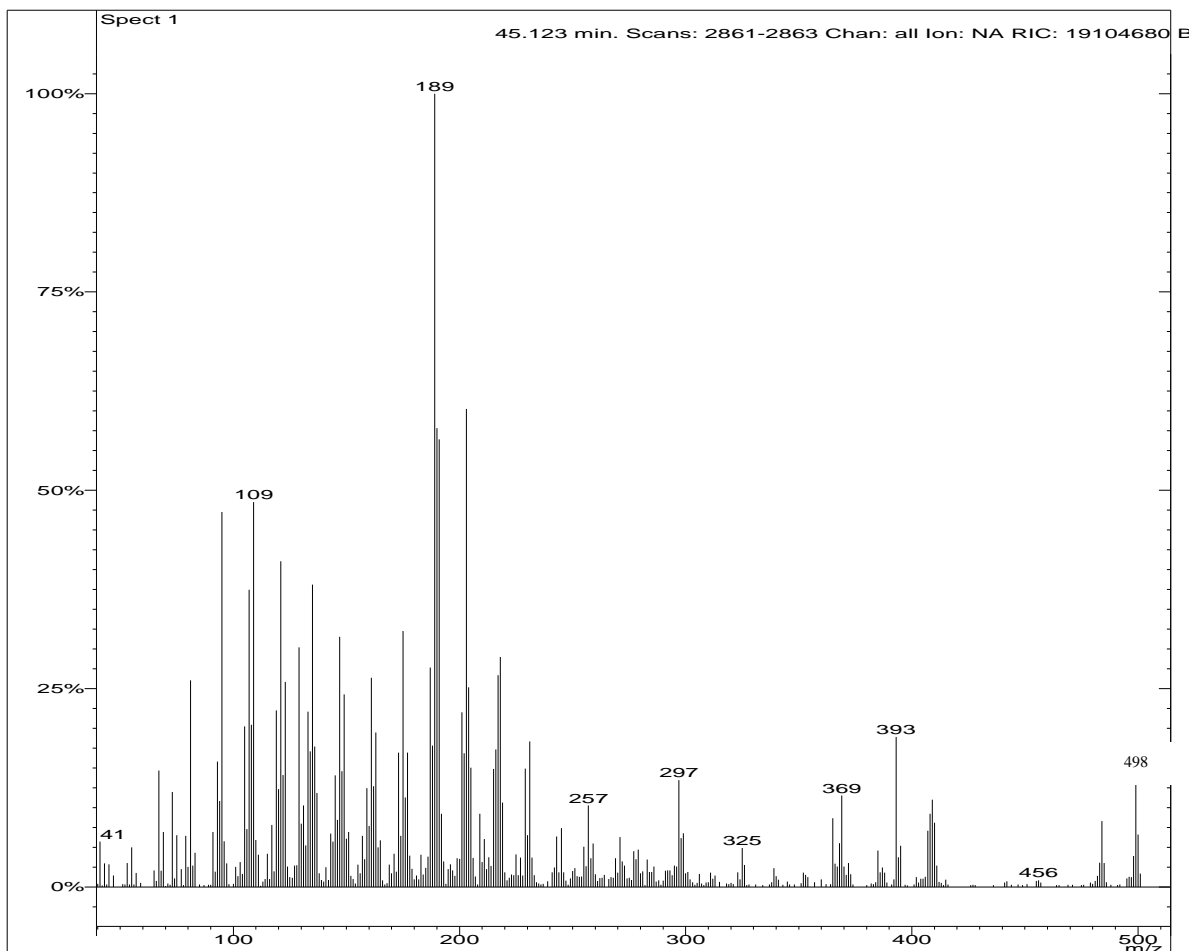
**Lupeol TMS**

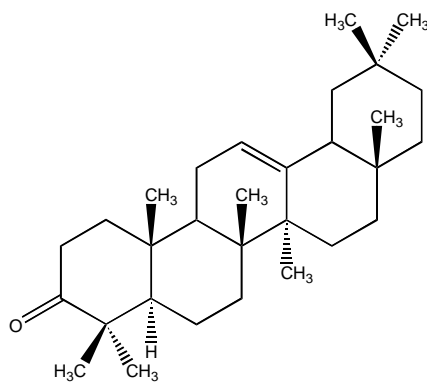
$C_{33}H_{58}OSi$

498 g.mol<sup>-1</sup>

Commercial product: Extrasynthèse

Gradient 1	tr = 43.67 min
Gradient 2	tr = 36.71 min



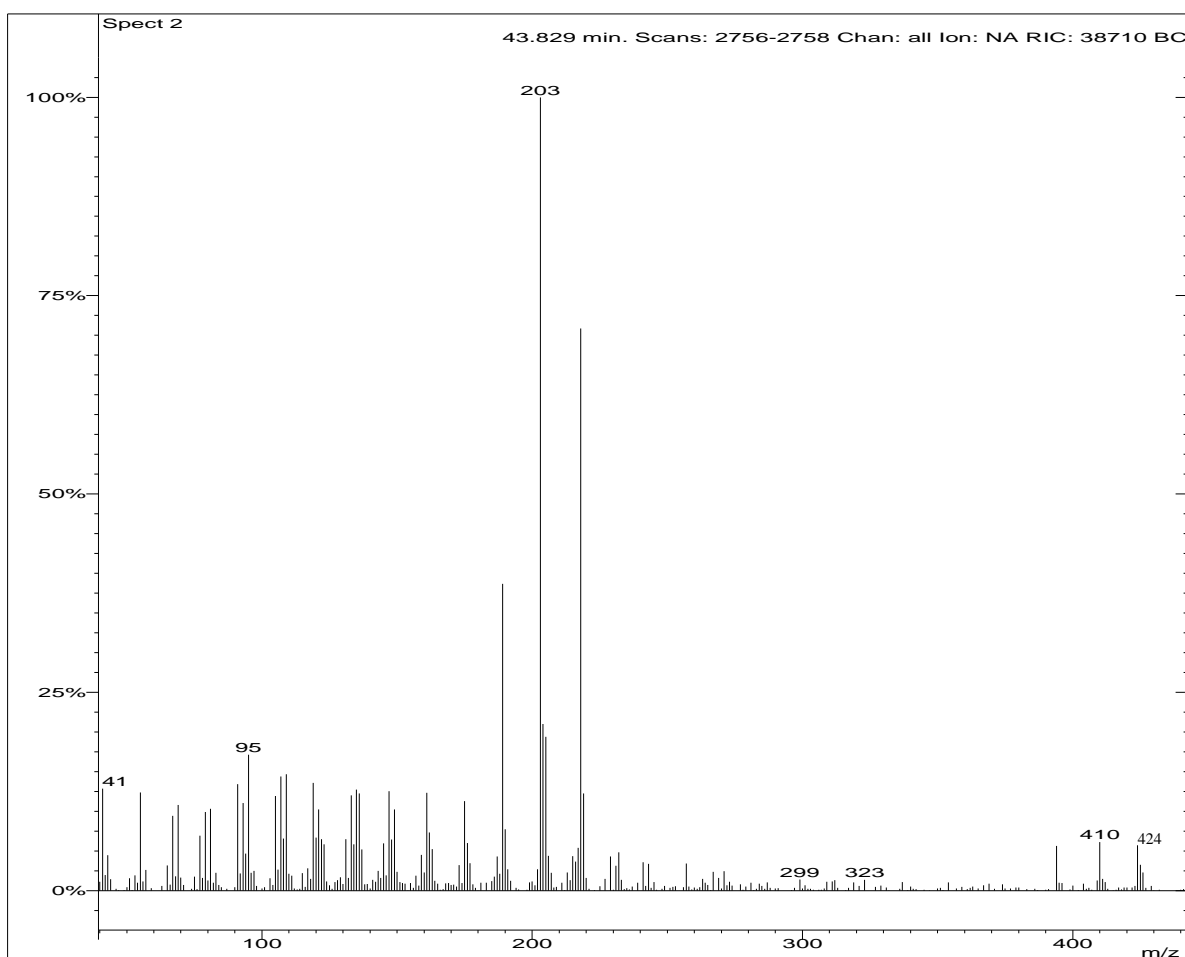


### $\beta$ -amyrone

$C_{30}H_{48}O$   
 $424 \text{ g}\cdot\text{mol}^{-1}$

Commercial product : BCP instruments

Gradient 1	tr = 42.48 min
Gradient 2	tr = 34.76 min





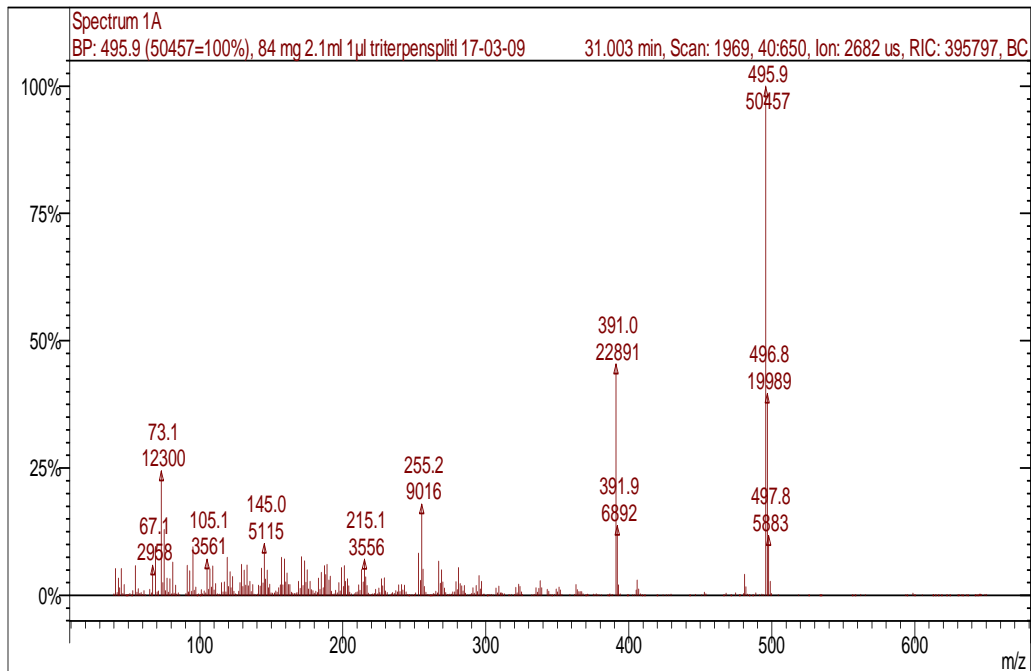
## Mass Spectra of the unknown compounds from certified resins

### Retention time under gradient 2

*B. bipinnata* and *B. stenophylla* markers

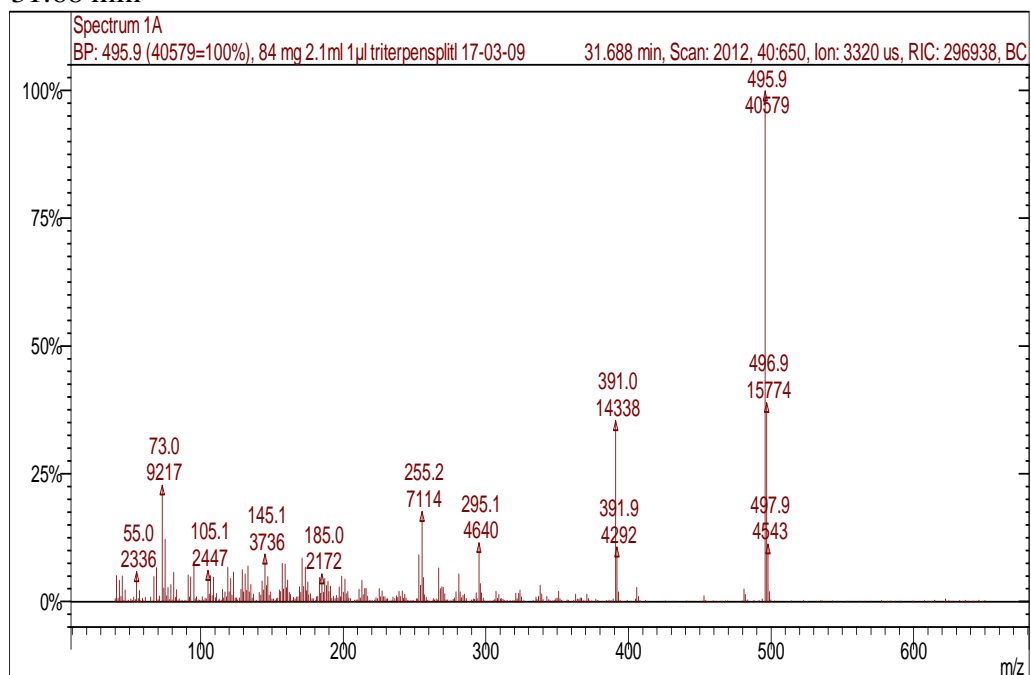
BS1

tr = 31.00 min



BS2

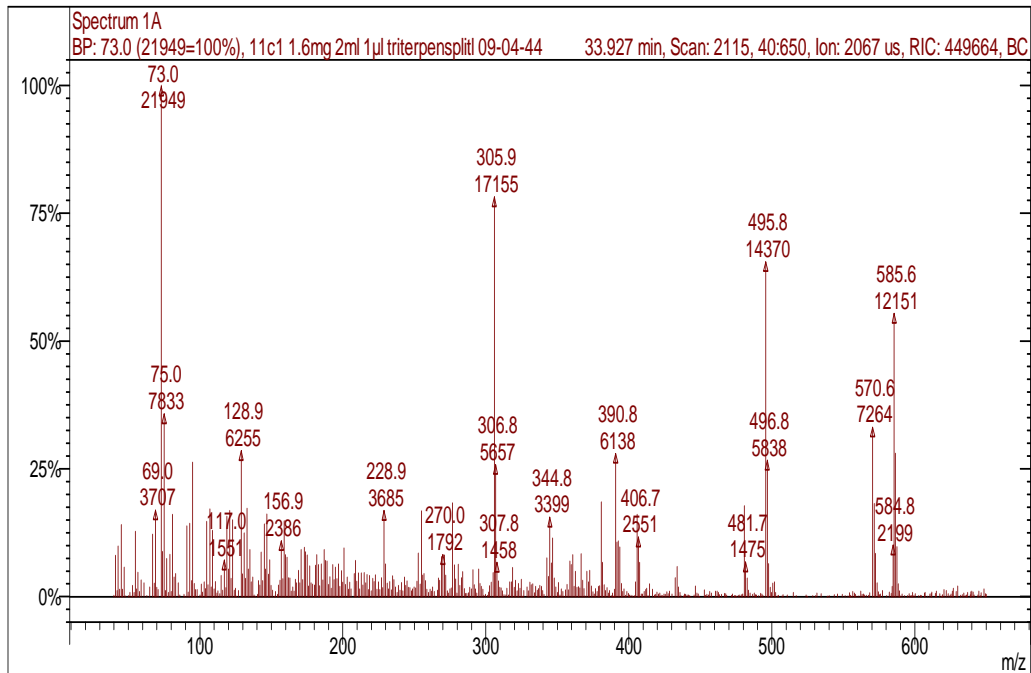
tr = 31.68 min



*B. bipinnata* and *B. stenophylla* markers

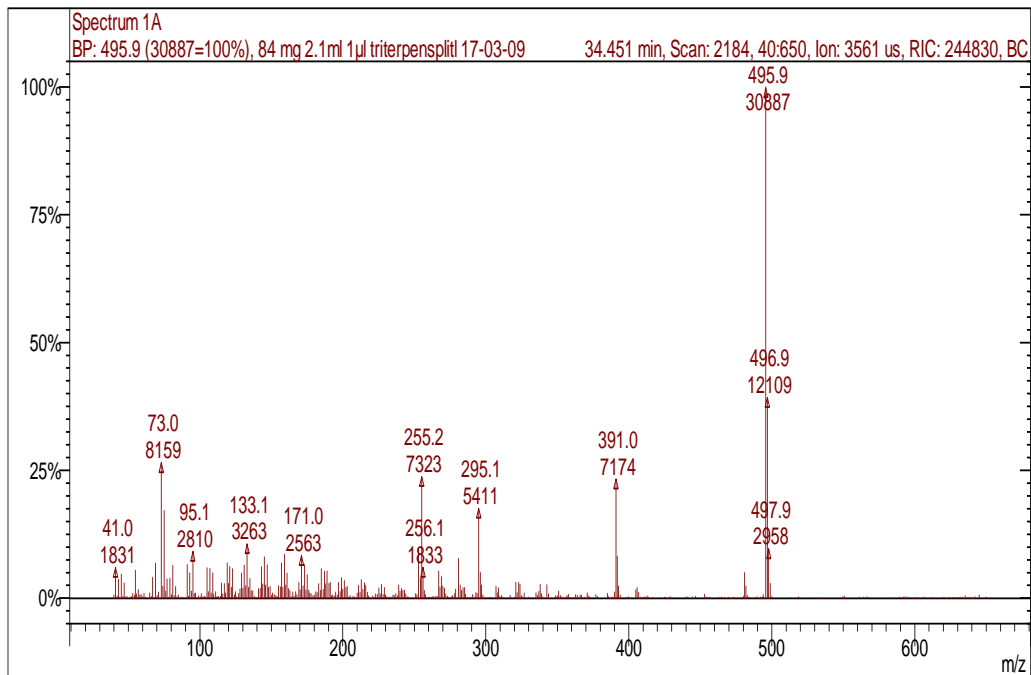
**BS3**

tr = 33.92 min



**BS4**

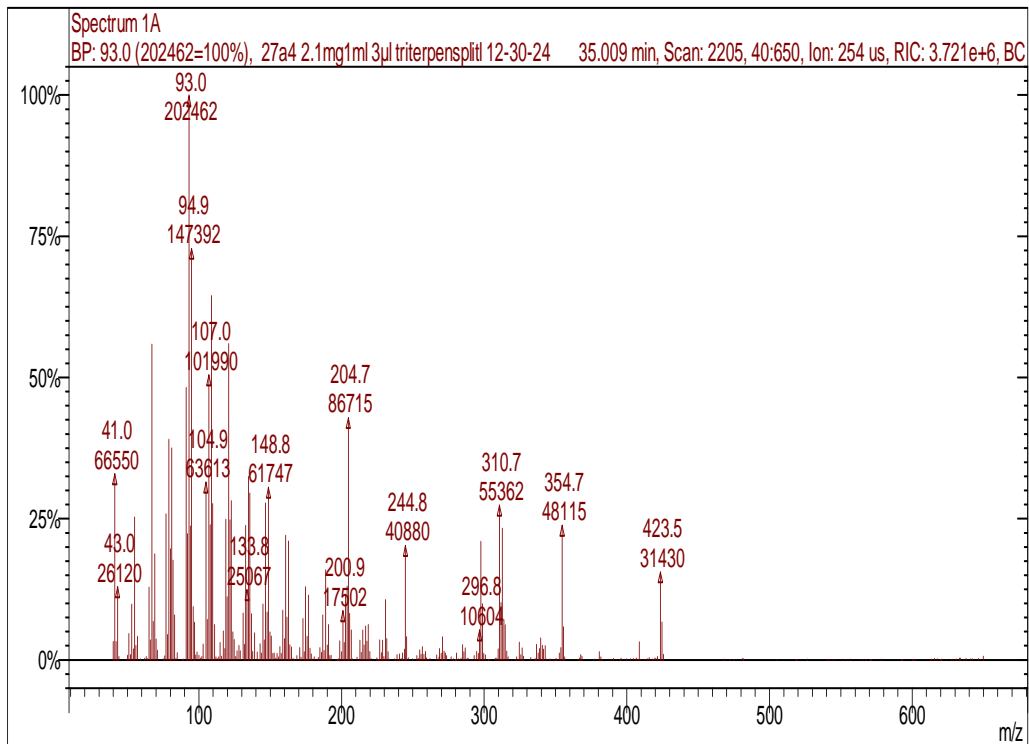
tr = 34.45 min



**Fig 118 *B.stenophylla*-*B.bipinnata* molecular markers  
*B. excelsa* markers**

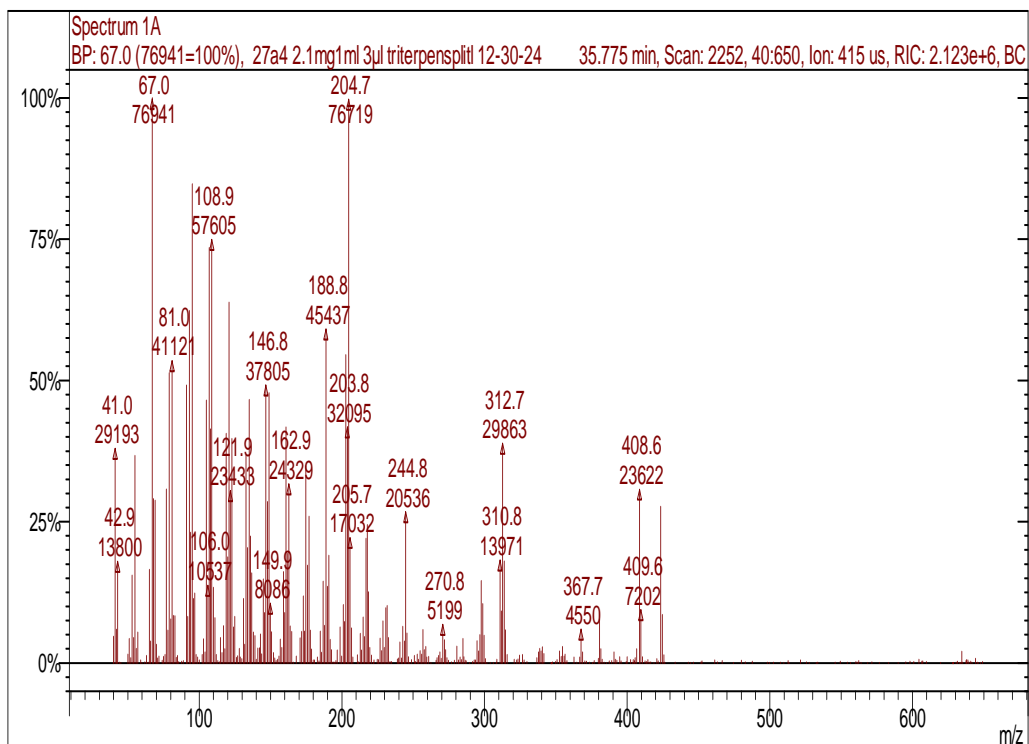
**E1**

tr = 35.00 min



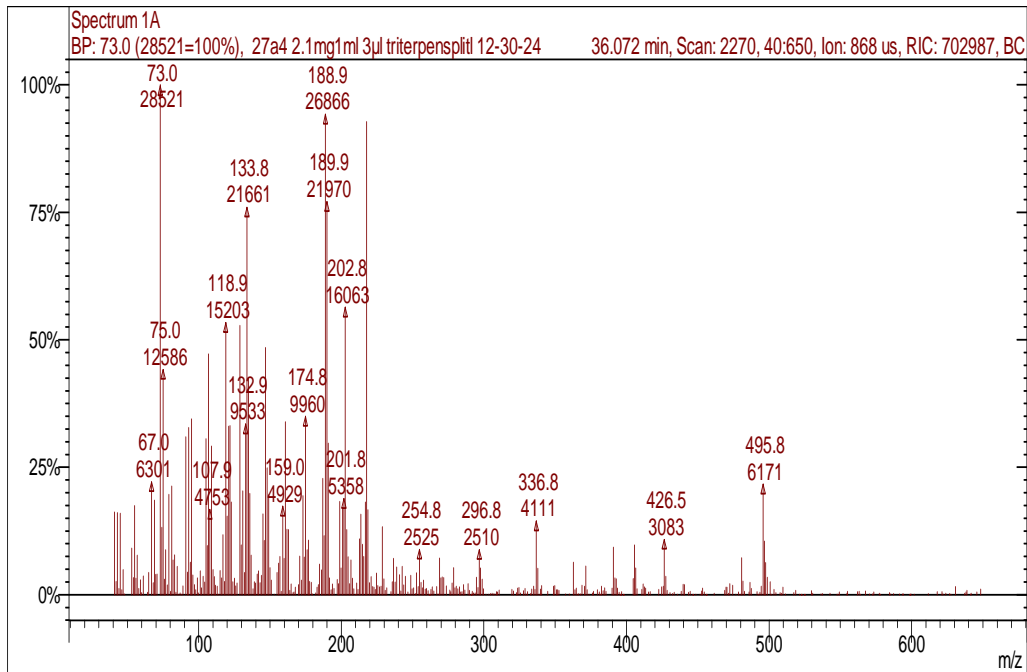
**E2**

tr = 35.77 min



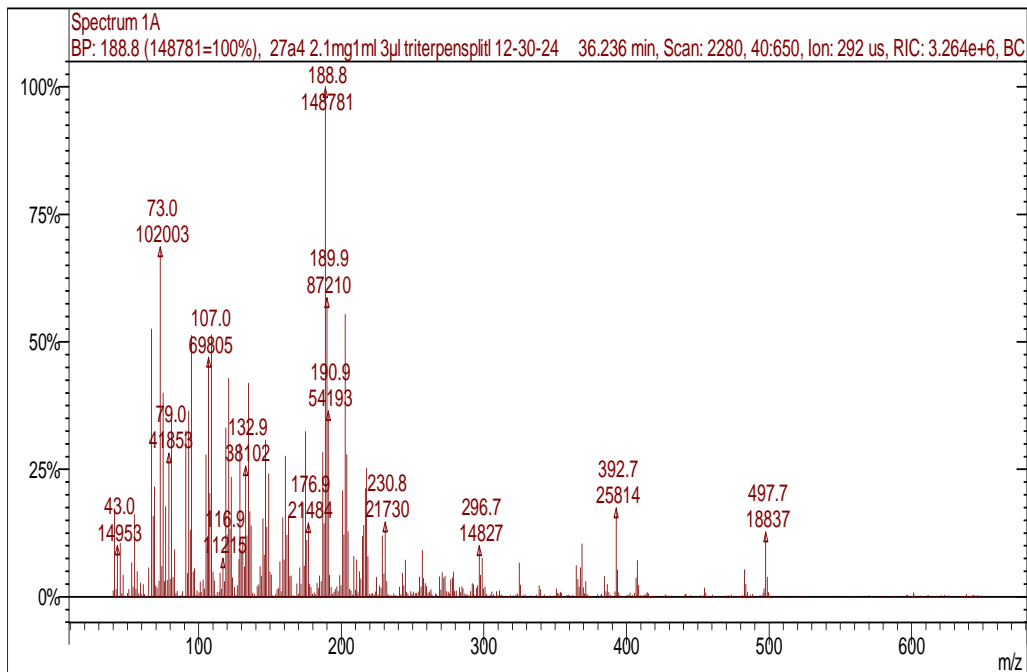
*B. excelsa* markers

**E3**  
tr = 36.07 min



**E4**

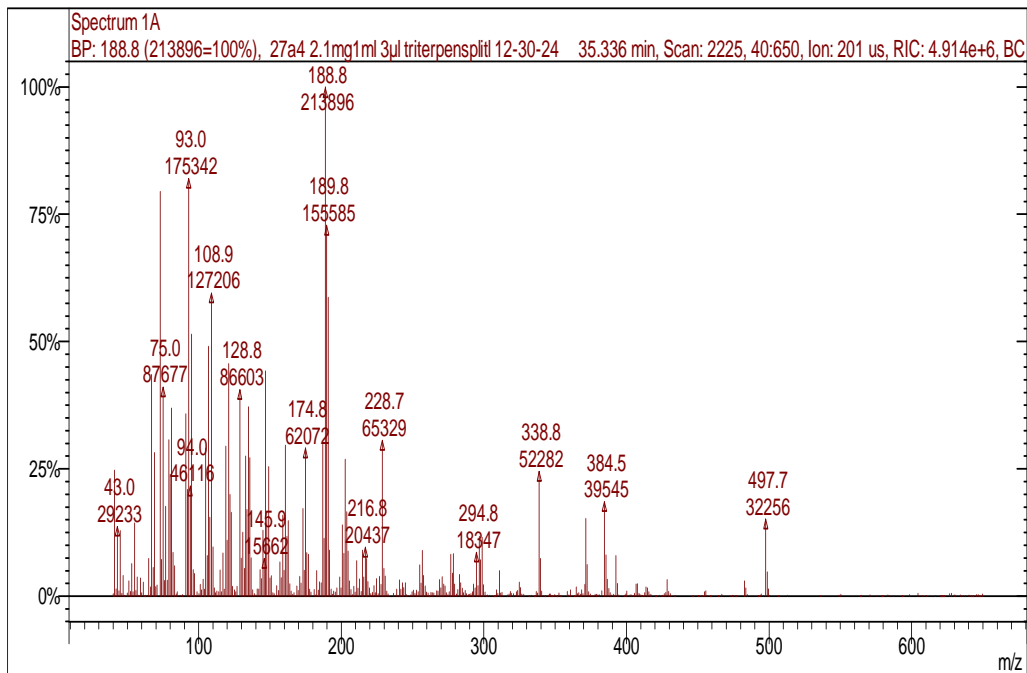
tr = 36.23 min



*B. excelsa*-*B. laxiflora* marker

**EL1**

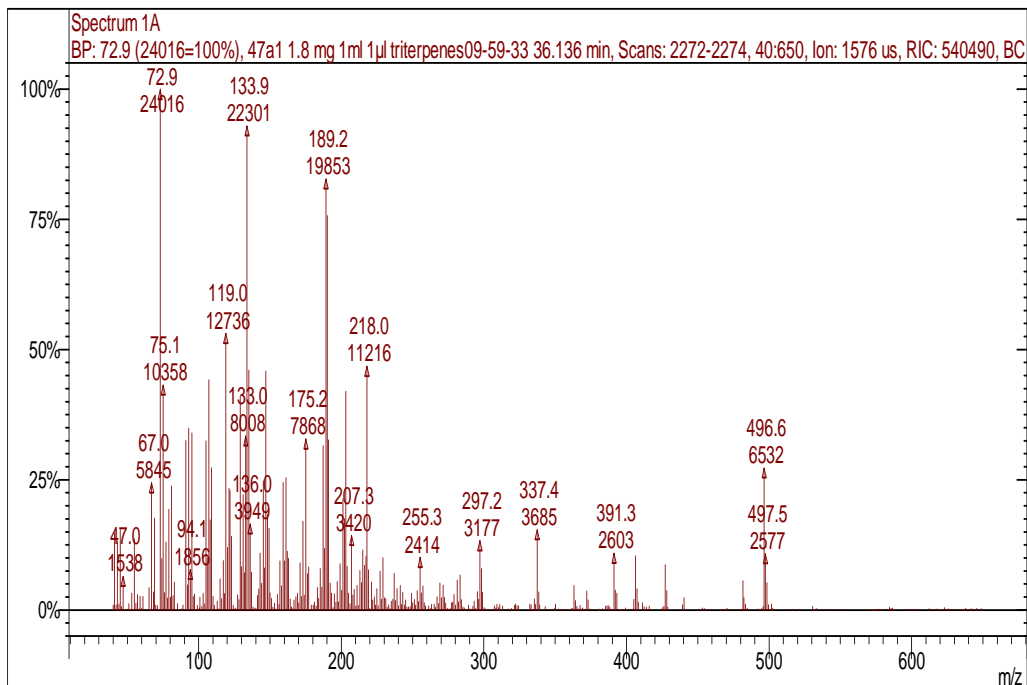
tr = 35.33 min



***B. laxiflora* markers**

**L1**

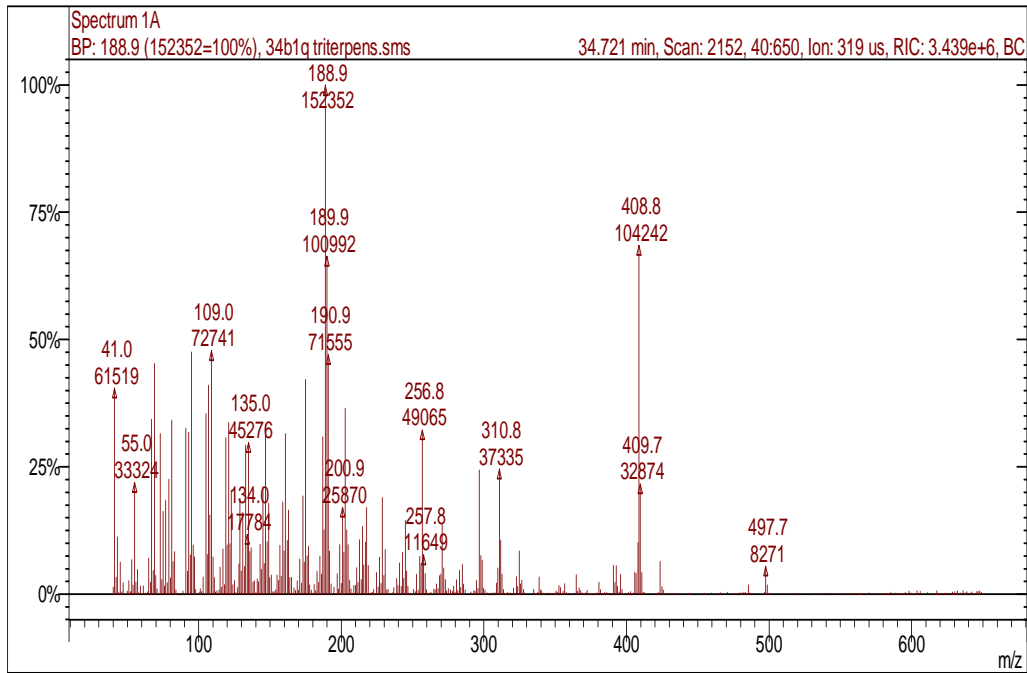
tr = 36.13 min



**Fig 119 *B. laxiflora* and *B. excelsa* molecular markers**

**G1**

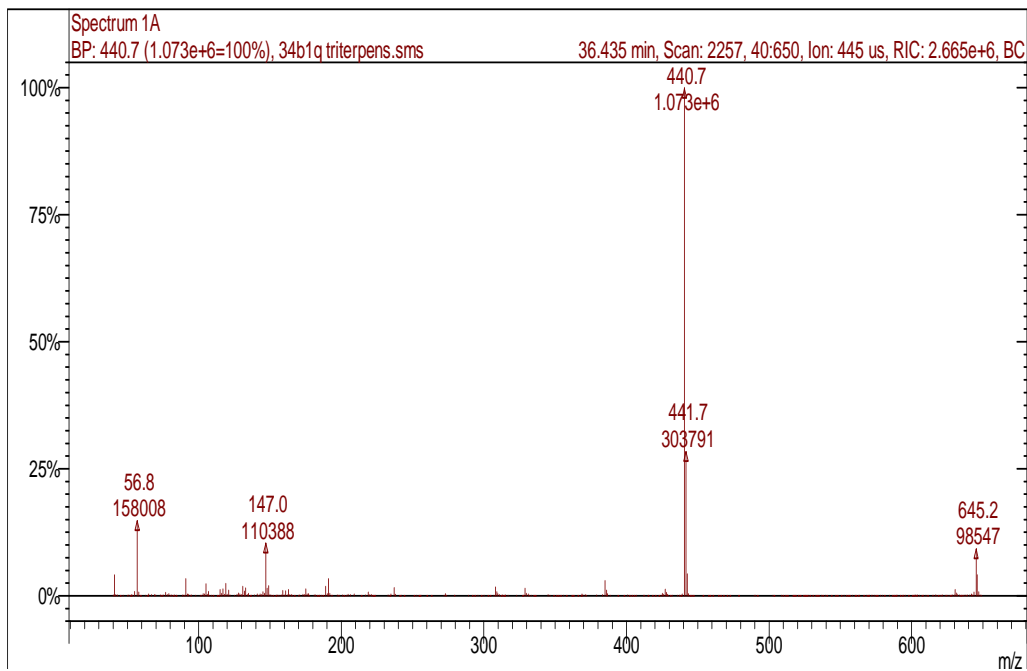
tr = 34.72 min



***B. grandifolia* markers**

**G2**

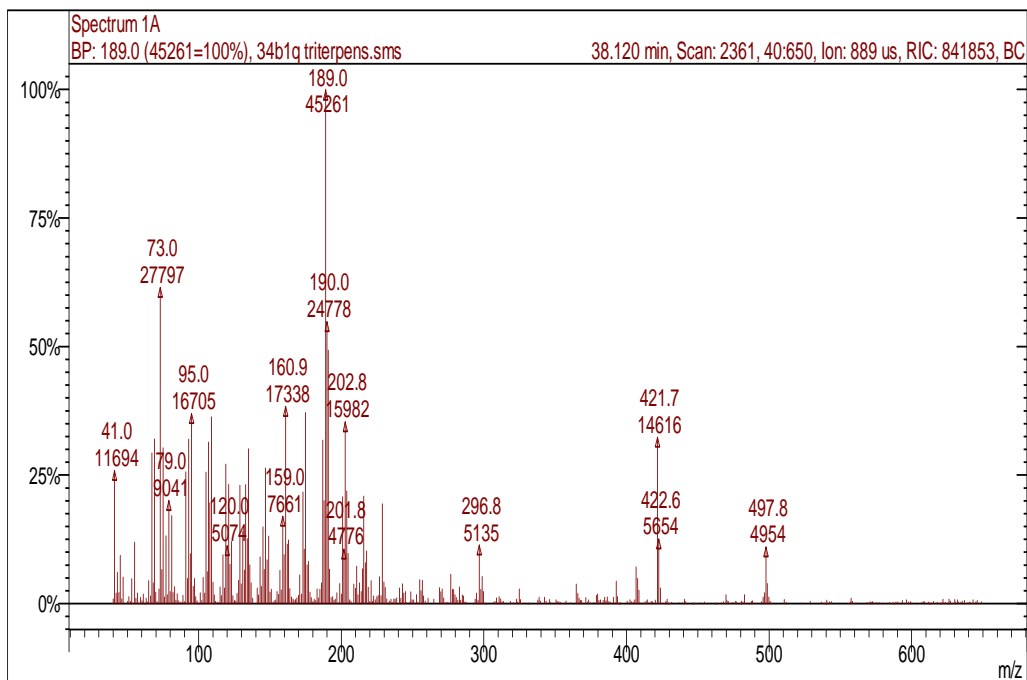
tr = 36.43 min



***B. grandifolia* markers**

**G3**

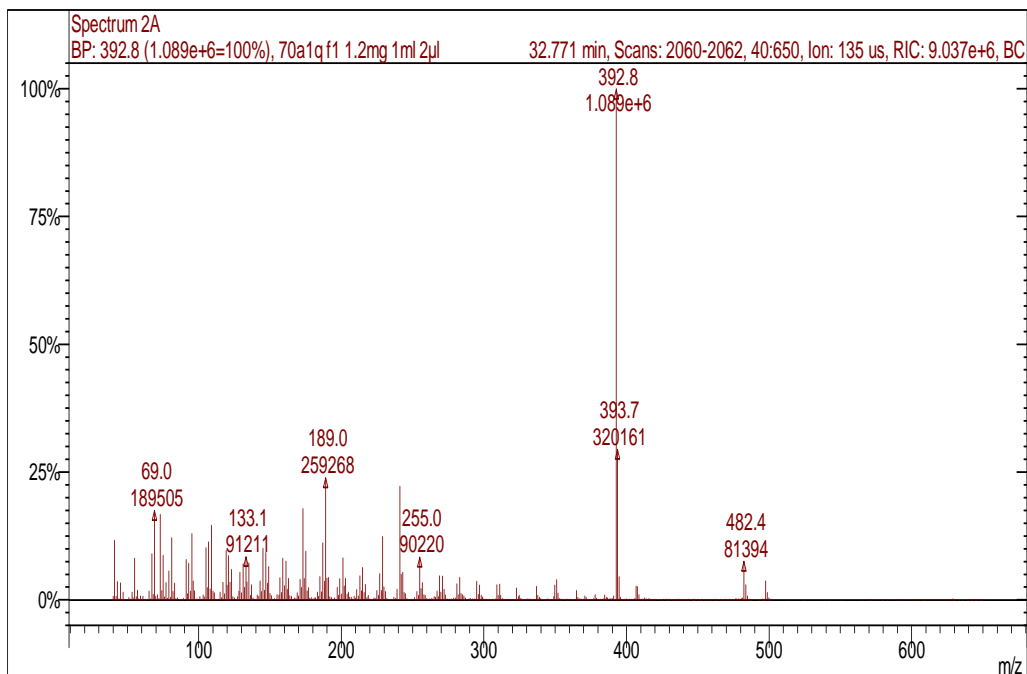
tr = 38.12 min



***B. grandifolia-simaruba* markers**

**GSI**

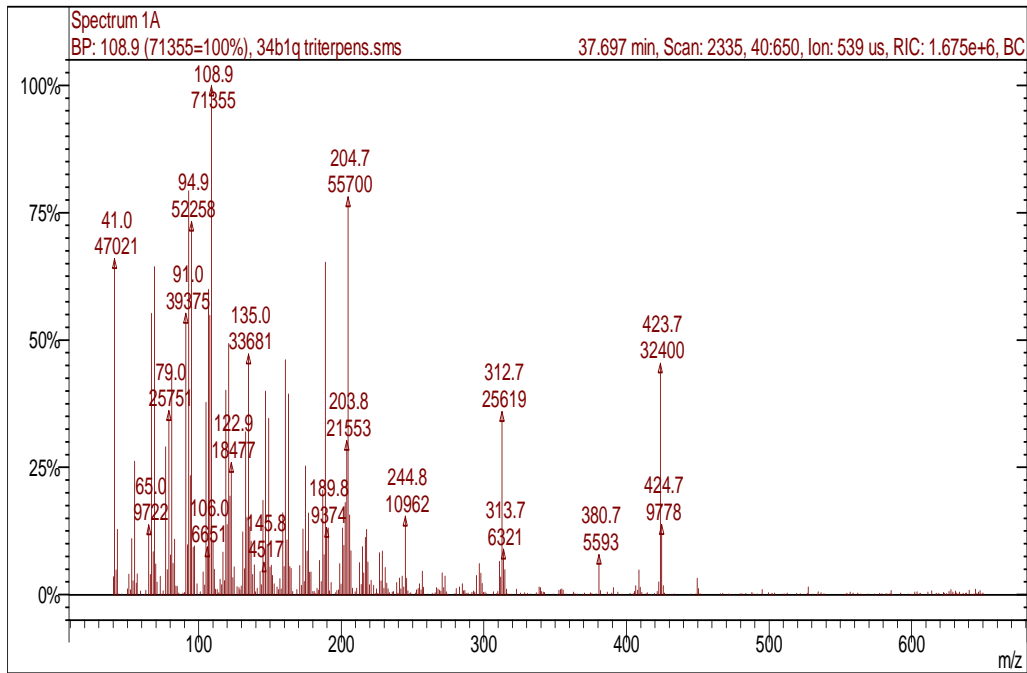
tr = 32.77 min



***B. grandifolia* markers**

**GS2**

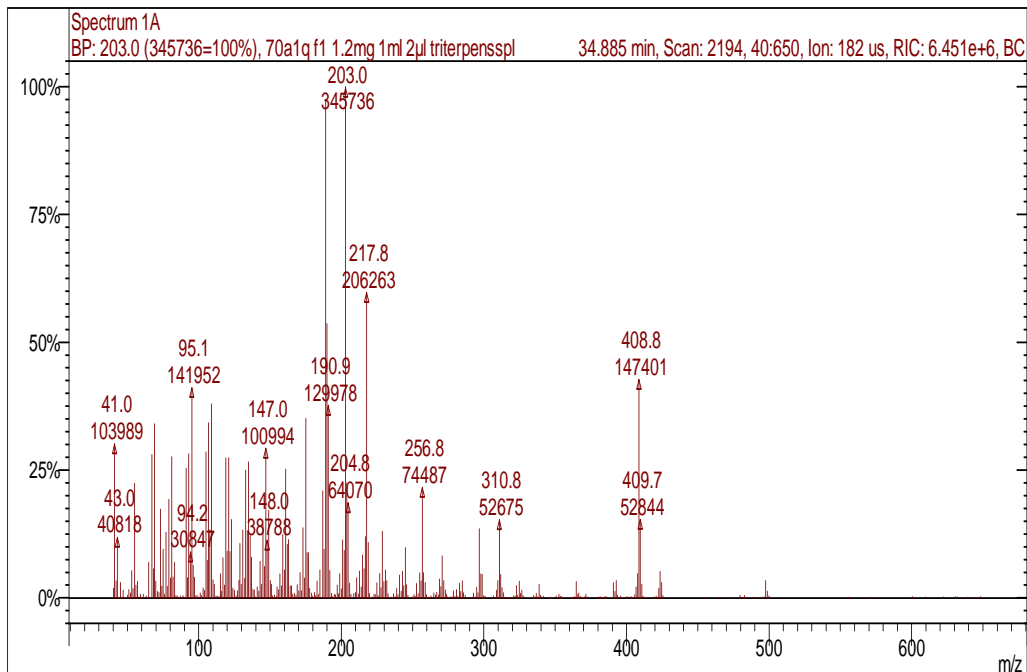
tr = 37.69 min



***B. simaruba* markers**

**S1**

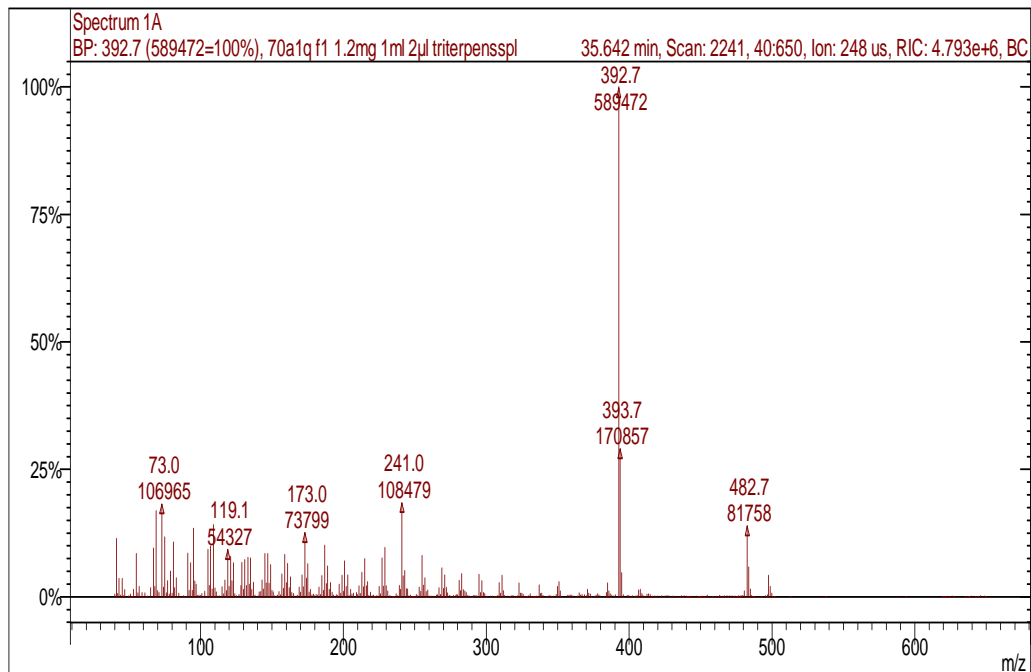
tr = 34.88 min



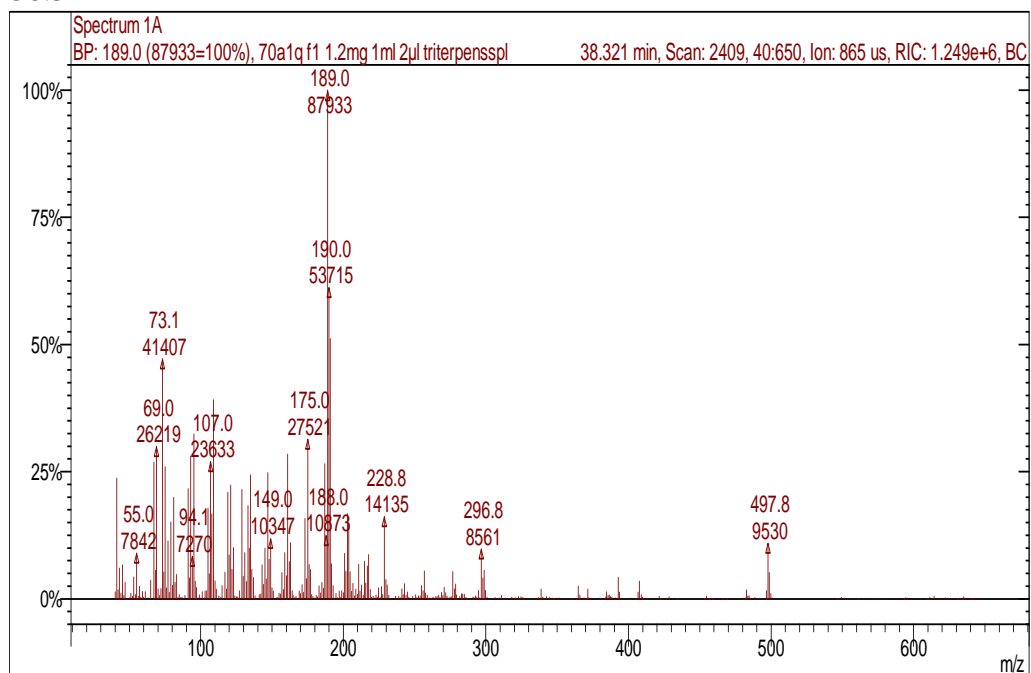


**B. simaruba** markers**S2**

tr = 35.64 min

**S3**

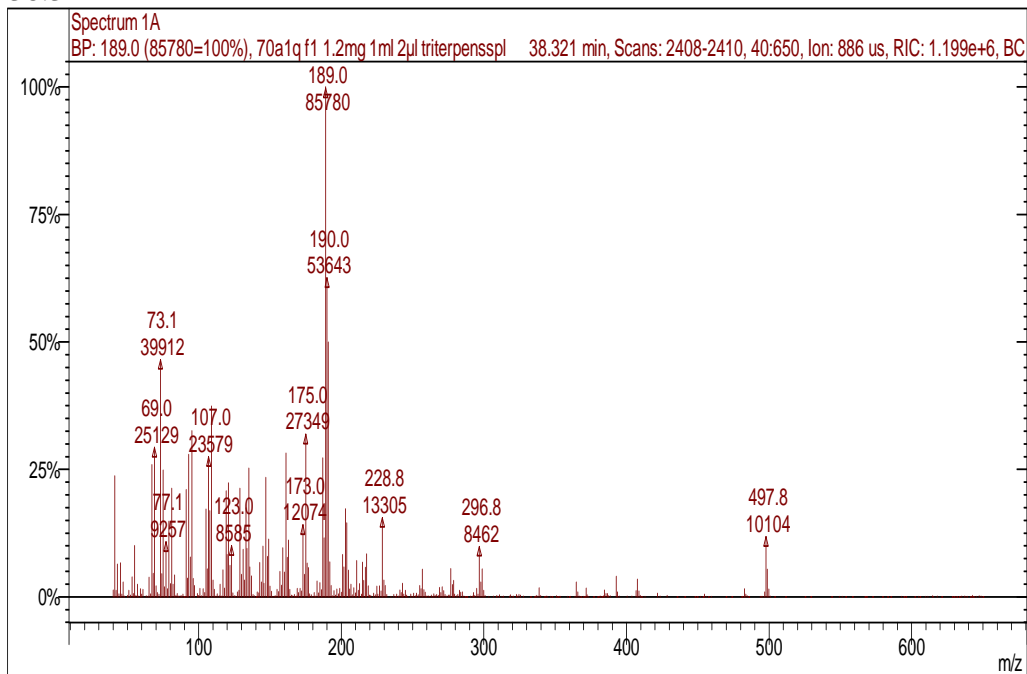
tr = 38.32 min



**B. simaruba markers**

**S4**

tr = 38.32min

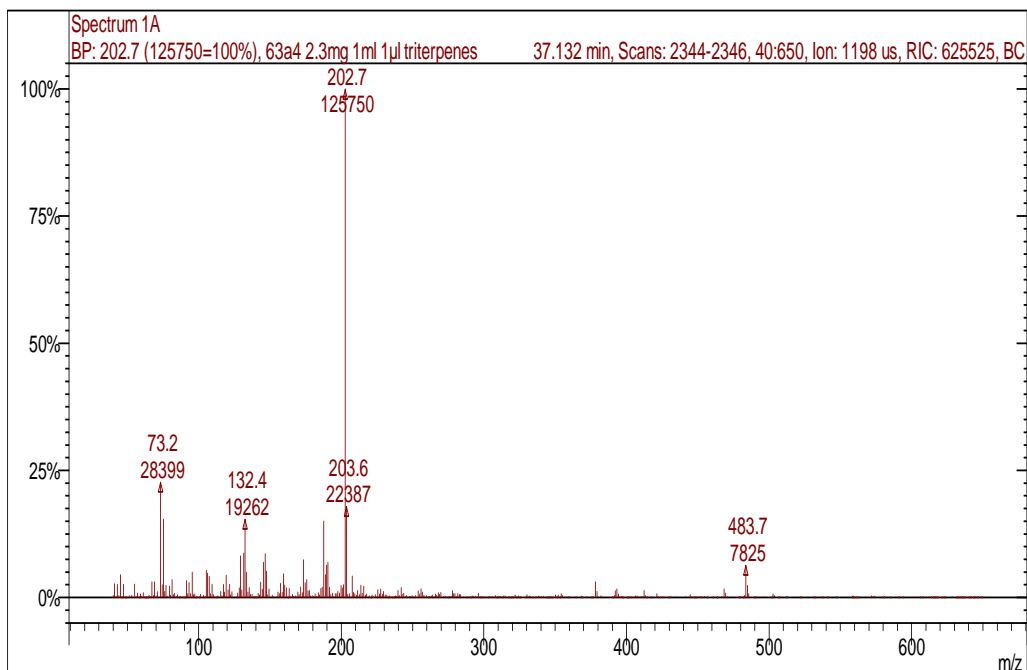


**Fig 120 B. simaruba and B. grandifolia mass spectra of molecular markers**

**B. penicillata markers**

**P1**

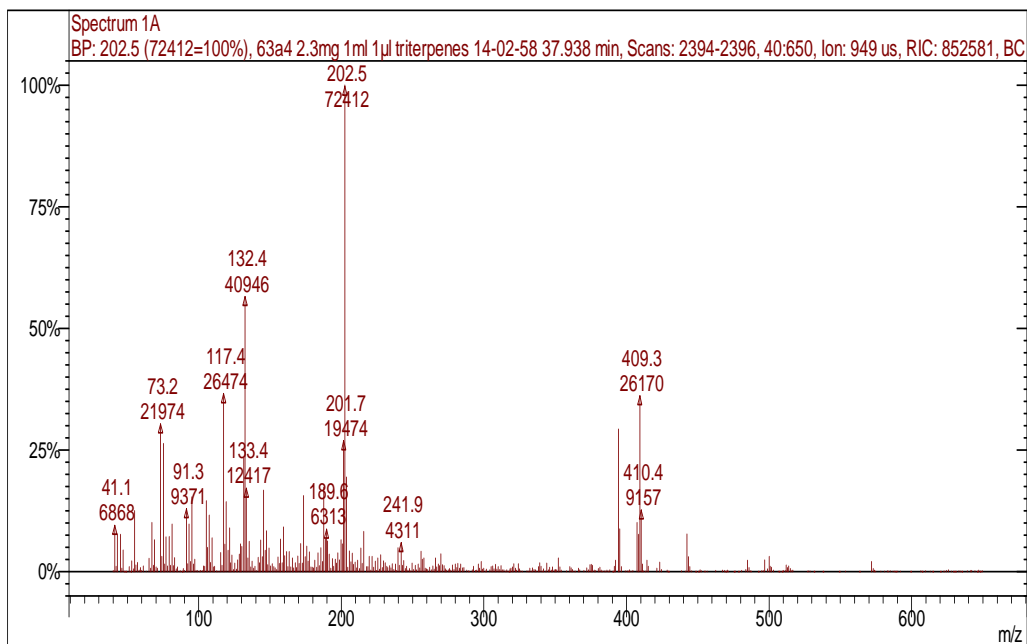
tr = 37.13 min



*B. penicillata* markers

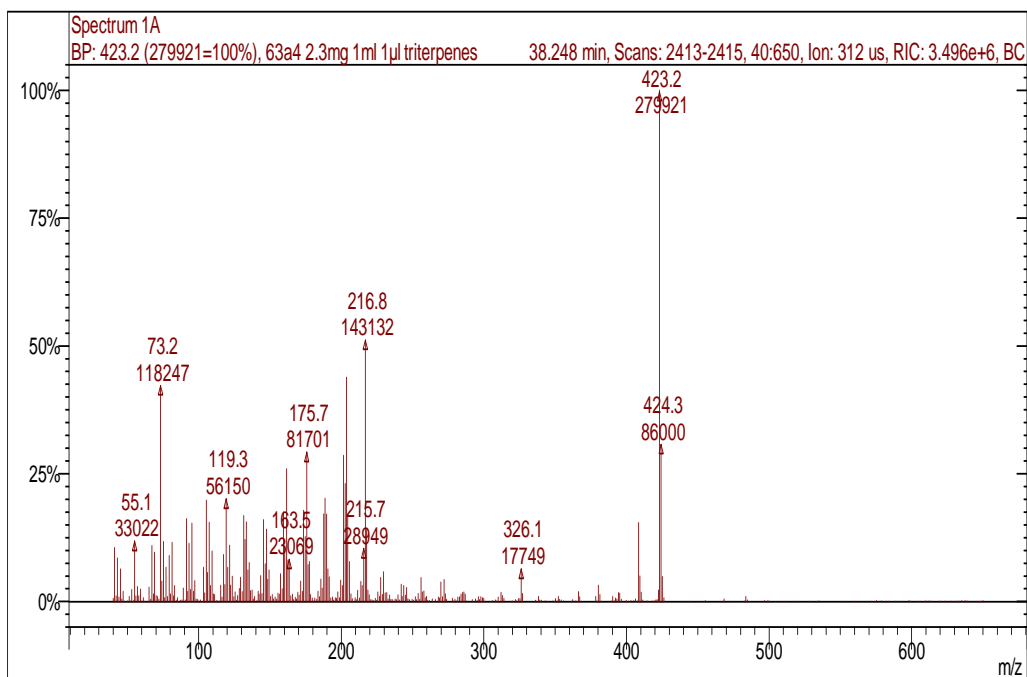
P2

tr = 37.93 min



P3

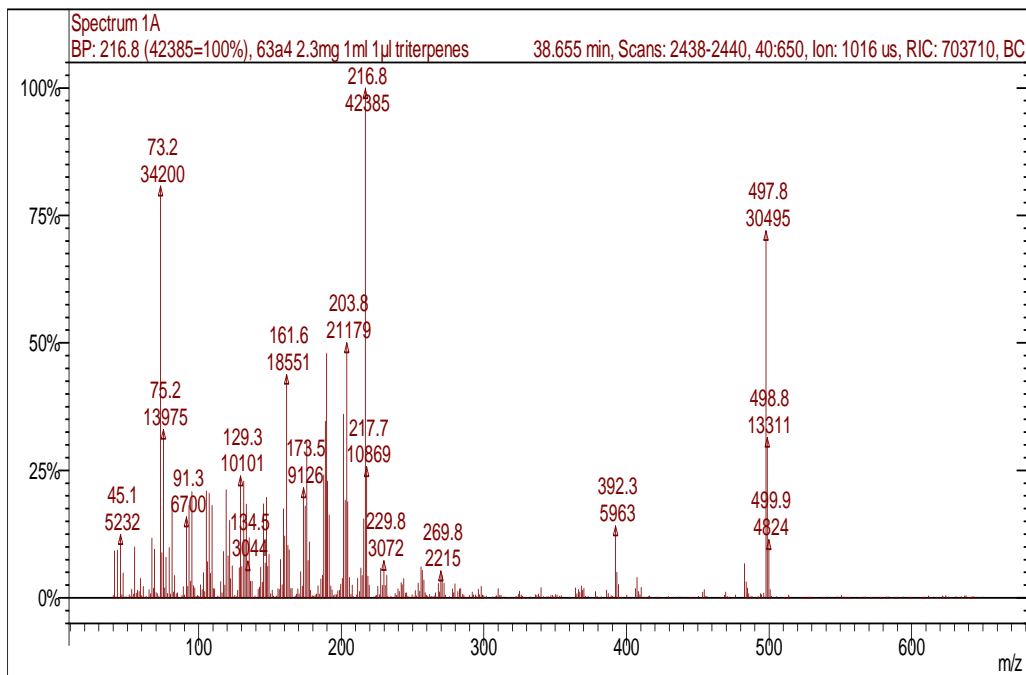
tr = 38.25 min



*B. penicillata* markers

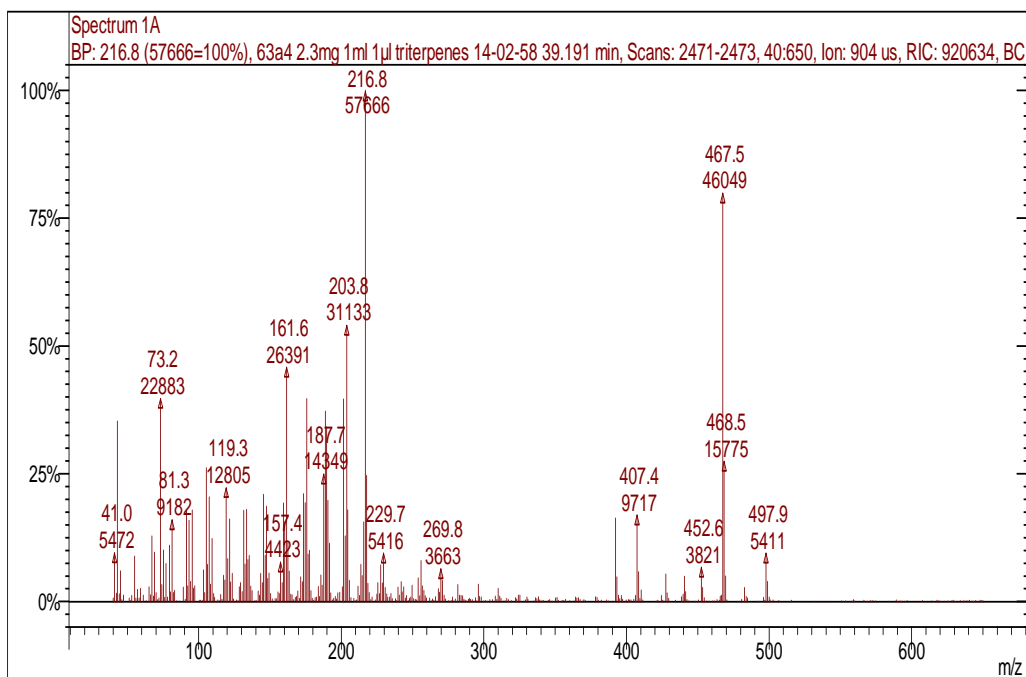
P4

tr = 38.65 min



P5

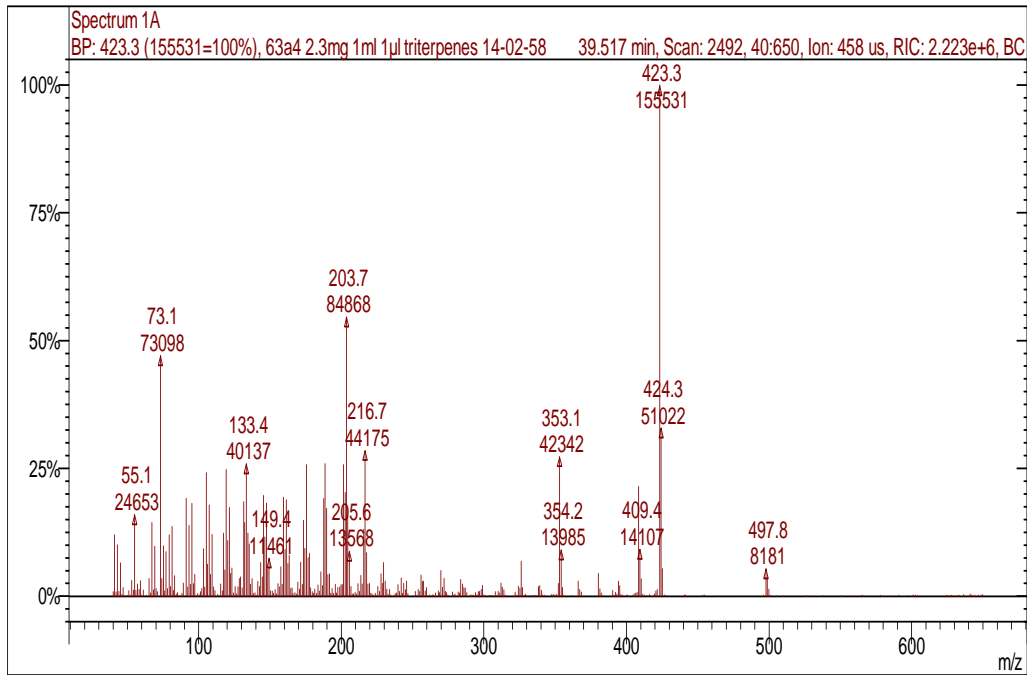
tr = 39.19 min



*B. penicillata* markers

P6

tr = 39.51 min



P7

tr = 40.00 min

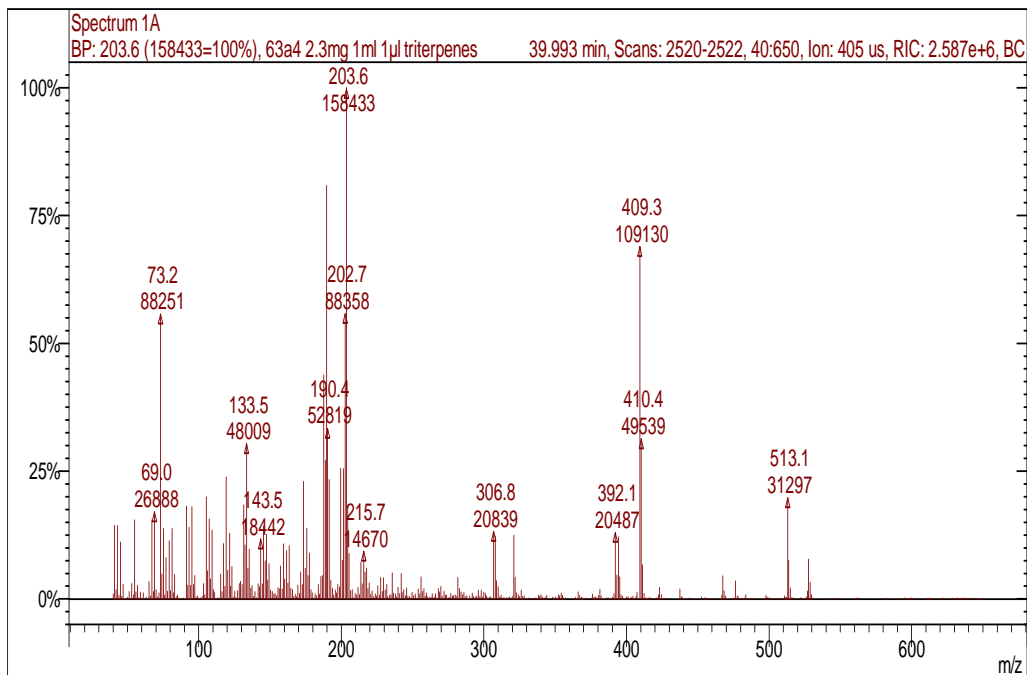
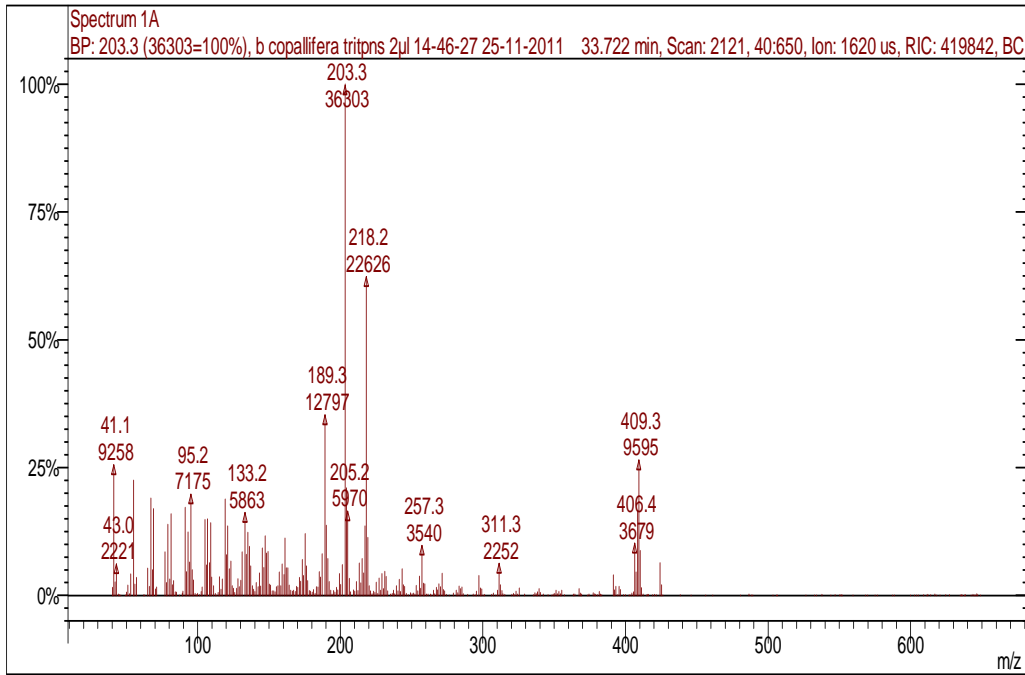


Fig 121 *B. penicillata* mass spectra of molecular markers

*B. copallifera* markers

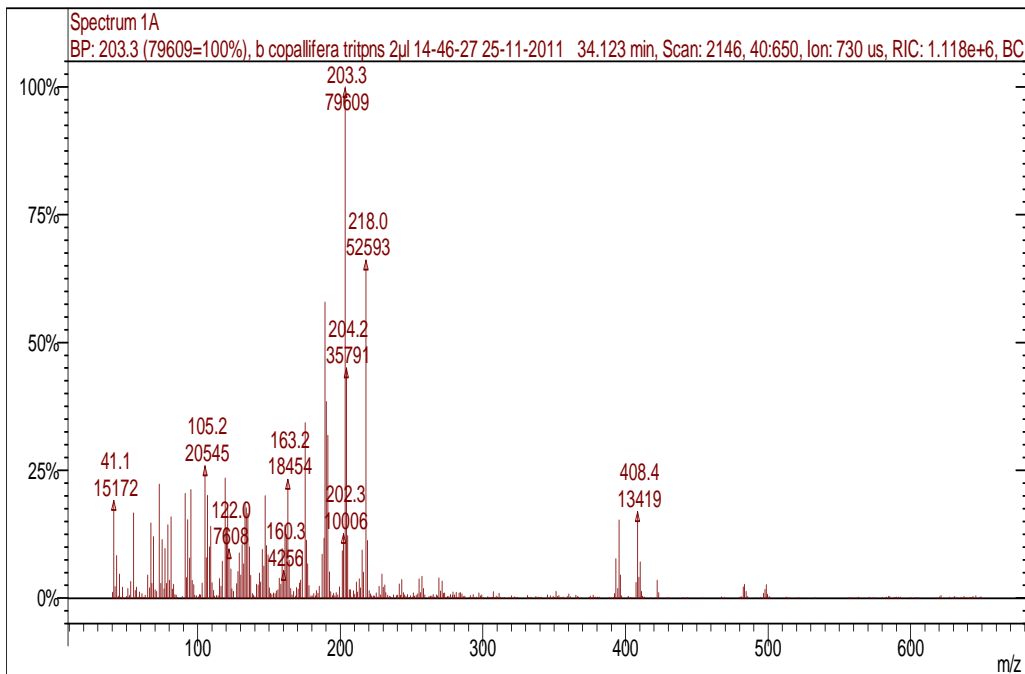
C1

tr = 33.72 min



C2

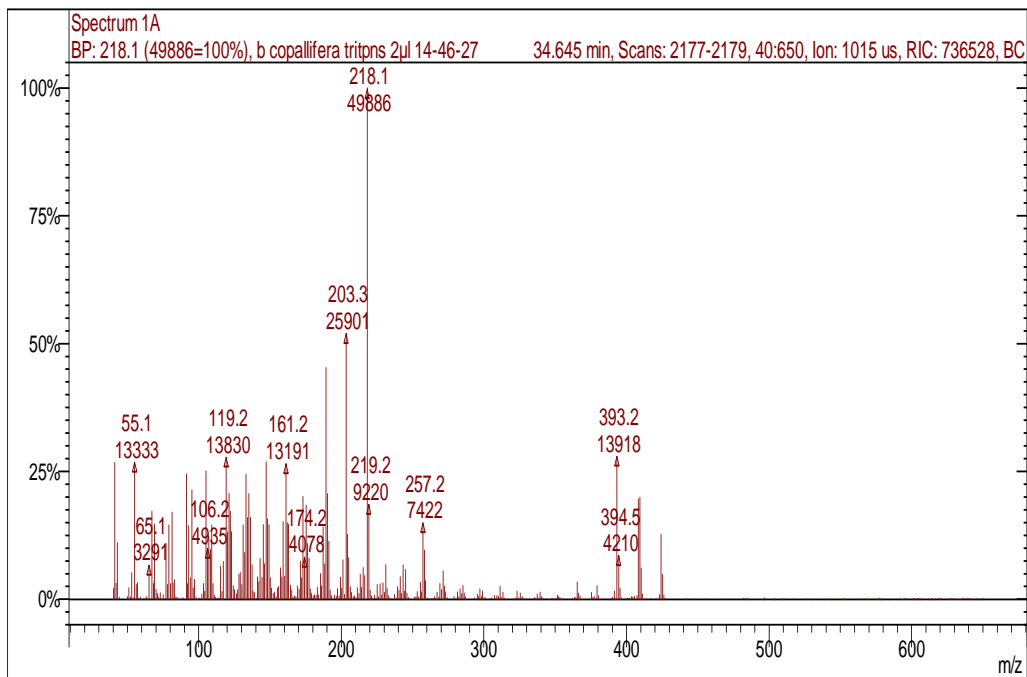
tr = 34.12 min



*B. copallifera* markers

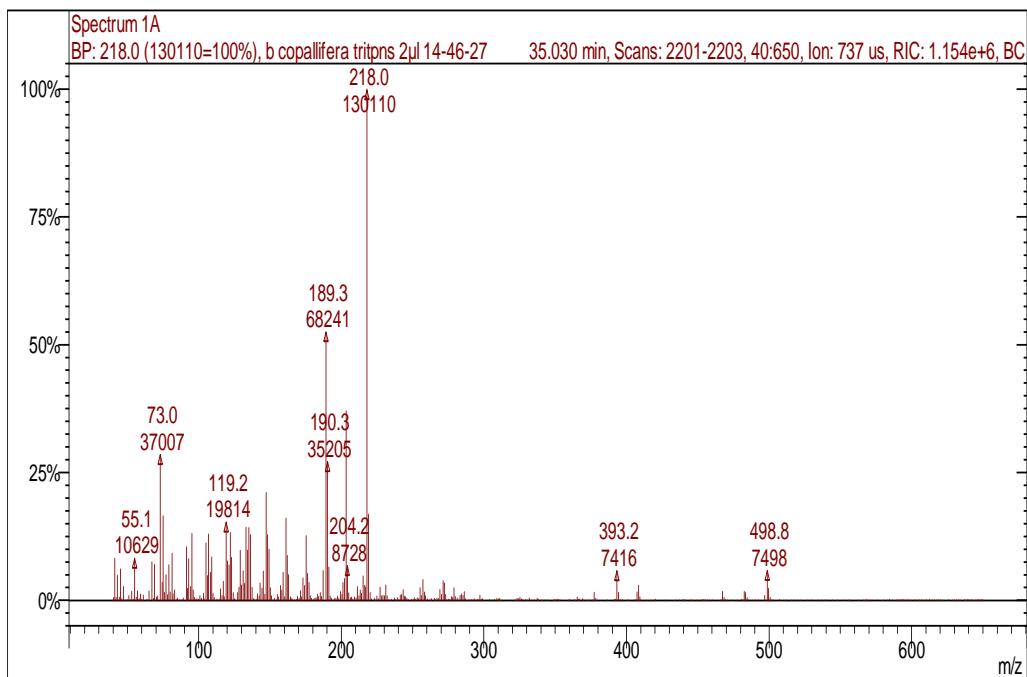
C3

tr = 34.64 min



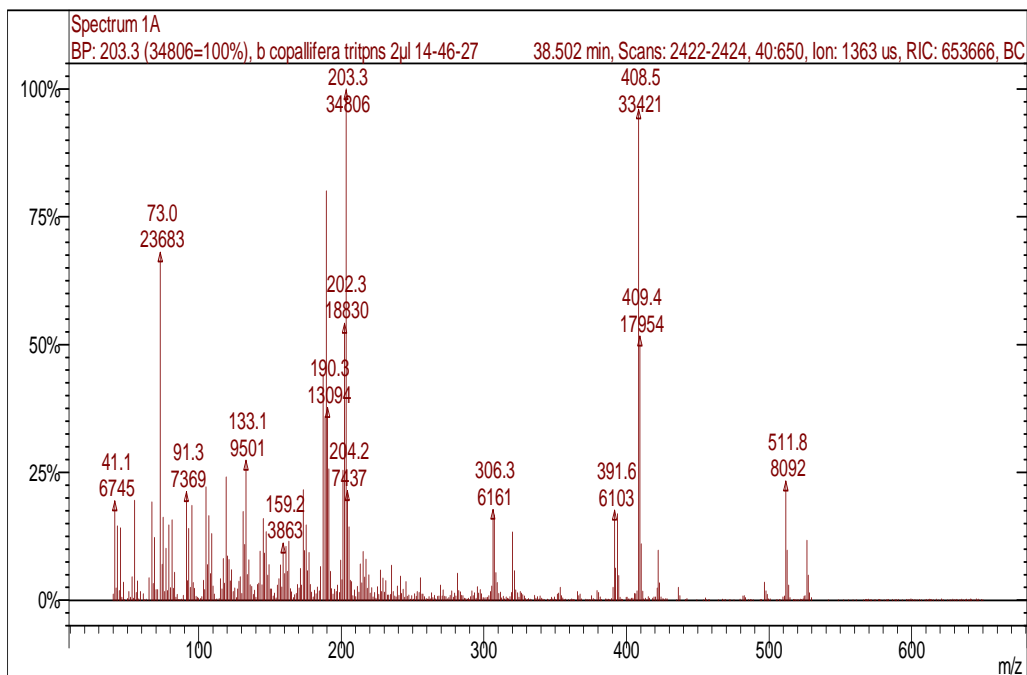
C4

tr = 35.03 min



## C5

tr = 38.50 min

Fig 122 Mass spectra of molecular markers for *B. copallifera*

Marker	Species	Retention Time (min)	Mw	Mass spectra data (70eV). Characteristic ions: m/z (%)
BS1	<i>B. bippinata</i>	31.00	496	189(6), 201(6), 215(7), 255(19), 391(45), 496(100)
BS2	<i>B. stenophylla</i>	31.68	496	185(5), 199(5), 213(4), 253(9), 255(18), 295(11), 391 (35), 496 (100)
BS3		33.92	586	73(100), 229(17), 306(78), 391(28), 496 (65.4), (586) (55)
BS4		34.45	496	95(9), 133(11), 171(8), 185(6), 199(6), 215(4), 255(25), 295(18), 391(21), 496(100)
E1	<i>B. excelsa</i>	35.00	424	93(100), 189(16), 205(43), 311(27), 355(24), 424(16)
E2		35.77	424	189(59), 205(100), 245(27), 313(39),



<b>E3</b>		36.07	496	409(31), 424(28) 73(100), 189(94), 203(56), 218(93), 336(14), 390(9.2), 427(11), 496(22)
<b>E4</b>		36.23	498	189(100), 203(55), 218(25), 393(17), 498(13)
<b>L1</b>	<i>B. laxiflora</i>	36.13	497	73(100), 134(93), 189(90), 203(42), 218(47), 337(15), 497(27)
<b>EL1</b>	<i>B. excelsa</i> & <i>B. laxiflora</i>	35.33	498	189(100), 203(55), 218(25), 393(17), 498(13)
<b>G1</b>	<i>B. grandifolia</i>	34.72	498	173(18), 189(24), 203(4), 229(12), 241(22), 393(100), 482(8), 498(4)
<b>G2</b>		36.43	646	59(15), 147(10), 441(100), 646(4)
<b>G3</b>		38.12	498	189(100), 203(35), 216(21), 229(19.3), 297(11), 422(32), 498(11)
<b>S1</b>	<i>B. simaruba</i>	34.88	498	95(41), 147(29), 189(100), 203(100), 218(60), 257(22), 311(15), 409(43), 498(3)
<b>S2</b>		35.64	498	73(18), 119(9), 173(12), 241(18), 393(100), 483(14), 498(4)
<b>S3</b>		38.32	498	189(100), 203(17), 229(16), 297(10), 498(12)
<b>GS1</b>	<i>B. grandifolia</i> & <i>B. simaruba</i>	32.77	498	189(100), 203(36), 218(17), 257(32), 297(24), 311(24), 409(68), 498(5)
<b>GS2</b>		37.69	424	109(100), 189(65), 205(78), 313(36), 424(45)
<b>C1</b>	<i>B. copallifera</i>	33.72	424	189(35), 203(100), 218(62), 409(26), 424(6)
<b>C2</b>		34.12	424	189(45), 203 (52), 218(100), 257.2(15), 393 (28), 409(20), 424(12)
<b>C3</b>		34.64	424	189(45), 203(52), 218(100), 257(15), 393

<b>C4</b>		35.03	498	(28), 409(20), 424(13) 189(52), 203(37), 218(100), 393(6), 467(2), 483(2), 498(6)
<b>C5</b>		38.50	526	189(80), 203(100), 408 (96), 512(23), 526(12)
<b>P1</b>	<i>B. penicillata</i>	37.13	484	132(15), 174(7), 188(15), 190(6), 203(100), 484(6)
<b>P2</b>		37.93	500	118(37), 132(57), 203(100), 394 (30), 409(36), 442(7), 500(3)
<b>P3</b>		38.24	424	176(29), 189(20), 204(44), 217(51), 424(100)
<b>P4</b>		38.65	498	162(44), 176(31), 190(48), 204(50), 217(100), 392(14), 407(4), 498(72)
<b>P5</b>		39.19	498	162(46), 176(40), 189(37), 204(54), 217(100), 392(16), 407(17), 468(80), 498(9)
<b>P6</b>		39.51	498	134(26), 176(26), 189(20), 204(52), 217(29), 353(28), 423(100), 498(6)
<b>P7</b>		39.99	528	189(81), 204(100), 409(69), 513(20), 528(8)

**Table 53 Summary of mass fragmentation for molecular markers for each studied species**

## **ABSTRACT**

In the present work, the molecular composition of series of resinous Aztec and Maya archaeological samples were investigated to determinate their nature and botanical origin.

Thus an analytical strategy was specifically designed. This analytical strategy included the analysis of botanically certified resins, freshly collected. It included as well the analysis of commercial samples bought in Mexican traditional markets.

The study of all the samples included microscopical techniques, Fourier Transformed Infrared Spectrometry (FTIR) , High Performance Liquid Chromatography coupled to Ultraviolet-visible spectrometry (HPLC-UV/Vis) and Gas Chromatography coupled to Mass Spectrometry (GC-MS).

The molecular study of these samples, in particular of their triterpenic composition allowed to:

- Establish the molecular profile of resins from certified botanical origin.
- Identify some of the triterpenic compounds present in samples.
- Identify triterpenic molecules that could be used as molecular markers for each botanical origin.
- Find the botanical origin of archaeological Aztec samples.
- Discard possible botanic origins for Maya archaeological sample.
- Have an overview of the origin of commercial samples of Mexican copal.
- Create a simple protocol that allows conservation and biomaterials professionals to establish the botanical origin of archaeological and commercial resins, used in conservation interventions.
- Observe the behavior of copal materials upon ageing, establishing potential markers for natural ageing in copal, under darkness.
- Asses that botanical origin of a sample can be found regardless the age of the resin.

**Discipline:** Chemistry, Archeometry.

**Key words:** Aztec, Maya, Mexican copal, triterpenoids, archeological chemistry, archeological figurine, aztec adhesive, plant resin, HPLC-UV/VIS, FTIR, GC-MS, PCA, LDA, *Bursera spp.*

**Contact the author:** paola.lucero@etd.univ-avignon.fr / paolaluce@gmail.com